How does sense emerge in the visual system? The cognitive visual system explored from categories to consciousness

Roger Koenig

Université de Toulouse

THÈSE

En vue de l'obtention du

DOCTORAT DE L'UNIVERSITÉ DE TOULOUSE

Délivré par :
Université Toulouse 3 Paul Sabatier (UT3 Paul Sabatier)

Cotutelle internationale avec :

Présentée et soutenue par :
A. Roger Koenig

Le mercredi 19 septembre 2012

Titre :
How does sense emerge in the visual system? The cognitive visual system explored from categories to consciousness — Comment le sens est-il extrait de l'information visuelle ? Le système visuel exploré des catégories à la conscience.

École doctorale et discipline ou spécialité :
ED CLESCO : Neurosciences, comportement et cognition

Unité de recherche :
Centre de Recherche Cerveau et Cognition (CerCo), UMR5549

Directeur(s) de Thèse :

Dr. Rufin VanRullen

Rapporteurs :

Dr. Thomas Carlson - Maryland Vision Science Lab - Maryland, USA
Dr. Jean Lorenceau - Cogimage, ICM - Paris, France

Autre(s) membre(s) du jury :

Dr. Bruno Rossion - IPSY, IoNS - Louvain-La-Neuve, Belgique
Dr. Lionel Naccache - CRICM, UPMC - Paris, France
Dr. Pier-Giorgio Zanone - PRISSMH - Toulouse, France

“In God we trust, all others bring data”.

William Edwards Deming

Publications

Revues internationales à comité de lecture

Koenig-Robert, R. & VanRullen, R. (2011). "Spatiotemporal mapping of visual attention". **Journal of Vision**. 11(14), 12.

Girard, P. & Koenig-Robert, R. (2011). "Ultra-rapid categorization of Fourier-spectrum equalized natural images: Macaques and Humans perform similarly". **PLoS One**. 6, e16453.

Vidal, R., Ramírez, OA., Sandoval, L., Koenig-Robert, R., Härtel, S. and Couve, A. (2007). "Marlin-1 and conventional kinesin link GABAB receptors to the cytoskeleton and regulate receptor transport". **Molecular and Cellular Neurosciences**. 35, 501-512.

Posters et Présentations à des conférences internationales

Koenig-Robert, R. & VanRullen, R. (2012). "Semantic Wavelet-Induced Frequency Tagging (SWIFT) tracks perceptual awareness alternations in an all-or-none fashion". Talk at the **12th Vision Sciences Society annual meeting**, Naples (Florida, USA).

Koenig-Robert, R. & VanRullen, R. (2011). "SWIFT: A new method to track object representations". Poster at the **34th European Conference on Visual Perception**, Toulouse (France).

Koenig-Robert, R. & VanRullen, R. (2011). "Frequency-tagging object awareness", Poster at the **11th Vision Sciences Society annual meeting**, Naples (Florida, USA).

Koenig-Robert, R. & VanRullen, R. (2010). "Spatiotemporal mapping of exogenous and endogenous attention", Poster at the **10th Vision Sciences Society annual meeting**, Naples (Florida, USA).

Girard, P. & Koenig-Robert, R. (2009). "Macaques and humans share the same mid-level cues for ultra-rapid categorization", Poster at the **31st Conférence internationale d'éthologie**, Rennes (France).

Abstract

How does sense emerge in the visual system? The cognitive visual system explored from categories to consciousness.

How does sense emerges in the visual system? In this thesis we will be focused on the visual system of human and non-human primates and their large capacity of extract and represent visual information. We studied several levels of visual representations from those related to the extraction of coarse visual features to the emergence of conscious visual representations. This manuscript presents six works in which we explored: (1) the visual features necessary to perform ultra-rapid visual categorization in monkeys and humans using psychophysics, (2) the spatio-temporal dynamics of visual attention in humans using psychophysics, (3) the neural correlates of high-level visual representations using EEG tanks to the development of an innovative technique called SWIFT, (4) the neural correlates of visual consciousness under binocular rivalry using EEG, (5) the synchrony of brain signals as a function of conscious recognition using intracranial electrodes implanted in epileptic patients and (6) the neural correlates associated with conscious perception in monkeys using intracranial electrodes. The results of these works allowed outlining a tentative model of visual perception aimed to dissociate attention and consciousness.

Keywords: visual perception, consciousness, attention, oscillations, EEG, ECoG, SSVEP, SWIFT.

Comment le sens est-il extrait de l'information visuelle ? Le système visuel exploré des catégories à la conscience.

Comment le sens est-il extrait de l'information visuelle ? Cette thèse est focalisée sur la capacité du système visuel d'humains et de singes à extraire et représenter l'information visuelle sur différents niveaux de complexité. Nous avons étudié différent niveaux de représentations visuelles, de la production de représentations visuelles primaires jusqu'à l'élaboration de représentations visuelles conscientes. Ce manuscrit présente six travaux dans lesquels nous avons exploré : (1) les attributs visuels nécessaires pour réaliser la tâche de catégorisation ultra rapide chez l'homme et le singe au moyen de méthodes psychophysiques, (2) la dynamique spatio-temporelle de l'attention visuelle chez l'homme au moyen de méthodes psychophysiques, (3) les corrélats neuronaux des représentations de haut niveau en EEG grâce au développement d'une nouvelle technique appelée SWIFT, (4) les corrélats neuronaux de la conscience visuelle dans la rivalité binoculaire en EEG, (5) la synchronie des signaux cérébraux en fonction de la reconnaissance consciente au moyen d'enregistrements intracrâniens chez des patients épileptiques et (6) les corrélats neuronaux associés à la prise de conscience chez le singe au moyen d'enregistrements intracrâniens. Les résultats de ces travaux nous ont permis d'ébaucher un modèle de la perception visuelle cherchant à dissocier l'attention et la conscience.

Mots-clés : perception visuelle, conscience, attention, oscillations, EEG, ECoG, SSVEP, SWIFT.

Résumé substantiel

Comment le sens est-il extrait de l'information visuelle ?

À chaque fois que nous ouvrons les yeux un phénomène remarquable a lieu : nous sommes capables de percevoir et de reconnaitre les éléments qui nous entourent de façon presque instantanée sans que cela ne nous demande aucun effort. La chose la plus surprenante est que nous pouvons associer une expérience subjective à ce processus : nous pouvons être conscients de ce que nous voyons.

Dans ce contexte, nous pouvons nous poser une série de questions, comme par exemple : Quels sont les phénomènes cérébraux qui sont à l'origine de l'extraction de l'information visuelle ? Quels processus permettent de rendre cette information consciente ? Et quelles sont les activités dans notre cerveau qui sont corrélées à la reconnaissance consciente de l'information visuelle ?

Différent travaux, réalisés surtout chez des modèles animaux, ont montré que dans un premier temps le traitement visuel est dédié à extraire l'information physique du stimulus et ce n'est que postérieurement que le sens de l'image est représenté de façon plus explicite pour finalement accéder à la conscience.

Ainsi, les signaux visuels voyagent dès la rétine où ils sont d'abord codés sous la forme d'impulsions électrochimiques grâce à un processus connu sous le nom de photo-transduction. Cette information est cheminée d'abord vers des structures sous-corticales comme le thalamus visuel, pour après activer des aires visuelles dites de bas-niveau. À ce niveau, un premier traitement de l'information visuelle est fait. Il permet notamment d'extraire des caractéristiques physiques de l'image comme son contraste local et son contenu en fréquences spatiales.

Dans ces stades précoces de traitement, selon le postulat classique du domaine des neurosciences visuelles, les représentations formées ne seraient pas associées à des catégories sémantiques et ce n'est qu'au terme d'une série de processus neuronaux

ultérieurs en charge de traiter cette information, que les représentations catégorielles émergeront.

Ainsi, des aires visuelles situées au-delà des aires visuelles de bas-niveau seraient à l'origine des représentations sémantiques. Dans ces aires, les neurones sont, en effet, sensibles à des caractéristiques visuelles comme la forme ou la couleur entre autres, qui permettraient d'associer les caractéristiques du stimulus à des classifications catégorielles. Dans certaines aires, les neurones sont même davantage sensibles à des attributs assez complexes comme des visages connus et des parties du corps. A ce niveau, l'activité des neurones est suffisamment sélective pour représenter les catégories sémantiques des stimuli qui sont présentés, permettant par exemple de classer une image comme contenant un animal ou un véhicule. Néanmoins, la dynamique temporelle des représentations permettant de classer des images complexes est, jusqu'à peu, restée méconnue. A quel moment précis les représentations neuronales permettant la catégorisation d'images naturelles sont-elles disponibles? Cette question a été intensivement traitée dans notre laboratoire depuis une série d'études menées afin de mesurer de façon précise le temps requis pour catégoriser une image complexe.

Force est de constater que le temps nécessaire pour catégoriser des images naturelles est particulièrement court : le temps de réaction se situe autour de 200ms pour des réponses manuelles et autour de 100ms pour des réponses oculaires ou saccades. Ces délais contraignent fortement le traitement de l'information au long de la voie visuelle. En prenant en compte les latences neuronales au long de différentes aires visuelles, les temps de réaction manuels (autours de 200ms) suggèrent que l'information visuelle n'a le temps de générer qu'un potentiel d'action par étape de traitement, dès son entrée rétinienne jusqu'à la réponse manuelle. C'est-à-dire que l'information serait traitée de façon purement *feed-forward* lors de cette tâche par la chaîne complète d'aires visuelles corticales depuis les aires visuelles de bas-niveau vers celles de haut niveau, pour ensuite activer le cortex préfrontal et les aires motrices. Par rapport aux tâches de saccades, les temps de réaction autour de 100ms sont encore plus contraignants, suggérant que l'information n'aurait même pas le temps d'être traitée par toutes les aires mentionnées auparavant. Ainsi, lors de la réalisation de la tâche de catégorisation visuelle rapide utilisant des réponses saccadiques, les aires oculomotrices (comme le FEF ou le colliculus supérieur) ne pourraient utiliser que

l'information provenant de l'analyse visuelle faite dans des aires de bas ou moyen niveau hiérarchique pour déclencher la réponse motrice. Ainsi, l'activité des aires en position basse et moyenne dans la hiérarchie encoderait explicitement des caractéristiques du stimulus, dites diagnostiques, permettant son classement dans des catégories sémantiques (par exemple animal, véhicule, visage, etc.).

La nature exacte des caractéristiques de l'image utilisées par le système visuel pour accomplir cette tâche reste débattue. Certaines études ont montré que des indices de très bas niveau codés dans des aires visuelles primaires, comme le contenu en fréquences spatiales de l'image (qui peuvent être dissociées des formes présentées, porteuses du contenu sémantique) peuvent influencer la catégorisation visuelle rapide. Alors, quels sont les attributs de l'image qui permettent cette catégorisation ? Cette question est abordée par la première étude de cette thèse dans laquelle nous avons réalisé une étude comparative chez le singe et l'homme tout en contrôlant les indices de bas niveau dans nos images. Nos résultats montrent que tant les êtres humains que les macaques peuvent réaliser la tâche de catégorisation ultra-rapide, lorsque les indices de bas niveau des images de différentes catégories sont contrôlés (spécifiquement le contenu en fréquences spatiales et le contraste). Nos résultats suggèrent aussi que les attributs de l'image utilisés pour la catégorisation chez l'homme et chez le macaque sont similaires et que ces attributs peuvent être contenus dans les basses fréquences de l'image (égal ou inférieur à 6 cycles/image), appuyant ainsi l'idée que les attributs nécessaires pour la catégorisation ultra-rapide pourraient reposer sur des représentations incomplètes de l'image.

Bien qu'il soit évident que la tâche de catégorisation visuelle rapide permette d'extraire de l'information catégorielle à partir d'une image complexe—ce qui correspond à un processus relativement complexe du point de vue cognitif—, elle semble ne pas avoir besoin de conscience pour être accomplie. En fait, il existe des études chez des patients agnosiques (des patients qui, à la suite de lésions cérébrales, ont des troubles pour reconnaitre explicitement des objets) montrant qu'ils peuvent réaliser la tâche de catégorisation rapide sans reconnaitre explicitement (*c.-à-d.* consciemment) les images. Des autres études qui ont utilisé des paradigmes de double tâche, afin de capturer l'attention sur un endroit de l'écran de présentation, ont notamment permis de montrer que la catégorisation visuelle rapide

peut être faite en absence (ou quasi absence) d'attention pour la catégorisation d'images naturelles.

Des nombreuses études ont montré qu'en l'absence d'attention, notre perception consciente est fortement dégradée. Ces études suggèrent alors que l'attention est la porte vers la conscience, ce qui veut dire que l'attention serait un préalable pour l'accès conscient à l'information visuelle. Ainsi, le rôle de l'attention visuelle est de sélectionner juste une partie de l'information qui est disponible pour la traiter au détriment de l'information qui n'est pas sélectionnée. Cette sélection peut être faite à plusieurs niveaux ; ainsi l'attention peut sélectionner, par exemple, une caractéristique des objets présentés (c'est ce qui est connu sous les termes d'attention basée sur les caractéristiques), comme leur couleur, et de cette façon focaliser le traitement sur les objets contenant la couleur choisie, ou elle peut sélectionner la forme d'un objet (attention basée sur l'objet), ou encore une partie du champ visuel (attention spatiale). Grâce à de nombreuses études, les propriétés de déploiement spatial de l'attention sont bien connues. Ceci a permis l'émergence du concept du focus de l'attention et de différents modèles qui ont tenté de corréler les propriétés spatiales du focus de l'attention avec le comportement lors de différentes tâches. Indépendamment, d'autres travaux de recherche se sont davantage concentrés sur le profil temporel d'activation de l'attention visuelle. Celle-ci est activée plus précocement par des stimuli saillants flashés brièvement (processus que l'on désigne sous les termes d'activation exogène de l'attention), que lorsqu'elle est dirigée vers un endroit du champ visuel par suite d'une action volontaire (activation endogène de l'attention). Néanmoins, les propriétés spatiales et temporelles de l'attention n'ont été que rarement étudiées conjointement. Ainsi, à ce jour, nous ne possédons aucune vision globale permettant de comprendre comment les composantes spatiales et temporelles de l'attention visuelle interagissent. Le motif spatial de l'attention change-t-il au cours du temps ? C'est dans la deuxième partie de cette thèse que nous étudierons cette problématique grâce à un dispositif expérimental innovateur qui nous a permis d'obtenir la première cartographie détaillée de l'attention visuelle dans l'espace et le temps.

Après avoir étudié l'attention qui semble être la clef des représentations conscientes, nous allons revenir à notre question initiale, à savoir, les représentations des objets visuels, afin d'étudier cette fois les représentations visuelles de haut niveau. Comme on l'a vu

précédemment, les représentations visuelles gagnent en complexité au cours du traitement visuel. Alors que les aires visuelles de bas-niveau encodent des attributs physiques de l'image, des aires de plus haut niveau contiennent des représentations plus complexes des objets visuels, notamment des représentations porteuses d'attributs sémantiques. Différents modèles proposent que ce ne soit qu'au terme de ce processus que ces représentations permettent la reconnaissance explicite des objets visuels. Comment peut-on dissocier les représentations des bas-niveau et celles qui sont à la base de la reconnaissance consciente des objets ? Dans une troisième série de travaux présentés dans cette thèse, nous avons développé un nouveau paradigme de stimulation appelé SWIFT (semantic wavelet-induced frequency-tagging) qui est basé sur des techniques de traitement du signal (transformée en ondelettes) et du SSVEP (steady state visual evoked potentials) afin de manipuler le contenu sémantique présenté aux sujets de façon périodique tout en égalisant les propriétés de bas-niveau de l'image. Le but de cette technique était d'activer périodiquement à une fréquence déterminée les aires cérébrales chargées de coder l'information sémantique pendant que les aires codant pour des attributs de bas-niveau sont stimulées avec un flux constant d'attributs de bas-niveau. Cette approche cherche ainsi à dissocier les activités de ces aires grâce à leurs profils d'activation au cours du temps, en identifiant notamment les aires codant l'information sémantique comme celles qui répondent périodiquement à la fréquence de modulation.

Ce protocole de stimulation a permis d'isoler l'activité cérébrale (enregistrée grâce à l'EEG) évoquée spécifiquement par la reconnaissance consciente des images naturelles. Des aires centro-pariétales n'ont pas montré de réponse en potentiels évoqués lorsque des séquences de stimulation SWIFT sans contenu sémantique ont été présentées, de même que lorsque ces séquences n'avaient pas encore été reconnues (dont le contenu sémantique n'est pas encore accessible). Une fois que le contenu sémantique a été révélé, les mêmes séquences qui n'avaient pas été reconnues précédemment, ont évoqué des réponses significatives ainsi que celles qui ont été reconnues spontanément. Ces résultats montrent que l'activité évoquée par SWIFT est sélective de la reconnaissance consciente des images. Nous avons aussi testé l'effet de l'attention spatiale sur les signaux enregistrés utilisant SWIFT. Nos résultats montrent que les signaux évoqués utilisant SWIFT présentent des modulations attentionnelles plusieurs ordres de grandeur supérieures à celles enregistrées

en utilisant des techniques traditionnelles, suggérant que ces signaux correspondent à des représentations de haut niveau, car il est connu que les effets attentionnels sont amplifiés au cours de la hiérarchie visuelle. Finalement, nous avons testé la dynamique temporelle des représentations évoquées par SWIFT. Nos résultats suggèrent que le système visuel ne peut produire qu'un maximum de 4 à 7 représentations conscientes par seconde.

Lors des expériences permettant de mettre en évidence la sélectivité des signaux évoqués par SWIFT par rapport à la reconnaissance consciente, le stimulus visuel était toujours visible par le sujet et seul son contenu sémantique (c.-à-d., la reconnaissance explicite des objets contenus dans la séquence) a été manipulé, pouvant être consciemment accessible ou pas. Ainsi, nous pouvons différencier deux processus grâce à ce protocole: la reconnaissance consciente du stimulus (que nous avons manipulée) et la visibilité consciente du stimulus (que nous n'avons pas manipulée lors de notre expérience). En conséquence nous nous posons la question suivante : Quel type de modulations du signal SWIFT obtiendrions-nous en manipulant l'accessibilité consciente aux stimuli d'une façon plus claire? C'est dans une quatrième expérience que nous avons étudié les modulations du signal SWIFT en utilisant la rivalité binoculaire. Pendant la rivalité binoculaire, des images différentes sont présentées à chaque œil et au lieu d'être fusionnées dans un même percept, elles entrent en compétition pour l'accès à la perception consciente qui alterne alors entre une image et l'autre. Ceci permet de présenter des stimuli qui ne sont pas consciemment perçus mais qui font tout de même l'objet d'un traitement visuel. Les résultats de travaux utilisant des techniques traditionnelles, ont montré que les modulations du signal sont modestes lorsque le stimulus passe de l'état consciemment perçu à l'état non-perçu. Ceci est dû au fait que les techniques traditionnelles enregistrent de façon confondue les activations résultant du traitement de bas-niveau de l'image (qui est largement non-conscient) et celles provenant des représentations de haut niveau qui sont plus proches de l'accès conscient. En utilisant SWIFT, nous avons montré des modulations en tout-ou-rien : l'activité est évoquée par SWIFT lorsque le stimulus est perçu consciemment, par contre aucune activité n'est évoquée lorsqu'il n'est pas perçu. Ceci indique que les activités évoquées par SWIFT correspondent à des représentations conscientes. Nos résultats suggèrent également que l'activité représentant l'accès conscient serait associée à une augmentation de la cohérence de la

dynamique temporelle de ces signaux au cours du temps et non à une augmentation de l'amplitude du signal.

Les résultats obtenus avec la technique SWIFT montrent qu'il est possible d'isoler les corrélats neuronaux des représentations de haut niveau, avec une spécificité remarquable pour les activités conscientes. Dans les deux derniers travaux présentés dans ce manuscrit, nous allons explorer une question fondamentale pour l'étude des représentations conscientes : Où et à quel moment les représentations conscientes émergent-elles dans le cerveau ? Afin de répondre à cette question nous avons utilisé des techniques permettant d'obtenir des enregistrements de l'activité neuronale avec une haute résolution spatiale et temporelle. Ces techniques correspondent à des enregistrements électriques intracrâniens qui ont été possibles grâce à des collaborations avec les équipes du Dr Denis Fize et Dr Emmanuel Barbeau. Ces collaborations sont toujours en cours ainsi que l'acquisition de données. Néanmoins des résultats préliminaires sont déjà disponibles et sont présentés dans cette thèse dans la forme de deux rapports indépendants.

Ainsi, le cinquième travail présenté dans ce manuscrit est consacré à l'étude des signaux obtenus grâce à la technique SWIFT enregistrés sur des électrodes intracrâniennes chez des patients épileptiques. Ces patients sont implantés avec des électrodes profondes pour des raisons médicales, afin de connaitre la localisation des foyers épileptiques lors d'épilepsies résistantes à de traitements pharmacologiques. Lors de cette expérience nous avons reproduit la tâche de reconnaissance consciente d'objet. Nos résultats montrent des comportements différents entre la synchronie, dite externe, de différentes aires cérébrales (la synchronie des signaux avec la stimulation SWIFT au cours des présentations) et la synchronie dite interne (la synchronie au sein de chaque aire cérébrale au cours des présentations) en fonction de la reconnaissance consciente des images. Ces résultats suggèrent des corrélats électrophysiologiques qui permettraient de dissocier les phénomènes attentionnels de la conscience.

Le sixième et dernier travail traite d'une étude chez un singe macaque implanté avec des électrodes intracrâniennes, cherchant à mettre en évidence des activités liées à la prise de conscience ainsi que l'exploration de la dynamique spatiale et temporelle de ces activités. L'animal, étant entrainé à faire une tâche de catégorisation animal/non-animal, a été l'objet

d'une étude lors d'une version modifiée du paradigme de reconnaissance consciente utilisé auparavant. Une analyse en potentiel évoqué a révélé l'existence de deux composantes principales dans nos enregistrements. Une première composante fut évidente à des délais précoces (avec une amplitude maximale vers les 100 ms) après l'apparition de l'information sémantique. Cette composante était présente pour tous les types de stimuli (cibles, distracteurs et fausses alarmes) et son amplitude semble être corrélée avec la réponse motrice de l'animal (go ou no-go). Une deuxième composante plus tardive (présente après 200 ms) était présente seulement pour les cibles classifiées en tant que telles, ce que l'on pourrait associer à la reconnaissance consciente chez l'animal. Il mérite d'être souligné que les activités enregistrées sont compatibles avec le modèle de l'espace de travail neuronal global d'accès à la conscience. Ces résultats mettent en évidence des corrélats électrophysiologiques associés à la reconnaissance consciente chez le singe qui sont comparables à ceux observés chez l'homme.

Dans la dernière partie de la thèse un modèle de perception visuelle est proposé. Ce modèle est compatible avec les résultats obtenus lors des différents travaux présentés ainsi qu'avec des éléments d'autres modèles. Il s'appuie sur une architecture hiérarchique du système visuelle dissociant notamment des processus conscients et non-conscients. Une dissociation à la fois hiérarchique et fonctionnelle est proposée pour l'attention et pour la perception consciente, et des hypothèses sont exposées concernant les bases électrophysiologiques pour identifier chacun de ces processus.

A. Introduction

I. Overview: sensing the world

Interpreting the world by extracting relevant information is critical for every living being in order to set an appropriate response to the environmental constrains. The extraction of information, in its most rudimentary sense, is made at all levels of the phylogenetic scale. Think for instance of a bacterium using a quite complex molecular machinery in order to recognize the host cell by acquiring information from its cell membrane proteins, or a tree modulating the turgor pressure of its leaves in response to the direction of the light in order to orient them toward the sun or a bat hearing the reverberations of its own voice coming from the walls in order to navigate into a cave using eco-location.

Different signals from the environment are thus more or less integrated by the sensing machinery of different living beings across the phylogenetic tree, allowing the emergence of only very peripheral representations of the environmental state in less-evolved creatures to more central and integrated representations in higher-order organisms.

Over millions of years, evolution has fashioned the organisms to be more efficient to extract information from their environment. The emergence of the first nervous systems in animals: the Coelenterates, between 600 and 540 million of years ago and subsequently the emergence of the first central nervous systems with the Bilateria animals marked a revolution in the integration of environmental information (Galliot & Quiquand, 2011). The possibilities for information integration and management increased rapidly as the neural systems grew bigger. Evolving neural systems allowed creatures to adapt better to their environment avoiding risks and finding new nutriment resources. The improvements in the way that living beings sensed the world were selected by their fitness value and thus perpetuated in future generations. The emergence of brains in evolution allowed setting internal plans in order to guide and predict the changes in a dynamic environment. Thus, central nervous systems and brains are thought to have primarily evolved because of the

need to integrate sensory information and predict motor behavior (see for instance Maturana & Varela, 1992; Llinás, 2002). The evolution of ever more sophisticated sensory organs diversified the possibilities of sensing the environment and interacting with it. One of the most sophisticated sensory organs designed by evolution is the eye. The importance of vision is attested by the fact that eyes evolved many times in an independent fashion in different species (Fishman, 2008; Lamb, Arendt, & Collin, 2009).

In primates, the sense of vision is by far the most developed. As a consequence, much of the primate cortex is devoted to visual processing. In the macaque monkey at least 50% of the neocortex is associated with vision, involving over thirty distinct areas (Desimone & Ungerleider, 1989; Van Essen & Gallant, 1994). Visual inputs allow primates to produce a virtually infinite repertoire of more or less complex behavioral responses, which in turn are pinpointed by neural representations with different levels of complexity.

Some behavioral responses guided by visual information such as oculomotor responses appeared early in evolution and rely on very rudimentary visual information which is represented by small neural circuits which generate reflexive responses (Martínez-García, Puelles, Donkelaar, & González, 2012). These reflex behaviors—such as vergence adaptation, saccadic movements and smooth pursuit—involve archaic areas within the central nervous system such as the brain stem and the cerebellum, but can be also modulated by cortical visual areas (Voogd, Schraa-Tam, van der Geest, & De Zeeuw, 2010). These visuomotor loops are poorly flexible, stereotyped behaviors that are executed automatically. The visual information managed by this kind of systems remains often subjectively unnoticed; that is, the visual input is not consciously perceived. However, non-conscious processes are not an exclusive property of small neural circuits and simple neural computations. In fact, quite complex cognitive operations such as extracting the semantic information of a rapidly flashed word is also possible in absence of conscious perception (Dehaene et al., 1998).

On the other hand, visual information can be the object of subjective sensation, that is, it can be consciously perceived. The emergence of consciousness in the phylogenetic scale marked a quite singular event. However it is unclear why evolution selected conscious perception. Taking a cognitive stance, the main role of consciousness would be the unification and integration of otherwise independent brain functions in a coherent whole

(Bransford, 1979; Baars, 2002). This would represent an evolutionary advantage for conscious animals which would integrate information in novel ways, thus enlarging their repertoire of internal representations and in consequence also their behavior (Baars, 1990; Baars, 2005; Shanahan, 2010; Ward, 2011).

While visual operations are relatively well understood at the level of single neurons and brain areas, its relationship with subjective experience has only recently begun to be studied scientifically. How does neural activity in the brain give rise to consciousness? An explanatory gap still lies between the function of neurons and our capacity to represent the world subjectively.

In this thesis we will be focused on the visual system of human and non-human primates and its large capacity of information extraction from the very fundamental mechanisms allowing extracting coarse features carrying on some semantic value to the search for neural correlates of conscious representations.

In the introduction we will see how visual information is extracted in a cascade of automatic processes and then integrated along the visual hierarchy. Then, we will focus on visual attention and we will see how this process enables the emergence of higher-level visual cognitive functions. Then we will focus on visual consciousness and the neural mechanisms allowing representing visual information consciously, completing the introduction with a brief summary of the current neurobiological theories of consciousness.

II. The visual system as a hierarchical network

a) The retina

The retina is the first center that processes visual information. The retina is a thin multi-layer tissue (no more than 250µm in humans) where the light focused by the eye's optical structures is projected (Alamouti, 2003). In the retina, photoreceptor cells transform light into neural activity in a process known as *phototransduction*. Photoreceptors come in two

types: rods and cones and are functionally specialized. Rods are 20 times more abundant than cones in the human retina and are specialized for low-light vision. They are exquisitely sensitive and can signal the absorption of single photons, however their response saturates at daylight illumination conditions (Baylor, Lamb, & Yau, 1979). Cones, on the other hand, support vision under daylight conditions (where the rods are nonfunctional). They are much less sensitive to light than rods, but have higher temporal resolution (Kefalov, 2012). Three types of cones mediate color vision in humans. They contain different photopigments with different light spectra sensitivity allowing representing color information as a trichromatic code. Information coming from rods and cones reaches the dendrites of bipolar cells (i.e. second order cells) which innervate ganglion cells (i.e. third order cells) whose axons constitute the optic nerve. Retinal circuitry includes other second order cells: bipolar, horizontal and amacrine cells. Second order cells jointly generate the response properties of ganglion cells (Lee, Martin, & Grünert, 2010, Figure 1). Ganglion cells respond to photic stimulation falling within the area covered by the photoreceptors functionally linked to them. This area is known as the *receptive field*. The number of photoreceptors converging into a single ganglion cell is related to the size of its receptive field. Large ganglion cell's receptive fields represent thus high photoreceptor convergence, leading to low visual acuity while small receptive fields represent low convergence generating high visual acuity. Ganglion cells located at the fovea have small receptive fields, whereas ganglion cells located at the periphery have larger receptive fields.

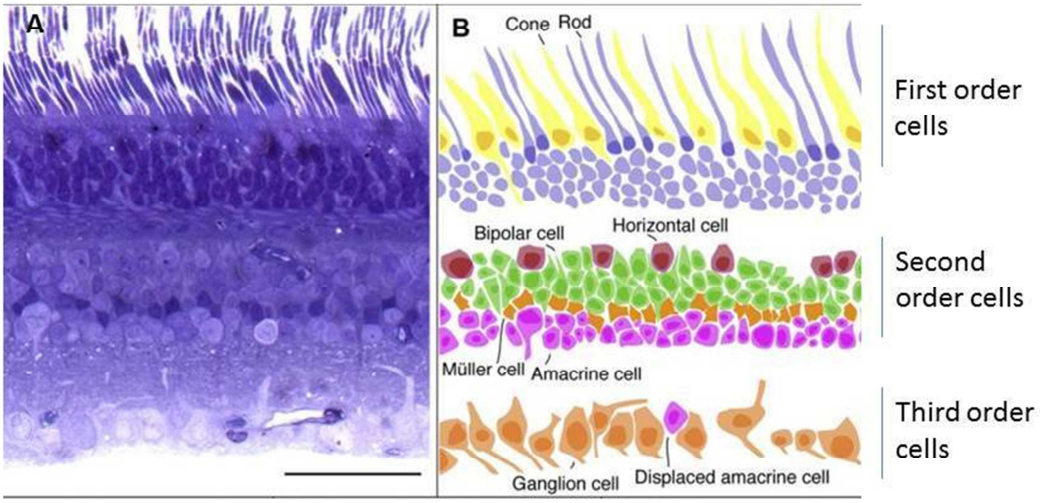

***Figure 1. Histological preparation and functional circuitry of primate retina**. **A.** Macaque monkey retina stained with Toluidine blue (Nissl). The bar represents 50 µm. **B.** Disposition of neuronal layers. Silhouettes show cell soma and nuclei from cells shown in panel A; inner and outer segments of some rod and cone receptors are also drawn (Modified from Lee et al., 2010).*

Pioneer electrophysiological studies on eel and frog optic nerve revealed that the firing rate augmented at both the onset and the offset of the light stimulation (Adrian & Matthews, 1927). These *on* and *off* responses were later found in isolated ganglion cells of frogs (Hartline, 1938). Some years after, independent studies showed that ganglion cell receptive fields have two distinctive functional zones: the *center* and the *surround* (Barlow 1953, Kuffler 1953). The activation properties of these zones vary among different cells. Some ganglion cells can be activated by light falling in the center of their receptive fields or by the light extinction in their surround. Cells with these properties are known as *on-center* cells (Figure 2, left panel). Other cells are activated by light extinction in their center and light onset in their surround, and are called *off-center* cells (Figure 2, right panel). A crucial feature of ganglion cell responses is that when light falls over both the center and the surround of the receptor field, the response of the cell is very weak if any –center and surround receptive field regions are antagonistic. This functional property is fundamental for the coding of visual information at the retina. While a digital camera encodes the absolute luminance at every pixel, the retina encodes *local luminance contrast*, since ganglion cells

only respond when there is a *luminance difference* within their receptive fields. Thus the critical feature of visual information encoded by the retina is local contrast.

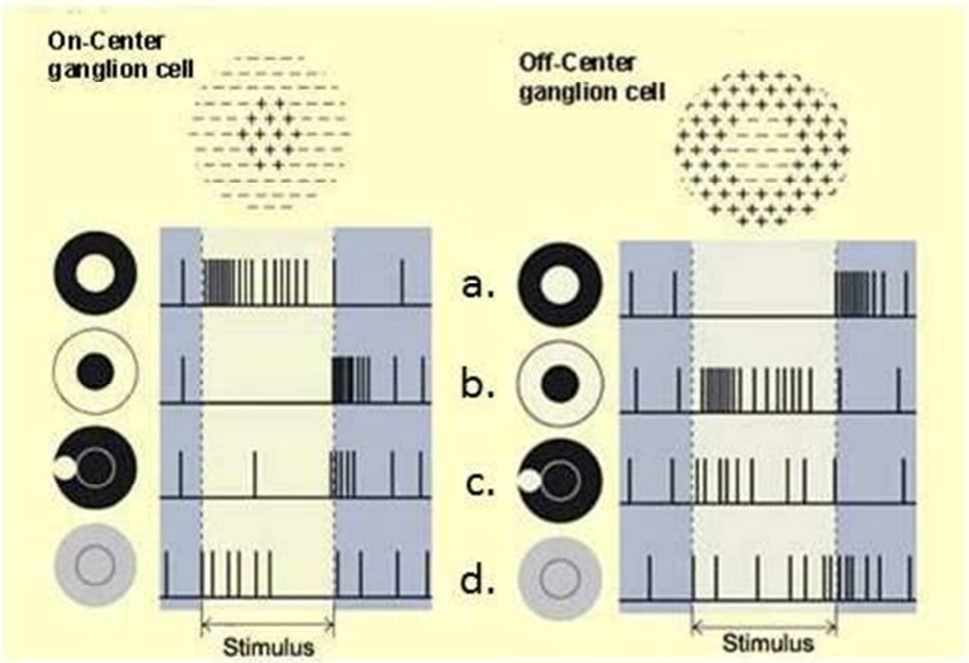

***Figure 2. On-center and off-center ganglion cells**. **A.** Illumination within the small central area produces an on-response in on-center cells (left), while an off-response in off-center cells (right). **B.** Illumination within the contour of the receptive field produces no response in on-center cells (left), while activates off-center cells (right). **C.** Light extinction in the surround elicits an off-response in on-center cells. Local illumination in the contour area of the receptive field produces more modest responses. **D.** Ganglion cells fail to be activated when both center and surround are simultaneously illuminated (Modified from Kuffler, 1953).*

b) The lateral geniculate nucleus

The lateral geniculate nucleus (LGN) of the thalamus is the principal target of the retinal projections in primates. This nucleus represents the major relay station of visual information coming from retina to primary visual cortex. The LGN is arranged in a laminar organization where distinctive ganglion cell projections are segregated. This segregation originates three

different pathways: magnocellular, parvocellular and koniocellular (Kaas, Huerta, Weber, & Harting, 1978).

In the primate LGN, four parvocellular layers receive projections from midget ganglion cells. These ganglion cells have small dendritic trees, thus receiving inputs from relatively few rods and cones (i.e. low degree of convergence). Parvocellular neurons are sensitive to color and have a finer spatial resolution than magnocellular neurons (Xu et al., 2001).

Magnocellular neurons in the two bottom layers LGN receive inputs from parasol ganglion cells. They have large dendritic trees and thus receive inputs from many rods and cones (i.e. high degree of convergence and thus low visual acuity). They can respond to low-contrast stimuli but are not sensitive to color (Wiesel & Hubel, 1966). In particular, these cells are responsible for resolving motion (Xu et al., 2001). The coarse (i.e. low-acuity) visual information carried by the magnocellular pathway can play a major role in cognitive tasks such as rapid-categorization as suggested by the first work presented in this thesis.

Koniocellular neurons are located between the magnocelullar and parvocellular layers in the LGN, and receive inputs from bistratified ganglion cells where visual information from short-wavelength cones converge. Throughout each koniocellular layer are neurons that innervate extrastriate cortex (i.e., visual areas beyond V1), and may sustain some visual behaviors in the absence of V1 (Hendry & Reid, 2000), which is the case of pathological conditions such as blindsight (Zeki, 1995).

Visual response latencies of parvocelullar neurons are longer than those of magnocellular cells, supporting the idea that visual cortex is activated first by magnocelullar projections providing a coarse preview of the visual world in the first wave of activity (see for instance Bullier, 2001). However, some authors have argued that due to the fact that parvocellular neurons are far more numerous than magnocellular neurons, convergence in cortex could reduce the magnocellular advantage by allowing parvocellular signals to generate detectable responses sooner than expected based on the responses of individual parvocellular neurons, and it could even reverse the magnocellular advantage (Maunsell et al., 1999).

Classically, the LGN has been considered as a simple relay system. However, in terms of numbers of synapses on the geniculate relay cells, retinal inputs provide only about 5% (Van

Horn, Erişir, & Sherman, 2000). The remaining 90%-95% of synaptic inputs are roughly equally divided among local inhibitory inputs, brainstem inputs and cortical feedback. These cortico-thalamic connections targeting the LGN and other thalamic nuclei have been highlighted as crucial features for models aimed to explain sensory representations (Mumford, 1991), attention (Koch and Ullman 1985, Kustov & Robinson, 1996), and conscious perception (Lumer, Edelman, & Tononi, 1997), among other functions.

There is also evidence supporting the idea that LGN relay cells can actively shape the temporal dynamics of activation of the primary visual cortex, having a key role in the generation of the cortical alpha rhythm (see for instance da Silva et al. 1973, Llinás 1988, (Lőrincz, Kékesi, Juhász, Crunelli, & Hughes, 2009), which would be fundamental in maintaining the functional connectivity among brain areas (Sauseng & Klimesch, 2008; Wang, 2010). Thus, the role of the LGN apparently goes further from the relay function proposed for classic views.

c) The primary visual cortex

The primary visual cortex (also known as area V1 or striate cortex) is the principal target of projections from the retina. The neocortex is organized in layers which are distinguishable using histological dyes (Brodmann, 1909). The primary visual cortex contains 6 layers, with layer 1 located at the cortex surface and layer 6 next to the white matter (Figure 3). Relay neurons in the LGN project principally on layer 4 (Wilson & Cragg, 1967, Figure 3A).

Magnocelullar and parvocellular pathways project on different subdomains of layer 4 (Figure 3A). Magnocellular projections are mainly found in layer 4Cα, while parvocellular projections are mainly found in layers 4Cβ and 4A (Lund, 1973; Blasdel & Lund, 1983). Other cortical layers can also receive thalamo-cortical projections. Collateral axonal projections from magnocellular and parvocellular neurons are also found in layer 6 (Lachica, Beck, & Casagrande, 1992), while the koniocellular pathway mainly projects on layer 1 and 2 (Casagrande, Yazar, Jones, & Ding, 2007).

Also, there are some koniocellular axons that project beyond the primary visual cortex, in regions such as V2 (Yoshida & Benevento, 1981; Fries 1981; Bullier and Kennedy 1983), V4 (Tanaka, Lindsley, Lausmann, & Creutzfeldt, 1990), the inferotemporal cortex (Hernández-González, Cavada, & Reinoso-Suárez, 1994) and the medial temporal area MT (Bullier & Kennedy, 1983 ; Sincich, Park, Wohlgemuth, & Horton, 2004), which, besides from supporting visuospatial behaviors in pathological conditions affecting V1 as discussed above, could also shortcut visual information in normal vision, producing the unexpected early neural responses (less than 80 ms) in higher level visual areas such as MT and the prefrontal cortex (Bullier, 2001).

While receptive fields in LGN are organized concentrically (with on- and off-centers and antagonistic surrounds), receptive fields in the primary visual cortex have a more complex organization. The pioneer works of Hubel and Wiesel in cat and monkey cortices led to the distinction of two kinds of neurons: simple and complex which have different receptive field properties (Hubel & Wiesel, 1959; Hubel & Wiesel, 1962; Hubel & Wiesel, 1965; Hubel & Wiesel, 1968).

Simple cells have from 2 to 4 easily distinguishable on and off regions in their receptive fields. On and off regions emerge as a consequence of the convergence of on-center and off-center LGN cells respectively (Tanaka 1983; Alonso, Usrey, & Reid, 2001). Simple cells show a *push-pull* organization within the regions of their receptive fields. Bright stimuli falling within off-regions and dark stimuli falling within on-regions inhibit neuronal response (Palmer & Davis, 1981; Ferster, 1988). Thus, when on- and off-regions are stimulated at the same time, the neural response is less important than responses obtained by stimulating on- and off-regions alone.

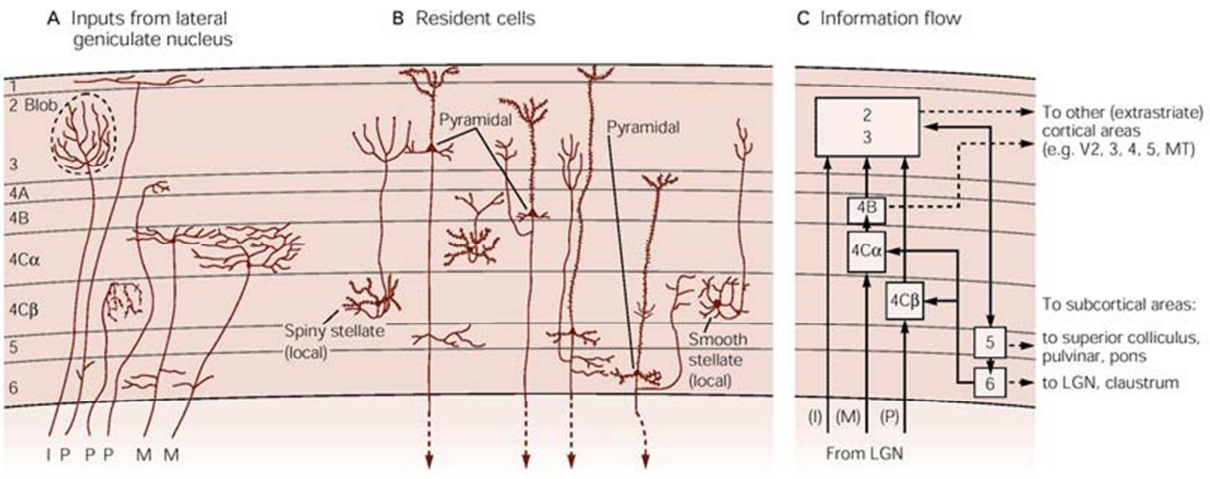

Figure 3. The six cortical layers introduced by Brodmann*. *A. V1 inputs from LGN. *Magnocellular afferences principally arrive to layer 4Cα of V1 while parvocellular inputs principally arrive to layers 4A and 4Cβ, with some inputs in layer 1. Collaterals from both pathways are found in layer 6. Koniocellular inputs are located mostly in layer 2.* ***B. Cell soma distribution.*** *Layer 1 is nearly aneuronal, composed predominantly of dendritic and axonal connections. Approximately 20% of the neurons in layers 2-6 are inhibitory interneurons (GABAergic) that make major contributions to the function of V1 circuits but do not project axons outside this area. Layers 2/3 contain many excitatory projection neurons.* ***C. Information flow.*** *Feedforward connections are made from neurons in layers 2/3 that send axons to extrastriate cortical regions (e.g. V2, V3, V4, MT, etc.). Feedback connections (not shown) are made from neurons in layers 5 and 6 to layers 2/3 and 5/6 (Modified from Lund, 1988).*

Complex cells have on- and off-regions that are not segregated spatially (Hubel & Wiesel, 1962). At any location of their receptive fields, complex cells generate an on-response to the onset of light stimulation, and an off-response to its extinction.

Neurons of the primary visual cortex are selective to orientation and direction (Hubel & Wiesel, 1968). While the vast majority of V1 cells show some degree of orientation selectivity, only approximately 25-35% of V1 cells are strongly directionally selective (Schiller, Finlay, & Volman, 1976; De Valois, Yund, & Hepler, 1982). Orientation selective neurons discharge strongly to luminance bars oriented in the preferred orientation and less strongly to light bars oriented in the non-preferred ones (Figure 4).

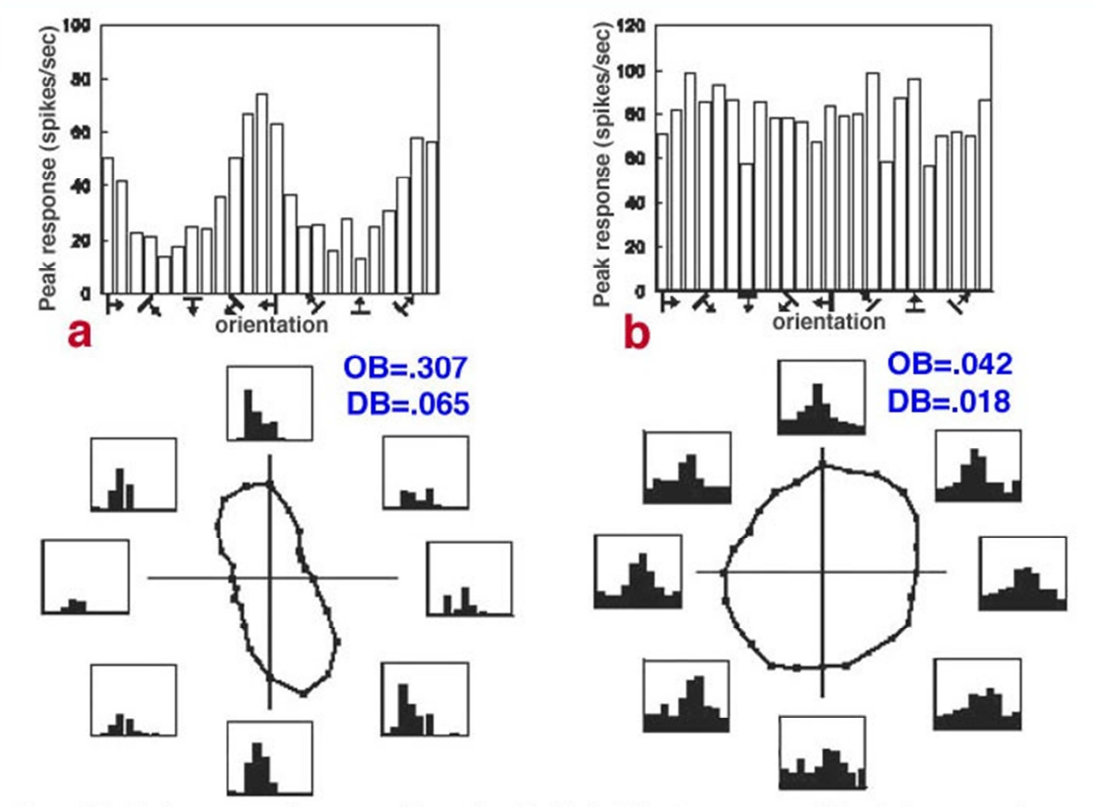

Figure 4. Orientation selectivity in V1 cells. *A tuning curve obtained from two macaque V1 cells in response to drifting luminance bars. The polar plots show responses to systematically varied orientations and directions.* ***A.*** *Responses from one orientation selective V1 cell* ***B.*** *Responses from one nonselective V1 cell. Histograms surrounding the polar plots demonstrate the cellular response as a function of time. Orientation bias (OB) and direction bias (DB) are measures of how selective a cell is (Modified from Schmolesky, Wang, Pu, & Leventhal, 2000).*

Neurons selective to the same orientation tend to be organized in *cortical columns* (Hubel & Wiesel, 1968). Each orientation column is about 30 to 100 µm wide and 2 mm deep, and cells within a column have receptive fields covering the same area of the visual field. Orientation selectivity varies systematically among adjacent columns, with adjacent columns showing similar orientation preferences (Hubel & Wiesel, 1968; Leventhal, Thompson, Liu, Zhou, & Ault, 1995).

Neurons of the primary visual cortex receive and send information from neurons within and beyond V1 by means of 3 different corticocortical connections: horizontal, feedforward and feedback connections (Salin & Bullier, 1995).

Horizontal connections link neurons within the same cortical area, linking columns with shared orientation preferences and represent the vast majority of synapses in V1. Horizontal connections are often made between neurons within the same layer (Binzegger, Douglas, & Martin, 2004). Feedforward connections, on the other hand, are made from lower to higher cortical areas. These connections are made from pyramidal cells of layers 2 and 3 to neurons in layer 4 in the target area (Figure 3C). Feedback connections are made from higher to lower cortical areas (Figure 3C). These connections are made from neurons in layers 5 and 6 to layers 2/3 and 5/6 (Rockland & Pandya, 1979; Maunsell & van Essen, 1983).

This connectivity pattern was used to propose a hierarchical organization among visual areas in the monkey brain (Felleman & Van Essen, 1991).

d) Visual area V2

In monkey V2 two-thirds of the projections are provided by V1 (Sincich, Adams, & Horton, 2003). V2 receptive fields are larger than those in V1 which is produced by the convergence of multiple V1 cells onto each V2 neuron. V2 cells are sensitive to depth, motion, color, and simple contours (Levitt, Kiper, & Movshon, 1994; Thomas, Cumming, & Parker, 2002).

Area V2 neurons show more complex responses than V1 neurons. They can be sensitive to border ownership (i.e., the object-appartenance of occluding contours defining the limits of such objects). Border ownership can be manipulated when the same local feature (contrast edge or line) is presented as part of different figures. For example, the same light-dark edge could be the left side of a dark square or the right side of a light square (Figure 5). More than a half of V2 neurons modulate their firing rate by border ownership, while less than one-fifth of V1 cells are sensitive to border ownership (Zhou, Friedman, & von der Heydt, 2000; Zhaoping, 2005). This information has an important role in the emergence of object recognition as it would be used in later stages on the processing to separate object from background (Orban, 2008).

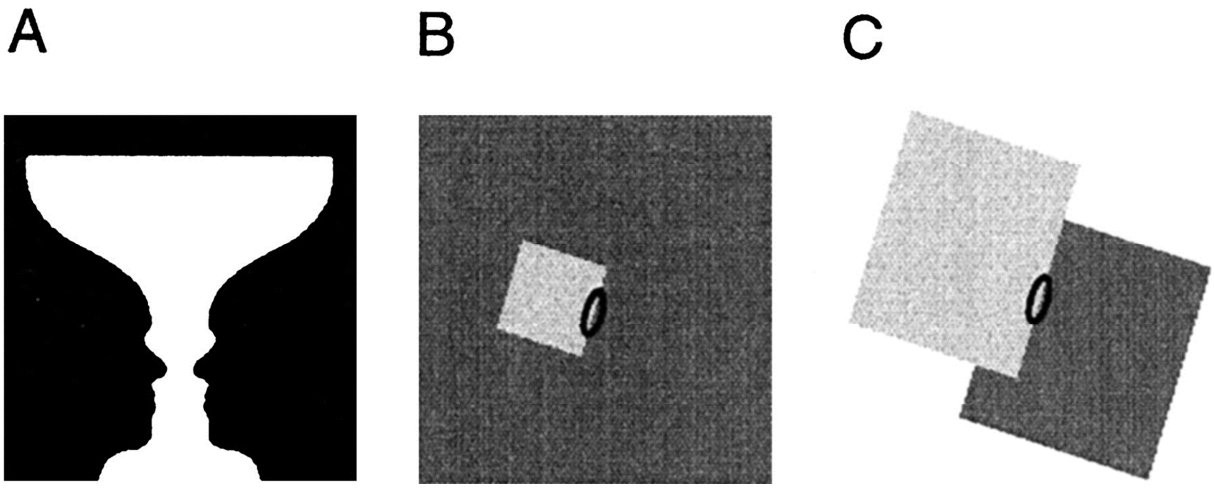

Figure 5. Perception of border ownership. A. *This ambiguous stimulus known as Rubin's vase illustrates the tendency of the visual system to interpret contrast borders as occluding contours and to assign them to one of the adjacent regions. In this example, figure-ground cues have been carefully balanced; however, the black and white regions are generally not perceived as adjacent; instead, perception switches back and forth, and the borders belong either to the vase or to the faces.* ***B****. Isolated patches of contrast are generally perceived as "figures" (i.e., visual objects seen against a background).* ***C****. Display which is generally perceived as two overlapping rectangles rather than a rectangle adjacent to an L-shaped object (From Zhou et al., 2000).*

Many neurons in V2 are also *end-stopped*. They respond strongly to short bars, lines or edges, while their response to long stimuli is reduced (Peterhans & von der Heydt, 1993). Moreover, monkey V2 neurons respond stronger to fairly complex geometric forms than to simple oriented bars or sinusoidal gratings (i.e. the preferred stimuli in V1). Most effective stimuli in V2 include polar gratings, circles, arcs, angles and intersections (Hegdé & Van Essen, 2000; Hegdé & Van Essen, 2003).

Neurons in area V2 have also a remarkable property which is more related to subjective perception than to the physical stimulus properties. They respond explicitly to both real and illusory edges (von der Heydt, Peterhans, & Baumgartner, 1984; Seghier & Vuilleumier, 2006). When the stimuli are modified in such a manner that subjective perception of illusory contours is weakened, V2 neurons also reduce their neuronal responses. In contrast, early single-unit studies have shown that cells in area V1 are apparently unable to *see* these nonexistent contours (von der Heydt et al., 1984). However, new evidence shows that these

responses can be also found in V1 (Seghier & Vuilleumier, 2006; Schmid, 2008; Zhan & Baker, 2008).

e) Ventral and dorsal visual pathways

It has been proposed that beyond area V2 visual information is divided in two pathways: the ventral and the dorsal visual pathways. Experiments in monkeys revealed selective impairments following lesions in the occipitoparietal and occipitotemporal visual cortices suggesting that temporal areas are relatively specialized in object recognition, whereas parietal areas would be specialized in carrying out spatial localization of stimuli, sensing of motion and visual guidance of motor actions (Mishkin & Ungerleider, 1982; Ungerleider and Mishkin 1982 ; reviewed in Mishkin, Ungerleider, & Macko, 1983 ; and Goodale and Milner 1992).

Anatomically, the dorsal pathway extends along the occipito-parietal and parietal cortices, while the ventral pathway includes the occipito-temporal and inferotemporal cortices (see Figure 6).

Clinical evidence for the ventral and dorsal pathways model has been found also in humans. Lesions in temporal regions have been associated with impairments in recognition of objects (such as faces and animals) and the inability to perceive colors; while lesions in the parietal cortex causes failures in perceiving movement, visuo-motor disorders and hemineglect—i.e., incapacity to notice objects in one side of the visual field—(Newcombe, Ratcliff, & Damasio, 1987; Warrington, 1982; Postma, Sterken, de Vries, & de Haan, 2000; Rizzolatti & Berti, 1990). Functional dissociation between these two pathways in humans has been also supported by functional neuroimaging studies in normal subjects (see for instance Ungerleider & Haxby, 1994).

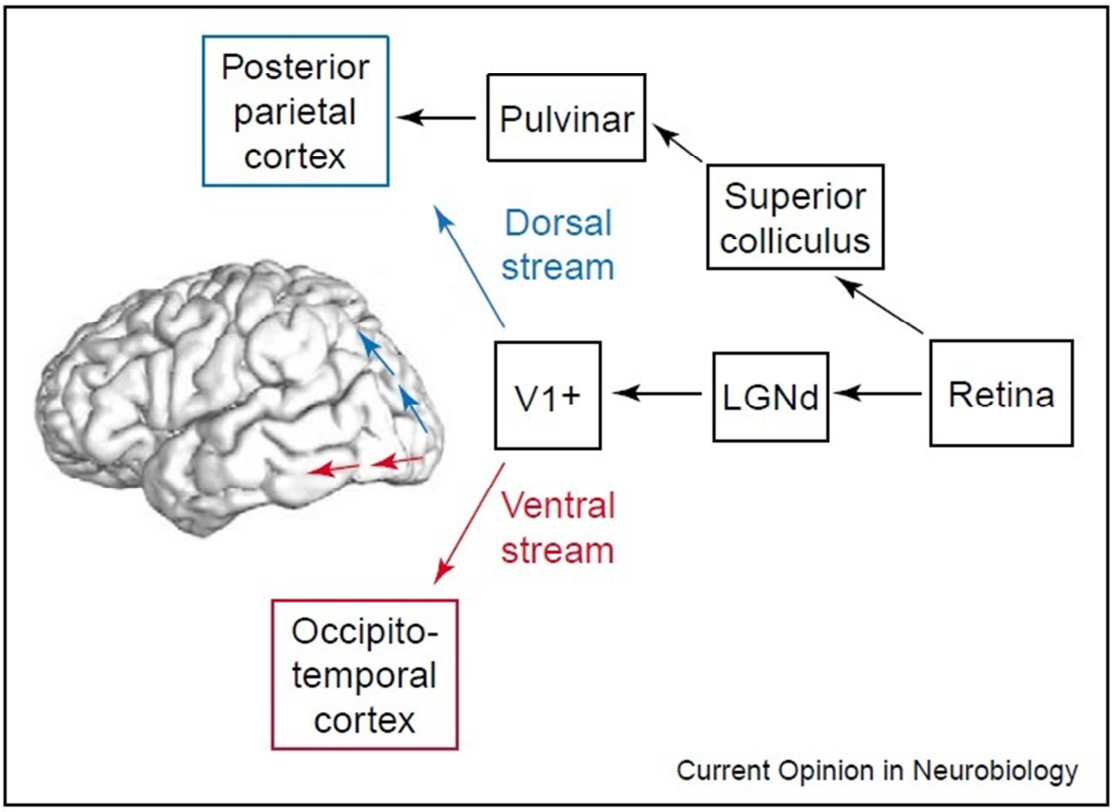

Figure 6. Schematic representation of the two streams of visual processing in human cerebral cortex. *The dorsal part of the lateral geniculate nucleus in the thalamus (LGNd) receives afferences from retina. The LGN projects mostly to primary visual cortex (V1). Within the cerebral cortex, the ventral stream (red) arises from early visual areas (labeled in the figure as V1+) and projects to regions in the occipito-temporal cortex. The dorsal stream (blue) also arises from early visual areas but projects instead to the posterior parietal cortex. The posterior parietal cortex also receives visual input from the superior colliculus through the pulvinar (Modified from (Melvyn A Goodale & Westwood, 2004).*

Although the two-stream idea has served as a useful scheme with which to understand the organization of the visual system, it is an oversimplification in several ways. For instance, some areas in the dorsal pathway exhibit selectivity for simple, two-dimensional geometric shapes that are comparable to those observed in the ventral pathway (Sereno & Maunsell, 1998); even though shape distinctions are finer in temporal structures belonging to the ventral pathway than in parietal areas (Lehky & Sereno, 2007). In any case, under an anatomical point of view, temporal and parietal areas exhibit a dense pattern of

interconnection (Baizer, Ungerleider, & Desimone, 1991), which suggests a high-degree of functional interaction between both visual pathways. Furthermore, recent evidence shows that functional dissociations may be less pure than previously suggested (see for example Farivar, 2009; Goodale & Westwood, 2004).

In the next section we will focus on the ventral pathway in order to explore the neural basis of object recognition.

f) The ventral visual pathway and object recognition

The ventral pathway in monkeys includes occipital and temporal visual areas such as V1, V2, V4 and the inferotemporal cortex IT (Desimone & Ungerleider, 1989). The different cortical areas in the ventral pathway contain populations of cells sensitive to shape, color, and/or texture. While progressing in the visual hierarchy, cells have larger receptive fields and tend to be selective to more complex stimuli (Enns, 2004). For instance, while most of V1 neurons serve as local spatial filters, signaling the presence of contours at particular positions and orientations in the visual field, as we have seen in Section c; an increasingly higher proportion of cells in higher areas (e.g., V2 and beyond) respond to illusory contours (as we have seen in Section D), across increasingly larger regions of the visual field. This integration of features would lead to the representation of complex object features representations at the higher steps of the ventral pathway (Grill-Spector, 2003; Blumberg & Kreiman, 2010), which would be coded explicitly by neural populations within the ventral pathway (Tanaka, 2003).

The selectivity for forms and complex object features in areas V4 and IT has been intensely studied in monkeys thanks to electrophysiological recordings. Neurons in area V4 are selective to 2D and 3D shapes (Desimone & Schein, 1987; Gallant, Braun, and Van Essen 1993; Hegdé & Van Essen, 2005; Hegdé & Van Essen, 2006). Compared to V2 cells, area V4 neurons respond more strongly to more complex geometrical patterns (Hegdé & Van Essen, 2007). Lesion studies in monkey have revealed that V4 is important for shape discrimination, recognition and for generalization (Schiller & Lee, 1991; Schiller, 1995). In humans, area V4v has been proposed as the homologous of area V4 in monkeys. It has been suggested that

area V4 would serve to code visual representations of intermediate complexity which would be completed by inferotemporal areas where more complex object features are coded (Pasupathy & Connor, 1999; Schiller, 1995).

Area V4 projects primarily to the inferotemporal cortex (IT) (Desimone, Fleming, & Gross, 1980; Baizer et al., 1991; Felleman and Van Essen 1991). Area IT is subdivided in posterior (PIT), central (CIT), and anterior (AIT) regions. In area IT one can find the neurons with the greatest object selectivity. Several studies revealed that some IT neurons are activated by several objects categories such as faces, flowers and hands, but are poorly activated by simple stimuli or scrambled versions of objects (Gross, Rocha-Miranda, & Bender, 1972; Desimone, Albright, Gross, & Bruce, 1984; Young & Yamane, 1992; reviewed by Logothetis & Sheinberg, 1996). These areas can be also activated by synthetic objects (i.e., non-natural stimuli) that are learned during intensive training (N K Logothetis, Pauls, & Poggio, 1995). In a series of studies using a systematic method to reduce stimulus complexity, it was shown that AIT neurons coding for related object features are organized in a column-like pattern (Fujita, Tanaka, Ito, & Cheng, 1992; Kobatake & Tanaka, 1994; Tanaka, 1996; Tsunoda, Yamane, Nishizaki, & Tanifuji, 2001; Tanaka, 2003) Figure 7.

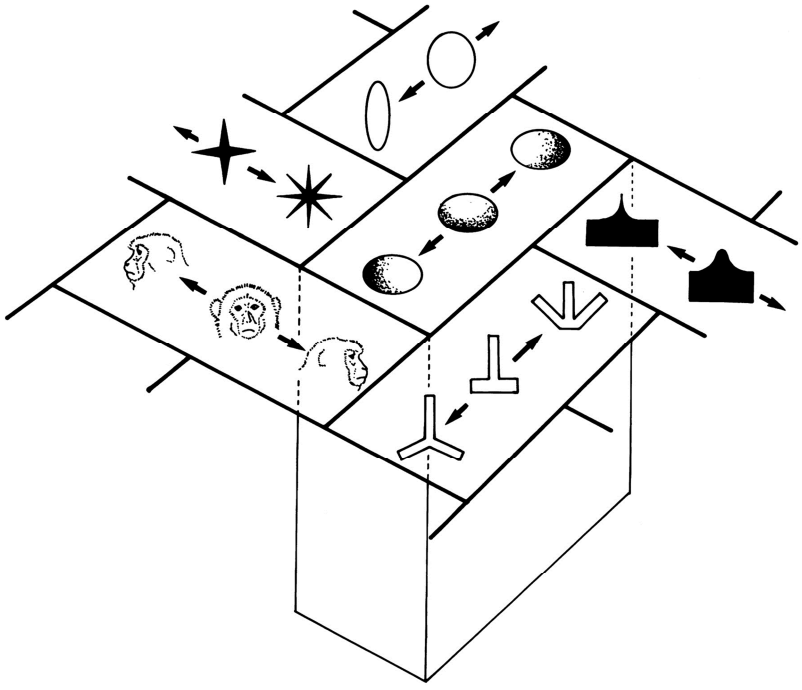

Figure 7. Schematic diagram of the columnar organization in TE*. Similar object features are thought to be grouped in adjacent columns. (From Tanaka, 2003).*

In the human brain, visual areas within the ventral pathway that show preferent responses to a group of object categories have also been identified. Using fMRI, regions responding more to objects than to scrambled stimuli were found in the lateral occipital complex (LOC), (Malach et al., 1995). Brain areas specialized for faces, the fusiform face area (FFA) (Puce, Allison, Gore, & McCarthy, 1995); (Kanwisher, McDermott, & Chun, 1997), and scenes, the parahypocampal place area (PPA) (Epstein, Harris, Stanley, & Kanwisher, 1999) have been also found.

A good deal of homology between different visual areas between monkeys and humans has been established as illustrated in Figure 8 (Denys et al., 2004 ; Orban, Van Essen, & Vanduffel, 2004; Pinsk et al., 2009; Nasr et al., 2011). The ventral surface of the human brain, extending from around the occipito-temporal border to the middle part of the temporal cortex (LO area), has been designated as the human homologue of the monkey inferotemporal cortex IT, Figure 8 (Tanaka, 1997; Orban et al., 2004). Activations around the occipito-temporal border are generally driven by complex object images without selectivity to a particular class of objects (Haxby et al., 1991; Tootell, Dale, Sereno, & Malach, 1996; Nancy Kanwisher, Woods, Iacoboni, & Mazziotta, 1997). In the middle part of the temporal cortex, some regions are activated more significantly by faces (Puce et al., 1995; Kanwisher et al., 1997) whereas other regions are more activated by non-face objects (Malach et al., 1995; Grill-Spector, 2003). The presence of regions activated specifically by letter strings has also been suggested (Puce, Allison, Asgari, Gore, & McCarthy, 1996; Borowsky, Esopenko, Cummine, & Sarty, 2007), however its actual existence is still debated (see for example Price & Devlin, 2003). It has been proposed that the functional modularity seen in the visual brain has probably evolved as a result of the differential characteristics of visual images of different object classes which led to the functional specialization of particular visual areas (Tanaka, 1997).

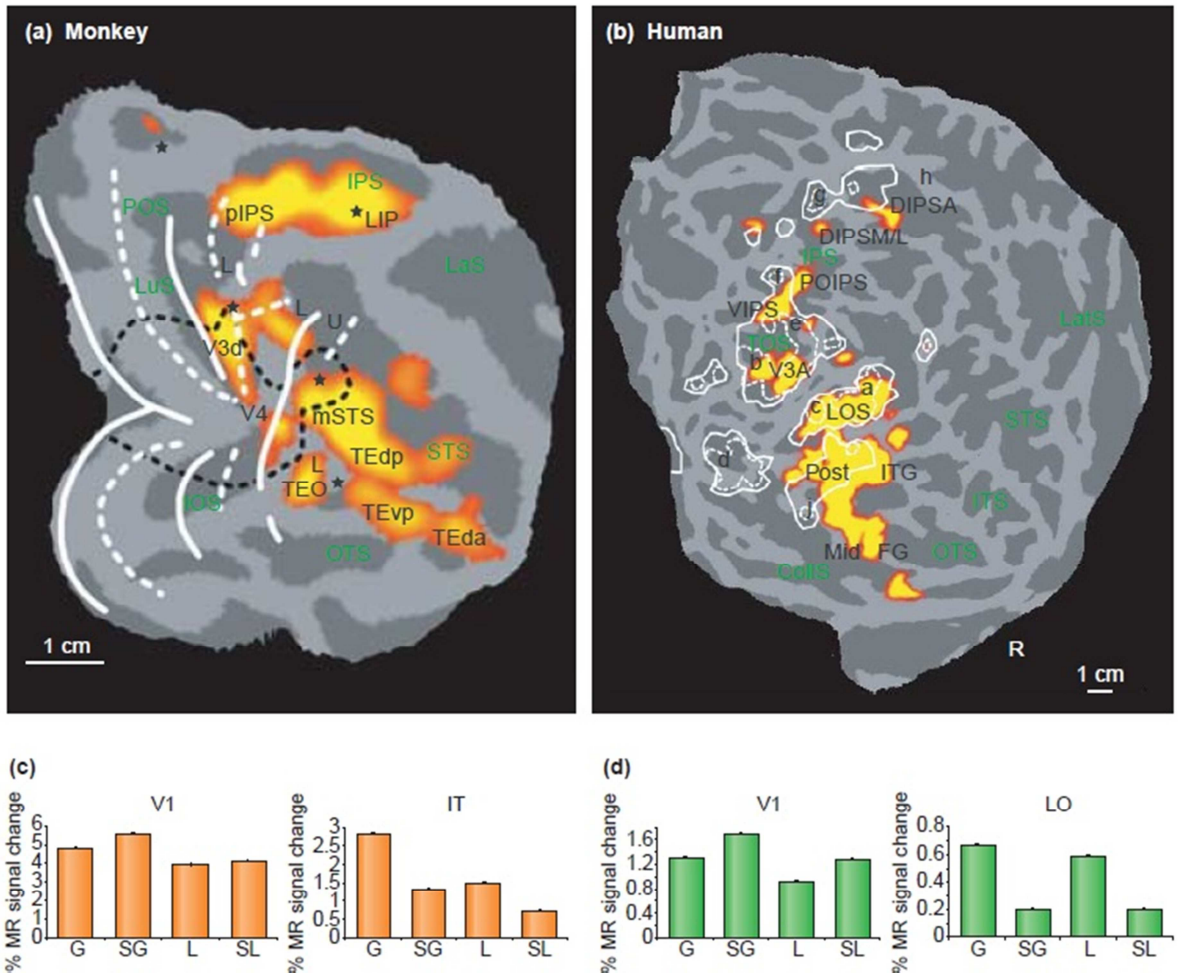

Figure 8. Object-related activation in human and monkey. *Flattened brain surfaces showing visual areas from V1 (left border) to more anterior areas (right border).* ***A.*** *Zones showing larger activity for viewing intact images of objects compared with viewing scrambled images in monkey* ***B*** *Zones showing larger activity for viewing intact images of objects compared with viewing scrambled images in humans.* ***(C and D) Activity profiles plotting percentage MR signal change compared with fixation baseline.*** *(G) Represents comparison with intact greyscale images; (SG): scrambled greyscale images; (L): intact drawings; (SL) scrambled drawings of objects. Note the similar activation profile of areas IT in monkeys and LO in humans (Modified from Orban et al., 2004).*

Beyond the ventral pathway we can find neurons that seem to be selective to single items. Single unit recordings in epileptic human patients implanted with electrodes for clinical reasons have revealed single neurons responding selectively to pictures (and also to the written name) of celebrities (e.g., politicians and actors) and landmarks (Quiroga, Reddy, Kreiman, Koch, & Fried, 2005; Kreiman, Koch, & Fried, 2000; reviewed in Quiroga et al. 2008). These neurons have been recorded in the medial temporal lobe (MTL) a multimodal

area which receives massive inputs from the ventral pathway (Lavenex & Amaral, 2000; Suzuki 1996; Saleem & Tanaka, 1996). Specifically, these neurons have been found in the parahippocampal complex (PHC) which involves structures such as hippocampus, amygdala, entorhinal cortex, parahippocampal cortex and perirhinal cortex. These areas are thought to maintain a memory of task-related information such as the identity or category of a target (Miyashita & Hayashi, 2000; Suzuki, 1996; Suzuki, 1999).

g) Visual hierarchy in perspective

There are several hallmarks of the hierarchic functional organization in the visual cortex. First, anatomically speaking, visual projections show convergence from a stage to another, which is associated with the integration of information at both the spatial and the feature level (Rust & Dicarlo, 2010). Monkey area V1 contains ~$190 \cdot 10^6$ neurons whereof ~$37 \cdot 10^6$ would project to the next area, while area AIT contains ~$16 \cdot 10^6$ neurons whereof ~$10 \cdot 10^6$ would send projections (Collins, Airey, Young, Leitch, & Kaas, 2010; O'Kusky & Colonnier, 1982). Convergence leads to an increase of the size of receptive fields from V1 (where they are smaller than 1° of visual angle) to IT (where they can include the entire visual field).

Functionally, neurons along the ventral pathway respond to more complex features as one ascends the hierarchy, as we have seen in the previous sections. However, these selectivities emerge progressively along the visual pathway and different areas can show a high degree of overlapping regarding their preferred stimuli. Indeed, there are commonalities of visual shape representation across different hierarchical levels, from V1 to V4, and they may reflect the replication of neural circuits used in generating complex shape representations at multiple spatial scales (Hegdé & Van Essen, 2007), rendering thus the functional divisions along the visual hierarchy less sharp than previously suggested.

Although median response times to photic stimulation across areas of the ventral stream tends to follow a hierarchical scheme, there is a high degree of temporal overlapping of the neural latencies across areas, as seen in Figure 9 (Schmolesky et al., 1998; Bullier, 2001). For instance, frontal areas which deal with executive functions are activated quite soon (see FEF, Prefrontal and Orbitofrontal, Figure 8B), all of them showing their earliest responses before

100 ms. These early responses seem to violate the premise that visual information is processed serially along the visual pathway, as is predicted by the bottom-up hierarchical theory popularized in the 70' (Marr, 1976). An alternative model (Bar 2003; Bar et al., 2006) proposes a *shortcut* mechanism in which early cortical visual areas or subcortical projections would send coarse, partially analyzed visual information through the magnocellular pathway, to the prefrontal cortex (PFC) (Kveraga, Boshyan, & Bar, 2007). This model conceives that possible interpretations of the crude visual input would be generated in the PFC and then sent back to the inferotemporal cortex (IT) subsequently activating relevant object representations which are then incorporated into the slower, bottom-up process (Fenske, Aminoff, Gronau, & Bar, 2006). This "shortcut" is meant to minimize the amount of object representations required for matching thereby facilitating object recognition.

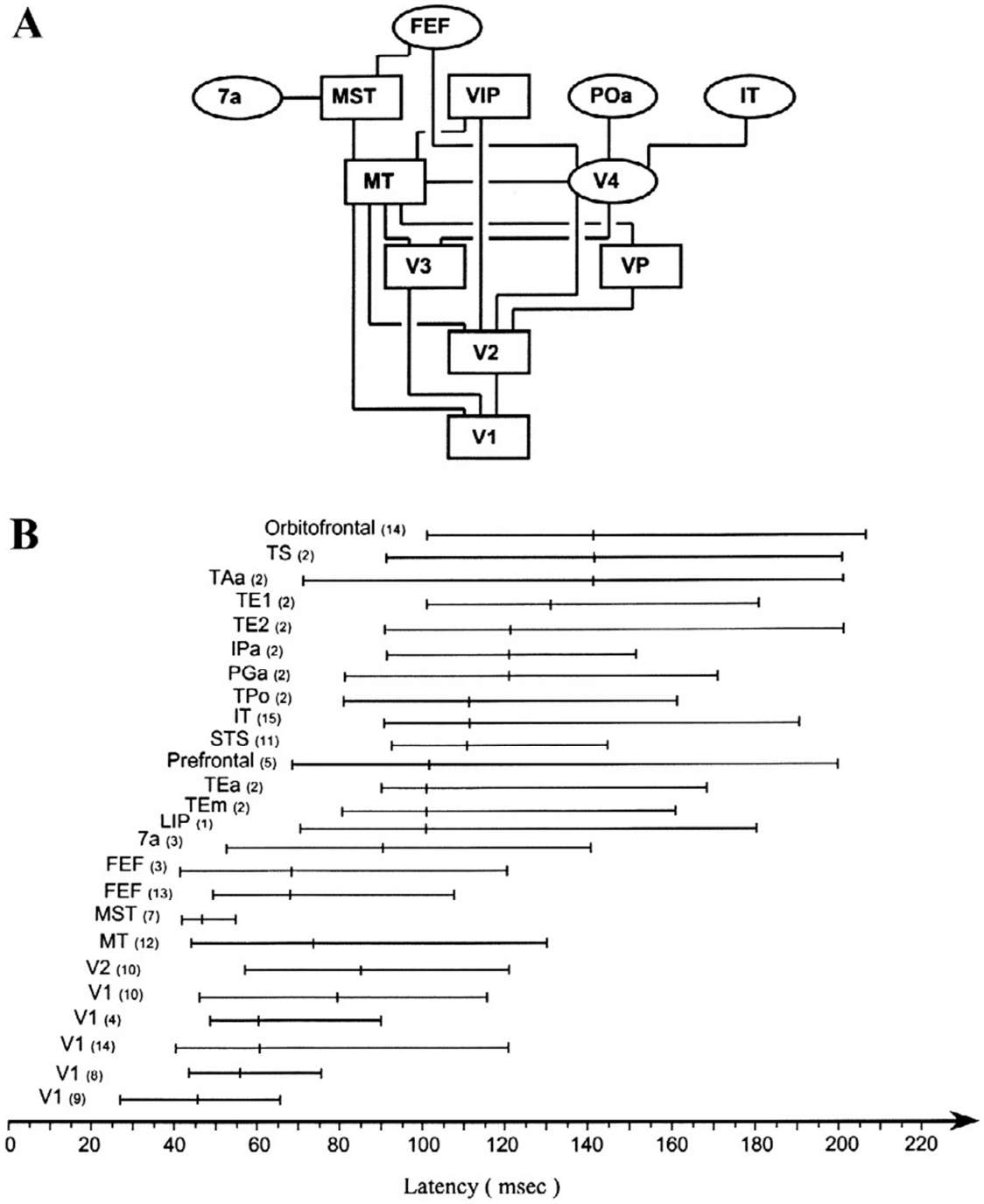

Figure 9. A. Hierarchical organization of cortical areas. *Bullier's model of visual system organization presenting the different cortical areas of the primate visual system arranged according to their feedforward-feedback connection patterns. Areas of low-order stages send feedforward connections to the upper levels whereas high-order areas send feedback connections to areas at a lower level.* ***B. Latencies of visual responses of neurons in different cortical areas.*** *For each area, the central tick marks the median latency and the extreme ticks the 10 and 90% centiles. Note that the shortest latencies do not always correspond to the lowest stages of the hierarchy. In particular, areas MT, MST, FEF have very short latencies despite their being placed at the highest levels of the hierarchy. (From Bullier, 2001).*

Thus, neural processing in the object recognition pathway does not seem to be a simple elaboration of information from lower order to higher order areas. At all stages, the neural connections are reciprocal, such that an area receiving feedforward projections from an area earlier in the ventral stream also provides feedback projections to that area (Spatz, Tigges, & Tigges, 1970; Felleman and Van Essen 1991; Salin & Bullier, 1995; Lamme, Supèr, and Spekreijse 1998; Anderson & Martin, 2009; Anderson & Martin, 2006; Anderson & Martin, 2005). Long-range nonreciprocal connections, such as from temporal areas back to V1, also exist (Kennedy & Bullier, 1985; Rockland & Van Hoesen, 1994; Rockland & Drash, 1996), and reversible inactivation of these connections can affect receptive field characteristics in V1 neurons (Huang, Wang, & Dreher, 2007). The role of feedforward excitatory projections is to provide bottom-up, sensory-driven inputs to subsequent visual areas, driving their responses (i.e., triggering action potentials in target neural populations), while feedback projections would not drive neural responses directly but would modulate their ongoing activity (Crick and Koch 1998; Sherman & Guillery, 1998). Functional properties of feedback are not yet fully understood. However, some functions of feedback connections are relatively well established, for instance feedback among early visual areas play a role in figure/ground segregation (Hupé et al., 1998; Roelfsema, Lamme, Spekreijse, & Bosch, 2002; Scholte, Jolij, Fahrenfort, & Lamme, 2008; Likova & Tyler, 2008) and selection of attentded objects by top-down attention (Neggers et al., 2007; Rossi, Pessoa, Desimone, & Ungerleider, 2009; Soltani & Koch, 2010).

All areas within the ventral stream also are heavily interconnected with subcortical structures, notably the pulvinar, claustrum, and basal ganglia (Spatz et al., 1970; Wong-Riley, 1977; Wong-Riley, 1978), which connections allowing visual information to travel back and forth from visual cortex to subcortical structures. In addition, each ventral stream area also receives subcortical modulatory inputs from ascending cholinergic projections from the basal forebrain, and ascending noradrenergic projections from the locus coeruleus (Tomycz & Friedlander, 2011). These projections are thought to play a role in the storage of information in the cortex, and the influence of arousal on information processing, respectively (Solari & Stoner, 2011).

All in all, these evidences denote that visual processing would be actually more complex than the strict hierarchic visual models propose. Nevertheless, hierarchical models of visual processing, although failing in describe the visual system in all its overwhelming complexity, have the advantage of serving of schematic frameworks allowing to explain certain visual functions with an elegant simplicity. In the next section we will briefly review the feedforward model of object categorization representing one of such hierarchic visual models.

h) Feedforward model of object categorization

How fast can a visual object be categorized? The categorization of complex visual images into semantic categories (i.e., animals, transport means, faces) challenges the visual system to group together visual objects that share some common properties despite their sometimes huge physical differences. Such a process is indeed performed quite efficiently by primates (humans, baboons and macaques) both rapidly and accurately (Thorpe, Fize, and Marlot 1996; Fabre-Thorpe, Richard, and Thorpe 1998; Martin-Malivel & Fagot, 2001).

By forcing the subject to respond as quickly as possible it has been thus possible to estimate a floor processing time to complete all the steps from sensory stimulation, through activation of relevant neural representations to decision making. In fact, this time is surprisingly short as was showed by a pioneer study in humans (Thorpe, Fize, and Marlot 1996). In this experiment, the subject had to perform a go/no-go categorization task deciding in each trial whether a briefly flashed natural image did or not contain an animal by releasing a button (go-response) when an animal was present on the screen. The fastest behavioral responses were registered under 300 ms after the stimulus onset, while the earliest differences between the ERPs waveforms of animals and non-animals were as early as 150 ms. This result settled a quite constraining temporal limit to visual object recognition models, suggesting that visual object categorization can be done within the fast feedforward sweep.

These results have been subsequently replicated showing minimum manual (go/no-go task) reaction times around 250 ms for humans (Fabre-Thorpe et al. 2001; Rousselet, Fabre-

Thorpe, & Thorpe, 2002; Rousselet, Macé, & Fabre-Thorpe, 2003) and, surprisingly, even more rapidly in monkeys that showed minimum reaction times around 180 ms (Fabre-Thorpe, Richard, and Thorpe 1998; Delorme, Richard, and Fabre-Thorpe 2000). The use of two images, one target and one distractor, flashed at the same time did not lengthen minimum reaction times, showing that this task can be performed, at least in some degree, in parallel (Rousselet et al., 2002).

Shortly after, using the same setup but this time measuring saccadic reaction times, it was shown that behavioral responses, in the form of a saccade to the animal target (saccadic choice task), could be registered even earlier, with the faster reaction times found at 120 ms after stimulus onset in humans (Kirchner & Thorpe, 2006) and 100 ms in monkeys (Girard, Jouffrais, & Kirchner, 2008). The shorter reaction times recorded in macaques are explained by the fact that conduction delays would be shorter because of the smaller size of their heads. Interestingly, saccadic reaction times toward faces are even faster, could be initiated as shortly as 100-110 ms after stimulus presentation in human subjects (S. M. Crouzet, Kirchner, & Thorpe, 2010). Intriguingly, it appears that these very fast saccades are not completely under instructional control, because when faces were paired with photographs of vehicles, fast saccades were still biased toward faces even when the subject was targeting vehicles.

Two hypotheses have been advanced to explain the fact that visual information can be processed and used by the motor system at such short latencies (Figure 10).

The first hypothesis, which explains go/no-go task involving manual responses with median reaction times around 250 ms (and 180 ms for minimal reaction times) recorded in monkeys, implies that the information must travel along the ventral pathway from V1 to the temporal structures and from them to prefrontal areas where motor responses are generated (Figure 10a). In this model (Thorpe & Fabre-Thorpe, 2001), selective responses to single objects generated at the end of the ventral stream in inferior temporal (IT) neurons (Tanaka, 1996; Booth & Rolls, 1998) would be sent to the prefrontal cortex (PFC). In these areas responses of IT neurons would be more related to features present in the stimulus (i.e., object based), while responses in the PFC would be more correlated with categorical decisions (i.e., decision based), regardless of the detailed physical features contained in the stimulus

(Freedman, Riesenhuber, Poggio, & Miller, 2001; Freedman, Riesenhuber, Poggio, & Miller, 2002; Freedman, Riesenhuber, Poggio, & Miller, 2003). Thus, activity in the PFC would trigger motor responses by activating pre-motor and motor areas (Figure 10a). Taking into account all the stages necessary to process the visual input and trigger the motor responses, manual reaction times around 200 ms severely constrain the neural mechanisms involved in such process. Taking into account the minimum and median latencies (Figure 10a, first and second number showed next to each area respectively) across the ventral visual pathway in addition to those seen in the frontal and motor cortices, there is little room for feedback processing to occur. This hypothesis thus constrains the visual processing to one spike per area along the hierarchy, thus precluding any possibility of feedback (Thorpe & Fabre-Thorpe, 2001; VanRullen & Thorpe, 2002; Guyonneau, Vanrullen, & Thorpe, 2004; Guyonneau, VanRullen, & Thorpe, 2005; VanRullen, Guyonneau, & Thorpe, 2005); Fabre-Thorpe, 2011).

The second hypothesis, which accounts for the saccadic choice task with faster minimum reaction times around 100 ms (Figure 10b), states that occulomotor areas (such as FEF and the superior colliculus) would trigger the saccadic categorical responses by accumulating evidence (i.e., presence or absence of a given category of stimulus within the picture) based on the information delivered by low- and mid-level ventral visual areas (Kirchner & Thorpe, 2006). This hypothesis was formulated considering the latencies in the ventral visual pathway aiming conciliating such short latencies with the comparatively late activations of the areas at the end of the ventral pathway (Figure 10b). The earliest and average latencies in areas at the end of the ventral stream (i.e., AIT: 80 and 100 ms respectively), suggest that the visual information cannot be processed until the last stages in the ventral hierarchy in order to trigger saccadic responses with latencies as fast as 100 ms after stimulus onset (Kirchner & Thorpe, 2006; Girard et al., 2008; Crouzet et al., 2010). The saccadic responses would thus be generated based on mid-level visual representations encoded not further than V4 (Kirchner & Thorpe, 2006). Thus the visual information would take a shortcut in the visual hierarchy, from V4 to the superior colliculus for instance, before being processed serially by all ventral visual areas up to IT. This is proposed since such saccadic short latencies do not seem to leave enough time for even a single feed-forward pass through the ventral stream (Kirchner & Thorpe, 2006; Crouzet & Thorpe, 2011).

Experiments using double tasks have shown that rapid visual categorization can be performed in near absence of attention (Li, VanRullen, Koch, & Perona, 2002; Reddy, Reddy, & Koch, 2006). In these experiments, a demanding discrimination task (discriminate randomly rotated Ts and Ls) is performed at fixation, while complex images containing objects are flashed in periphery. At the end of the trial, the subject has to respond to the central task (presence of a T) where her attention was engaged and perform a forced choice task related to the presence or not of an animal in the peripherally flashed image. Results show that both animal/non-animal and face gender categorizations are performed quite well under little presence of spatial attention in these dual-task setups. These results support the idea that visual categorization can be made pre-attentively, in an automatic fashion, presumably away from conscious control.

Furthermore, a study on patients affected by visual agnosia (a deficit on the perception of visual objects produced by a damage in ventral visual areas) showed that rapid visual categorization is performed accurately even though the subject is largely unaware of the identity of objects (Boucart, Moroni, Despretz, Pasquier, & Fabre-Thorpe, 2010). In this study, one patient suffering from posterior cortical atrophy which led to an object agnosia was tested in a go/no-go forced choice task. The patient was able to perform superordinate categorization of animal pictures versus distractors (landscapes, food, inanimate objects), as well as human faces versus animal faces with a performance well above chance ranging between 70 and 86% respectively, even though this patient could not recognize her own face! However, categorization at the basic level (dog versus animals) was performed at chance. This supports the idea that rapid visual categorization at the superordinate level could be performed based on incomplete representations of stimuli, probably relying solely on distinctive features among categories but not on complete object representations nor overt recognition. Interestingly, when these distinctive features are relatively similar (categorization at the basic level, such as in the dog versus animal task) the categorization process seems to need more refined visual representations, which would not be available in the case of the agnostic patient discussed above.

All in all, these results suggest that visual categorization, even though it is a fairly high-level cognitive task, could be made remarkably efficiently without the need for awareness. Attentive processes, which seem largely irrelevant for rapid-visual categorization, are

perhaps the key to higher level processes and ultimately the key to consciousness. In the next section we will briefly review the huge literature on visual attention and trying to emphasize its role in visual perception and ultimately in the access to conscious representations of the visual wolrd.

A. Go/no-go task categorization model

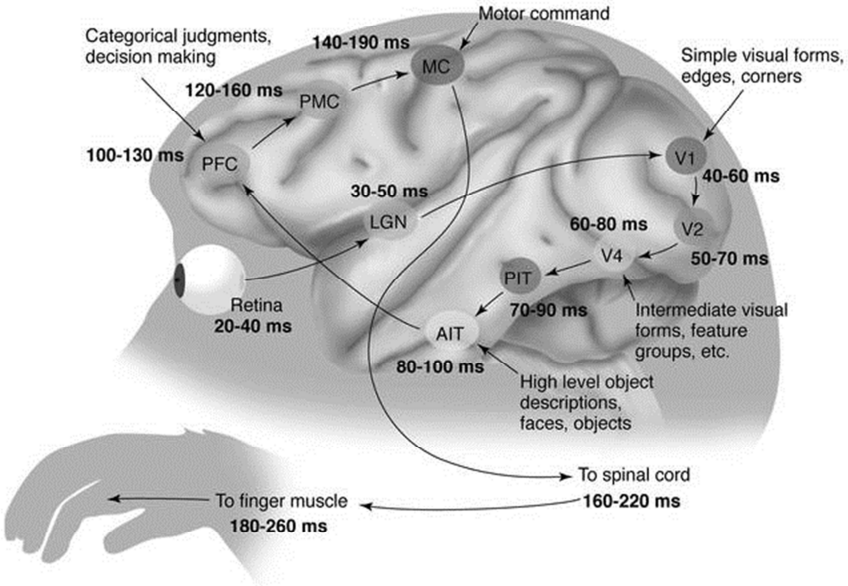

B. Saccadic task categorization model

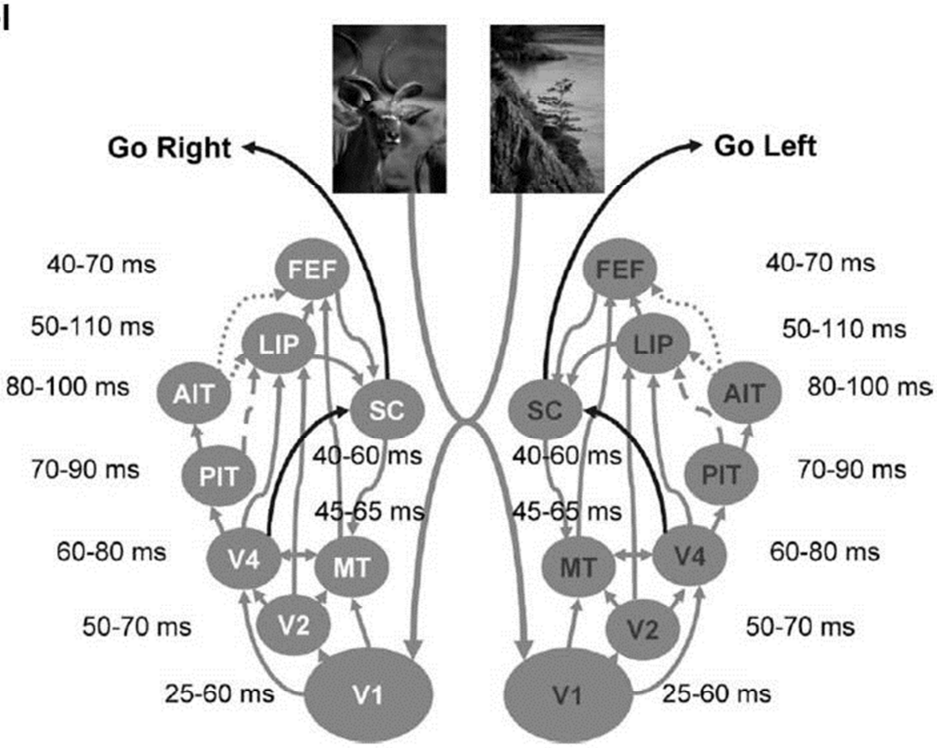

Figure 10. Go/no-go and saccadic categorization models. *Two different models have been proposed in order to account for categorization reaction times obtained with two different response paradigms.* ***A. Go/no-go task categorization model.*** *This model was proposed in order to account manual reaction times around 200 ms and involves a feedfoward pass from lower (V1) to higher (AIT) visual cortices which would activate the PFC which in turn triggers the manual response. The neuronal latencies recorded in these areas preclude the involvement of feedback iteration within this process.* ***B. Saccadic task categorization model.*** *This model was proposed in order to account saccadic reaction times around 100 ms and involves a partial processing of visual information within the ventral stream, with a putative role of V4 and lower areas in sending evidence to visuomotor areas such as the FEF and superior colliculus which would accumulate this evidence in order to decide of the presence of a given category in the stimulus. Dotted and dashed arrows denote connections that are either insignificant or absent. (Modified from Thorpe & Fabre-Thorpe, 2001 and Kirchner & Thorpe, 2006).*

III. Visual attention

a) Selective processing of sensory information

The experience of vision feels like a faithful representation of the external physical reality. At first sight, the visual world seems to be completely accessible and in a glimpse, that is, we often have the impression that we are aware of all that we look at; but it is only an illusion. The truth is that our visual system selects only a part of the available information to process it preferentially, neglecting the rest, which is apparently relegated to beneath the screen of consciousness. This selection process is what we known as *attention*. This fact is illustrated in a very compelling fashion by the *change blindness* phenomenon, where conspicuous changes between two scenes can be totally missed (even during minutes!), as illustrated in Figure 11 (Rensink, O'Regan, & Clark, 1997; Ronald A Rensink, 2002; Simons, Franconeri, & Reimer, 2000).

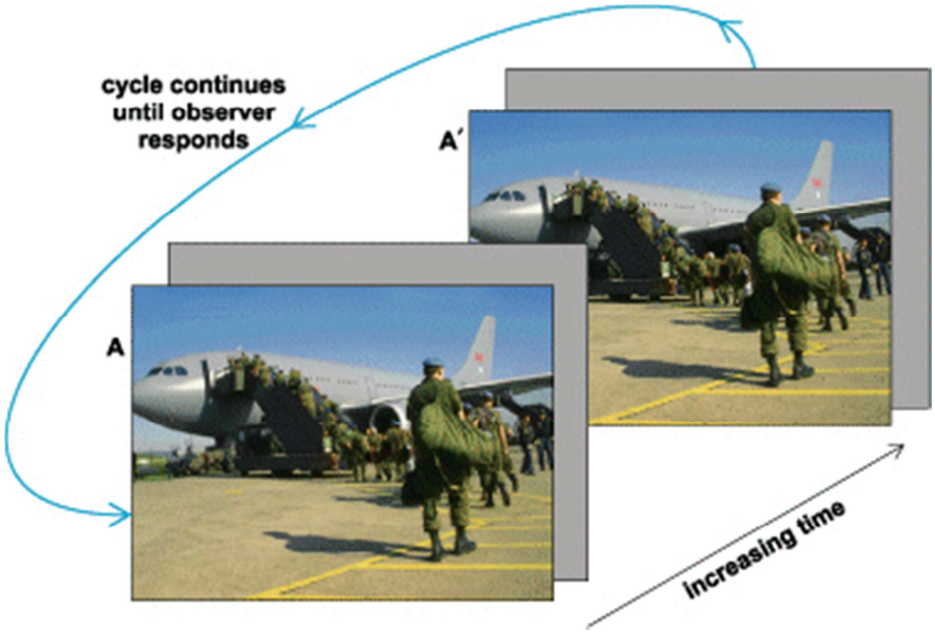

Figure 11. Change blindness. *The observer views a continuous cycling of images between original picture A and altered picture A'. A blank screen appears between both images avoiding that changes would detected as a pop-out effect. Each picture frame is presented during about a half second, while the blank screen is showed during about 200ms. The images alternate until the observer sees the change. In this example, the change is the appearance and disappearance of the airplane engine.(Modified from Rensink, 2005).*

This phenomenon denotes the inability to consciously access visual information which is not directly attended. This compelling phenomenon has been taken as an argument for the idea that the perceived richness of our visual world is only an illusion resulting from a constructive process in our minds which is aimed to mask (or counterbalance) the relatively sparseness of our actual sensorial perception (Blackmore, Brelstaff, Nelson, & Trościanko, 1995; Blackmore, 2005).

Another phenomenon which is closely related to change blindness is inattentional blindness (Neisser & Becklen, 1975; Mack & Rock, 1998; Simons & Chabris, 1999; Most et al., 2001). This phenomenon consists in the failure to experience a conspicuous object or event when the observer is engaged in an attentionally-demanding task elsewhere, and does not expect the object or event. This is exploited by the illusionists in the presentation of "magic shows" in the performance of some tricks by focusing the audience's attention upon some distracting element, away from elements of the scene under manipulation by the performer, which is called misdirection by magicians. In many ways, both inattentional and change blindness are similar. However, inattentional blindness is concerned with first-order information—the presence of quantities—while change blindness involves second-order information—the transitions between quantities (Rensink, 2000). The two therefore refer to somewhat different aspects of the visual world, with somewhat different mechanisms likely involved in each; however they illustrate compellingly the idea that visual awareness would strongly dependent on visual attention (Rensink, 2000; Mack & Rock, 1998; Simons & Chabris, 1999; Simons & Rensink, 2003).

At this point, a fundamental question naturally arises: why does a massively parallel system such as the brain need attention to select information in the first place? We can distinguish two different schools which propose two different explanations about the need for attention in the visual system. The first school alludes to an intrinsic processing capacity limit of the perceptual system, which was mainly inspired by making the analogy between the visual system and the capacity limited computers (Broadbent, 1987; Ullman 1984; Tsotsos 1997; Sanders, 1997). The second school attributes the need for selection to the unaffordable metabolic cost that would entail the processing of all the available sensory information (Attwell & Laughlin, 2001; Laughlin, 2001; Lennie, 2003; Howarth, Gleeson, & Attwell, 2012).

In any case, the main function of attention is to select sensory information and to allocate perceptual resources in order to process it more efficiently than the remaining information. This selection is manifested as higher perceptual sensibility where attention is deployed, which is measurable behaviorally in different ways, for example as an increase in performance in perceiving selected visual attributes in several dimensions, as we shall see in the next section.

b) Attending to different dimensions of the visual world

Benefits produced by attention can involve qualitative perceptual improvements of attended stimuli such as enhanced contrast sensitivity (Cameron, Tai, & Carrasco, 2002) or improved spatial resolution (Yeshurun & Carrasco, 1999). Furthermore, attention improves performance in detecting or discriminating a target, which are performed faster, more accurately or both (Posner, 1980; Posner, Snyder, & Davidson, 1980).

Attention can select visual information using one of a combination of the following strategies: it can select a region of the visual field, which is known as *spatial attention*, therefore, the zone selected by spatial attention is called the *focus of attention* (Shulman, Remington, & McLean, 1979; Posner, Snyder, and Davidson 1980; Posner 1980; Sagi & Julesz, 1986). Attention can also select a visual attribute, such as color, to focus on objects bearing such attribute regardless of their location, which is known as *feature based attention* (Treisman, 1988; Wolfe, Cave, & Franzel, 1989; Dehaene 1989; Treisman & Sato, 1990). And, finally, attention can also be directed toward groups of features enclosed within discrete objects, which is known as *object based attention* (Duncan, 1993; Vecera & Farah, 1994; Behrmann, Zemel, & Mozer, 1998; Scholl & Pylyshyn, 1999; Driver, Davis, Russell, Turatto, & Freeman, 2001).

In the spatial domain, the most obvious way to orient and deploy attention is to look at the attended location. By doing so, we place the foveal area over the attended object which benefits from the higher visual acuity at the center of the visual field. This kind of spatial orienting of attention is known as *overt attention*. We can also attend to a region of the visual field, which is different from the foveal area, while keeping fixation elsewhere. This

form of attention spatial orienting is known as *covert attention* (Posner 1980; Wright & Ward, 2008). The differences between these two types of attention orienting were already acknowledged in the seminal works of Hermann von Helmholtz (Helmholtz, 1867). Overt and covert orienting of attention are complementary in everyday life (i.e., think while you play a collective sport as basketball and you pay attention overtly to the ball while you covertly attend to your team mates in order to hide your next move). The spatial deployment of the focus of attention seems to be quite flexible, adapting its spatial properties in order to match the requirements of the task at hand. Several models have been proposed in order to account its spatial properties. In the next section we will briefly review some of these models.

c) Models of spatial attention deployment

Several models have been proposed in order to represent the different spatial properties of the spatial attention deployment over the visual field. Each model elaborates predictions about the size and the form of the focus of attention, as well as the size and distribution of enhancing and inhibitory zones. Spatial attention has been considered as a *spotlight* (Shulman et al., 1979), lightening with a fixed shape, a part of the visual field and moving from object to object in order to render them noticeable. A modification of the spotlight metaphor was later suggested in the *gradient* model (LaBerge & Brown, 1989), which introduces a transition zone between the focus of attention and the periphery. In other models which take another body of evidence into account, spatial attention has been compared to *zoom-lenses* which would be adaptable to the size and spatial frequency of the attended objects (Eriksen & St James, 1986; Shulman & Wilson, 1987). Another account for explaining the spatial properties of visual attention is represented by the *suppressive annulus* (Tombu & Tsotsos, 2008 ; Cutzu & Tsotsos, 2003) derived from the selective tuning model (Tsotsos et al., 1995) in which a inhibitory zone would surround the facilitation zone of attention. These different models, derived from different sets of experimental evidences, seem to be different faces of a same phenomenon, and presumably they actively interact in everyday vision.

d) Two ways to activate attention: endogenous and exogenous

As early as in the 19th century, William James, one of the founders of contemporary psychology, defined two types of attention (James, 1890). On the one hand, we have a type of attention which is reflexive and involuntary, while on the other hand we have another type of attention which is voluntary. We now know these two types of attention as exogenous and endogenous attention (Nakayama & Mackeben, 1989; Cheal & Lyon, 1991; Hein, Rolke, & Ulrich, 2006; Yeshurun, Montagna, & Carrasco, 2008; Chica & Lupiáñez, 2009). Exogenous attention corresponds to an automatic orienting response to a spatial location triggered by abrupt-onset or salient stimuli and is mostly reflexive (i.e., bottom-up) with little contribution from volitional states (Yantis & Jonides, 1990; Giordano, McElree, & Carrasco, 2009). Endogenous attention, on the other hand, corresponds to a voluntary process allowing us to monitor information at a given location at will, being triggered by higher level mechanisms (i.e., top-down) and largely depending on the subject's expectations and knowledge (Yantis & Jonides, 1990; Hopfinger, Buonocore, & Mangun, 2000; Giordano et al., 2009; for reviews on exogenous and endogenous attention see Egeth & Yantis, 1997; Corbetta and Shulman 2002). Exogenous attention is transient, meaning it rises and decays quickly if not stabilized by top-down mechanisms, peaking at about 100–120 ms; whereas endogenous attention is slower, taking around 300 ms to be deployed and it can be sustained as long as necessary to perform the task (Nakayama & Mackeben, 1989; Müller and Rabbitt 1989; Cheal & Lyon, 1991; Cheal, Lyon, & Hubbard, 1991; Remington, Johnston, & Yantis, 1992; Hein et al., 2006; Liu, Stevens, & Carrasco, 2007).

Neural circuits underlying these two forms of spatial orienting of attention are thought to share some neural mechanisms (Corbetta and Shulman 2002; Wright & Ward, 2008). Some areas within a dorsal frontoparietal network would be shared by top-down and stimulus-driven attention (specifically the right frontal eye field and the right intraparietal sulcus), while the ventral frontal cortex and the temporoparietal juntion would be dedicated to stimulus-driven orienting mechanisms (Corbetta & Shulman, 2002).

e) Attention at the neuronal level

As we have seen, the role of visual attention is to select a particular source of visual information among all the available information. Now, the question is: how is this selection implemented at the neuronal level? Several studies have revealed that the firing rate of neurons in several visual areas is actively modulated by attention. Let's consider a monkey V4 neuron which is maximally activated by vertical bars (i.e., preferred stimulus, figure 12, black top line) and poorly activated by horizontal bars (i.e., non-preferred stimulus, figure 12, black bottom line) within its receptive field. When both vertical and horizontal bars are presented together, the intensity of the cell response is intermediate between the preferred and the non-preferred stimulus (dotted line). Now, when attention is deployed over the preferred stimulus while both bars are presented, the response is comparable to the one to the preferred stimulus *alone* (figure 12, top gray line). Said otherwise, the cell seems to ignore the presence of the non-preferred stimulus, thus attention would *filter* the irrelevant stimulus. Conversely, if attention is deployed over the non-preferred stimulus, the response is comparable to the response to the non-preferred stimulus alone; again, attention makes the cell to ignore the unattended stimulus, said otherwise, it filters non-attended stimuli. The effects of attention under these conditions are quite clear: the response of the population is biased towards its normal response to the attended stimulus when it is presented alone. This behavior has been observed in several areas of the monkey visual system from V2 to MT and IT (Moran & Desimone, 1985; Miller, Gochin, & Gross, 1993 ; Rolls & Tovee, 1995; Chelazzi, Miller, Duncan, & Desimone, 1993; Treue & Maunsell, 1996; Luck, Chelazzi, Hillyard, & Desimone, 1997; Reynolds, Chelazzi, & Desimone, 1999; Rolls, Aggelopoulos, & Zheng, 2003).

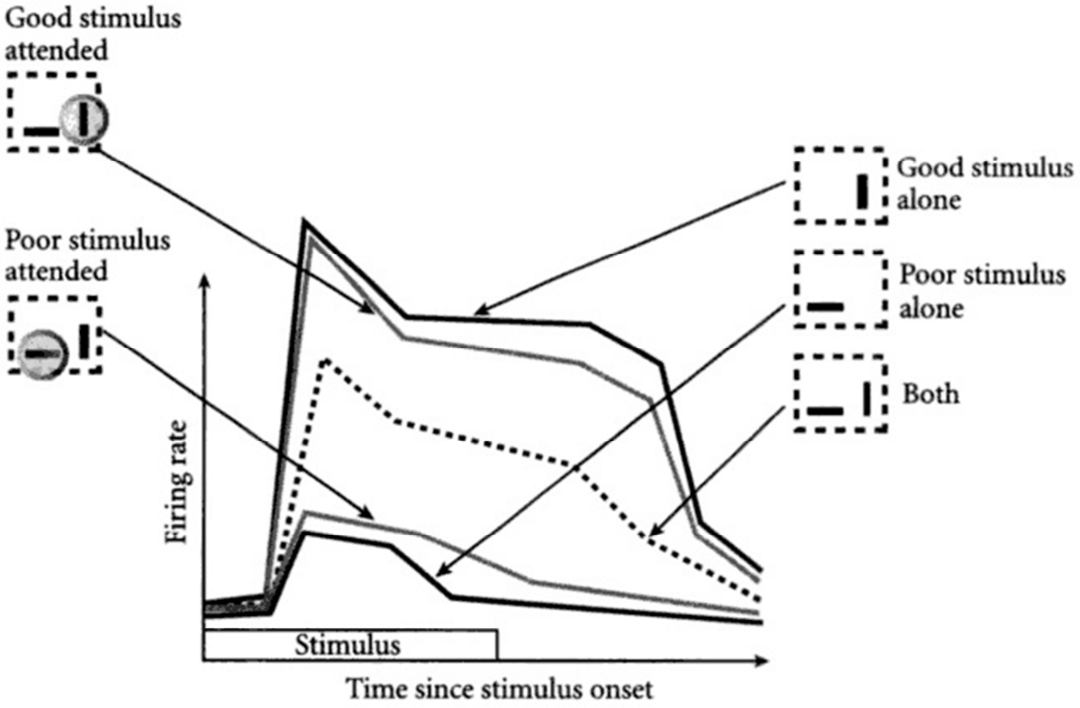

Figure 12. Attention at the neuronal level. *When more than one object is located within the receptive field of a cortical neuron, competitive interactions between both stimuli have been observed. Attention has the role to resolve the competition in favor of the attended item. The responses of a hypothetical V4 cell are shown. The cell responds best to a lone vertical bar of light and poorly to a horizontal one within its receptive field. When attention is directed away from both, the response amplitude to their joint appearance is intermediate between the responses to the individual bars. If attention is focused on the vertical bar, the cell behaves as if the distracting horizontal bar was removed. If attention shifts to the horizontal bar, the neuron fires weakly, as if its trigger feature, the vertical bar, has been filtered out (Modified from (Reynolds & Desimone, 1999).*

f) Attention as a network

Thanks to studies in functional neuroimaging in humans, two functional networks have been proposed to support visual attention: the ventral attention network and the dorsal attention network, which are somehow related to the ventral and dorsal pathways discussed previously.

The ventral attention network detects salient and behaviorally relevant stimuli in the environment, especially when unattended and is thought to support exogenous attention (Arrington, Carr, Mayer, & Rao, 2000; Corbetta, Kincade, Ollinger, McAvoy, & Shulman, 2000; Kincade, Abrams, Astafiev, Shulman, & Corbetta, 2005; Vossel, Thiel, & Fink, 2006). The ventral attention network is lateralized in the right hemisphere and includes regions such as the temporoparietal junction (TPJ) cortex and ventral frontal cortex (VFC).

The dorsal attention network enables the selection of sensory stimuli based on internal goals or expectations (Corbetta and Shulman 2002), thus supporting endogenous attention and links them to appropriate motor responses. Regions included in the dorsal attention network are the intraparietal sulcus (IPS), superior parietal lobule (SPL), and dorsal frontal cortex along the pre-central sulcus, near or at the frontal eye field (FEF) (Kastner, Pinsk, De Weerd, Desimone, & Ungerleider, 1999; Corbetta et al., 2000; Hopfinger et al., 2000).

The damage in the functional interconnectivity between these two networks leads to severe cognitive deficits, often involving visual awareness, such as spatial neglect (He et al. 2007). Neglect patients are unaware of large objects, even people, towards their neglected side of the visual field –which is contralateral to the brain damage (usually after a ventral frontal or temporoparietal stroke). They may eat from only one side of a dish, write on one side of a page, make-up only the non-neglected side of their face. The spatial bias of neglect depends on a physiological imbalance between left and right dorsal parietal cortex (IPS/SPL), which is caused by structural and physiological abnormalities in the ventral attention network (Corbetta & Shulman, 2011). Interestingly, neglect patients seem to lose their capacity to consciously access to the visual contents included in the neglected side of their world. Interestingly, these patients do not notice anything wrong with their perception; the neglected area of their visual field is basically gone, without leaving any trace of its previous existence.

Pathologies such as neglect and phenomena such as inattentional and change blindness highlight the close relationship between attention and consciousness. In the next section we shall concentrate on consciousness and evaluate its putative relationships with attention.

IV. Consciousness

We have briefly reviewed how the visual world is processed by the visual system. We have seen how the *meaning* of the visual information is extracted by different specialized modules in the visual hierarchy. Along the visual processing, visual information can trigger motor responses (such as in ultra-rapid categorization), it can be selected by attention, and eventually enter to consciousness. Which are the mechanisms allowing the access of visual representations into the realm of consciousness? How can we account for the neural activities supporting awareness?

The study of consciousness is the study of the nature of our existence. Differently from other studies that are related to objectively measurable phenomena such as physics, the study of consciousness is aimed to explain the subjective mental world, which involves the scientific challenge of deal and measure subjective inner states in the mind of subjects. Currently, we lack a comprehensive view of how these subjective states emerge from brain activity. In this section we shall briefly review current views regarding this fascinating subject.

a) What is consciousness for?

> *"…Suppose also that the machines have been carefully programmed and fed with great quantity of data of an appropriate kind. The manufacturers are claiming that the devices actually think. Perhaps they are also claiming them to be genuinely intelligent. Or they may go further and make the suggestion that the devices actually feel—pain, happiness, compassion, pride, etc.—and they are aware of, and actually understand what they are doing. Indeed, the claim seems to be being made that they are conscious".* From *'The emperor's new mind'* by Roger Penrose, 1990.

From a cognitive point of view, consciousness is surmised to have substantially different functions from attention. These include summarizing all information that pertains to the current state of the organism and its environment, making this summary available to planning and executive areas of the brain; which would lead, among others, to detect anomalies and errors, decision making, language, inferring the internal state of other animals, setting long-term goals (van Gaal, de Lange, & Cohen, 2012; Bor & Seth, 2012; Shanahan, 2010; Edelman, and Tononi 2000; Butler, 2012).

As we stated at the very beginning of this introduction, consciousness would help to set flexible means of behavior which are pinpointed by the integrative function of consciousness. Thus, cognitive theories relate consciousness to constructive functions, allowing the unification and integration of diverse components in a coherent whole (Bransford, 1979; Baars, 2002; Ward, 2011). This integrative framework would lead to interaction of specialized modules in the brain in an "on-demand" fashion in order to create flexible behaviors to resolve the task at hand (Baars, 1990; Baars, 2005; Shanahan, 2010).

This would probably had a fitness advantage for conscious animals over the non-conscious ones and thus consciousness would has been selected by evolution (Judd, 1910; Fetzer, 2002; Butler, 2008; Shanahan, 2010). However, it is not easy task to demonstrate that consciousness is an adaptation in the strict sense; that is, that it was originally selected for because it increased the fitness of its bearers. In fact, this point is still hotly debated and some authors have considered that consciousness would have no immediate use and it would thus be a mere epiphenomenon, implying that creatures without any conscious sensation would be able to behave indistinguishable from conscious ones (see for instance (Kirk, 1974; Flanagan, 1994; Chalmers, 1996).

My guess is that unless we understand how consciousness *actually works* at the neurobiological level we will hardly be aware of the adaptive advantages related to it.

b) The hard and the easy problem of consciousness

> *"[A lot of writing] addresses the 'easy' problem of consciousness: How does the brain process environmental stimulation? How does it integrate information? How do we produce reports on internals states? These are important questions, but to answer them is not to solve the hard problem: Why is all this processing accompanied by an experienced inner life?"* From "*The conscious mind"* by (Chalmers, 1996).

The mystery of consciousness has many faces. Different explanatory levels have been distinguished and addressed for both philosophic and biological points of views. Here we introduce the so-called hard and easy problems of consciousness.

The hard problem of consciousness can be summarized as follows: Why do physical phenomena occurring in the brain give rise to our subjective experience? There seems to be a dichotomy between physical world (and the laws governing it) and our subjective experiences, which are summarized by the concept of qualia. The concept of qualia (singular quale) comes from philosophy and it is referred to the subjective inner conscious experience in its most fundamental sense. Qualia are related to the conscious feeling associated to any conscious experience, for instance the redness of red or the warm sound of an oboe, which are only accessible by direct experience but are largely ineffable by other means. No matter how hard one tries, it is impossible to communicate the qualia of red—or redness—to a born blind person, neither we can remotely imagine how does it fell to perceive the world by using echolocation as dolphins or bats do—however, there are indeed blind subjects capable to fairly 'navigate' by hearing the echo emitted by the surrounding objects (Schenkman & Nilsson, 2010; Schenkman & Nilsson, 2011; Teng, Puri, & Whitney, 2012).

Several questions about consciousness must be resolved in order to acquire a full understanding about the relationship between qualia and brain processes. These questions include, but are not limited to, whether being conscious could be wholly described in physical terms, invoking emergent material properties from complex neural interactions. In the case that consciousness could not be explained exclusively by physical events in the brain, it implies that consciousness would be governed by different laws from those of

physical systems and require an explanation in a non-physical background, or the discovery of new physical interactions—such as those proposed by the quantum consciousness theory (Penrose, 1990; Hameroff, 1998). For philosophers who state that consciousness is nonphysical in nature (see for example Chalmers, 1996), there remains a question about what mechanisms (other than physical ones) could support consciousness.

The so-called easy problem, on the other hand, can be enunciated as follows: what are the brain processes that are correlated with our subjective experience? In this case the problem of why certain physical phenomena in our brains are accompanied by a subjective experience is not directly addressed.

While the hard problem of consciousness is difficult (if not impossible) to address scientifically, the easy problem is a scientifically tractable problem and it can now be approached using the modern tools of neurobiology. Therefore, we will only concentrate on the so-called easy problem of consciousness.

c) Is attention necessary for conscious perception?

Intuition tells us that attention would be necessary to be aware of something. Think about all the errors that we make when we do not pay attention; an overwhelming body of data have demonstrated that our sensory sensitivity and reaction times are severely impaired when we are not attending. As discussed above, the compelling phenomena of change blindness and inattentionnal blindness (Mack & Rock, 1998; Rensink et al., 1997), suggest that whatever remains outside the spotlight of attention cannot be seen (or if it is vaguely experienced in some way, at least cannot be later recalled or reported).

However, some scholars argue that consciousness can sometimes occur in total absence of attention (Koch & Tsuchiya, 2007; Boxtel, Tsuchiya, & Koch, 2010), but it is still highly debated (see for instance Prinz, 2010). Other authors acknowledge that consciousness can occur in absence of attention, but in this case all content of consciousness would remain out of the reach of working memory and would thus be hard to be reported (Lamme, 2003; Koivisto, Kainulainen, & Revonsuo, 2009). Phenomenologically, the former case of

attentionless consciousness would be equal to a very vague feeling of "seeing something". This kind of consciousness would be close to the philosophical concept of consciousness called *phenomenal consciousness* or *primary consciousness* (Block 1995; Block, 2008), which would account for rich subjective experience that is hardly reportable and elusive to memory encoding (note that under this point of view, the richness of perception would not be an illusion and phenomena such as change blindness would be explained by the failure in the processes allowing to report the overwhelming richness of such subjective states). Phenomenal consciousness would be thus preattentive, and it would have no particular limit on the amount of information held in it.

Access consciousness (or reflective consciousness), on the other hand, refers to a kind of consciousness which is available for use in high-level cognitive processes such as thinking, speech, or action planning. Access consciousness is limited in capacity (as attention), allowing accessing a limited number of representations at a given time (Block, 2008).

Due to the nature of phenomenal consciousness which is information hardly accessed by other modules allowing overt report such as language and higher cognitive functions as memory, it is hard to study it in laboratory conditions. Consequently, here we shall only consider access consciousness, which is always verbally reportable and relies on attention.

d) Is attention sufficient for conscious perception?

The concept of attention has sometimes almost replaced the concept of consciousness, and the underlying suggestion is that consciousness might be identical to attention or at least not fundamentally different from it (Posner, 1994; O'Regan & Noë, 2001; Mole, 2008; De Brigard & Prinz, 2009; Posner, 2012). However, attention and consciousness seems to be dissociable and the study of attention would not become automatically the study of consciousness.

Attentional selection and enhancing of visual information can take place at levels of processing that are outside or before consciousness, in other words, we can attend to objects which are not consciously perceived. For example, an emotional word or image can draw attention and cause larger responses in the brain even if not consciously perceived

(Carlson et al. 2012; Carlson et al. 2011). It has been also showed that blindsight patients can use consciously perceived cues to enhance unconscious processing of visual targets (Kentridge, Heywood, & Weiskrantz, 1999; Kentridge, Heywood, & Weiskrantz, 2004). When a target was presented in their blind visual field, blindsighted patients responded faster and more accurately when it was validly cued by a consciously perceptible arrow pointing to it, than when it was invalidly cued. In both cases, the patients still claimed that they could not see the target. Spatial visual attention can enhance invisible stimuli processing in normal subjects too (Ward and Jackson 2002; Kentridge, Nijboer, & Heywood, 2008; Lu, Cai, Shen, Zhou, & Han, 2012). It has been also shown that attention is necessary for priming invisible words (suppressed by a combination of forward and backward masking). In conditions without attention, the same word fails to elicit an effective priming (Naccache, Blandin, & Dehaene, 2002). A recent study in functional imaging using binocular suppression has shown a clear neural dissociation between attention and consciousness in V1 (Watanabe et al., 2011). While BOLD signal was enhanced by attention for both visible and invisible targets, visibility itself did not elicit any significant effect on BOLD signal in V1, indicating that attention can enhance non-conscious neural representations.

e) The neural correlates of visual consciousness

Which are the neurons that pinpoint consciousness? Historically, several brain areas –within the visual cortex as well as beyond it—have been argued to support visual experience. For instance, René Descartes believed that the pineal gland was the seat of consciousness and thought (Descartes, 1649). Today we are more prudent and there are few that would attribute all conscious functions to a single brain structure. Before reviewing the brain areas that have been found as correlated with visual conscious experience, we have to distinguish between the enabling factors and the neural correlates of consciousness proper. While the neural correlates of consciousness (NCC) are defined as the minimal neuronal mechanisms that are jointly sufficient for any one specific conscious percept (Koch, 2004), the enabling factors stand for the brain processes that are needed for any form of consciousness to occur at all. These factors include maintaining a certain level of vigilance (i.e. while asleep in a dreamless sleep or in coma no conscious perception is possible). Several areas have been

identified as enabling factors. Some examples include the mesencephalic reticular formation (MRF) that controls the level of arousal or wakefulness in animals and when it is damaged produces stupor or coma (Steriade, Oakson, & Ropert, 1982; Jones, 2003). Another subcortical area is the locus coeruleus which sends diffuse connections to many brain areas from thalamus to frontal and visual cortex and regulate some aspects of the sleep-wake cycle (Luppi et al., 2006; Gottesmann, 2008).

In experiments involving the reversible suppression of the visibility of a stimulus by dichoptic suppression, several areas of the brain respond selectively to the visual stimulus. Indeed, the selectivity to conscious perceived stimuli is increased along the visual hierarchy. While about 20% of V1 neurons are activated selectively by consciously perceived stimuli, about 40% of V4 and MT cells can show selective responses, and the proportion of consciousness selective neurons can reach about 90% in temporal visual areas in monkeys (Leopold & Logothetis, 1996; Logothetis 1998). Activations in higher visual areas in the human brain, such as the fusiform face area, can also be tightly correlated with conscious reports, suggesting that the representations supported in these regions are readily brought to consciousness (Tong et al. 1998). However, non-conscious visual stimulation can also activate these regions (Jiang & He, 2006), and it is also possible to decode categories in these areas from invisible stimuli (Sterzer, Haynes, & Rees, 2008). These results suggest that the activity in these areas is not sufficient for consciousness. All in all we lack a comprehensive view on where in the brain we find the NCC.

f) Current theories of consciousness

A science that deals with consciousness requires a theory of consciousness that explains what consciousness is and how it fits with available data. Discussing all current theories of consciousness goes beyond the scope of this introduction and some remarkable theories have thus been not included here. Here we will briefly review some of the most influential theories of consciousness.

1. The neurobiological theory of consciousness of Crick and Koch

Crick and Koch outlined a research program for the study of consciousness rather than a detailed theory. According to them, we should not try to precisely define consciousness at this stage, because it is impossible, and we should not worry about explaining the hard problem (such as the existence of qualia); these problems can be left for later. They proposed that what neuroscientist can and must do is to concentrate on finding the neural correlates of consciousness which are defined as the smallest set of brain mechanisms sufficient for some specific phenomenal state (Crick & Koch, 1990; Crick and Koch 2003). In their theory, essential nodes located in sensory areas are connected to a wider network represented by high-level, executive areas located in frontal areas of the brain which could interact at distinctive frequency bands—such as the gamma frequency— (Crick and Koch 1998b; Crick and Koch 1998c; Crick & Koch, 1995; Koch, 2004). The authors suggest the existence of a subset of anatomically and physiological special types of neurons within the network that would be necessary to pinpoint consciousness. The importance of the early works of Crick and Koch was to consolidate the study of consciousness as a valid scientific endeavor; contrarily to the previous thought standing that consciousness would be a subject of exclusive philosophical study.

2. The dynamic core and the information integration theory

The dynamic core is a holistic functional cluster involving the recurring neural activity in the thalamocortical system as a key element which would represent a functional cluster composed by neuronal groups that interact with each other (Lumer et al., 1997; Edelman & Tononi, 2000). The spatiotemporal coordination of activity within this cluster would thus bind the different perceptual elements into coherent objects and further to unified conscious perceptual states (Edelman, and Tononi 2000). This activity is not identified with particular types of neurons nor localized in specific brain areas. Rather, different neural populations can participate in the dynamic core at different times, and it is the integrated activity of these otherwise unrelated components that would correlate with conscious

states. In the scope of this theory, conscious information would have two main features: (1) it is highly integrated (that is, it always appears as a globally unified field of experience) and, at the same time, (2) it would be highly differentiated (that is, every single conscious state is different from all possible states). Thus, what counts for the emergence of consciousness would be how much integrated information is generated by the system (Tononi 2004b), and the level or deepness of consciousness would be defined by the differentiation of a particular mental state from the number of different possible states available at one particular moment (Edelman, and Tononi 2000). Therefore, only integrated information can access consciousness, if a particular neural group is excluded from the dynamic core, its activity would not be capable to elicit any conscious sensation. On the other hand, if the activity of the dynamic does not achieve differentiability from the rest of the system (which can be accounted by their activity profile) its state would not be differentiable from other states of the system and it would thus not be informative. This is exemplified by epileptic seizures (where the subject often loses consciousness) in which the pattern of activity among vast areas of the brain is highly indistinguishable since different brain areas are highly synchronized.

3. Recurrent processing theory

In the theory of recurrent processing the crucial factor to the emergence of awareness is the direction of processing in the visual cortex. As we have previously seen, a first wave of activity travels from early visual cortex to executive areas. This feedforward sweep would carry a non-conscious representation of visual information and thus the information cannot be verbally reported yet, but it would be able to drive rapid, unconscious, reflex-like actions (Lamme 2000). After the feedforward sweep all areas remain active and two kind of neural connections come into play. Within each visual area, neurons start to interact through horizontal connections, generating local recurrent activity. Between lower- and higher-level areas, recurrent interactions are settled through feedback connections. These types of interactions establish a resonant processing which would be associated with consciousness. The emergence of consciousness according this model would be triggered by the exchange and integration of information among different brain areas through recurrent processing, binding together different stimulus features. When recurrent processing reaches parietal

and frontal cortex, the contents of perception would become fully accessible to higher cognitive functions as memory and would thus become reportable. However, this theory also considers awareness beyond reportability which would be represented by the recurrent activity prior to the reaching of the parieto-frontal network (Lamme, 2003; Lamme, 2004).

4. Micro-consciousness theory

Whereas several theories identify consciousness with information integration, the micro-consciousness theory of consciousness argues that stimuli features, once extracted –that is, explicitly represented by a neural population—would become consciously accessible in the form of a *micro-consciousness* (Zeki & Bartels, 1999; Zeki, 2003; Zeki, 2008). This theory implies that consciousness is fundamentally non-unified and its neural correlates are distributed and restricted to the sensory cortex; and the quality of being conscious of a certain visual feature would only depend in the degree of activation of the cortical area coding for it (Moutoussis & Zeki, 2002). There would thus be no single unified neural mechanism of consciousness to be found since the nature of the neural correlated of consciousness would be fragmented. This theory states that when we are presented with a complex visual stimulus, each feature of it would emerge independently at different moments defined by their processing and explicit representation by different neural populations. This asynchrony would pass unnoticed because it is above the temporal resolution of our phenomenal experience.

5. The Global Workspace theory of consciousness

The global workspace theory is a simple and elegant cognitive architecture relating conscious experiences with the interaction of specialized brain modules that would allow to make the sensory (and inner) information accessible to different modules (Baars, 1990). The term "global workspace" comes from artificial intelligence, where it refers to a fleeting memory domain that allows for cooperative problem-solving by large collections of specialized programs. The global workspace theory therefore assumes that the brain can be viewed as a group of highly specialized modules which would interact through a functional

architecture which supports their interactions: the global workspace. As we have seen previously, there is evidence which is consistent with the hypothesis that much of the brain consists of highly specialized regions. For example, detailed sensorial processing of visual information, such as the encoding of spatial frequency content of an image in the early visual cortex or the figure/ground segregation process are performed automatically by specialized group of neurons and remain largely unconscious. On the other hand, the outcome of the visual processing is a conscious holistic experience of objects and scenes which would be accounted by the access of the information processed earlier in these automatic modules. The global workspace theory predicts that conscious experience would evoke highly distributed activity in visual and non-visual regions of the brain in order to interconnect several distributed, functionally specialized modules. In the global workspace theory this is called "broadcasting" of global messages to multiple target functions (Baars, 1990; Baars, 2002; Baars, 2002; Baars, 2005; Shanahan, 2010).

5.1 The global neuronal workspace and its neurocomputational implementation

An inheritor of the global workspace theory is represented by the global neuronal workspace model, which is a neurocomputational and neurobiological model introduced by Dehaene and colleagues (Dehaene, Kerszberg, & Changeux, 1998; Dehaene, Sergent, & Changeux, 2003). This model was aimed to explain processes underlying effortful tasks (Dehaene et al., 1998) and eventually it became a testable model to explain the access to consciousness (Dehaene et al., 2003; Dehaene, Changeux, Naccache, Sackur, & Sergent, 2006; Dehaene & Changeux, 2011). The global neuronal workspace distinguishes two main computational spaces: a unique global workspace composed of distributed and heavily interconnected neurons with long-range axons, and a set of specialized and modular processors (Figure 13a) including perceptual, motor, memory, evaluative, and attentional units. In this model, the activation of the workspace would be necessary in tasks that are not solvable by the activity of specialized processors alone. Thus, the workspace architecture would selectively include specific processor neurons in order to solve the task at hand.

The global neuronal workspace is thus composed by two main components: a bottom-up network that propagates sensory stimulation across the hierarchy of areas (Figure 13b), and a long-distance, top-down network that sends amplification signals back to all levels below it (Figure 13b). Although a variety of processor areas project to the interconnected set of neurons composing the global workspace, only a subset of inputs effectively accesses it at any given time (Figure 13b, top). The access of different components to the global workspace would be gated by feedback modulatory projections sent from neurons located in high-level areas to more peripheral processor neurons (Figure 13b, bottom). These projections may selectively amplify or extinguish the feedforward inputs from processing neurons, thus including, at a given time, a specific set of processors in the workspace while suppressing the contribution of others (Dehaene et al., 1998; Dehaene et al., 2003; Dehaene & Changeux, 2011).

The key feature of the global neuronal workspace is the presence of a distributed set of cortical neurons characterized by their ability to receive and send back to homologous neurons in other cortical areas through long-range excitatory projections (i.e. through reciprocal connections). These neurons are known as *workspace neurons*. As we have previously seen, long-range corticocortical connections, mostly originate from the pyramidal cells of layers 2 and 3, which send and receive inputs from other cortical areas. Thus, the extent to which a given brain area contributes to the global workspace would be simply related to the fraction of its pyramidal neurons contributing to layers 2 and 3 interconnectivity (Figure 13c). In addition, the stability of workspace activity would be established by strong vertical and reciprocal connections, via layer 5 neurons, with corresponding thalamic nuclei (Figure 13c, Dehaene et al., 1998).

The global workspace is thus characterized by the coherent activation of a subset of all available workspace neurons, while the rest of workspace neurons would be inhibited. The functional architecture of the neuronal global workspace precludes the coexistence of multiple dominant representations and thus only allows one workspace representation to be active at any given time. This all-or-none invasive property distinguishes the dynamics of the global neuronal workspace from peripheral processors which allow several parallel representations to coexist (Dehaene & Changeux, 2005). When a representation invades and has access to the workspace it can remain active in an autonomous manner and resist

changes in peripheral activity. If it is negatively evaluated, or if attention fails, it may however be spontaneously replaced by another discrete combination of workspace neurons (Dehaene et al., 1998).

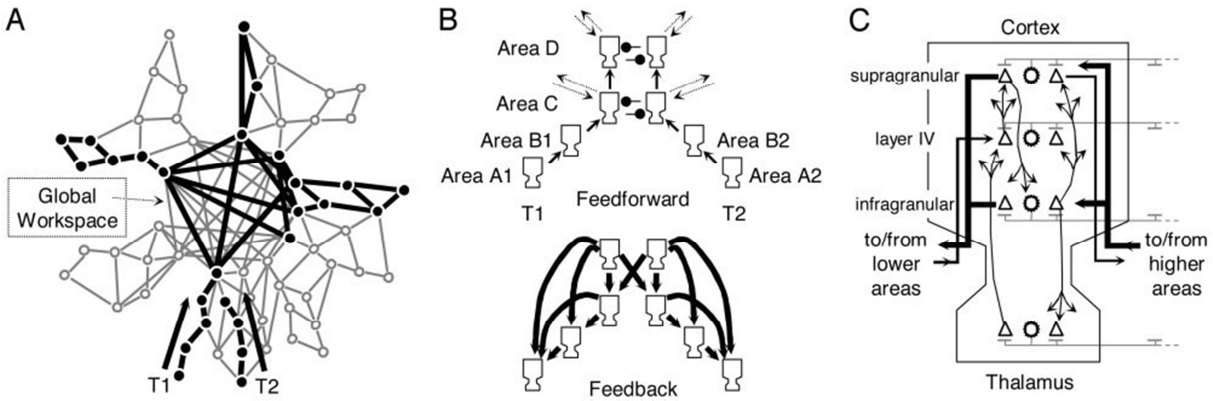

Figure 13. The neuronal global workspace model of conscious access. A. *Scheme showing the functional architecture supporting the global workspace. Multiple specialized processors represented by different brain areas (schematized by the peripheral projections of the network) reach accessibility to a central network (the central core of the network) transiently allowing the communication of these modules with a global neural network composed by high-level areas. A first stimulus (T1) invades the workspace, allowing that initially unrelated areas become an interconnected assembly and thus the information from T1 is shared among different processors, thus supporting conscious reportability. The invasion by T1 blocks the entrance of a second stimulus T2 to the global workspace, thus avoiding its conscious reportability.* ***B.*** *Subset of thalamo–cortical columns showing the feedforward activation in different zones (top) and the competitive interactions at higher-level areas (Area C and D) in order to gain control of the global workspace. Feedback activity from high-level areas broadcast information of the winning stimulus among different processors located at different hierarchical levels.* ***C.*** *Structure of a single simulated thalamo–cortical column, reproducing the laminar distribution of projections between excitatory neurons (triangles) and inhibitory neurons (circles). (Modified from Dehaene et al., 2003).*

5.2 Spatio-temporal dynamics of the global neuronal workspace

The global neural workspace model predicts a non-linear, all-or-none-like threshold access to consciousness which have been successfully tested experimentally (Sergent, Baillet, & Dehaene, 2005; Del Cul, Baillet, & Dehaene, 2007). In a visual masking paradigm different masking strengths were used to manipulate the visibility of a target number, while measuring both objective performance and subjective visibility (Del Cul et al., 2007). As previously reported (Breitmeyer & Öğmen, 2006), both objective performance and subjective visibility had a non-linear relationship with the masking strength: at strong masking strength the stimulus was largely non-conscious and once the strength of mask was decreased to a threshold value, the visibility of the stimulus increased suddenly, in a non-linear fashion. The intrinsic properties of the global neuronal workspace explain well the all-or-none dynamics seen in those experiments (Dehaene & Changeux, 2005; Del Cul et al., 2007).

Figure 14 illustrates the schematic predictions that may be expected from the global neuronal workspace model. The example showed in Figure 14 stands for an experiment using visual masking, where the masking strength is modulated with a consequent effect in conscious visibility. However the same principle can be applicable to other examples where the conscious access is modulated as a result in the manipulation of other stimuli variables. In this example, the first wave of activation should be indistinguishable for all stimuli in early visual areas, independently if they would or not reach consciousness afterwards. Then, higher order areas would be more activated as the strength of the mask decreases (or more generally speaking, as the amount of relevant stimuli features increases) which is illustrated as higher amplitude in the first wave of activity reaching occipito-temporal and parietal cortices in Figure 14. After that, when the information reaches higher cortical areas, particularly the prefrontal cortex, activation should diverge in a nonlinear manner, either eliciting high-levels of activity, or decaying back to baseline; in an all-or-none fashion which is as a consequence of the global workspace ignition (or failure to ignite) by the sensorial information. This phenomenon is thus correlated by a late wave of activation in frontal areas illustrated in the right panel of Figure 14. Finally, the activation of the global network induces feedback activity which reactivates areas including parietal, temporal and occipital areas thus creating a second, late peak of activation in such areas, which replicates itself the all-or-none behavior of the global workspace.

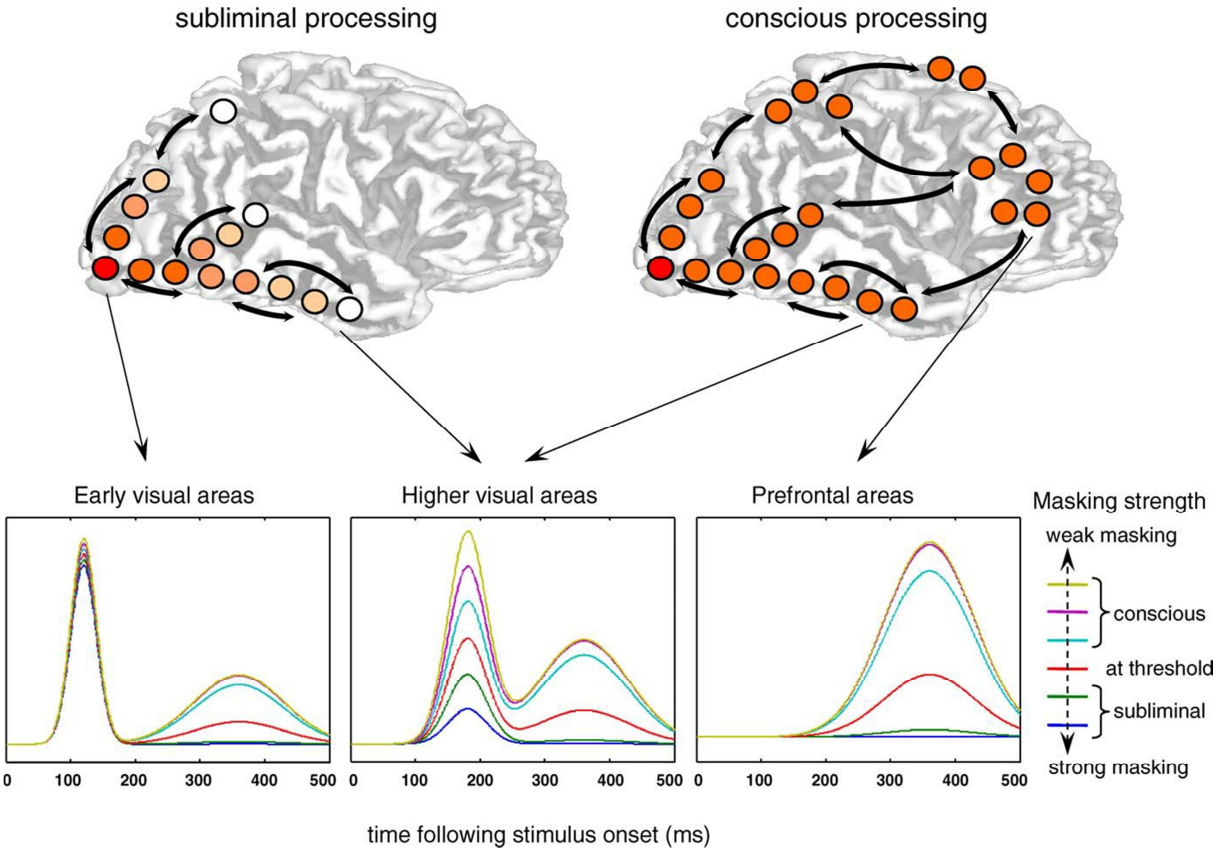

Figure 14. Brain activations as predicted by the global neuronal workspace model of consciousness. *Top, depth of cortical processing: subliminal stimuli (left panel) should evoke a strong activation in extrastriate visual cortex, but their intensity should quickly decrease in higher visual areas; only conscious stimuli (right panel) should trigger a late surge of activation in a global prefronto-parietal network. Bottom, schematic time course of activation as a function of masking strength. Masking is expected to have little effect on early visual activation but to modulate the strength of activation in higher visual areas. Furthermore, there should be a nonlinear effect of masking strength in prefrontal cortex, with a similar late top-down activation peak occurring simultaneously in visual areas. (From (Del Cul et al., 2007)*

The global neuronal workspace has been tested in a variety of cognitive paradigms including Stroop's test, attentional blink, visual masking and others experiments involving the psychological refractory period (Dehaene et al., 1998; Dehaene et al., 2003; Del Cul et al., 2007; Hesselmann, Naccache, Cohen, & Dehaene, 2012). However it is still unclear whether this model can account for other paradigms involving conscious access and if it is a valid model for general conscious access. In the last work presented in this thesis I present evidence supporting this model in a recognition task performed by monkeys.

V. Thesis aims

In this thesis we will be focused on the visual system of human and non-human primates and their large capacity of information extraction from fundamental mechanisms allowing extracting coarse visual features associated to some semantic values to the emergence of the neural correlates of conscious recognition.

First we will explore the image features that the visual system can use in order to distinguish between categories of complex visual stimuli under high temporal constraints. This was done by studying ultra-rapid categorization, a paradigm allowing exploring the minimal set of neural processes that allow categorizing semantic categories. In this chapter we will explore to which extent the global low-level visual features are necessary to perform ultra-rapid categorization, and test if these features are used similarly by two different primate species: macaque and humans, in order to infer to which extent they use similar strategies.

Then, we will explore visual attention, which is the door to higher-level cognitive processes such as consciousness. In this part we will focus on the relationship between the spatial deployment and temporal dynamics of both endogenous and exogenous attention in humans and we will ask if the spatial pattern of attention deployment evolves across time, a question largely deferred by direct analysis. We will tackle this question by introducing a new method to explore spatial attention in the temporal domain using psychophysics.

We will then focus on high-level representations of objects: the paramount product of the visual processing. Is there a way to specifically extract such representations? In this part we will focus on a new stimulation method called SWIFT which allows isolating brain activity underlying high-level visual representations. In a first work we will focus on the development of this technique and the test of its capacity in isolating the neural correlates of conscious object recognition, the interaction of these representations with attention and we will explore the temporal dynamics of high-level representations.

In a second work involving the innovative SWIFT method we will show how this technique tracks conscious objects representations which are modulated in an all-or-none fashion

under binocular rivalry and we study the nature of brain activity underlying conscious representations.

In the final part, two ongoing studies will be presented. The aim of these studies is to couple the SWIFT technique with intracranial recordings—a unique technique that allows obtaining both high temporal and high spatial resolution measures of brain activity—in order to address the following question: where and when do conscious representations emerge? The first study involves intracranial recordings in epileptic patients and the second intracranial recordings in macaque monkey.

The relationship among these works is represented in Figure 15. A main axis of research is aimed to decipher the nature of the neural representations used in different sense-extraction processes at different levels of the visual system. This axis regroups four different works dealing with different cognitive phenomena from ultra-rapid categorization to conscious object recognition. Two more works explore parallel questions which were important in order to gain a deeper insight into the main problem of how does the brain extract the sense from the visual world. The first parallel study was aimed to visual attention as a cornerstone in the access of visual representations to consciousness. In a second work we thus examined the following problem: What are the spatiotemporal dynamics of visual attention? After studying how the shape of the doors of perception is modulated across time, I was interested in seeing what was behind these doors, and thus in the third work I return to my original quest trying to answer the following question: can we isolate the neural correlates of high-level representations? In this work we developed a new method in order to isolate the neural correlates of conscious object recognition. This method allowed extracting neural activities specifically representing the conscious recognition of natural images. Later on we were confronted with the question: can we isolate the neural correlates of visual consciousness under binocular rivalry using the SWIFT technique? This parallel question was tested in the fourth work. In this work we used the binocular rivalry paradigm in order to manipulate visual conscious representations. We thus measured the evoked responses under conscious and non-conscious states under binocular rivalry using the SWIFT technique. The final two works are aimed to gain insight into the following question: where and when are the neural correlates of conscious object recognition generated in the brain?

We used our novel technique in combination with intracranial recordings allowing high temporal and spatial resolution in two models: humans and monkeys.

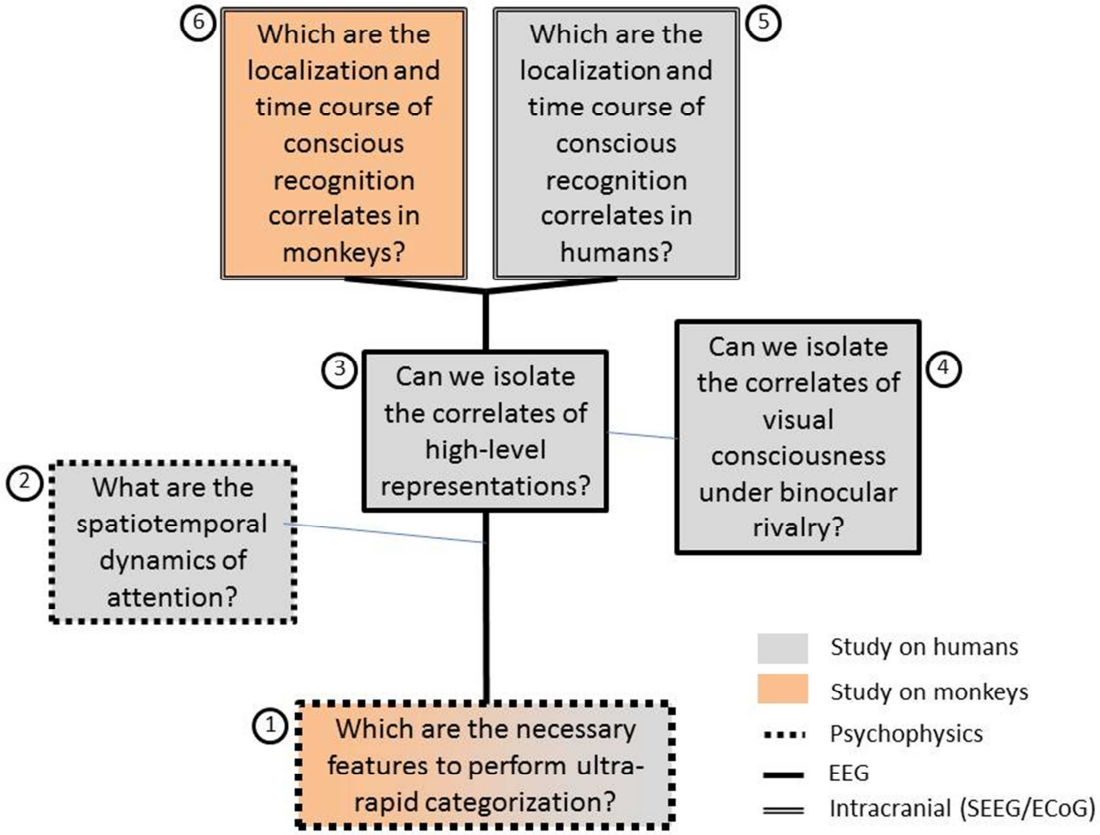

Figure 15. Schematic diagram representing the relationship among the works presented in this thesis*. A main axis of research, regarding the nature of the neural representations used in the sense-extraction process in the visual system, from ultra-rapid categorization to conscious recognition, is represented by the bold black line. Parallel questions which were important in order to gain a deeper insight into the main problem are represented by thinner lines. Different models and techniques were used in the different studies which are indicated by a visual code.*

B. Looking for the necessary features to categorize a natural image in a glimpse

As discussed above, ultra-rapid categorization imposes strong constraints on the brain mechanisms underlying the processing of complex stimuli. Ultra-rapid categorization relying on saccadic choice task show the earliest reliable reaction times around 100 ms (Kirchner & Thorpe, 2006; Girard et al., 2008; Crouzet et al., 2010). Taking into account the neuronal latencies across the ventral pathway and the time for the execution of the occular motor response, it seems that the visual information would not have enough time for even a single feed-forward pass through the ventral stream up to IT and it is probable that visual information would take shortcuts at some level of the visual pathway in order to reach the oculomotor areas (from V4 to the superior colliculus for instance), before that it would be processed by all ventral areas (Kirchner & Thorpe, 2006; Crouzet & Thorpe, 2011). Thus ultra-rapid categorization could rely on incomplete object representations represented by its constituent features. These features could be represented by simple shapes that could be used as diagnostic features to differentiate stimuli categories (Ullman, Vidal-Naquet, & Sali, 2002; Sigala & Logothetis, 2002; Sigala, 2004; Wang et al. 2011). Thus, neurons in ventral areas would be tuned to these diagnostic features allowing categorizing visual stimuli before a complete representation of the object would emerge (Sigala & Logothetis, 2002). Another line of thought sustains that important features involve even lower-level visual attributes such as global statics of the image rather than form-like object features (Torralba & Oliva, 2003; Oliva & Torralba, 2006; VanRullen 2006). Distinctive global statistic (which can be irrespective of the local configuration that one associates to an object form) within a category would serve to differentiate among several stimuli using low-level cues. For instance, the strong salience of faces which are easily discriminable among other objects, could be partly explained by their spatial frequency amplitude spectrum (VanRullen 2006; Honey, Kirchner, & VanRullen, 2008). Let's see how the spatial frequency amplitude spectrum can account for the saliency of object categories, specifically faces.

I. The paper of Honey et al. 2008

In an ingenious experiment, it has been shown that the conspicuity of faces is in partly due to the Fourier 2D amplitude spectrum (Honey et al., 2008). One face and one vehicle images were simultaneously presented with different contrasts while subjects were asked to saccade as fast as possible to the image with higher contrast. Subjects made saccades to face images more often than to transport images when both images had the same contrast (Figure 16). This confirmed the already reported bias towards faces in ultra-rapid categorization (Crouzet, Thorpe, & Kirchner, 2007). In a second step, faces and transport means images were scrambled in their spatial configuration to the same extent. For one subject group, the scrambling was done on the orientations of wavelet components (local orientations) while preserving their location (Figure 17a-b, top row). This manipulation completely abolished the face bias for the fastest saccades (Figure 18b). For a second group, the phases (i.e., the location) of Fourier components were scrambled while preserving their orientation (i.e., the 2-D Fourier amplitude spectrum, Figure 17a-b, bottom row). Even when no face was visible (100% scrambling), the fastest saccades were still strongly biased toward the scrambled face image (Figure 18a). These results suggest that the ability to rapidly saccade to faces in natural scenes depends, at least in part, on low-level information contained in the Fourier 2-D amplitude spectrum. Thus it has been argued that visual features necessary to perform ultra-rapid categorization involving natural images such as faces could be extracted from the activities of cortical neurons in the bottom of the visual hierarchy such as neurons in the early visual cortex (Crouzet & Thorpe, 2011).

A previous work (Joubert, Fize, Rousselet, & Fabre-Thorpe, 2008) has showed that human subjects are still capable to categorize natural scenes and man-made scenes that have been equalized in their 2D Fourier amplitude spectrum, showing only a slight drop of accuracy and increase in manual reaction times.

Can monkeys also categorize equalized natural images? That is, can they extract the relevant meaningful attributes of the image in the absence of differential low-level cues (i.e., the Fourier amplitude spectrum) between categories, despite their lack of language and cultural

background? And, if they do, at what speed can they do so? Secondly, do they use the same strategies than humans in order to categorize natural images?

In the next work we will try to answer these questions. This work started a Masters study conducted by the supervision of Pascal Girard, who allowed me to make the first steps in cognitive neuroscience involving primates, for which I am very grateful. This work turned into collaboration when I started my PhD training under the supervision of Rufin VanRullen. Thus the next paper is the fruit of this collaboration.

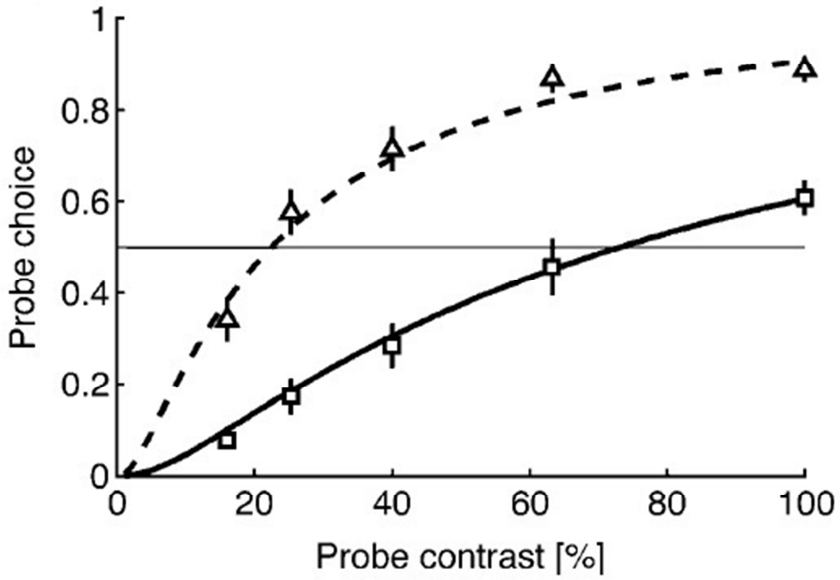

Figure 16. Probe choices for the unscrambled images as a function of the contrast of the probe*. Choices of faces and transports are represented by triangles and squares respectively. Faces are systematically perceived as more salient (i.e., as having more contrast). Note that the reference stimulus always had a contrast of 0.4. Error bars represent standard error of the mean. (Modified from (Honey et al., 2008).*

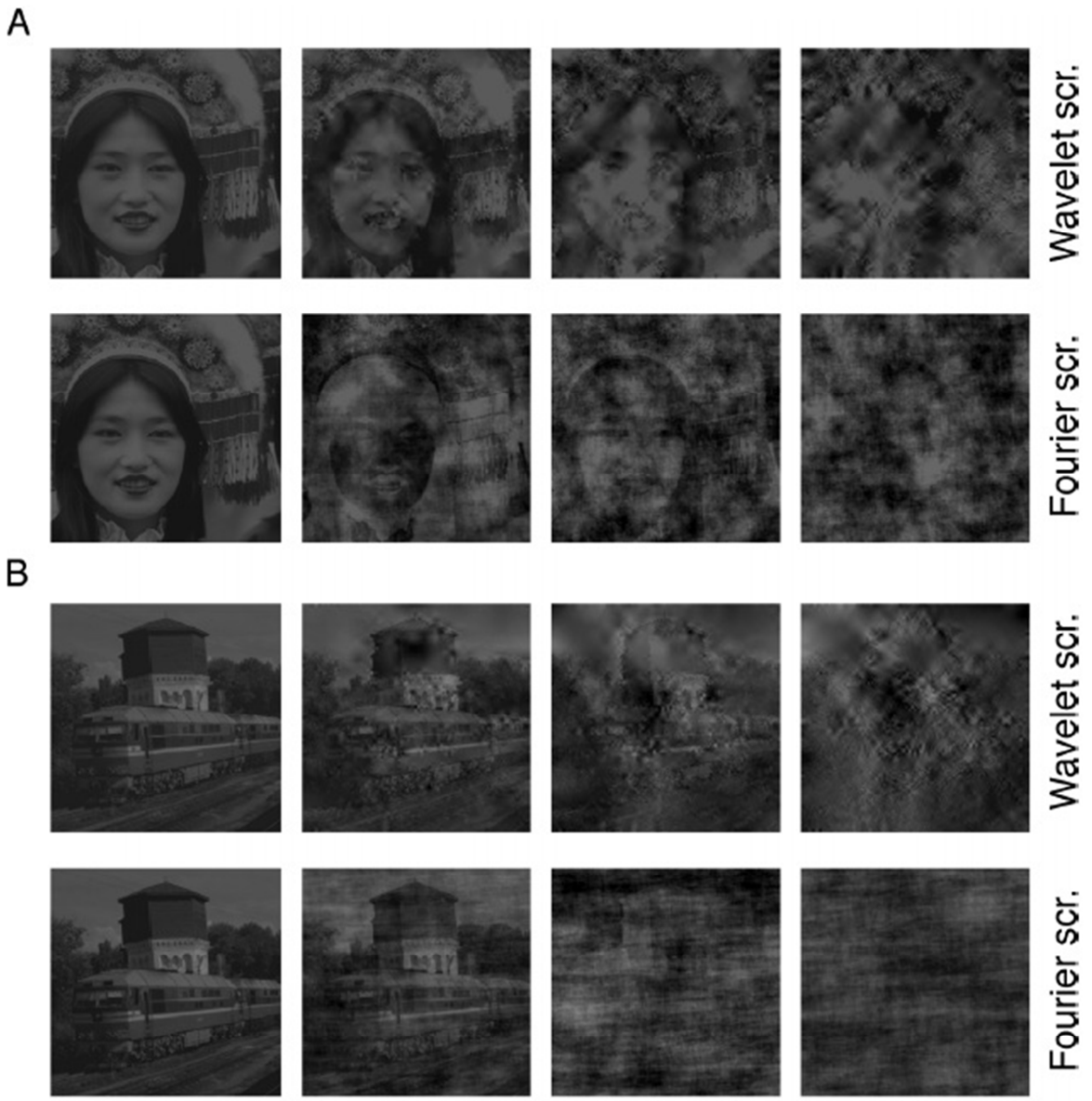

Figure 17. Examples of stimuli used in the work of Honey et al. A. Face images. *Top row shows faces scrambled at different levels in the wavelet domain (i.e., local orientation scrambling). Bottom row shows faces using phase-scrambling in the Fourier domain (i.e., conservation of image orientations but disruption of their relative positions in the image) at different levels.* ***B.*** *The same for transport images. Scrambling levels from left to right: 0%, 30.25%, 55%, and 100% (Modified from (Honey et al., 2008).*

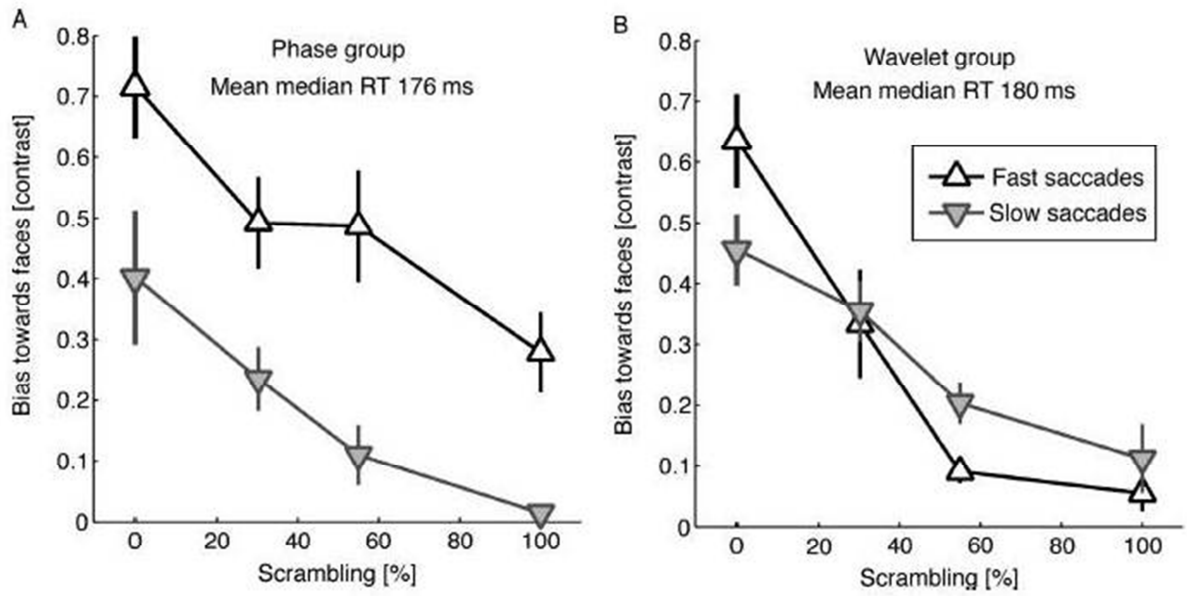

Figure 18. Face biases in both groups A. Phase group. *Bias toward faces was strong at all scrambling levels for fast saccades (upside-up white triangles), while this bias was weaker for slow saccades (upside-down grey triangles), becoming non-significant at high-levels of scrambling. Crucially, at 100% scrambling (where the image is no longer recognizable) the bias remain strong and highly significant for fast saccades.* ***B. Wavelet group.*** *Bias at 100% scrambling, in the wavelet group, are no longer significant. The means of the median reaction times in each group are indicated in each plot. Error bars represent 95% confidence intervals (Modified from (Honey et al., 2008).*

II. PAPER 1. Girard and Koenig-Robert, PLoS One, 2011.

OPEN ACCESS Freely available online

PLoS one

Ultra-Rapid Categorization of Fourier-Spectrum Equalized Natural Images: Macaques and Humans Perform Similarly

Pascal Girard[1,2,3]*, **Roger Koenig-Robert**[1,2]

1 Université de Toulouse, UPS, Centre de Recherche Cerveau et Cognition (CerCo), Toulouse, France, **2** Centre National de la Recherche Scientifique (CNRS), CerCo, Toulouse, France, **3** Institut National de la Santé et de la Recherche Médicale (INSERM), Toulouse, France

Abstract

Background: Comparative studies of cognitive processes find similarities between humans and apes but also monkeys. Even high-level processes, like the ability to categorize classes of object from any natural scene under ultra-rapid time constraints, seem to be present in rhesus macaque monkeys (despite a smaller brain and the lack of language and a cultural background). An interesting and still open question concerns the degree to which the same images are treated with the same efficacy by humans and monkeys when a low level cue, the spatial frequency content, is controlled.

Methodology/Principal Findings: We used a set of natural images equalized in Fourier spectrum and asked whether it is still possible to categorize them as containing an animal and at what speed. One rhesus macaque monkey performed a forced-choice saccadic task with a good accuracy (67.5% and 76% for new and familiar images respectively) although performance was lower than with non-equalized images. Importantly, the minimum reaction time was still very fast (100 ms). We compared the performances of human subjects with the same setup and the same set of (new) images. Overall mean performance of humans was also lower than with original images (64% correct) but the minimum reaction time was still short (140 ms).

Conclusion: Performances on individual images (% correct but not reaction times) for both humans and the monkey were significantly correlated suggesting that both species use similar features to perform the task. A similar advantage for full-face images was seen for both species. The results also suggest that local low spatial frequency information could be important, a finding that fits the theory that fast categorization relies on a rapid feedforward magnocellular signal.

Citation: Girard P, Koenig-Robert R (2011) Ultra-Rapid Categorization of Fourier-Spectrum Equalized Natural Images: Macaques and Humans Perform Similarly. PLoS ONE 6(2): e16453. doi:10.1371/journal.pone.0016453

Editor: Gonzalo de Polavieja, Cajal Institute, Consejo Superior de Investigaciones Científicas, Spain

Received October 25, 2010; **Accepted** December 16, 2010; **Published** February 4, 2011

Funding: The work was funded by Centre National de la Recherche Scientifique. The funders had no role in study design, data collection and analysis, decision to publish, or preparation of the manuscript.

Competing Interests: The authors have declared that no competing interests exist.

* E-mail: pascal.girard@cerco.ups-tlse.fr

Introduction

The macaque monkey provides one of the closest animal models for studies of the mechanisms of human brain function [1] including cognitive processes such as visual categorization. Recent studies have revealed that monkeys can categorize natural scenes very efficiently (review in [2]). They have shown that Rhesus macaque monkeys are as accurate as humans in categorization tasks involving large sets of images [3–5]. Furthermore, these studies also revealed that the categorization can be extremely fast, with behavioural responses reaching a minimum of 100 ms in a forced-choice saccadic task [4]. It is important to stress that such values place severe constraints on the processing involved in such elaborate cognitive tasks. In particular, it is well established that selectivity to complex stimuli is present in the inferotemporal cortex of the macaque (for a recent review, see [6] but neuronal latencies are such that little processing time is available between stimulus onset and a motor output at 100 ms [7–9].

One relatively simple hypothesis can be put forward to explain these extremely fast reaction times in cognitive tasks: subjects could perform the categorization on the basis of low-level attributes of the images, putatively processed in lower order areas with faster neuronal responses. Such a hypothesis is supported by the work of Oliva and Torralba who have shown that the gist of a natural scene can be grasped on the basis of the spatial frequency content of the image [10]. In the same vein, in humans, fast saccades are still biased toward images of faces in which phase components are randomized and thus must presumably depend on the 2D amplitude spectrum of the images [11]. Hence, in a categorization task, one cannot formally exclude the possibility that images belonging to one category (animal targets for instance) have a spectral content different from that of images of other categories. This is an important issue since former studies have shown that monkeys can use low-level cues that are unrelated to a category per se, for instance a colour patch, to classify stimuli [12]. One solution to avoid a low-level response bias toward one category consists in normalizing all the images of the study in term of mean luminance and RMS contrast and equalizing them in spectral energy. A recent study [13] showed that human subjects are still able to categorize natural scenes and man-made scenes

that have been equalized by giving them the same averaged power spectrum. The main consequences of the equalization process were a slight drop of accuracy and an increase in manual reaction time. Our first aim was to determine whether monkeys can also categorize equalized images and at what speed. In the present study, we successfully trained one rhesus macaque monkey to perform a forced-choice saccadic categorization task of equalized images of animals in natural scenes.

Our second aim was to compare the performance of the monkey with that of human subjects with the same set of equalized images. When tested in the same conditions and with the same images, monkeys are somewhat less accurate but faster than human in a manual go-nogo categorization task of animals in naturalistic scenes [14]. Recent work has emphasised the striking similarity between the cortical representation of categories in both species of primates using passive presentation of numerous natural stimuli [15,16]. Multidimensional analyses of fMRI in humans and neuronal responses in macaques showed that inferotemporal cortex contains separate representations for animate and inanimate objects in which subcategories like face and bodies are distinguishable. Under the methodological constraint of equalized images, we further explored whether monkeys and humans use the same strategies to categorize the same images in the demanding force-choice saccadic task. We focused on several important characteristics of the images such as the angle of view with which the faces were displayed. Humans are readily able to categorize many different species as animals, even odd-looking ones such as ant-eaters or armadillos. Because humans have an obvious cultural advantage, we examined the similarity of categorization across various types of animals. Both species achieved fast reaction times and have a comparable overall accuracy. They also had a similar accuracy on individual images and gave precedence to full-face and close-up views of the faces of the animal targets.

The last question was related to the theoretical possibility that fast categorization could rely on the quantity of relevant information contained in the low spatial frequencies. Authors have postulated that low spatial frequencies could allow building up a quick hypothesis about the content of the image [17] to help recognition or categorization. In the forced-choice saccadic task, there is little time to elaborate a full description of the image and efficiency could rely on the use of low spatial frequencies. Since images were equalized and the phase was not disrupted, they had all the same global frequency content. However, if the target in the image was more salient because of the combination of local low spatial frequencies, it should have been more easily categorized in the saccadic task, considering the hypothesis of Bar. We investigated the potential role of low spatial frequencies in humans, in a rating psychophysical task.

Methods

Ethic statement

All experiments on human subjects were approved by the local ethical committee 'Comité Consultatif de Protection des Personnes dans la Recherche Biomédicale Toulouse II' (permit N° 'Avis N°2-03-34/Avis N°2'). All subjects gave informed written consent to participate in the experiment.

All experiments on the monkey subject were in conformity with the ethical rules of the EEC (EEC, Directive No. 86–609, November 24, 1986). All procedures were in accordance with the Weatherall report, 'The use of non-human primates in research' and were fully approved by the local ethical committee named 'comité regional d'éthique pour l'expérimentation animale de Midi Pyrénées (permit N° MP/04/04/01/05). The surgical procedures necessary for head fixation are described in [4]. No extra surgical procedure was necessary at any time during the present experiment. The general health status of the animal could be monitored every day by competent and authorized personal. The animal was paired-housed during the whole duration of the experiment.

Behavioural task

One female rhesus macaque monkey (*Macaca mulatta*, age: 13 years, weight: 3 kg) was used in this study. The animal was already expert in the categorization of images by means of saccadic eye movements (monkey M1 in [4]). We used the same behavioural task as in the former study but with a new set of images. The animal sat in front of a screen (Iiyama vision masterpro 512, 75 Hz frame-rate) with the head immobilized (see [4]). Every trial required first the monkey to fixate a central dot (0.15°, 300 to 450 ms fixation period). A gap period with a blank screen (200 ms) followed the fixation dot, then 2 pictures appeared simultaneously (centered on the horizontal meridian at 5 degrees eccentricity, one in each hemifield) with a presentation duration of 400 ms. One image contained an animal ("target") and the other did not ("distractor"). As soon as the pictures appeared, the monkey was allowed to make a saccade onto the target. Eye movements were monitored by an ISCAN camera (120 Hz). A drop of water was given after each correct trial; errors were indicated by a low white-noise sound and sanctioned by a slightly prolonged inter-trial delay. We kept careful records of the weight of the water-deprived monkey and gave extra water if needed.

Nine human subjects (3 male and 6 female; mean age 26±4 years) were involved in the same categorization task as the monkey in the same experimental setup and room. They were instructed to make a saccade to the picture that contained an animal. The same CORTEX (NIMH CORTEX) program, in a DOS operating system, was used to monitor the behaviour of both the humans and the monkey. The human subjects sat in front of the same screen as the animal, at the same distance (57 cm); the monkey experiments have been terminated 6 months before and the experimental setup cleaned. Human subjects had their head stabilized by a chin and front device. Their eye movements were monitored with the same camera and software as the monkey. On each correct trial, the subjects could hear the sound of the monkey reward system. All subjects gave informed written consent to participate in the experiment.

Stimuli

All images were 8-bit BMP gray level pictures of natural scenes (243×356 pixels, 5×7 degrees of visual angle). About half were taken from the Corel Database and the other half were taken from internet searches in order to display a larger variety of animal species in the targets (see Table S1) and to have a large number of distractors displaying salient objects. All images in the study were first equalized in luminance (mean grey value = 128) and in RMS contrast (standard deviation of 20.4). In a second step, they were equalized in spectral energy. Equalization was performed by the following operation: we computed the mean power spectrum of the whole set of images (targets+distractors). Then, we applied the mean power spectrum to each image while keeping the original phases [18]. Examples of images before and after the equalization process can be seen in figure 1. The background of the monitor was set to a uniform gray (luminance 14 Cd/m^2).

In each daily session, the monkey saw 50 pairs of images, 10 of which were composed of completely new images while the remaining ones were familiar. All pairs were displayed in a randomized order and appeared several times in the session. New

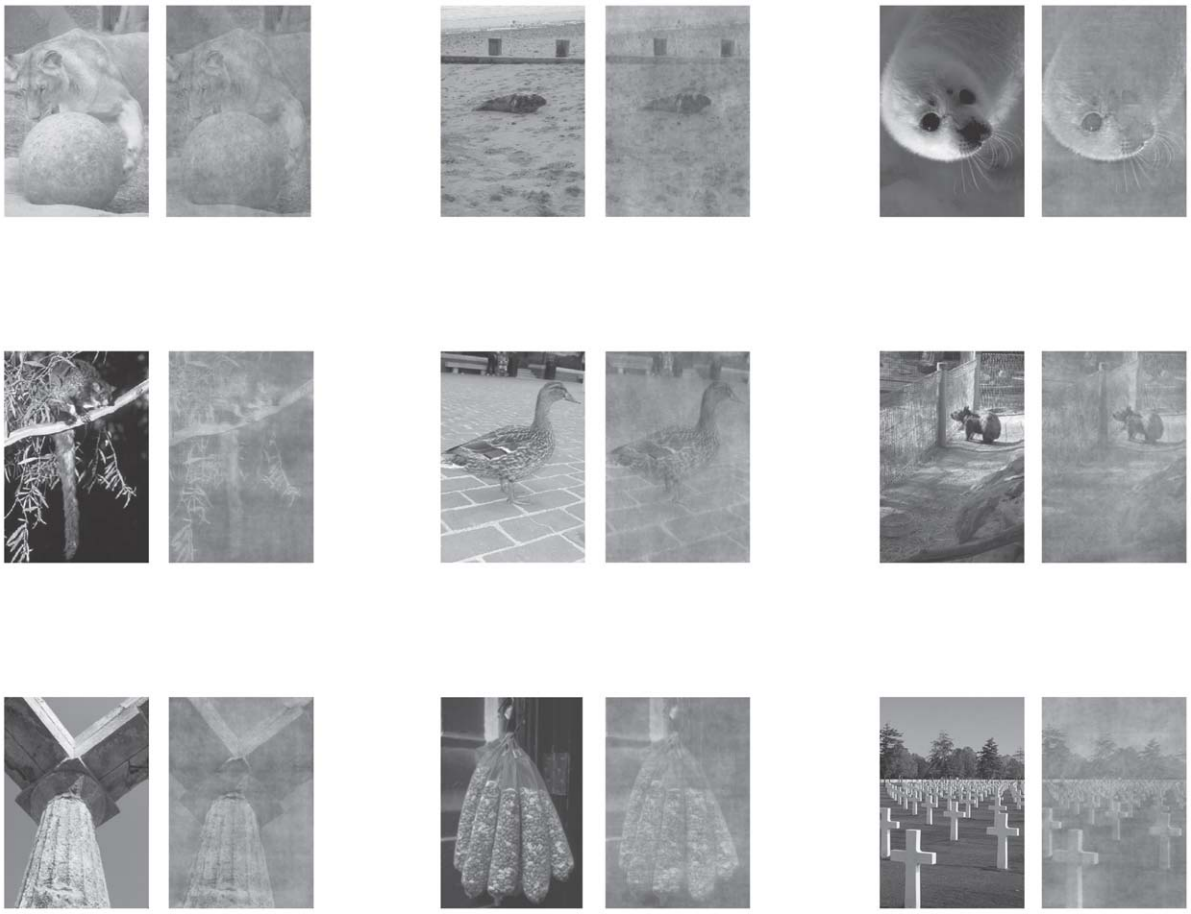

Figure 1. Examples of stimuli. Examples of targets (first 2 rows) and distractors (bottom row) in original grey-level view (left side of each pairs) and equalized version (right side). As illustrated here, distractors often contained salient objects and the target animals could be difficult segregate from the background. In this figure, images appear easier than in the experimental situation since the reader is primed by the original picture.
doi:10.1371/journal.pone.0016453.g001

pairs were composed of pictures that had never been presented to the monkey in either a non-equalized or an equalized version. Although they were repeated along the session, they were considered as new for all trials since they appeared in one session only. Since the monkey performed 51 sessions, it saw 510 different new pairs. Familiar pairs were composed of familiar images taken from a previous study ([4]) in which they were never presented in the equalized version. All the familiar images were present in every session and the pair members were randomly shifted from session to session. Since the animal had not performed the task for several months, we started the experiment with two "warming-up" sessions (two days) in which she performed the task only on familiar non-equalized images (these sessions are not taken into account in the result section). From the third day onwards, only equalized images were presented.

Humans saw only equalized images. In order to draw comparisons, we selected among the 510 new pairs, the 382 pairs that have been presented at least ten times to the macaque, in a given session, and for which we have been able to compute the reaction time offline for each trial (less than 10 trials per pair were available for each of the remaining new pairs and they were not presented to humans). Each human subject saw these pairs, in a random order, in a unique session of 1000 to 1500 trials. Because the humans were not head-fixed as the monkey was, many trials were rejected. The great majority of rejections (15% of the trials) were caused by break in the fixation period. Another 1.6% of the trials were saccades that we rejected offline. We needed 9 human subjects to reach a sufficient number of trials (at least 10 for each pair) for comparison with the monkey.

Saccadic latencies

We computed saccadic latencies as in [4]. We determined a threshold as the maximum value of the derivative of the horizontal eye trace during the fixation period. The saccadic latency of a given trial was taken as the time between stimulus onset (photodiode signal) and the time at which the derivative crossed the threshold. We then checked that the eye position signal did not return to fixation level for at least five consecutive points. The minimum saccadic reaction time (minimum RT) was defined as the first 10 ms bin of the distribution that contained significantly more correct responses than errors (chi-square test, $p<0.05$). This bin had to be followed by 5 consecutive bins reaching the same criterion.

Role of low spatial frequencies

We sought to link the performance obtained in the saccadic task to the low spatial frequency content of the images. All 382 pairs of equalized images that were used in humans were low-pass filtered (2DGaussian with a cut-off frequency of 6 cycles/image [19]. Each target randomly appeared left or right of the midline and each pair

of images was displayed during unlimited time. We asked 5 naïve human subjects to rate the presence of an animal in each pair by entering on a keyboard two answers (left/right presence and rating from 'just guessing' to 'clearly seen' on a 1 to 5 scale). Images that were rated 5 were considered by the subjects as clearly containing an animal whereas a rating of 1 meant they were just guessing. In the analysis of the data, a rating index was computed by multiplying the ratings by −1 if the subject localized an animal in the distractor image or multiplying by 1 in case of correct response; hence, as there were 5 subjects, the rating index could vary form −5 to 5 excepting 0. There were no time constraints and no head restraint in this task. The subjects were in the same age range as the subjects that participated in the saccadic task. They had normal or corrected to normal vision and had not seen the images before.

Results

Monkey performance accuracy

The monkey performed the task remarkably well. The overall score of the animal, based on 24237 saccades, was 74.35% correct (figure 2). However, as expected given the degraded aspect of the images, the performance was lower than she had achieved previously with non-equalized images (79.3%, $\chi2 = 125.35$, df = 1, P<0.0001). In order to rule out any rote learning strategy that would have allowed the monkey to solve the task by memorizing stimulus/reward association, we assessed the ability of the monkey to categorize equalized images in the 510 new pairs. The overall mean score of all trials with new images (n = 4859) was 67.48% correct responses, which is significantly above chance ($\chi2 = 306.43$, df = 1, P<0.0001) but below the performance obtained with non-equalized new pairs in the former study ($\chi2 = 22.48$, df = 1, P<0.0001). The performance was good across the different images since among the 510 new pairs, the monkey performed above 50% correct for 371 pairs and 90 pairs elicited 100% correct responses. Even more important is the response to the very first trial on which a given pair appears, since in that case we are absolutely sure that the monkey could not respond on the basis of a simple stimulus-reward association. The mean percentage of correct responses for the very first occurrence of each of the 510 pairs of new images was 68.43% and clearly above chance level ($\chi2 = 35.87$, df = 1, P<0.0001). If we restrict the analysis to the 382 pairs that were presented at least 10 times, the overall score was 67.25% correct (4025 trials) and above chance level ($\chi2 = 247$, df = 1, P<0.0001). The median accuracy on the different pairs was 70%, 97 pairs gave above or equal to 90% correct responses, 52 pairs gave 100% correct responses, and only 5 pairs were systematically miscategorised (figure 3).

The monkey made significantly more correct responses to familiar images than to new images (76.08% correct, $\chi2 = 150.62$, df = 1, p<0.00001). This performance was significantly below the score of 80% obtained in the previous experiment on familiar pictures ($\chi2 = 82.06$, df = 1, p<0.0001). Interestingly, responses to familiar images were rapidly better than those to new images: the performance of the first occurrence of the 40 familiar targets was 78% correct on the first session where they appeared. The median accuracy on different familiar images was 78.5%. Despite this overall high level of accuracy, the monkey did not exceed chance level on 3 familiar images. These 3 targets depicted respectively a panther, a lemur and a giraffe. This strengthens the view that the performance of the saccadic task did not depend on rote learning: even these 3 images were familiar ones, they were paired with a different distractor at each session and the monkey could not learn them.

Human performance accuracy

Each human subject took part in one experimental session only. They each saw the 382 new pairs that have been presented at least 10 times in the monkey. Each subject performed between 1000 and 1500 trials of which a substantial proportion (15% on a total of 10080) were aborted or rejected (1.6%) since it was not possible to keep the subjects' head as still as in the head-fixed monkey's experiment. However, we decided that the human subjects should not participate in more than one session to avoid a familiarisation with the images. As a consequence, the overall score was based on 8371 saccades. The overall level of accuracy of the human subjects was 63.74%. All subjects performed above chance level with the worst one reaching 54.64% and the best one 79.84% correct responses. The performance is substantially less than the 90% correct reported with non-equalized images [20]. Figure 2 shows the accuracy for both the monkey and the human subjects for the present and the former study.

Saccadic latencies

Figure 4 shows the distribution of saccades latencies obtained for the 382 equalized new pairs that were common to the humans and the monkey. The monkey performed the task very quickly: the median reaction time for correct trials was 121 ms and the minimum reaction time was 100 ms (latency range 95–104 ms). If we consider all 510 pairs of new images used in the monkey, median and minimum reaction time were not different and the distribution of saccades latencies is very similar to the one shown in figure 4 (not shown). Familiar images (monkey only) also lead to a median reaction time of 121 ms but a slightly shorter minimum reaction time (90 ms, not shown).

Correct trials in humans displayed longer latencies than correct trials in the monkey (Mann–Whitney, $U = 1.34 \times 10^7$, n1 = 2707, n2 = 5336, $P<0.0001$). The median human reaction time (correct trials) was 172 ms and the minimum reaction time was 140 ms (range 135–144 ms). The median reaction time was considerably shorter than the 228 ms reported by Kirchner and Thorpe ([20]). Individual median reaction times (correct trials) ranged between 159 and 197 ms except for one subject at 255 ms.

Inter-species comparisons

This second part of our study was intended to explore the similarities between humans and monkey by making extensive comparisons on the 382 common individual target images.

The examination of the human saccadic distribution in figure 4 (and saccadic distributions of individual subjects) suggests that reaction times below the 120 ms are likely to be anticipatory saccades. Indeed, the overall performance for saccades below 120 ms is 40% correct only. Such anticipatory saccades were virtually absent in the monkey distribution (only 3 latencies were below 80 ms). Hence, for comparison with the monkey, we kept human latencies that were between 120 ms and 400 ms (7907 saccades, 65% correct) and monkey latencies between 80 ms and 400 ms (4022 saccades, 67.25% correct). On this set of data, the performances of both species were quite similar, although the monkey was statistically slightly more accurate ($\chi2 = 6.35$, df = 1, p = 0.0118).

An important issue was to test whether both primate species use a similar strategy by looking at the performance on the same pairs of images. The relationship between the performance of the humans and the monkey on individual images is shown with the linear regression plot in Figure 5A. The regression equation ($Y = 42.744 + 0.322 * X$; $R^2 = 0.177$) indicates that there was a slight tendency for humans and the monkey to perform similarly on each pair of images. Another way to express the similarity of

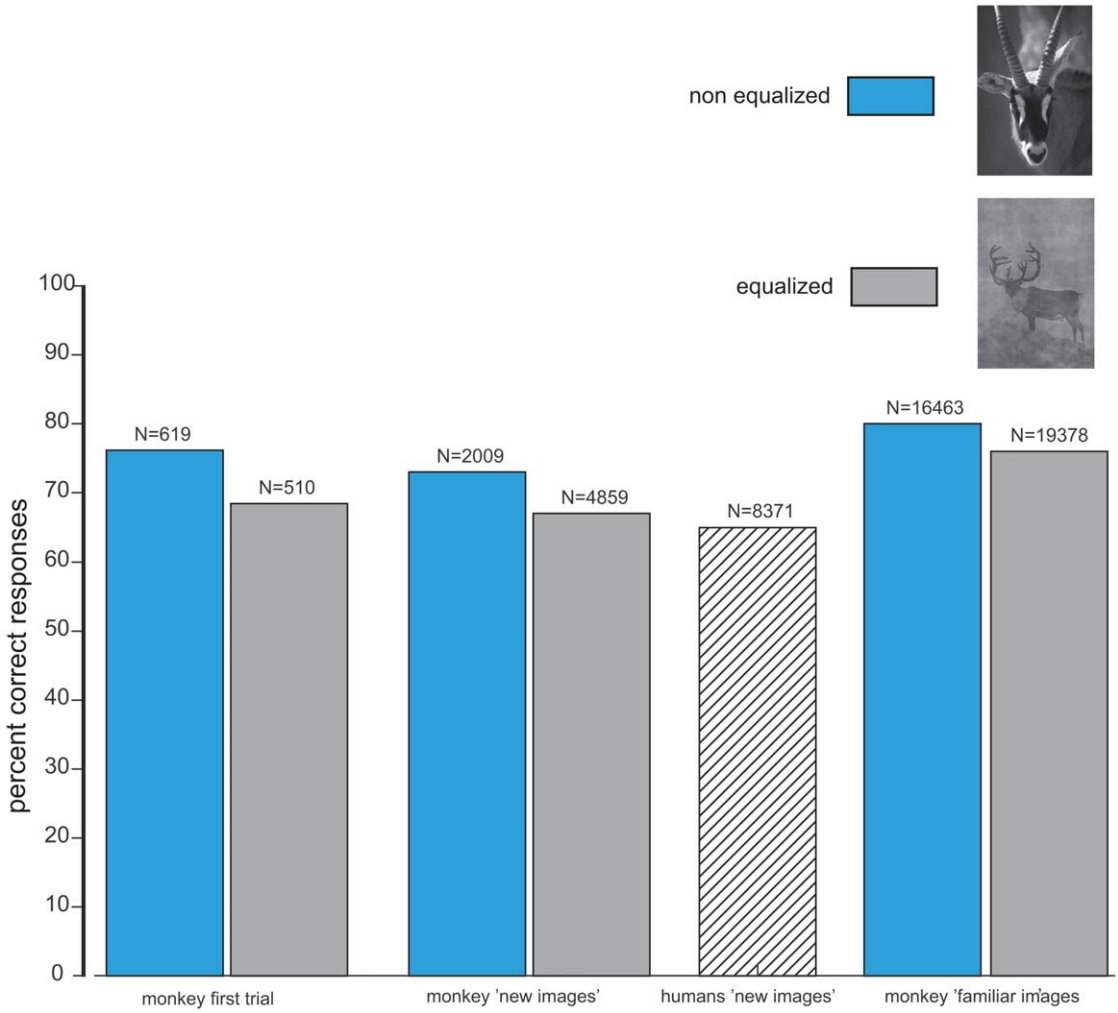

Figure 2. Performance accuracy. Bar plot of the percent correct responses obtained by humans and the monkey on equalized (grey) or non-equalized images (blue, former study). The number of trials is indicated on top of each bar.
doi:10.1371/journal.pone.0016453.g002

performance between both species is by using the distribution of the difference of percent correct responses (Figure 5b). The distribution is approximately centred on zero and shows that most targets did not elicit more than 10–20% difference of performance between the monkey and humans (the median of the distribution is at 5% difference). However, since the distribution is quite broad, there were a number of images on which the monkey and the humans performed differently.

We further explored which characteristics of the images could lead to similar responses in both species. We only focused on the content of the targets and not on that of the distractors. The first characteristic we examined was the presence of faces, which are potentially attracting features in the targets. To compare human and monkey performances, we split the images into several subcategories according to the status of the face. Each target could be either a close-up view of a face or a full-body presentation; these two kinds of targets were further split in two groups according to the orientation of the face (full-face view or profile view). Only targets belonging to the class of mammals were included in this analysis and 15 images were excluded because they contained several individuals with different head orientations; hence the analysis relied on 268 images. The monkey and the humans had a similar response profile with respect to faces (figure 6). Face close-up views elicited better responses than full-bodies, this being particularly prominent in the monkey (U Mann-Whitney; monkey: $U = 3664$, $p<0.0001$; humans: $U = 4565$, $p = 0.0079$. Median latencies were slightly shorter for face close-up than for full-bodies, but only in the monkey (monkey: $U = 4908$, $p = 0.046$; humans: $U = 5715$, $p = 0.67$). Furthermore full-face presentations elicited better scores than profile views (Monkey: $U = 6933$, $p = 0.013$, humans: $U = 6934$, $p = 0.013$). Full-face presentations elicited shorter median latencies than profile views in the monkey (Monkey: $U = 7107$, $p = 0.03$, humans: $U = 7365$, $p = 0.074$). Within close-up and full body categories (figure 6), the performance for full-face was always above that for profile views but this did not reach statistical significance in both monkey and humans. Finally, in terms of minimum latencies, face close-up views were better for the monkey (90 ms) than other views (100 ms) whereas in humans, all kind of views elicited a 140 ms minimum reaction time except profile views (170 ms). In summary, full-face or face close-up views were the most efficient stimuli both in terms of accuracy and speed.

A potential difference between the monkey and the humans is that the latter will have already seen exemplars of many species on different media, something that is much less likely for our monkey, who was born in captivity. Hence, we examined if both the

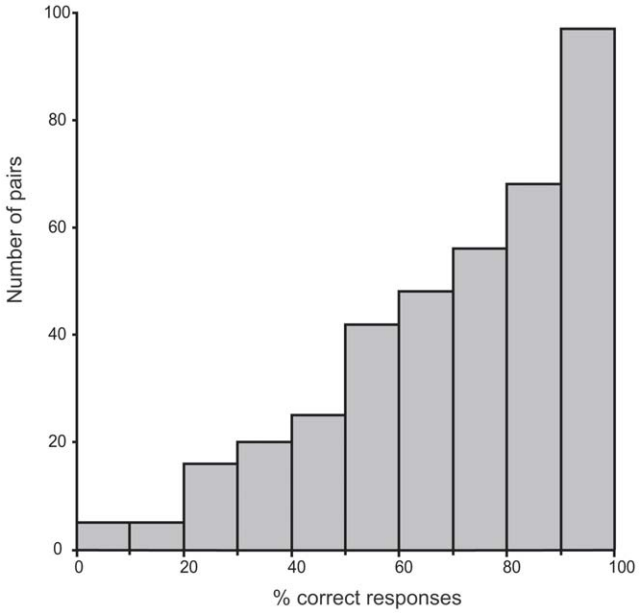

Figure 3. Accuracy on individual pairs of images. Distribution of the percentage of correct responses of the monkey with individual new pairs of stimuli that were presented for at least 10 trials.
doi:10.1371/journal.pone.0016453.g003

monkey and humans respond similarly to the different families of animals depicted in the targets. The term family here corresponds in most cases to the appropriate taxonomic family (Table S1) for mammals and birds but corresponds to the class for insects and fish, and the order in the case of reptiles. Note that although we chose a wide spectrum of animal prototypes, the experiment was not designed to present an even number of targets in each family. Figure 7a shows the respective performances of the monkey and humans on the different families of animals (corresponding to the 382 pairs in common). The monkey performed above 50% correct for most families. In most cases, the monkey was close to and even better than humans. The monkey was successful in categorizing some of the oddest animals (according to human standards) like the hedgehog (erinaceidae, 71% correct), the aardvark (orycteropodidae, 66.6% correct). She had difficulties for armadillos (dasypodidae, 44% correct) that differ from many species by having a very odd texture that was still visible in the equalized pictures. Both humans and monkey had difficulties with myrmecophagidae (anteaters) and procyonidae (coatis, raccoons). Figure 7b shows that the mean percent correct responses obtained by humans and the monkey on the different families are positively and significantly correlated (regression equation: $y = 33.426 + 0.542 * x$; $R^2 = .342$, $P<0.0001$).

The overall good performance of the monkey on various families could potentially result from the fact that, among the different species of target animals, some were also used (although on different images) in the familiar images that were repeated across sessions (for instance, the bald eagle was one of the familiar images and 5 other new pictures contained a bald eagle (see Table S1) This concerned 92 images out of the 382 targets. The monkey performed better on the images containing a familiar species (overall performance 72% correct) than on those depicting an unfamiliar one (overall performance 66% correct). This difference was significant ($\chi 2 = 12.4$, $df = 1$, $P<0.0005$). This was also the case if we consider only the very first presentation of each image (75% correct for familiar species and 64% for new species). Interestingly, humans, who never saw the familiar images of the monkey and had only one session, performed similarly on both

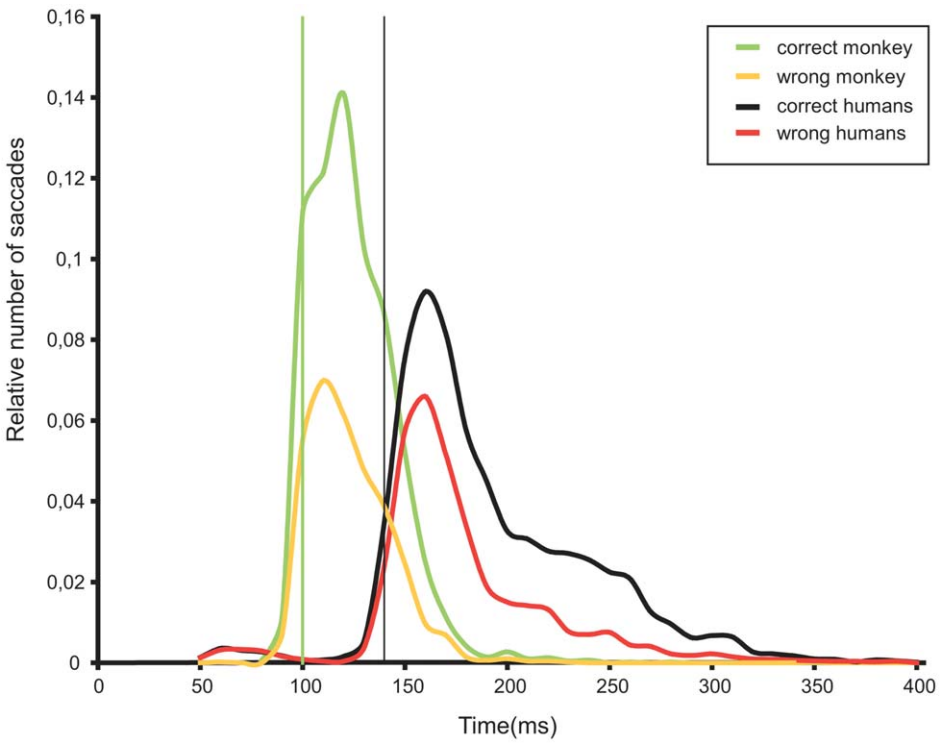

Figure 4. Distribution of correct and incorrect saccades (relative number of trials) for humans and the monkey. Vertical bars indicate the minimum reaction times (for monkey in green and humans in black).
doi:10.1371/journal.pone.0016453.g004

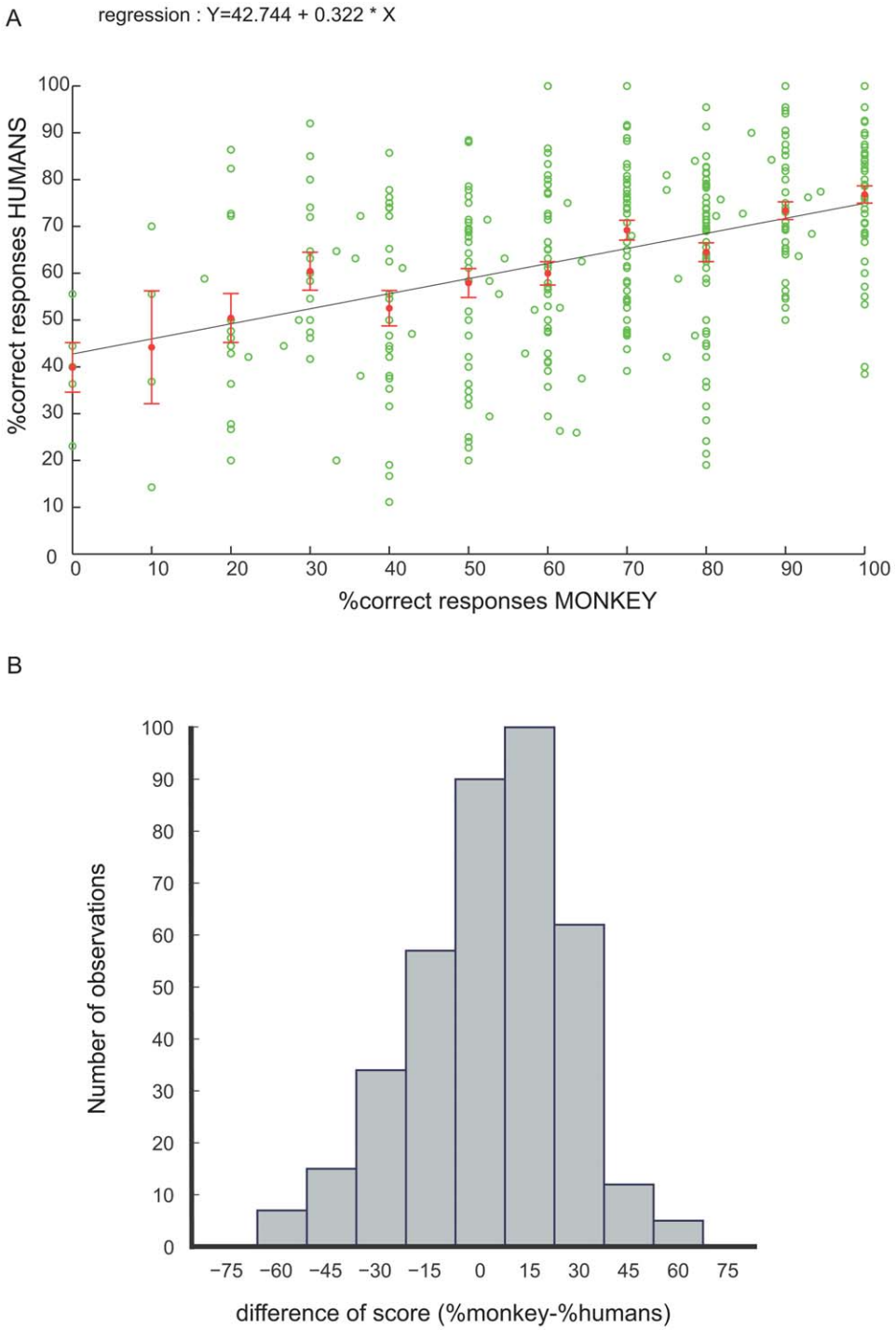

Figure 5. Comparison of accuracy of humans and monkey. 5a: regression plot of the percentage of correct responses for humans as a function of the score of the monkey for each individual pair of stimuli. Red dots indicate the mean score of humans for each 10% correct bins. Error bars show the standard error of the mean. 5b: histogram of the difference in performance of the monkey and the humans on individual pairs of images.
doi:10.1371/journal.pone.0016453.g005

groups of images (overall respective performances were 66% and 64.5% correct; $\chi 2 = 1.56$, df = 1, P = 0.21). Hence, in the monkey, the advantage for familiar images generalized to other exemplars of familiar species. Could familiarity generalize to similar animal species that were not strictly the same? For instance, if a familiar image depicted a leopard, could the monkey give better responses to cats or tigers that were not represented in the familiar pictures? These 'close-to-familiar' species involved 103 images (excluding the former 92 with familiar species in the strict sense). The monkey performed better on this subset of images (68.4%) than on non-familiar images (64.4%) but the significance was much lower ($\chi 2 = 5.11$, P = 0.0239). Humans, like the monkey, performed

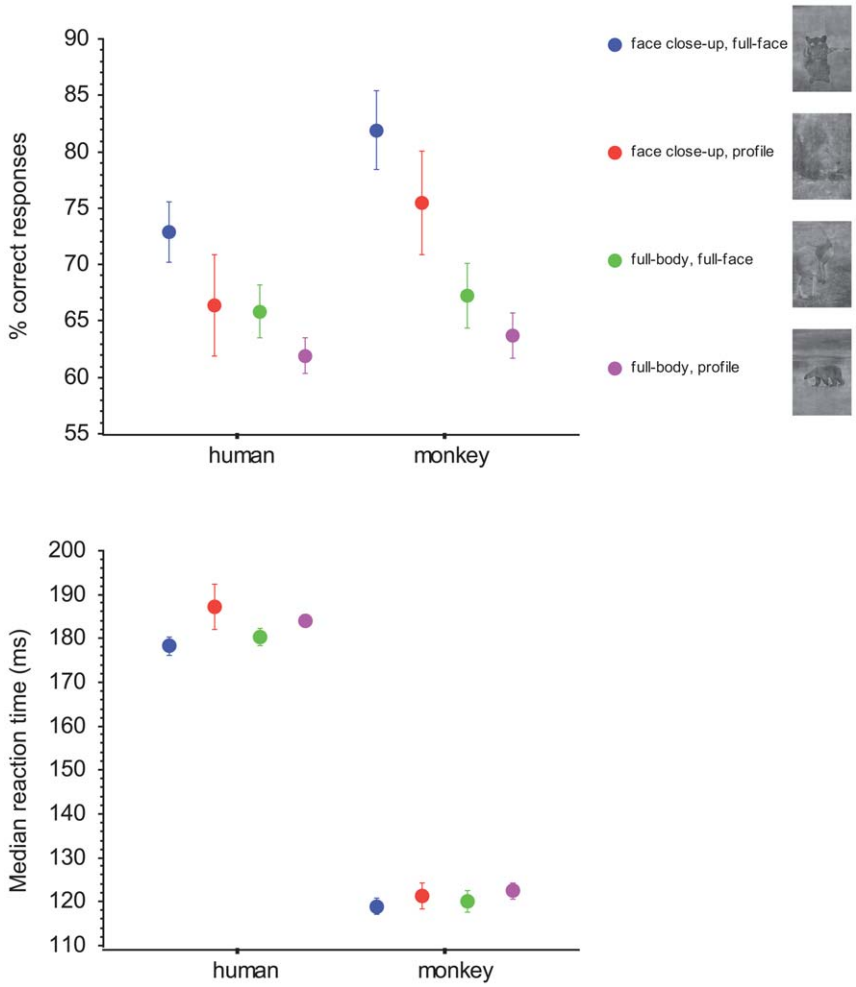

Figure 6. Advantage for faces. Percentage of correct responses and median reaction times of the monkey and human subjects to different views of the face in the target stimuli (mammals).
doi:10.1371/journal.pone.0016453.g006

better on the subset of 'close-to-familiar images' (66.6% and 63.4% respectively, $\chi 2 = 6.51$, $P = 0.01$). For both the monkey and humans, there was no difference in term of speed for familiar versus non-familiar species (monkey: $U = 1962441$, $P = 0.0927$; humans: $U = 5556532$, $p = 0.2078$). For the monkey, the median reaction time was 120 ms for both familiar and non-familiar species and the minimum reaction time was 100 ms in both cases.

Role of low spatial frequencies

In this experiment, the low-pass filtered images had an extremely degraded visual aspect. However for some of them, one can clearly detect the animal in the picture (figure 8a). The five new human subjects (who did not take part in the experiment with saccades) managed to correctly locate the animal in 75.76% of the pairs. The performance increased with confidence in ratings. Humans rated 60% of the trials as 1 (example of targets from those trials in fig. 8a right). Although 1 meant pure guessing, they performed above chance (67.73% correct, $\chi 2 = 74.87$, $df = 1$, $P<0.0001$) in that case. When they were sure of their choices (rating 5, 9% of the trials, figure 8a left), they reached 96% correct responses. For intermediate ratings (2, 3 and 4), the respective performances were 83.28, 89.63 and 89.67% correct. It is then interesting to compare the score of the forced-choice detection of the 5 subjects with low-pass filtered-images with the performance obtained in forced-choice saccadic detection by the monkey and the previous human subjects. For each trial made by a subject, we computed the rating index such that the rating given for each pair of images is multiplied by -1 if the response is incorrect and by 1 if correct. Figure 9a shows the mean percent correct responses of the humans and the monkey to individual pairs in the saccadic task as a function of the median rating index obtained by the 5 human subjects on the same filtered pairs. The example in figure 8b illustrates an extreme case of a pair with a median rating index of -3 and that led to 19% and 40% correct responses in humans and monkey respectively in the saccadic task. The data showed a similar trend for the humans and the monkey: the best performance in the saccadic task is obtained for those pairs that had the higher rating index. We did not observe a correlation of the median rates with median latencies for both species (figure 9b).

Discussion

Main results

These results confirm the ability of primates to perform this high-level task by means of saccadic responses [4,20]. The main result of the present paper is that even with images equalized in Fourier-spectrum, both monkeys and humans can efficiently

A

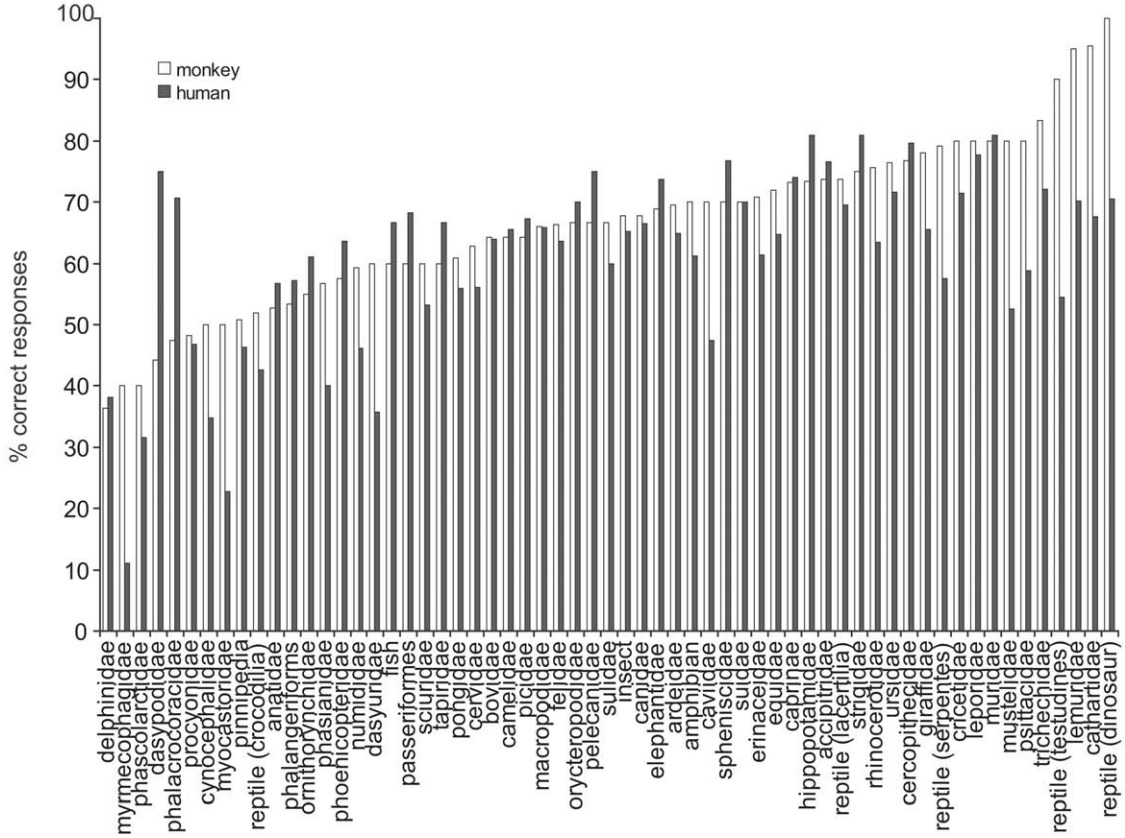
% correct responses
monkey
human
delphinidae
myrmecophagidae
phascolarctidae
dasypodidae
phalacrocoracidae
procyonidae
cynocephalidae
myocastoridae
pinnipedia
reptile (crocodilia)
anatidae
phalangeriformes
ornithorynchidae
phasianidae
phoenicopteridae
numididae
dasyuridae
fish
passeriformes
sciuridae
tapiridae
pongidae
cervidae
bovidae
camelidae
picidae
macropodidae
felidae
oryctéropodidae
pelecanidae
suidae
insect
canidae
elephantidae
ardeidae
amphibian
cavidae
sphenisciidae
suidae
erinaceidae
equidae
caprinae
hippopotamidae
accipitridae
reptile (lacertilia)
strigidae
rhinocerotidae
ursidae
cercopithecidae
giraffidae
reptile (serpentes)
cricetidae
leporidae
muridae
mustelidae
psittacidae
trichechidae
reptile (testudines)
lemuridae
cathartidae
reptile (dinosaur)

B

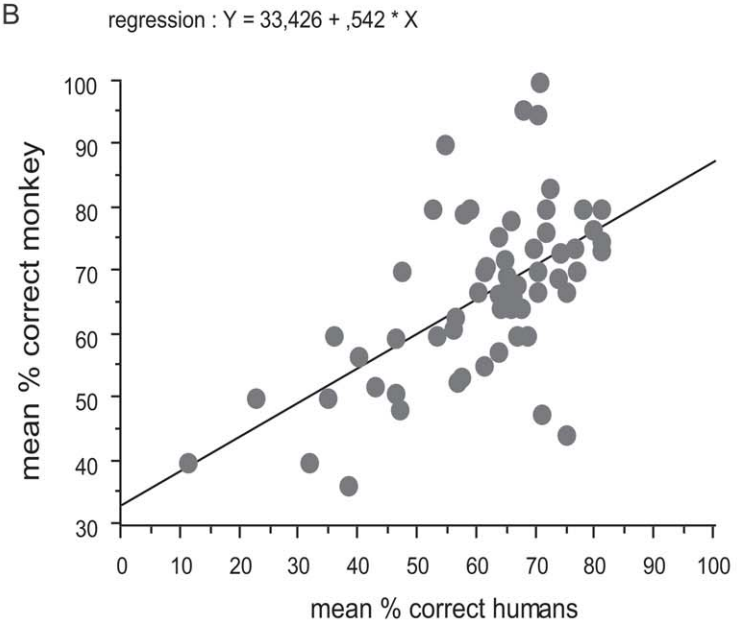
regression : Y = 33,426 + ,542 * X
mean % correct monkey
mean % correct humans

Figure 7. Responses to different animal families. 7a: bar plots of the respective percentage of correct responses for humans and for the monkey to different animal families. The number of stimuli contained in each family is very variable. 7b: mean percent correct responses of the monkey to different families of animals plotted against corresponding responses of human subjects. Also shown is the regression line.
doi:10.1371/journal.pone.0016453.g007

perform the ultra-rapid categorization of animals in natural scenes. Despite the degraded visual aspect of the stimuli, each subject performed above chance level. Importantly, the monkey also readily performed well above chance on equalized images. The monkey made accurate discriminations on images that were completely new, and even on the very first presentation (68.5% correct). The performance on first trials is an important issue considering the work of Cook and Fagot [21] who found that baboons can form long-term memory traces of numerous images from the first trial of presentation. Note here that the degraded aspect of the images is such that the performance with new images is below usual acquisition criteria for discrimination learning (for instance 75% correct in [12]) but mean accuracy on new images was above chance and comparable (if not better) than human subjects.

The use of equalized images rules out the possibility that target animals could be discriminated solely on the basis of a bias in the global statistics of contrast, luminance or spatial frequency content as suggested by computational studies [22]. However, we cannot make the suggestion that the amplitude spectrum has no contribution to the task. Indeed, the most noticeable effect of equalization was a moderate reduction in performance in comparison to the results obtained with 'intact' images'. Reductions of performances have also been reported by other authors who recently assessed in humans the role of the amplitude spectrum and its interaction with the phase content in similar tasks [23,24]. In our study, this reduction was similar in humans and the monkey since both species reached an overall level of accuracy around 65%–68%. In the monkey, the decrease from 73 to 68% (for new images) is in the same range as the decrease of 6% observed in monkeys that performed an animal categorization task when the luminance is altered [25]. Joubert and collaborators [18] also found a decrease of 6% in human accuracy with equalized images in a go/no-go task but on a different category discrimination (natural vs. man-made "context"). However, the mean accuracy of our human subjects was much lower (63.74%) than in Kirchner and Thorpe's experiments (90%) that also used saccadic responses. This drop in accuracy was in the range of the 16% drop in accuracy observed by Wichmann and collaborators when their human subjects performed a saccadic categorization of

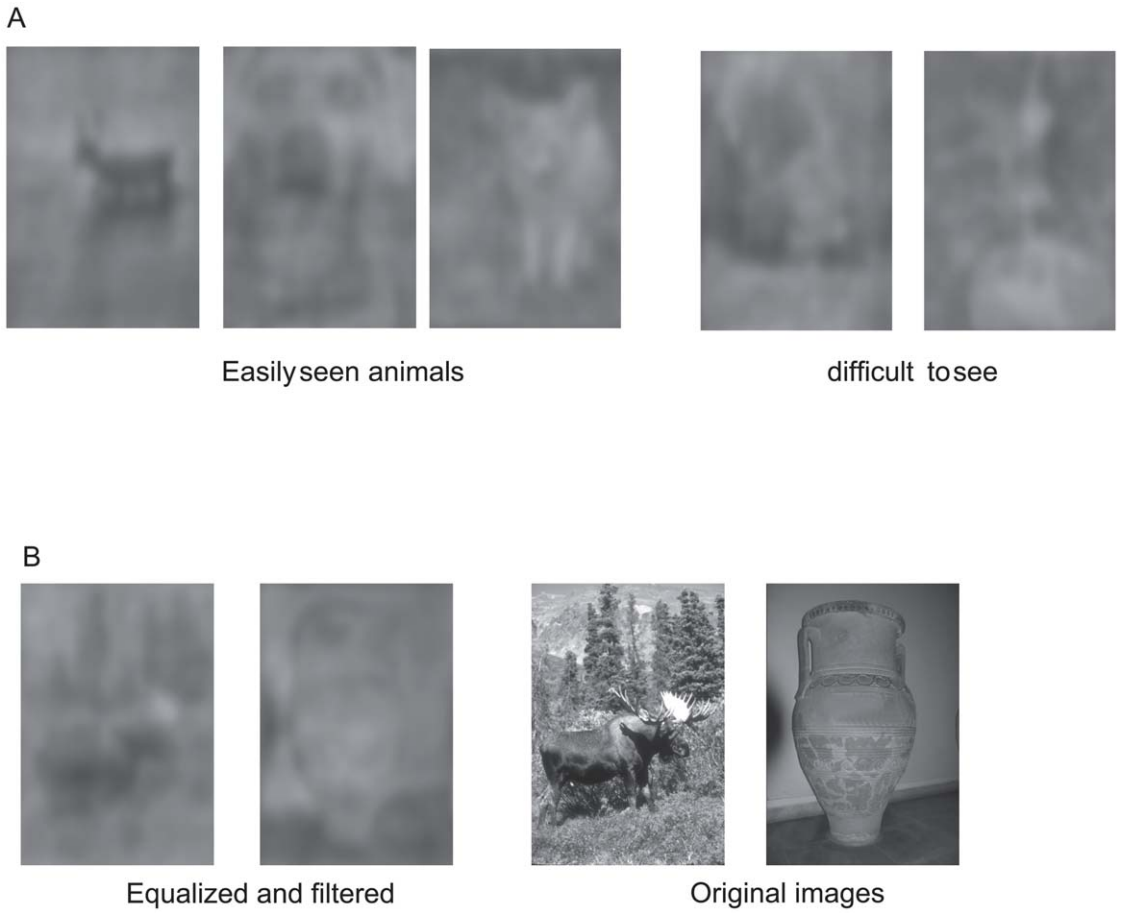

Figure 8. Examples of low pass-filtered equalized images. 8a: targets with various levels of visibility (3 left images are easily visible, 2 rightmost images are difficult). 8b: example of a pair that was miscategorised by both the humans and the monkey. The equalized and filtered version is shown on the left side and the original images on the right.
doi:10.1371/journal.pone.0016453.g008

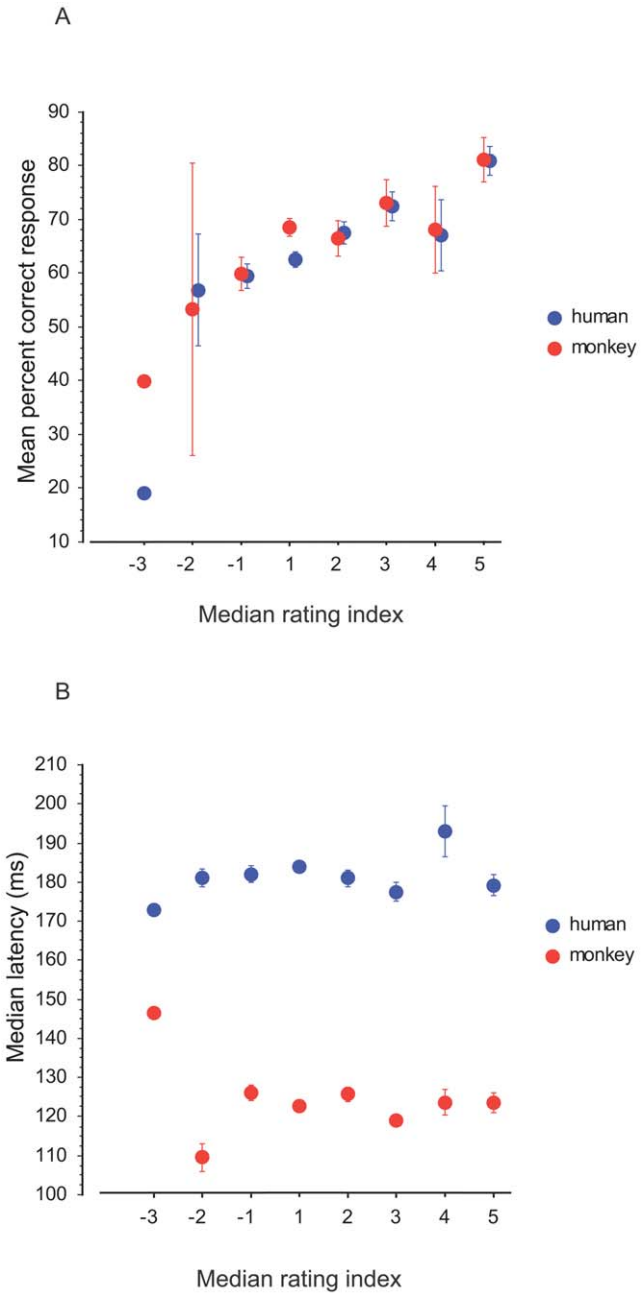

Figure 9. Role of low spatial frequencies. Scores obtained by humans and monkey in the saccadic experiment are plotted as a function of the median ratings given by different human subjects. Ratings ranged from 1 to 5 and were multiplied −1 for wrong responses.
doi:10.1371/journal.pone.0016453.g009

animals on a subset of images in which both the target and the distractor were 'difficult'[24]. These authors suggested that this difficulty might be a consequence of how photographers adjust the depth-of-field: difficult animals were not segregated from the cluttered background whereas difficult non-animals were segregated from a blurred background (hence being confusable with a portrait of a living subject). We think that the relatively low mean scores of our subjects comes from the fact that we have chosen our images with a bias towards difficulty and the use of distractor stimuli that nearly always contained a salient object. The results of the rating experiment suggest that it was the case. Let us consider the case of a pair of stimuli such that an animal was very well segregated and the distractor a uniform desert scene: as low pass filtering would not strongly affect the appearance of the target, subjects would have given a rate of 5. However, this was rarely the case (for instance we took care to select distractors with salient objects rather than with uniform landscapes) and the subjects actually reported that they were guessing for 60% of the low-pass filtered pairs, a result that argues strongly that our image set was particularly biased in favour of difficult image pairs.

Mechanisms of the categorization task

In our task, subjects are under time constraints that would encourage the use of processing strategies that could have been inherited from a common ancestor [2]. One possibility for an efficient categorization is a coarse holistic analysis of objects based on fast processing of low spatial frequencies [7,17,26]. The model of Bar [17] is an interesting framework which postulates that a coarse (low spatial frequencies) global magnocellular afferent information rapidly reaches the orbitofrontal cortex. This region then sets up predictions about what the stimulus was and sends back possible matches to be validated in ventral regions including inferotemporal cortex. The advantage is a reduction in the number of possible solutions to make recognition more efficient. Let us examine whether our data are consistent with this framework:

In the rating task, the human subjects saw a low-pass filtered version of the images and could correctly detect the animal in the majority of cases. Performance was correlated with the percentage of correct responses obtained with saccadic responses to the non-filtered versions of the images. This means that images were correctly categorized more often when they were easily understandable in their low-pass filtered version. Furthermore, it should be recalled that in the saccadic task, the images were centred at 5° of eccentricity, where low spatial frequency processing is even more important than in the rating task, which used free viewing. Interestingly, the performance of our human subjects with equalized images compares in terms of percent correct responses with that obtained by other authors with images below 10% contrast, a condition in which discriminability was reduced [25]. Performance was also close values obtained when categorization is done in the far peripheral visual field [27] where the influence of the magnocellular pathway is dominant.

More evidence about a predominant contribution of the magnocellular pathway to the categorization task comes from the reaction times of the subjects. Both species performed the task with very fast reaction times that were in the range of the latencies reported for non-equalized images. Minimum reaction times for both the monkey and the humans were virtually unchanged with respect to previous studies [4,20]. However median reaction times decreased in particular with human subjects (56 ms shorter). This could result from the fact that we used 400 ms presentation time instead of 20 ms in Kirchner and Thorpe's study. Indeed, recent studies [11,28] used 400 ms presentation time in a face detection task and obtained mean median reaction times, in humans, of about 180 ms, roughly equivalent to the median reaction times of 172 ms seen with our subjects. The extreme rapidity of the saccades places strong constraints on the brain mechanisms underlying the processing of complex stimuli. The minimum saccadic reaction times around 100 ms and the distribution of neuronal latencies in different cortical areas [7,29] preclude the possibility that the categorization process uses multiple iterations between brain regions before the motor response. There is indeed converging evidence from different experimental techniques that visual information rapidly reaches the cortical frontal regions. Brain recordings in patients have demonstrated very short latencies in the

frontal eye fields [30] reaching the amazing value of 45 ms with depth electrodes [31]. MEG and FMRI experiments in humans show that in a picture recognition task, the orbitofrontal cortex is rapidly activated by visual signals carrying low spatial frequencies (the reported MEG activity starts to develop before 100 ms), that could well originate from fast dorsal magnocellular pathways [32]. Our results point to a fast recognition mechanism based on low frequency contents that fits with Bar's framework, although our use of equalized scenes makes it unlikely that a simple categorization rule could be used. Intermediate level cues such as specific contours [33–35], may reflect the set of templates elaborated in frontal regions (after the arrival of the fast feedforward magnocellular information) in order to generate a set of initial hypotheses.

Have we some evidence of such 'templates' from our data? Faces are known to have a special significance and attractiveness in primates [36–38]. Recent fMRI investigations in both macaques and humans revealed that more brain areas are devoted in face processing than in other body parts [39]. Furthermore, fMRI reveals that face patches have the same relative size in the cortices of humans and monkey [40]. In agreement with these studies, we found in both the monkey and humans a similar trend towards much higher performance with full-face and close-up views of faces with respect to profile and full-body views. Although there is clear evidence of a special status of conspecific faces through expertise [41–43], we found that close-up view of full-faces of a large variety of animals (at least mammals) were also more attractive than profile views and full bodies. Hence prototypes of faces are the most obvious candidates as default templates used for guessing the identity of the input stimulus in fast categorization. Our results fit with the recent results of Crouzet and collaborators [28] who found an excellent saccadic detection of conspecific faces in humans and of Fletcher Watson et al [44] who found systematic attraction by faces in free-gazing of natural scenes. Reactions are extremely fast in all these studies. However, more experiments are required to decide between two alternatives. The first one would rely exclusively on feedforward mechanisms, with no time for the use of feedback. The second possibility is that a fast top-down signal carrying the most probable guess (the face) comes into play to trigger fast reaction times. However in that case, because of the saccadic response constraint, it would have no time to be compared with the slower detailed information arriving into the ventral pathway to validate the guess (latencies were not longer for difficult pairs and this was also the case in the study by Wichmann et al. [24]).

Role of familiarity

In addition, our results seem to indicate that the formation of templates can be quite rapidly modulated 'on line' over the period of the experiment sessions. Humans seem to be perfectly able to categorize even very unusual animal species as animals (at least for vertebrates). Each one of us is able to recognize a platypus or an anteater as an animal, and we can even do the same thing for very unusual prehistoric or even imaginary species [45]. The contribution of innate or cultural factors to picture recognition may not be a trivial issue but some studies have shown that people remote from the imaged-overloaded 'modern' civilization can recognize the presence of animals in pictures [46]. Since macaque monkeys do not normally have access to human media (although they could see some occasional TV programs as enrichment in our animal facility), it was interesting to assess the monkey's cognitive capacities in categorizing diverse types of animals. As a whole, the monkey performed similarly to humans for a large variety of families of mammals and members of other animal classes. Nevertheless, the correlation of the performances of both species on individual pairs of stimuli was rather modest. It is then important to emphasize the fact that the monkey made correct responses even if the animal targets belonged to a species that had never been presented before, although she performed more accurately on images that contained a species already presented in familiar images. In contrast, humans do not get advantage from their cultural background in the task since the percentage of correct responses obtained by humans and monkey on the non-familiar images are very similar (humans perform below the level reached by the monkey with familiar images). Hence the higher scores obtained with familiar species by the monkey is likely to be caused by a priming by the familiar images that were randomly interleaved with new ones rather than a natural propensity of monkeys to recognize these species or an inadvertent bias towards 'easy features' contained in these images. The effect of familiarity seems to occur rapidly since responses to first presentation of familiar species are about 10% better than responses to first presentations of new species. Determining to what extent this familiarity process takes place in the frontal cortical regions would be an interesting future experiment since, in the framework of Bar's model, this may influence the selection of the templates that are used to perform the task.

Supporting Information

Table S1 Details of animal species used in the study. Each line corresponds to one target. Columns indicate the class, the family, the common name and the scientific name. Last two columns indicate whether the image was used in humans and whether the animal target belonged to the familiar species seen by the monkey. At least 165 species were used. 97 could be determined with certainty; the others were undetermined and could belong to more than 68 different species. For mammals and birds, these species belonged to 56 different taxonomic families (53 used in both monkey and humans), with the following deliberate misclassifications: passeriforms (order), caprinae (subfamilia), phalangeriforms (suborder) for possums, echidna and okapi were deliberately misclassified in erinaceidae and equidae respectively, according to their aspect. Reptiles, amphibians, insects and fish were considered under the class name only.
(XLS)

Acknowledgments

Denis Fize for help in the design of stimuli, Angeline Mantione, Bénédicte Leveillé for animal husbandry, Pascal Barone, Simon Thorpe and Lionel Nowak for discussion.

Author Contributions

Conceived and designed the experiments: PG. Performed the experiments: PG RKR. Analyzed the data: PG RKR. Wrote the paper: PG.

References

1. Passingham R (2009) How good is the macaque monkey model of the human brain? Curr Opin Neurobiol 19: 6–11.
2. Fabre-Thorpe M (2003) Visual categorization: accessing abstraction in non-human primates. Philos Trans R Soc Lond B Biol Sci 358: 1215–1223.
3. Delorme A, Richard G, Fabre-Thorpe M (2000) Ultra-rapid categorisation of natural scenes does not rely on colour cues: a study in monkeys and humans. Vision Res 40: 2187–2200.
4. Girard P, Jouffrais C, Kirchner H (2008) Ultra-rapid categorisation in non-human primates. Anim Cogn 11: 485–493.
5. Mace MJ, Richard G, Delorme A, Fabre-Thorpe M (2005) Rapid categorization of natural scenes in monkeys: target predictability and processing speed. Neuroreport 16: 349–354.
6. Tompa T, Sary G (2010) A review on the inferior temporal cortex of the macaque. Brain Res Rev 62: 165–182.

7. Nowak LG, Bullier J (1997) The timing of information transfer in the visual system. In: Rockland KS, Kaas JH, Peters A, eds. Extrastriate visual cortex in primates. New York: Plenum Press. pp 205–241.
8. Liu H, Agam Y, Madsen JR, Kreiman G (2009) Timing, timing, timing: fast decoding of object information from intracranial field potentials in human visual cortex. Neuron 62: 281–290.
9. VanRullen R, Thorpe SJ (2002) Surfing a spike wave down the ventral stream. Vision Res 42: 2593–2615.
10. Oliva A, Torralba A (2006) Building the gist of a scene: the role of global image features in recognition. Prog Brain Res 155PB: 23–36.
11. Honey C, Kirchner H, VanRullen R (2008) Faces in the cloud: Fourier power spectrum biases ultrarapid face detection. J Vis 8: 1–13.
12. D'Amato MR, Van Sant P (1988) The person concept in monkeys (Cebus apella). J Exp Psychol Anim Behav Process 14: 43–55.
13. Joubert OR, Fize D, Rousselet GA, Fabre-Thorpe M (2008) Early interference of context congruence on object processing in rapid visual categorization of natural scenes. J Vision 8: 1–18.
14. Fabre-Thorpe M, Richard G, Thorpe SJ (1998) Rapid categorization of natural images by rhesus monkeys. Neuroreport 9: 303–308.
15. Kiani R, Esteky H, Mirpour K, Tanaka K (2007) Object category structure in response patterns of neuronal population in monkey inferior temporal cortex. J Neurophysiol 97: 4296–4309.
16. Kriegeskorte N, Mur M, Ruff DA, Kiani R, Bodurka J, et al. (2008) Matching categorical object representations in inferior temporal cortex of man and monkey. Neuron 60: 1126–1141.
17. Bar M (2003) A cortical mechanism for triggering top-down facilitation in visual object recognition. J Cogn Neurosci 15: 600–609.
18. Joubert OR, Rousselet GA, Fabre-Thorpe M, Fize D (2009) Rapid visual categorization of natural scene contexts with equalized amplitude spectrum and increasing phase noise. J Vis 9: 1–16.
19. Bar M, Kassam KS, Ghuman AS, Boshyan J, Schmidt AM, et al. (2006) Top-down facilitation of visual recognition. Proc Natl Acad Sci U S A 103: 449–454.
20. Kirchner H, Thorpe SJ (2006) Ultra-rapid object detection with saccadic eye movements: Visual processing speed revisited. Vision Res 46: 1762–1776.
21. Cook R, Fagot J (2009) First trial rewards promote 1-trial learning and prolonged memory in pigeon and baboon. Proc Natl Acad Sci U S A 106: 9530–9533.
22. Torralba A, Oliva A (2003) Statistics of natural image categories. Network 14: 391–412.
23. Gaspar CM, Rousselet GA (2009) How do amplitude spectra influence rapid animal detection? Vision Res 49: 3001–3012.
24. Wichmann FA, Drewes J, Rosas P, Gegenfurtner KR (2010) Animal detection in natural scenes: Critical features revisited. J Vis 10: 1–27.
25. Mace MJ, Delorme A, Richard G, Fabre-Thorpe M (2010) Spotting animals in natural scenes: efficiency of humans and monkeys at very low contrasts. Anim Cogn 13: 405–418.
26. Bullier J (2001) Integrated model of visual processing. Brain Res Brain Res Rev 36: 96–107.
27. Thorpe SJ, Gegenfurtner KR, Fabre-Thorpe M, Bulthoff HH (2001) Detection of animals in natural images using far peripheral vision. Eur J Neurosci 14: 869–876.
28. Crouzet SM, Kirchner H, Thorpe SJ (2010) Fast saccades towards faces: Face detection in just 100 ms. J Vis 10: 1–17.
29. Schmolesky MT, Wang Y, Hanes DP, Thompson KG, Leutgeb S, et al. (1998) Signal timing across the macaque visual system. J Neurophysiol 79: 3272–3278.
30. Blanke O, Morand S, Thut G, Michel CM, Spinelli L, et al. (1999) Visual activity in the human frontal eye field. Neuroreport 10: 925–930.
31. Kirchner H, Barbeau EJ, Thorpe SJ, Regis J, Liegeois-Chauvel C (2009) Ultra-rapid sensory responses in the human frontal eye field region. J Neurosci 29: 7599–7606.
32. Kveraga K, Boshyan J, Bar M (2007) Magnocellular projections as the trigger of top-down facilitation in recognition. J Neurosci 27: 13232–13240.
33. Biederman I, Cooper EE (1991) Priming contour-deleted images: evidence for intermediate representations in visual object recognition. Cognit Psychol 23: 393–419.
34. Biederman I, Ju G (1988) Surface versus edge-based determinants of visual recognition. Cognit Psychol 20: 38–64.
35. Lloyd-Jones TJ, Gehrke J, Lauder J (2010) Animal recognition and eye movements: the contribution of outline contour and local feature information. Exp Psychol 57: 117–125.
36. Pascalis O, Petit O, Kim JH, Campbell R (1999) Picture perception in primates: The case of face perception; Picture perception in animals. Cahiers de Psychologie Cognitive 18: 889–921.
37. Sugita Y (2008) Face perception in monkeys reared with no exposure to faces. Proc Natl Acad Sci U S A 105: 394–398.
38. Gilchrist ID, Proske H (2006) Anti-saccades away from faces: evidence for an influence of high-level visual processes on saccade programming. Exp Brain Res 173: 708–712.
39. Pinsk MA, Arcaro M, Weiner KS, Kalkus JF, Inati SJ, et al. (2009) Neural representations of faces and body parts in macaque and human cortex: a comparative FMRI study. J Neurophysiol 101: 2581–2600.
40. Tsao DY, Freiwald WA, Knutsen TA, Mandeville JB, Tootell RB (2003) Faces and objects in macaque cerebral cortex. Nat Neurosci 6: 989–995.
41. Dufour V, Pascalis O, Petit O (2006) Face processing limitation to own species in primates: a comparative study in brown capuchins, Tonkean macaques and humans. Behav Processes 73: 107–113.
42. Dahl CD, Wallraven C, Bulthoff HH, Logothetis NK (2009) Humans and Macaques Employ Similar Face-Processing Strategies. Curr Biol 19: 509–513.
43. Gothard KM, Brooks KN, Peterson MA (2009) Multiple perceptual strategies used by macaque monkeys for face recognition. Anim Cogn 12: 155–167.
44. Fletcher-Watson S, Findlay JM, Leekam SR, Benson V (2008) Rapid detection of person information in a naturalistic scene. Perception 37: 571–583.
45. Dixon D (1981) After man: A zoology of the future. New York: St Martin's Press: 124.
46. Deregowski JB, Muldrow ES, Muldrow WF (1972) Pictorial recognition in a remote Ethiopian population. Perception 1: 417–425.

III. Discussion

This work demonstrates that ultra-rapid categorization in macaque monkeys is not performed relying solely in low-level cues such as the mean Fourier amplitude spectrum, which has been shower earlier for humans (Joubert et al., 2008). Even with images equalized in their Fourier amplitude-spectrum, both monkeys and humans can efficiently perform the ultra-rapid categorization of animals in natural scenes. Despite the difficulty generated by degraded visual aspect of the stimuli, the task was performed significantly above chance by both monkey (67%) and humans (65%). However, these performances were lower than in previous studies (Girard, Jouffrais, and Kirchner 2008; Kirchner & Thorpe, 2006). This is certainly due to the degraded image aspect produced by the amplitude spectrum equalization. It is worth also mentioning that the deliberate choice of difficult distractors (i.e., distractors involving objects in complex scenes rather than simple landscapes) could also play a role in lowering the performances. Remarkably, despite the abovementioned, saccadic minimum reaction times (100 ms in monkeys and 140 ms in humans) were basically not different from those recorded in previous studies, involving monkeys (Girard et al., 2008) and humans (Kirchner & Thorpe, 2006; Crouzet et al., 2010). Our results also suggest that local low spatial frequency information could be important to the categorization performance, specifically regarding the hit rate reached on particular images. This finding is consistent with theories of top-down facilitation of object recognition involving the coarse and rapidly delivered magnocellular information (Bar 2003; Bar et al., 2006).

Even though we showed that by eliminating the amplitude-spectrum difference between categories, categorization is performed efficiently and, importantly, fast reaction times are unaffected; we still don't know if more complete representations of the object are required to perform ultra-rapid categorization. Unlike a feature based representation, which would be coded earlier in the visual cortex, an object based representation would require the activation of neurons of the ventral pathway which explicitly represent visual object categories, such as neurons located in the temporal lobe of monkeys in high-level visual areas such as the inferotemporal cortex (IT).

IV. Attempting a cooling study in high-level visual areas

Are neurons of the IT cortex necessary to perform ultra-rapid categorization? In order to test the causal role of IT neurons in ultra-rapid categorization, we developed a second experiment in which we used an inactivation approach. A number of strategies have been adopted to cool and thus deactivate neural tissue. We chose cooling deactivation due to its technical advantages, such as the fact that it does not lead to functional changes in the deactivated tissue after chronic application, and due to the full reversibility of cooling-induced effects (Lomber, Payne, & Horel, 1999). The cryoloop technique for cooling was originally described by Salsbury & Horel (1983). Using the cryoloop technique it is possible to customize the shape of the cooling devise in order to inactivate the target region in a more specific fashion than in techniques involving cryotips for example (see Figure 19). More recently, cryoloops have been chronically implanted subdurally in cats by (Lomber & Payne, 1996). The cryoloop method has been successfully used to test the involvement of area V4 in shape discrimination in match-to-sample task (Pascal Girard, Lomber, & Bullier, 2002). We used such an approach to test the causal role of anterior temporal areas in ultra-rapid categorization. One macaque monkey was implanted with a cryoloop aimed to inactivate TEO cortex. The same monkey used in the previous study was implanted and tested in an ultra-rapid animal/non-animal categorization task. However, we did not find any compelling result, neither in reaction times nor accuracy (data not shown). Post-mortem analysis revealed that, unfortunately, the cryoloop was placed more anteriorly than expected, resulting in the inactivation of cortical areas beyond the visual cortex.

Thus, the question whether complete object representations are necessary for ultra-rapid categorization or not is still unanswered, and waits for a definitive response.

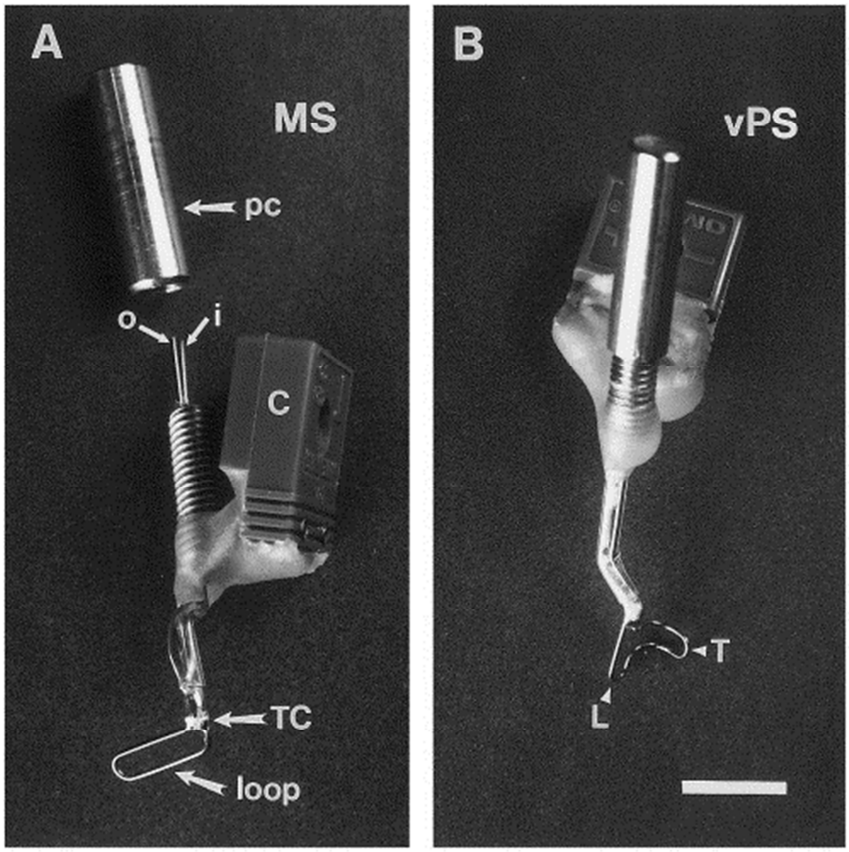

Figure 19. Cortical cryoloops. A. *Cryoloop constructed to be placed in the left middle suprasylvian (MS) sulcus of the cat. Protective cap (pc) has been removed to expose the ends of the inflow (i) and outflow (o) tubes. Tubes descend through the threaded cylinder and the heat-shrink Teflon tubing to the actual loop which is exposed to the cortical surface. The microthermocouple (TC) is attached to the union of the cryoloop. Its wires ascend through the heat-shrink Teflon tubing to the connector (C) affixed to the dental acrylic.* ***B.*** *Cryoloop constructed to be placed in Right ventral-posterior suprasylvian (vPS) showing a similar overall construction. Scale bar, 10 mm. (From Lomber et al., 1999).*

As discussed in the introduction, there is a body of evidence supporting the fact that ultra-rapid categorization is performed automatically and pre-attentively (VanRullen and Koch 2003; Li et al., 2002; Reddy et al., 2006; Honey et al., 2008). Moreover, it was shown that agnostic patients (with disorders involving the conscious recognition of objects) can perform rapid categorization (Boucart et al., 2010).

Ultra-rapid categorization is useful to study the minimal mechanisms to process visual stimuli in order to class them into semantic categories. In order to study conscious objects representations, less stringent approaches are needed. As we have discussed in the introduction, attention is the door to higher-level and conscious representations. In the next section we will temporary set aside our study on visual representations in order to study the dynamics of attention: the key to higher level representations.

C. Where and when spatial is attention deployed?

Attention is the key to the doors of conscious perception. Selecting a part of all available information, it guides the visual system towards the elements of the visual field that deserve to be treated as priority. It allows making sense of the plethora of information arriving from our sensory systems by filtering irrelevant stimuli. It can select stimuli attributes belonging to a variety of dimensions—color, location, shape, etc. In the case of spatial attention, stimuli lying within the part of the visual field where it is deployed are processed faster and/or more accurately. The deployment of spatial attention takes some time and it fades away after a while. Even though many studies of spatial attention have been separately focused on its spatial deployment or temporal dynamics, few studies have considered its spatiotemporal dynamics as a subject of study.

Thus, no systematical approach has succeeded in generating a complete picture of where and when the doors of perception are opened by spatial attention. Does the spatial pattern of attention evolve across time?

I. The paper of Tse, 2004

Few works have directly addressed the question of how spatial attention evolves over time. One of these attempts is the work of Peter Tse (Tse, 2004), in which a mapping of attention in space and time was performed using a change blindness paradigm. The experimental setup consisted in a colored point-pattern (Figure 20a, frame 1) which was showed during 306 ms (Figure 20a, frame 2). After that, an exogenous cue was flashed during 47 ms at 1 of 4 possible locations (Figure 20a, frame 3). This pattern was maintained for a certain amount of time (12, 82, 153 or 447 ms) followed by a blank screen flashed for 47 ms (Figure 20a,

frame 4). After that, the pattern was presented again, but one of the points changed its color (Figure 20a, frame 5). The task was to detect the square that changed its color.

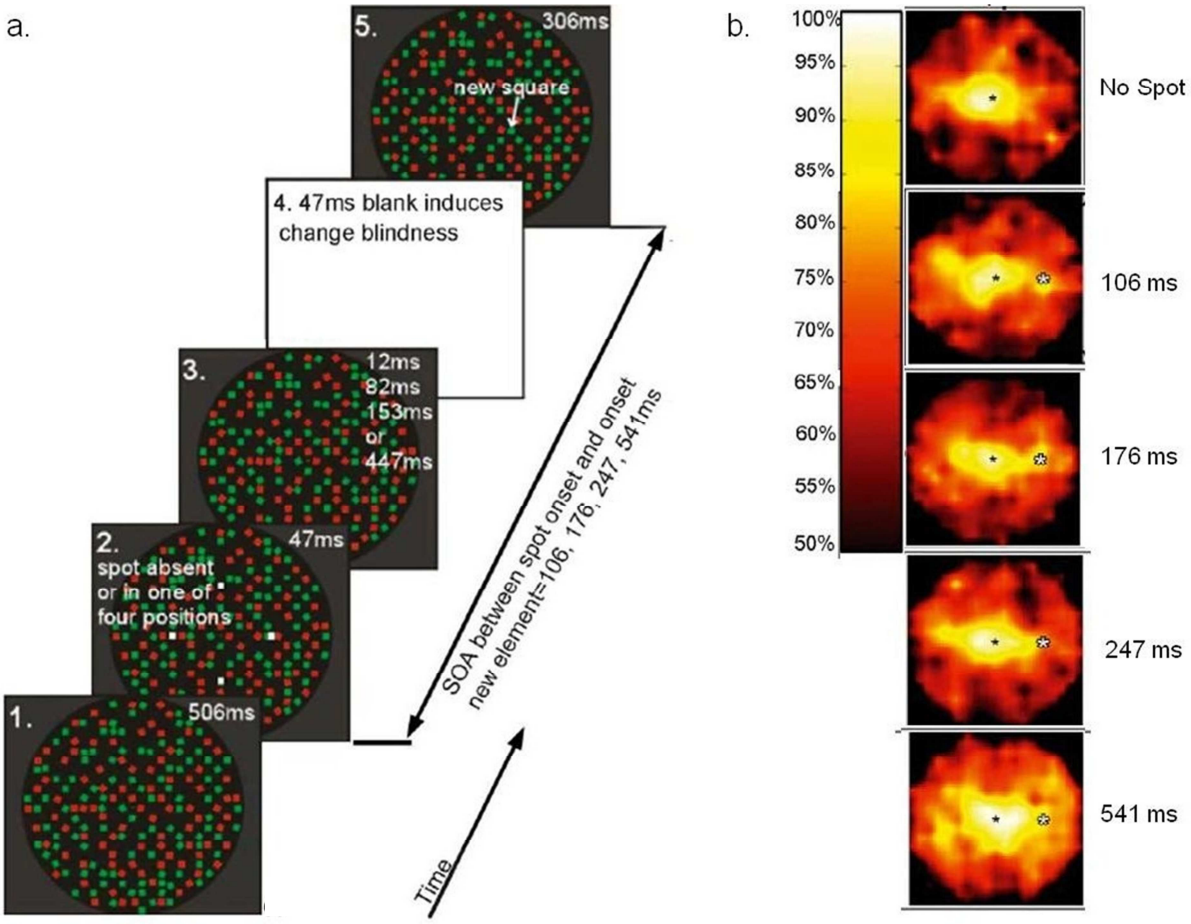

Figure 20. Experimental design and main results of Tse's study. *The trial sequence is illustrated in* ***A.*** *On cued trials, a spot appeared in Frame 2, and Frame 3 was presented for one of three durations. On non-cued trials, there was no spot in Frame 2, and Frame 3 always lasted 12 ms. In the final frame of the sequence (Frame 5) on both cued and noncued trials, a new square was shown in one of 149 positions of the array; these positions represented a subset of the overall grid that fit within an imaginary 25° circle centered at fixation. The new square always appeared in a random position that had been unoccupied on previous frames within a given trial. The final frame always contained one and only one new element. The observers' task was to maintain fixation and report whether the new element was red or green.* ***B.*** *Average spatial maps showing*

the attention effects as a color code. The attention effect is represented as the percentage correct for no-cue trials (top panel, 'no spot') and cued trials (the cue position is represented by a white star) with each SOA. Each of the 149 tested locations shown in panel A could have a maximum of 30 correct responses. The fixation point is indicated at the center of each map (Modified from Tse, 2004).

The principal result of this work is an enhancing attentional effect opposite the cued location, which, in some cases, was greater than the one at the cued location. Still, this work failed to show any clear modulation of the attentional pattern across time. By and large, the interdependence between spatial and temporal dimensions of attention remains an unanswered question: How does the spatial pattern of attention evolve across time?

II. Paper 2. Koenig-Robert & VanRullen, Journal of Vision

Spatiotemporal mapping of visual attention

Roger Koenig-Robert CerCo, UPS, Université de Toulouse III, Toulouse, France, & CNRS, UMR5549, CHU Purpan, Toulouse, France

Rufin VanRullen CerCo, UPS, Université de Toulouse III, Toulouse, France, & CNRS, UMR5549, CHU Purpan, Toulouse, France

The spatial distribution and the temporal dynamics of attention are well understood in isolation, but their interaction remains an open question. How does the shape of the attentional focus evolve over time? To answer this question, we measured spatiotemporal maps of endogenous and exogenous attention in humans (more than 140,000 trials in 23 subjects). We tested the visibility of a low-contrast target presented (50 ms) at different spatial distances and temporal delays from a cue in a noisy background. The cue was a non-informative salient peripheral (5°) stimulus for exogenous attention and a central arrow cue (valid 66.6%) pointing left or right for endogenous attention. As a measure of attention, we determined, for each distance and delay, the background contrast compensation required to keep performance at 75%. The spatiotemporal mapping of exogenous attention revealed a significant enhancement zone from 150 to 430 ms, extending up to 6° from the cue. Endogenous attention maps showed a peak at the cued side at 400 ms and between 8 and 10° from the cue. Modeling suggests that the data are compatible with a constant spotlight shape across time. Our results represent the first detailed spatiotemporal maps of both endogenous and exogenous attention.

Keywords: attention, detection/discrimination, contrast sensitivity

Citation: Koenig-Robert, R., & VanRullen, R. (2011). Spatiotemporal mapping of visual attention. *Journal of Vision, 11*(14):12, 1–16, http://www.journalofvision.org/content/11/14/12, doi:10.1167/11.14.12.

Introduction

Selective attention allows a sensory system to extract relevant information from the massive data influx reaching peripheral sensors. In order to do that, attention can use one or more of the following mechanisms: signal enhancement (i.e., amplitude increase of the task-relevant sensory inputs; Carrasco, Penpeci-Talgar, & Eckstein, 2000; Carrasco, Williams, & Yeshurun, 2002; C. C. Liu, Wolfgang, & Smith, 2009; Lu & Dosher, 2000), external noise exclusion (i.e., inhibition of non-relevant information; Dosher & Lu, 2000; Lu, Lesmes, & Dosher, 2002), and internal noise reduction (i.e., decrease in the variance of the perceptual processing; Mitchell, Sundberg, & Reynolds, 2003). Attention can also select relevant information by orienting or allocating the processing resources toward or away from a given signal source. In the visual domain, spatial orienting of attention can involve either eye movements toward a visual stimulus, which is known as overt spatial attention, or a selection of a part of the visual field without moving the eyes, known as covert spatial attention (Posner, 1980). A large body of behavioral evidence has dissociated two distinct forms of covert attention orienting: stimulus-driven orienting or *exogenous attention* and goal-driven orienting or *endogenous attention* (Cheal & Lyon, 1991; Chica & Lupiañez, 2009; Corbetta & Shulman, 2002; Egeth & Yantis, 1997; Hein, Rolke, & Ulrich, 2006; Nakayama & Mackeben, 1989; Yantis & Jonides, 1990; Yeshurun, Montagna, & Carrasco, 2008).

Exogenous attention is triggered by abrupt-onset or salient stimuli and is mostly reflexive (i.e., bottom-up) with little contribution from volitional states (Corbetta & Shulman, 2002; Egeth & Yantis, 1997; Giordano, McElree, & Carrasco, 2009; Yantis & Jonides, 1990). On the other hand, endogenous attention is triggered by higher level mechanisms (i.e., top-down) and depends on the subject's expectations and knowledge (Corbetta & Shulman, 2002; Egeth & Yantis, 1997; Giordano et al., 2009; Hopfinger, Buonocore, & Mangun, 2000; Yantis & Jonides, 1990). Whether it is induced by exogenous or endogenous cues, the orientation of spatial attention toward a stimulus increases the perceptual performance (i.e., detection and/or discrimination) for stimuli falling within a neighboring spatial region (Eckstein, Peterson, Pham, & Droll, 2009; Egeth & Yantis, 1997; Huang & Dobkins, 2005; Lu & Dosher, 2000; Pastukhov, Fischer, & Braun, 2009; Posner, 1980; Shulman, Remington, & McLean, 1979; Talgar, Pelli, & Carrasco, 2004). Furthermore, this selection is not instantaneous but takes a certain time to develop and to subside (Müller & Rabbitt, 1989; Nakayama & Mackeben, 1989; Olivers & Meeter, 2008). These two attributes of visual attention, its spatial deployment pattern and its temporal dynamics, have often been studied in isolation. Over the years, a great amount of knowledge has been achieved about each of these two attributes independently.

doi: 10.1167/11.14.12 Received January 16, 2011; published December 12, 2011 ISSN 1534-7362

Concerning the spatial deployment of attention, most data have come from studies in psychophysics (Cheal & Lyon, 1991; Eriksen & St. James, 1986; Posner, 1980; Sagi & Julesz, 1986; Shulman et al., 1979) but also from neuroimaging (Hopf et al., 2005; Kanwisher & Wojciulik, 2000; Reddy, Kanwisher, & VanRullen, 2009) and neurophysiology (Chelazzi, Duncan, Miller, & Desimone, 1998; Desimone & Duncan, 2000; Luck, Chelazzi, Hillyard, & Desimone, 1997; Spitzer, Desimone, & Moran, 1988). In these studies, the spatial pattern of attention is generally studied at a fixed time after the cue onset, corresponding to the expected peak of the attention effect (Posner, 1980; Sagi & Julesz, 1986). Thus, regarding its key spatial properties of filtering and enhancement, the focus of attention has either been modeled as a spotlight (Shulman et al., 1979), as a gradient (LaBerge & Brown, 1989), as a zoom lens (Eriksen & St. James, 1986; Shulman & Wilson, 1987), or as an inhibition beam (Tsotsos, 1990).

In the temporal domain, several studies of attention have characterized the time course of both exogenous and endogenous attention at a given spatial location—generally corresponding to the focal point of attention. The temporal dynamics of attention have been addressed in psychophysical studies (Fuller, Rodriguez, & Carrasco, 2008; Hein et al., 2006; T. Liu, Stevens, & Carrasco, 2007; Lyon, 1990; Mackeben & Nakayama, 1993; Müller & Rabbitt, 1989; Nakayama & Mackeben, 1989; Sagi & Julesz, 1986; Shimozaki, 2010; Theeuwes, Atchley, & Kramer, 2000; Weichselgartner & Sperling, 1987), in ERP studies, measuring the evoked electric responses in the brain (Clark & Hillyard, 1996; Harter, Miller, Price, LaLonde, & Keyes, 1989; Hillyard, Teder-Sälejärvi, & Münte, 1998; Mangun, 1995; Nobre, Sebestyen, & Miniussi, 2000), and also in single-unit recordings in non-human primates (Busse, Katzner, & Treue, 2008). These studies have revealed that attention peaks at about 80–150 ms after an exogenous cue, while the deployment of endogenous attention, triggered by a symbolic cue, takes about 300–500 ms and can be maintained at least for a few seconds (Ling & Carrasco, 2006b).

In most previous studies, however, the spatial pattern of attention has been implicitly thought to be fixed, only modulating its amplitude along the time domain. Hence, the temporal fluctuations of attention would be comparable regardless of the probed location, and its spatial extent would not depend on the exact probing time. Nevertheless, this assumption has rarely been tested directly (Kristjánsson & Nakayama, 2002; Tse, 2004). Using a change blindness-based paradigm, Tse succeeded in building up a map of exogenous attention deployment (over 149 positions) as a function of time (4 SOAs: 12, 82, 153, and 447 ms). Their principal result is an enhancing effect opposite the cued location, which, in some cases, was greater than the one at the cued location. Nevertheless, this work failed to show any clear modulation of attentional pattern across time. By and large, the interdependence between spatial and temporal dimensions of attention remains an unanswered question: Does the spatial focus of attention evolve along time? To address this question, we quantified the spatial deployment of attention as a function of post-cuing time in one single paradigm, for both exogenous and endogenous attention.

We tested the relative visibility of a low-contrast target presented at different distances (spatial sampling) and stimulus-onset asynchronies (SOAs) from the cue (temporal sampling) to build up a spatiotemporal map of attention effects, for both exogenously and endogenously driven attention. One original aspect of our paradigm is that we used a compensation technique to equalize the visibility of the target across screen positions, cue–target distances, and SOAs. In short, instead of adapting the intensity of the target to the various experimental conditions, we kept the target identical and varied the contrast of the noisy background using independent staircases for target eccentricity and several combinations of cue–target distance and cue–target SOA. The amount of background contrast modulation required to keep the target detection rate at 75% was taken as a reflection of the magnitude of attention at a particular distance and SOA from the cue (see Figure 1a and Methods section for more details). In our paradigm, the background noise contrast actually enhances the visibility of the target instead of interfering with its detection as in usual noise protocols (Lu et al., 2002; Talgar et al., 2004). This is because the target is only detectable if the background noise pattern has a sufficient contrast (the target is designed to be invisible when the background noise contrast is zero; see Figure 1a and Methods section). The use of noise in our paradigm does not imply that we favor the noise exclusion function of attention over its signal enhancement one. The conceptual framework underpinning our paradigm is that attention deployment enhances contrast sensitivity at the target location, a fact that has been very well documented (Cameron, Tai, & Carrasco, 2002; Carrasco et al., 2000; Ling & Carrasco, 2006a; Pestilli & Carrasco, 2005; Pestilli, Ling, & Carrasco, 2009). In order to test the dependency of the spatial deployment pattern across time, we compared our results to a model with null space–time interaction. The data for both exogenous and endogenous attention were well explained by the model, suggesting that the shape of the attention focus is constant over time (i.e., only its magnitude varies).

The development of this paradigm allowed us to obtain the first detailed spatiotemporal maps of both endogenous and exogenous visual attention. Moreover, the apparent

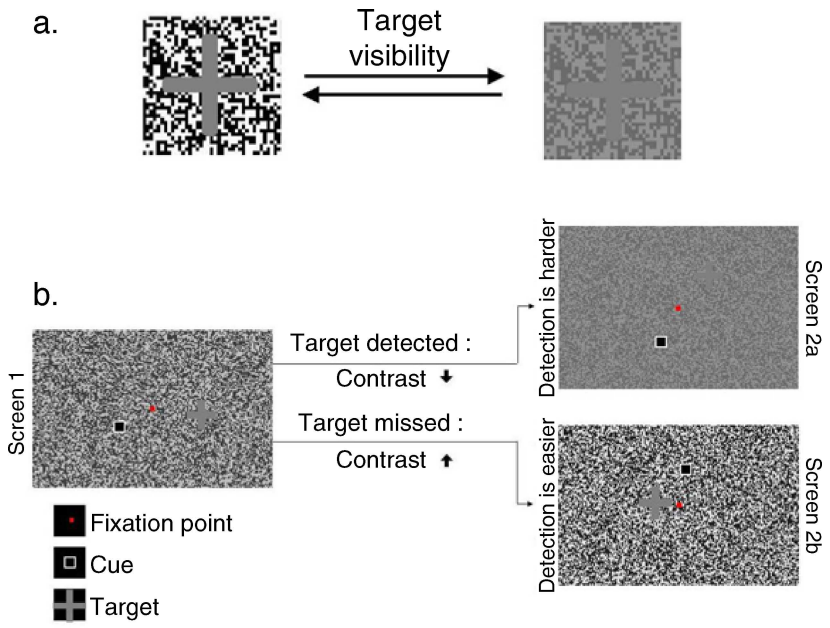

Figure 1. (a) Compensation paradigm. The background contrast is modulated in order to enhance or reduce target visibility, which in turn remains at the same luminance, fixing its detection rate at 75%. (b) An example of contrast compensation: Global contrast function defines the average contrast value all over the screen, fixing target detection rate at 75%. When the target is systematically detected, the background contrast decreases, making target detection harder (screen 2a). Inversely, when the target is systematically missed, the background contrast rises, making target detection easier (screen 2b). This adaptive staircase procedure allows maintaining the overall hit rate at 75%.

lack of reorganization of attention deployment pattern over time constrains the possible neural mechanisms that could underlie this cognitive function.

Methods

Subjects

All subjects were between 20 and 35 years old and had normal or corrected-to-normal visual acuity. They all gave informed consent. Thirteen subjects participated in the exogenous attention mapping and 10 subjects in the endogenous attention mapping.

Spatiotemporal mapping of attention

We used a detection task to quantify attention along the spatiotemporal domain. The target consisted of a gray cross (1°) that was present for 50 ms on 75% of trials, superimposed on a random background pattern of dark/light gray pixels, with the same mean luminance as the target (Figure 1a). The contrast of the background pixels was manipulated online and independently for each subject using a staircase method (Johnson, Chauhan, & Shapiro, 1992). Thus, the relative target visibility was modulated to equate detection performance at 75%: When the background contrast was zero, the target was invisible, as target and background had the same mean luminance; increasing the background contrast made the target more visible (Figure 1a). Thus, attention was measured as the contrast modulation of the background necessary to maintain performance at 75%.

In our paradigm, the background contrast (Cbg) was varied in space and time, modulated by 3 staircase-based functions, running simultaneously: *a global contrast function* (Cglob), *an eccentricity function* (Cecc), and *a spatiotemporal attention function* (Att) as follows:

$$\mathrm{Cbg}_{(f,x,t)} = (\mathrm{Cglob} + \mathrm{Cecc}_{(f)}) \cdot (1 + \mathrm{Att}_{(x,t)}). \quad (1)$$

The global contrast (Figure 1b) and eccentricity functions (Figure 2) provided the baseline for the actual attention measurement made using the spatiotemporal attention function (Figures 3 and 4). Note that the global contrast (Cglob) and eccentricity (Cecc) functions are in absolute units of contrast (between 0 and 1), while the spatiotemporal attentional (Att) function is only modulatory, with an expected value of 0 when attention has no effect.

The *global contrast function* compensated for intersubject variability, acting as a gain function. This function was a constant that modulated background contrast over

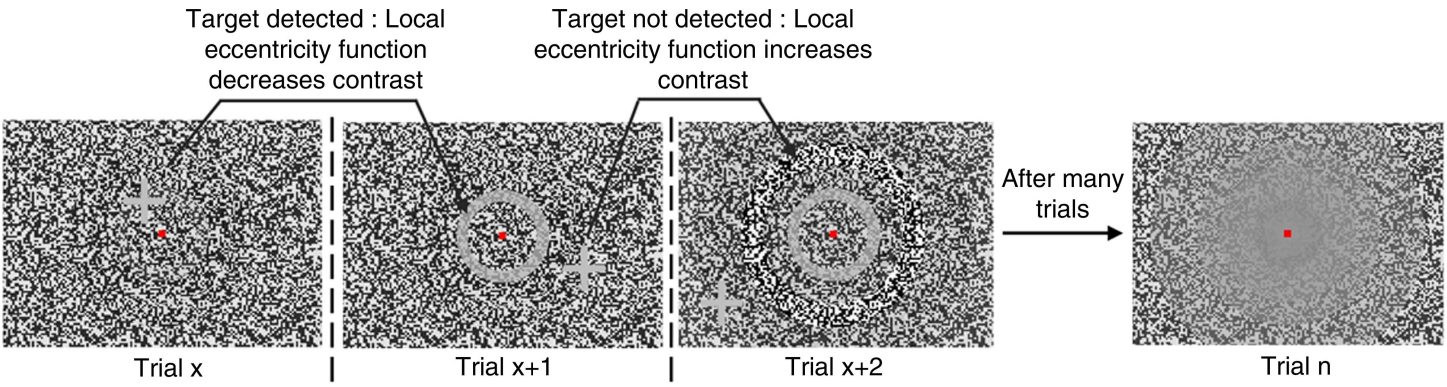

Figure 2. Eccentricity function. Seven concentric segments modulate the background contrast, in addition to the global contrast function, in order to fix performance at 75% no matter the eccentricity of the target. Note that, after a certain number of trials, the contrast at fixation is smaller than in the periphery, thus compensating for higher visual acuity at the fovea.

the entire screen area (Figure 1b). Contrast threshold was determined by one pair of staircases (one initiated at a low-contrast value and the other at a high-contrast value) in order to maintain performance at 75% no matter the eccentricity, the cue–target distance, or its SOA from cue onset.

The *eccentricity function* compensated for visual acuity differences between fovea and periphery. This was a function of distance from fixation point ($_f$) and modulated the background contrast independently over 7 concentric segments centered at the center of the screen (Figure 2), updating its contrast depending on target eccentricity from fixation point in each trial. The contrast threshold for each segment was determined by a pair of staircases in order to maintain performance at 75% along all eccentricities.

Finally, the *spatiotemporal attention function* compensated for the effects of attention in both space and time. This was a function of distance (d) and delay (t) from cue, dynamically modulating the background contrast at different distances and delays from the cue (Figures 3 and 4). The screen area was divided in discrete segments centered at the cue position (spatial sampling) and trial duration was divided as well in discrete time steps (temporal sampling). The contrast threshold was determined independently using one staircase pair for each spatiotemporal coordinate, in order to maintain performance at 75% at every cue–target presentation distance and delay.

Each one of these staircase-based functions was updated on every target-present trial (75% of trials), converging to threshold value after a certain number of trials (Figure 5). The convergence criterion was defined as reaching a difference smaller than 1% contrast between the 2 thresholds in a given staircase pair. In this manner, the global contrast function converged to its threshold value quickly (in ~600 trials), defining the gain value. Then, the eccentricity function converged after ~1000 trials, making target visibility equal all over the screen no matter the eccentricity, except for the effects of attention that we aimed to determine. Finally, the attention spatiotemporal function (i.e., our measure of attention) converged to its threshold, making target equally visible no matter the distance and delay from cue.

Exogenous attention mapping

In exogenous attention mapping, we used a non-informative high-contrast peripheral cue flashed either for 66.6 ms (in the low-resolution condition, see below) or for 50 ms (in the high-resolution condition; Figure 3). The peripheral cue consisted of a dark square with white edges, measuring 0.2°. It was located randomly at 5° eccentricity. The target, a gray cross of 1°, was presented in 75% of trials. Since uniform target placement over the screen area would generate a bias (higher probability of appearing at higher eccentricities), we placed the target in a semi-random way: In each trial, we chose a random cue–target distance among those that had received the fewest number of trials so far.

We sampled the spatiotemporal domain by placing the target at 56 coordinates (7 distances × 8 time coordinates) in a low-resolution condition (6 subjects, 4,000 trials each). Cue–target distance was semi-randomly selected in each trial (as explained above) and then nested into 7 bins: 0.5, 1, 2, 4, 6, 8, 12°. Eight cue–target delays were probed: 0, 66.6, 133.3, 200, 266.6, 333.3, 400, 466.6 ms.

In a high-resolution condition (7 subjects, 10,000 trials each), we sampled the spatiotemporal domain by probing attention at 154 coordinates (14 distances × 11 delays). Cue–target distance was semi-randomly selected in each trial and then nested into 14 bins: 0.1, 0.5, 1, 1.5, 2, 2.5, 3, 4, 5, 6, 7, 8, 10, and 12°. Eleven cue–target SOAs were probed: 0, 50, 100, 150, 200, 250, 300, 350, 400, 450, 500 ms.

Target location control experiment

We developed a control experiment to ensure that the semi-random target presentation did not provide information regarding the target position (i.e., the subject could

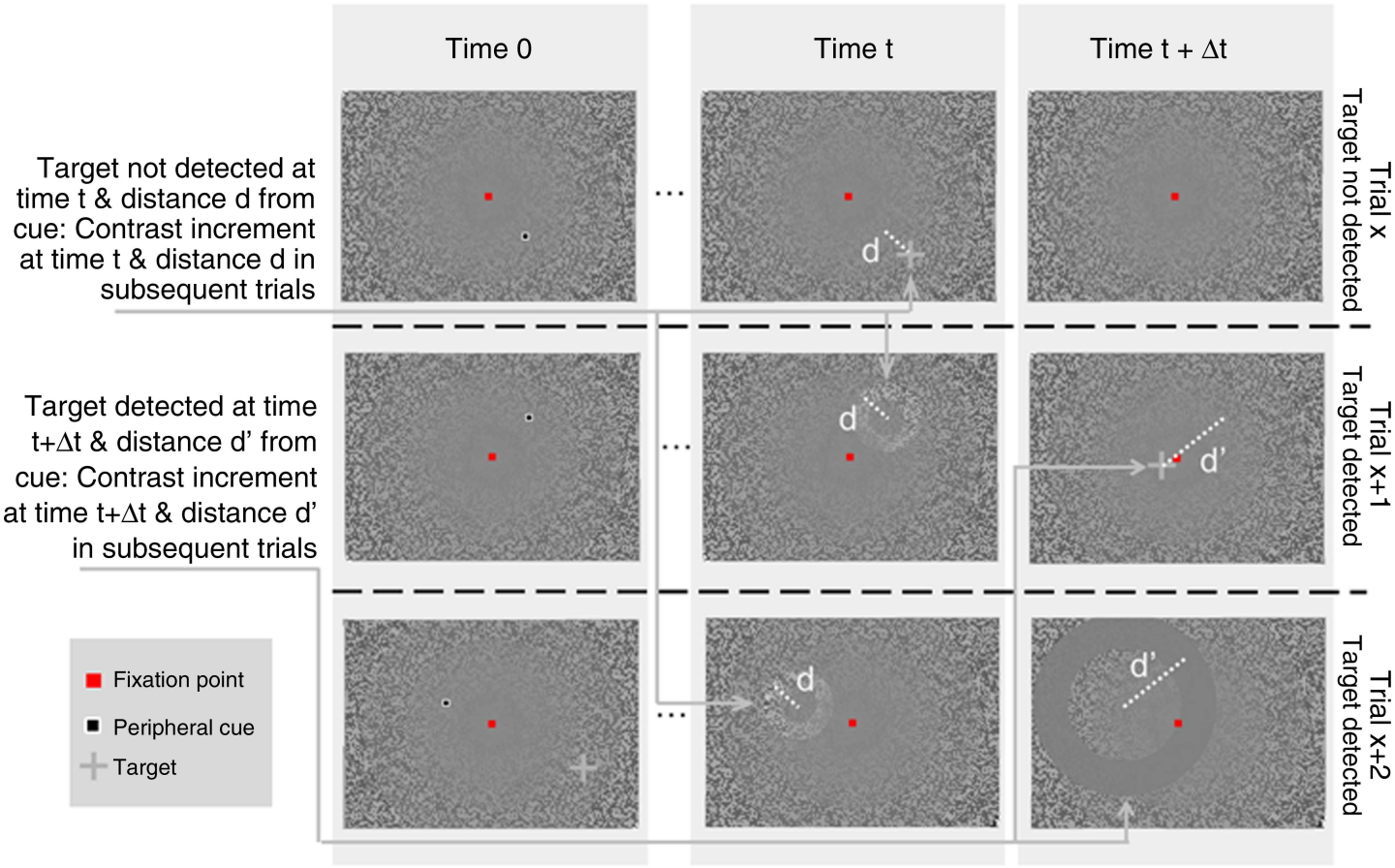

Figure 3. Exogenous attention mapping. The horizontal axis represents time, showing time 0 and 2 contiguous sampling time steps separated by Δt. The vertical axis represents 3 consecutive trials. The cue was shown randomly at any location at 5° from fixation. The target was flashed at a semi-random location over the screen and then nested into a space bin (see Methods section). The target could appear at different SOAs from cue onset (temporal sampling, see Methods section). One pair of staircases per spatiotemporal coordinate was used to modulate the background contrast to fix performance at 75%. In this example, the target appears at time t and distance d, in the first trial of the sequence (trial x). The subject does not detect the target in trial x, so the background contrast in the next trial (trial $x + 1$) will be raised at time t and distance d; the target on this trial will be presented at a different time step (here the next step, at time $t + \Delta t$) and at another distance (d'). This time the target is detected, so the contrast at this spatiotemporal coordinate will be decreased. As a consequence, in the third trial of the sequence (trial $x + 2$), different modulations of local contrast (enhancing at distance d and diminution at distance d') will be shown at two consecutive time steps (time t and time $t + \Delta t$). The cumulative effect of this procedure (designed to fix performance at 75% in all spatiotemporal coordinates) over many trials will represent the attention function.

have guessed the position of the target). We restrained target presentation to the horizontal midline, thus avoiding the geometric bias for higher eccentricities. In this manner, we presented the target in a completely random way, positioning it uniformly over the screen midline. Four of the 13 subjects participated in this experiment (2 for the low-resolution condition and 2 for the high-resolution one).

Endogenous attention mapping

In endogenous attention mapping, we used an informative (66.7% of time) central cue pointing left or right. The cue was presented for the entire duration of the trial (700 ms). The target was presented on 75% of trials and flashed for 100 ms, placed randomly (uniform distribution) over the horizontal screen midline (Figure 4). Ten observers participated in this experiment.

We sampled the spatiotemporal domain at 70 coordinates (10 distances and 7 delays). Cue–target distance was randomly selected on each trial and then nested into 10 bins: −11, −7, −3, 0, 2, 4, 6, 8, 10 and 12°. The distance of 0° stands for the central cue position, positive distances define the cued side, and negative ones define the uncued side. Seven SOAs were probed: 0, 100, 200, 300, 400, 500, and 600 ms.

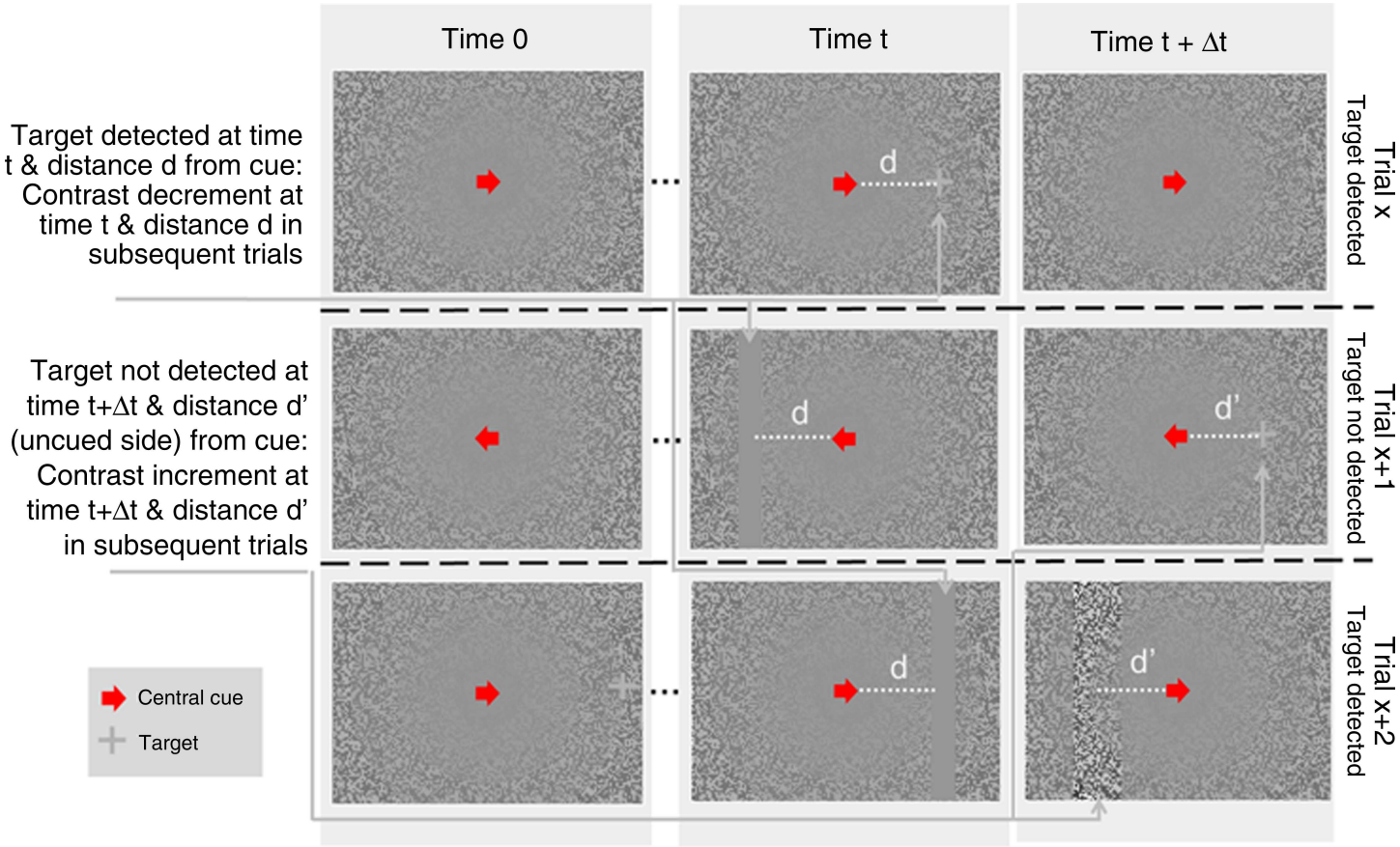

Note: The distance markers are shown here for illustrative purposes only and were not shown in the experimental screen

Figure 4. Endogenous attention mapping. The horizontal axis represents time, showing time 0 and 2 contiguous sampling time steps separated by Δt. The vertical axis represents 3 consecutive trials. A central cue (valid 66.6% of time) directed attention to either the left or the right of the fixation point. The target was flashed for 100 ms in a random position over the horizontal screen midline and then nested in a space bin (see Methods section). The target could appear at different SOAs from cue onset (temporal sampling, see Methods section). One pair of staircases per spatiotemporal coordinate was used to modulate background contrast to fix performance at 75%. In this example, the target appears at time t and distance d, in the first trial of the sequence (trial x). The subject detects the target in trial x, so the background contrast in the next trial (trial $x + 1$) will be decreased at time t and distance d; in this trial, the target will be presented at a different time point (in our example, at the next time step, time $t + \Delta t$) and at another distance (d'). This time the target is not detected, so the contrast at this spatiotemporal coordinate (time $t + \Delta t$ and distance d') will be increased. As a consequence, in the third trial of the sequence (trial $x + 2$), different modulations of local contrast (diminution at distance d and enhancing at distance d') will be shown at two consecutive time steps (time t and time $t + \Delta t$). The cumulative effect of this procedure (designed to fix performance at 75% in all spatiotemporal coordinates) over many trials will represent the attention function.

Stimulus generation

Stimuli were generated in Matlab, using the Psychophysics Toolbox extensions (Brainard, 1997; Pelli, 1997). Two distinct setups were used: one with a resolution of 800 × 600 pixels and a 100-Hz vertical refresh rate (corresponding to the high-resolution condition of the exogenous mapping experiment) and the other using a resolution of 1680 × 1050 pixels and a 60-Hz vertical refresh rate (corresponding to the low-resolution condition of the exogenous mapping experiment, as well as the endogenous mapping experiment). Absolute luminance was not calibrated, since the manipulated variable in our paradigm was relative luminance (i.e., contrast variation).

Procedure

Subjects were placed at 56 cm from the screen and were instructed to maintain fixation at the center of the screen. They were trained to detect the target (presented in 75% of trials) over a noisy background for a few practice trials before starting the experiment. They could respond by pressing two keys indicating target presence or absence.

Incorrect responses were fed back through a beep. Subjects had no time limitation to give their answer. A new trial began when response was given.

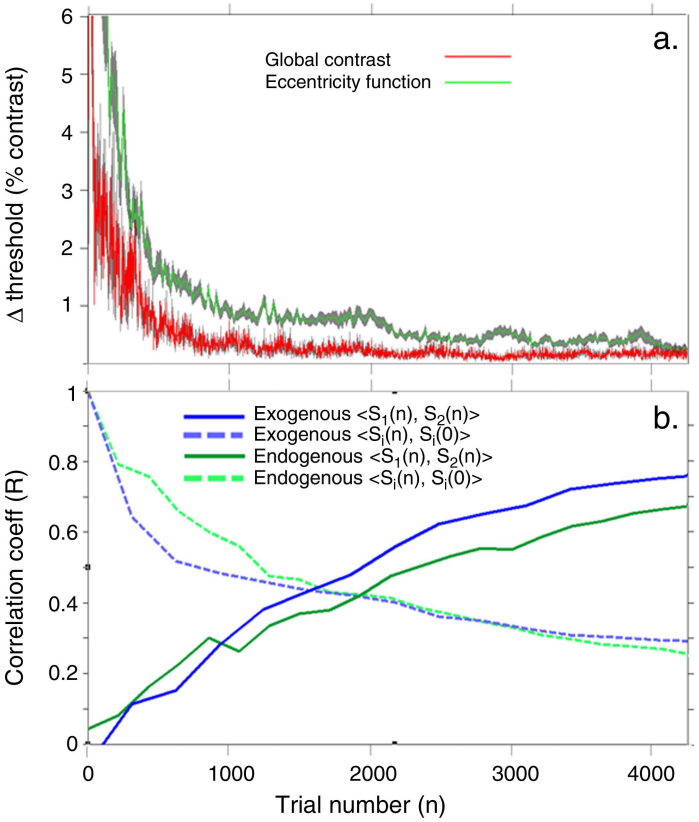

Figure 5. Staircase threshold evolution. Threshold values of all functions were updated at every target-containing trial. (a) Staircase threshold difference as a function of trials. The red line represents the threshold difference between the two global contrast staircases (differing only in their initial values, one low contrast and one high contrast) as a function of trials, for all subjects. The green line represents the mean threshold difference between staircases of a pair, averaged over the 7 pairs used in the eccentricity function. Gray shaded area represents the standard error of the mean (*SEM*). The convergence criterion was a threshold difference less or equal to 1%. Note that the global contrast staircases converge earlier (~600 trials) than the eccentricity ones (~1000 trials). (b) Correlation between threshold values for the attention function. The solid lines represent the mean correlation values between two thresholds in a pair averaged across all spatiotemporal coordinates. The blue line represents the exogenous attention function and the green line represents the endogenous attention one. Note that the correlation across spatiotemporal coordinates between both staircases (S1 and S2), which were initialized at random values, increases as a function of trials, implying that it represents a meaningful attention function. On the other hand, the dashed line represents the mean correlation value of each staircase threshold (Si(*n*)) with its initial state (Si(0)). Note that the correlation diminishes across trials, showing that thresholds evolve from an arbitrary value (at trial 0) to a meaningful value.

Exogenous attention mapping participants performed 4,000 trials each in the low-resolution condition (~4 h, across many sessions) and 10,000 trials each in the high-resolution condition (~10 h, across many sessions). Endogenous attention mapping participants performed 5,000 trials each (~5 h, along many sessions). Subjects received financial compensation for their participation.

Results

Exogenous attention mapping

First, we verified that our method was efficient at determining spatiotemporal attention effects by evaluating the convergence of the contrast thresholds for the attention function. The contrast for each spatiotemporal coordinate had been adjusted using two independent staircases (one randomly initialized at a low-contrast value and the other at a high value). We calculated the correlation (across spatiotemporal coordinates) between the estimated contrast thresholds of these 2 staircases and confirmed that this correlation increased throughout the experiment (Figure 5b, blue line). In the same time, the correlation (across spatiotemporal coordinates) between a given staircase and its initial (randomly determined) value decreased steadily across trials (Figure 5b, dashed blue line). Thus, the contrast thresholds were slowly evolving during the experiment to reflect a meaningful attentional function rather than an arbitrary initial state. Because the two independent staircases tended to provide similar results, and in order to increase statistical power, for the following analyses we pooled the corresponding trials and computed offline the threshold contrast value at each spatiotemporal coordinate.

Each threshold value corresponds to an estimate of attention at a given spatiotemporal coordinate. Contrast modulations below the baseline reflect a positive effect of attention (i.e., the background contrast must be diminished to compensate for the effect of attention and maintain performance at 75%; see Equation 1), while contrast modulations above the baseline indicate inhibitory effects of attention (i.e., the background contrast must be raised to compensate for the effect of attention). To visualize the spatiotemporal attention function, we interpolated (bicubic 2D interpolation) the original sampling grids (7 × 8 points for the low-resolution condition and 14 × 11 for the high-resolution condition) to a 100 × 100 point grid. One representative subject for the high-resolution condition is shown in Figure 6a.1 and one for the low-resolution condition in Figure 6a.2. The *X*-axis corresponds to target delay from cue onset and the *Y*-axis to target distance from the cue. Attentional effects (percentage of background contrast compensation, see Equation 1) are color coded (from red to yellow representing attention enhancement, from blue to cyan representing inhibition, and black cor-

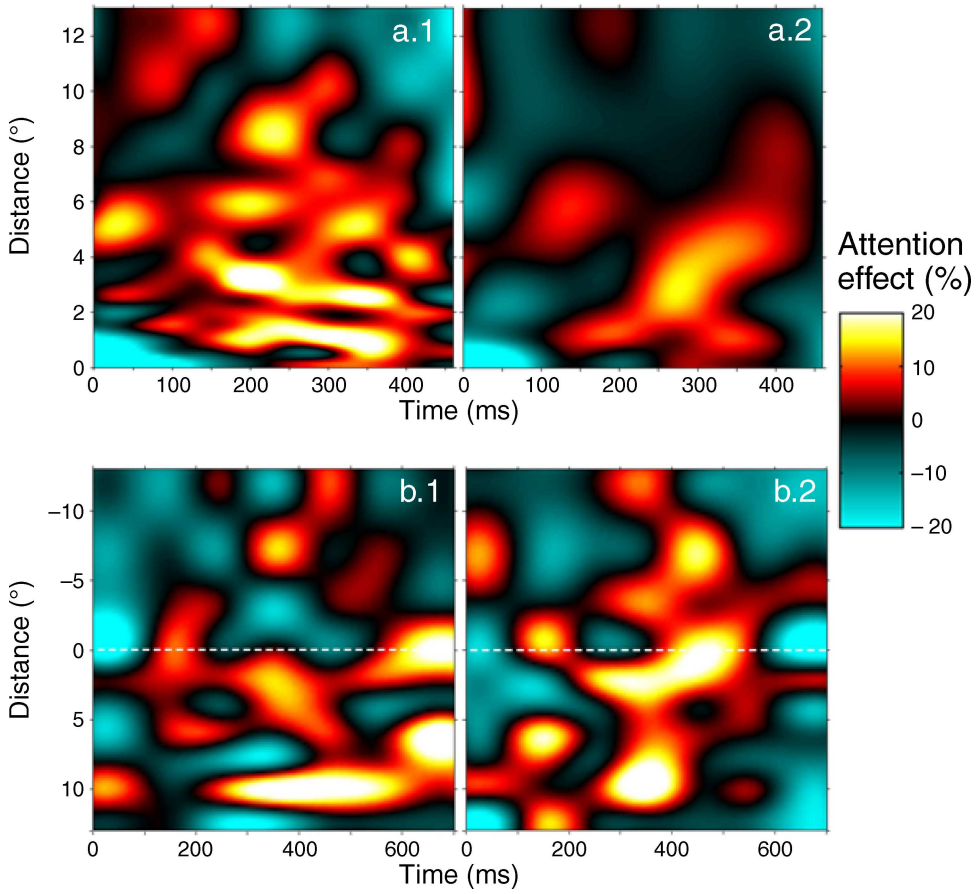

Figure 6. Individual mapping data. The *X*-axis represents target delay from cue onset, and the *Y*-axis represents distance from the cue. Attentional effects are color-coded: from red to yellow representing attention enhancement, from blue to cyan representing inhibition, and black corresponding to the baseline. (a) Two representative subjects from the exogenous attention mapping experiment. Panel a.1 shows a representative subject from the high-resolution condition. Panel a.2 shows a representative subject from the low-resolution condition. (b) Endogenous mapping. The *X*-axis represents target delay from cue onset, and the *Y*-axis represents distance from the cue. Positive distances represent the cued side, negative ones represent the uncued side, and zero is the cue position. Two representative subjects are shown in panels b.1 and b.2. Note that attention enhancement in individual subjects can reach more than 20% of amplitude.

responding to the baseline). We then calculated the grand average across all subjects. Figure 7a shows the grand-average attention map for exogenous attention over 13 subjects. A progressive enhancement of attention can be seen from 50 to 150 ms. This enhancement attains a plateau from 200 to 350 ms, peaking at the spatial region extending up to 3° from the cue.

There is also a clear inhibitory effect starting at the origin (i.e., cue–target delay and distance = 0) and extending over 150 ms and 1°. This negative effect can be explained by the high contrast of the cue causing forward masking and inhibiting target detection (Enns & Di Lollo, 2000; Foley & Boynton, 1993), particularly at a short delay from the cue onset and at small distances from it. By definition, an optimal cue for capturing attention exogenously must be highly salient; thus, we believe that such forward masking was unavoidable in our paradigm.

In order to verify that the spatiotemporal attention pattern was reproducible across subjects, we calculated the Pearson correlation coefficient (across 100 × 100 spatiotemporal coordinates) between all possible pairs of subjects. The mean correlation coefficient across all 78 possible pairs ($C_{13}{}^2 = 78$) was $r = 0.2574$. We compared this result to the null hypothesis that the measured attention pattern was simply due to noise. To do this, we randomly scrambled the attention map of each subject (in its original 7 × 8 or 14 × 11 format, later interpolated over a 100 × 100 grid) and we calculated the Pearson correlation between all subject pairs as previously. This procedure was repeated 10,000 times and revealed that the probability of obtaining a correlation coefficient $r = 0.2574$ due to chance was less than $p < 10^{-4}$. Thus, the measured spatiotemporal attentional pattern is not simply due to noise but is consistent across subjects.

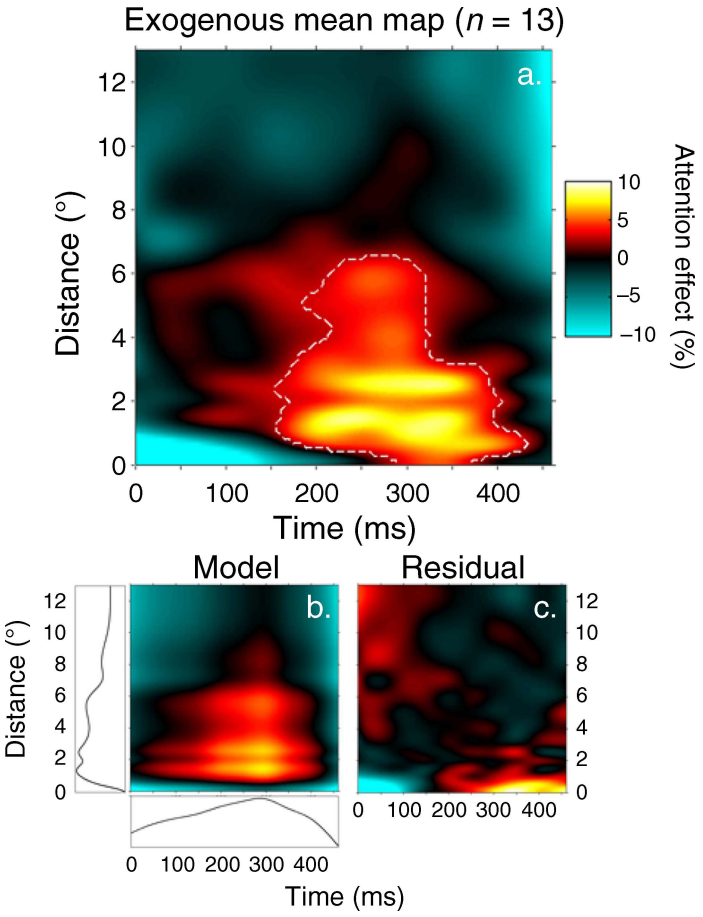

Figure 7. Exogenous attention map. (a) Mean attention effect. A progressive enhancement of attention can be seen from 50 ms with a peak at 275 ms, extending up to 8° from the cue. The dashed line represents enhancing effects above 3%, which are significant at $p < 10^{-4}$ (bootstrap procedure). (b) Null space-time interaction model. The model was approximated as the linear combination of the spatial profile (the attention map averaged across time, left panel) and the temporal profile (the attention map averaged across space, lower panel), see text for details. (c) Residuals from null space-time interaction subtraction. Each subject model map was subtracted from its actual attention map and the residuals were then averaged. Values departing from zero represent effects underestimated by the model. Residuals were largely non-significant ($p = 0.8$, bootstrap procedure) suggesting that exogenous attention does not change its deployment pattern over time, being only modulated in its amplitude over time.

In order to further quantify this consistency of attention effects across subjects, we computed the significance of the main spatiotemporal region of attentional enhancement by means of a cluster analysis. (A cluster analysis takes into account the interdependence among the neighboring spatiotemporal coordinates and is thus more appropriate than classical parametric tests that assume independence of each point on the map.) Thus, we calculated the size of the cluster defined by all adjacent points above 3% contrast modulation in Figure 7a: The cluster size was 1695 points (out of 100 × 100 = 10,000 possible spatiotemporal coordinates). We then applied a bootstrap analysis to estimate the significance of this cluster size by comparing it with the null hypothesis that the same cluster size could be found due to chance. To achieve this, we shuffled the assignment of correct and incorrect responses to each trial for a given subject: The average performance would remain unchanged, but the delay and distance from cue would become meaningless variables. Thus, we recomputed contrast threshold value for every spatiotemporal coordinate and subject, obtained a grand-average attention map, and then reassessed the largest cluster size defined by all adjacent points above 3% contrast modulation—this time under the null hypothesis. We iterated this procedure 10^4 times and found no cluster size equal or larger than 1695 points. Therefore, this bootstrap analysis reveals that attentional enhancement effects above 3% can be considered highly significant ($p < 10^{-4}$). These significant enhancing effects include the zone from 150 to 430 ms after cue onset and up to 6° of eccentricity.

To finish, we controlled that the semi-random cue position choice (see Methods section) was not used by subjects to anticipate the target position. We compared the control group of 4 subjects (where the target was located with a uniform random distribution over the screen horizontal midline) against the test group of 9 subjects (where at each trial a random location was chosen among those that had received the fewest number of trials so far). We calculated Pearson's correlation coefficient between pairs of subjects belonging to the same group (i.e., control group or test group) or pairs belonging to different groups (one control subject with one test subject). The mean correlation into the same group was $r = 0.3193$ and across the groups, $r = 0.2430$. Bootstrap analysis (shuffling the assignment of subjects to the control or test group and repeating the pairwise correlation $n = 10^4$ times) showed no significant difference between control and test groups (t-test, $p = 0.104$). Thus, even if semi-random target placement could have provided information to anticipate the target position, test subjects did not appear to use it in a significant manner.

Endogenous attention mapping

As previously, we first evaluated the convergence of the contrast thresholds for the spatiotemporal attention function. We calculated the correlation (across spatiotemporal coordinates) between the estimated contrast thresholds of the 2 randomly initialized staircases and confirmed that this correlation increased throughout the experiment (Figure 5b, green line). In the same time, the correlation (across spatiotemporal coordinates) between a given staircase and its initial (randomly determined) value decreased steadily across trials (Figure 5b, dashed green

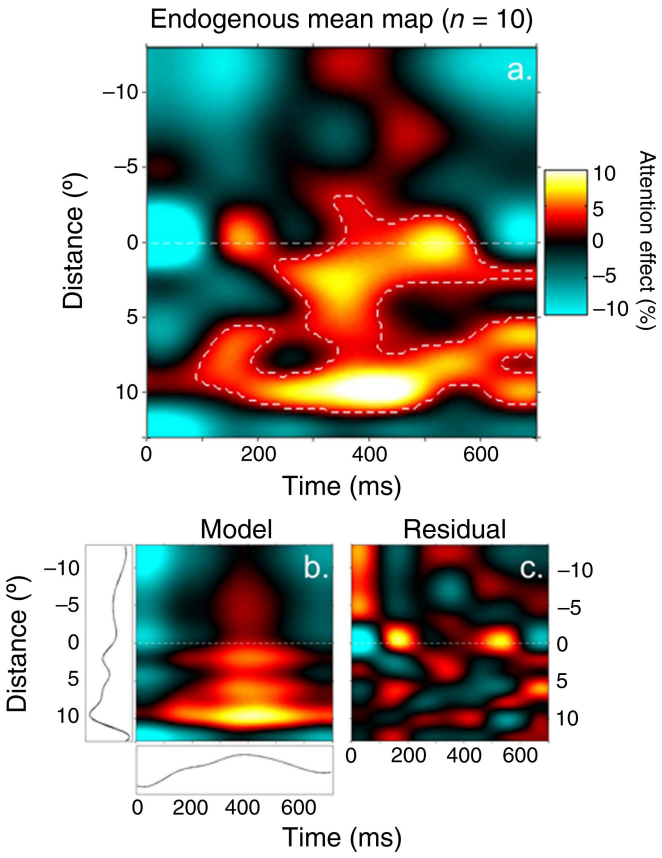

Figure 8. Endogenous attention map. The *X*-axis represents target delay from cue onset, and the *Y*-axis represents distance from the cue. Positive distances represent the cued side, negative ones represent the uncued side, and zero is the cue position. (a) Mean attention effect. An early (100 ms) enhancing effect centered on the cue is shown, with a later deployment of attention at the cued side peaking between 8 and 10° at about 400 ms after cue onset. The dashed line represents enhancing effects above 3%, which are significant at $p = 10^{-4}$ (bootstrap procedure). (b) Null space–time interaction model. The model was approximated as the linear combination of the spatial profile (the attention map averaged across time, left panel) and the temporal profile (the attention map averaged across space, lower panel; see text for details). (c) Residuals from null space–time interaction subtraction. Each subject model map was subtracted from their actual attention map and the residuals were then averaged. Values departing from zero represent effects underestimated by the model. Note that residuals were largely non-significant ($p = 0.7$, bootstrap procedure) suggesting that endogenous attention does not change its deployment pattern over time, being only modulated in its amplitude over time.

line). Again, this implies that the contrast thresholds were slowly evolving during the experiment to reflect a meaningful attentional function rather than an arbitrary initial state. Then, we pooled the trials from the two staircases and computed offline the threshold contrast value at each spatiotemporal coordinate.

To visualize the spatiotemporal attention function, we interpolated (bicubic 2D interpolation) the original sampling grids (7 × 10 points) to a 100 × 100 point grid. Two representative subjects are shown in Figures 6b.1 and 6b.2. The *X*-axis corresponds to time from cue onset and the *Y*-axis to distance from the cue. Attentional effects are color-coded (red/yellow representing attention enhancement, blue/green representing inhibition, and black corresponding to the baseline). We then calculated the grand average across all subjects. Figure 8a shows the grand-average attention map for endogenous attention over 10 subjects. The average map shows an early (100 ms) enhancing effect centered on the cue, with a later deployment of attention at the cued side peaking between 8 and 10° at around 400 ms after cue onset.

In order to verify that the spatiotemporal attention pattern was reproducible across subjects, we calculated the Pearson correlation coefficient (across 100 × 100 spatiotemporal coordinates) between all possible pairs of subjects. The mean correlation coefficient across all 45 possible pairs ($C_{10}^2 = 45$) was $r = 0.184$. We compared this result to the null hypothesis that the measured attention pattern was simply due to noise. To do this, we randomly scrambled the attention map of each subject (in its original 7 × 10, later interpolated over a 100 × 100 grid) and we calculated the Pearson correlation between all subject pairs as previously. This procedure was repeated 10,000 times and revealed that the probability of obtaining a correlation coefficient $r = 0.184$ due to chance was less than $p < 10^{-4}$. Thus, the measured spatiotemporal pattern of endogenous attention is not simply due to noise but is consistent across subjects.

In order to further quantify this consistency of attention effects across subjects, we computed the significance of the main spatiotemporal region of attentional enhancement by means of a cluster analysis, as previously. We calculated the size of the cluster defined by all adjacent points above 3% contrast modulation in Figure 8a: The cluster size was 929 points (out of 100 × 100 = 10,000 possible spatiotemporal coordinates). We then applied a bootstrap analysis to estimate the significance of this cluster size by comparing it with the null hypothesis that the same cluster size could be found due to chance, as previously (see Exogenous attention mapping section). We found a maximum cluster size equal to 929 points in a single bootstrap iteration out of 10^4. Therefore, this analysis reveals that attentional enhancement effects above 3% can be considered highly significant ($p = 10^{-4}$).

Attention movies

To illustrate the deployment of attention in a more intuitive fashion, we created movies of exogenous and endogenous attention effects (see Supplementary materials: exogenous_attention.mov, endogenous_attention.mov).

The movies represent the experimental screen, centering the attention effects over the peripheral cue for exogenous attention mapping, and over the central cue for the endogenous one.

Space–time interdependence

Our compensation method was efficient at providing a detailed spatiotemporal map of exogenous and endogenous attention. One important question to address is whether the shape of the attentional focus changes over time from cue onset. To assess this, we compared our results to a null space–time interaction model. The modeled attention maps (Figure 7c for exogenous attention and Figure 8c for endogenous attention) were approximated as the linear combination of the spatial profile (i.e., the attention map averaged across time) and the temporal profile (i.e., the attention map averaged across space) as follows:

$$\mathrm{Att}_{(x,t)} = k(S_{(x)} \cdot M_{(t)}) + b, \quad (2)$$

where the spatiotemporal attention function $\mathrm{Att}_{(s,t)}$ is decomposed in two parts: one spatial subfunction $S_{(s)}$ that corresponds to the shape of the attentional focus and one activation function $M_{(t)}$ that reflects the magnitude of attentional modulation as a function of time. The constant b represents baseline (i.e., average value of the spatiotemporal attention function), and k is a constant of proportionality obtained as follows:

$$k = 1/\iint (\mathrm{Att} - b)\,dx\,dt, \quad (3)$$

defining S and M as

$$S_{(x)} = \int (\mathrm{Att} - b)\,dt, \quad (4)$$

$$M_{(t)} = \int (\mathrm{Att} - b)\,dx. \quad (5)$$

We calculated the modeled map for each subject and then subtracted it from the original map. The remainder of this subtraction is the attention effect that cannot be explained by a null space–time interaction. The residuals of the exogenous (Figure 7d) and endogenous (Figure 8d) mapping do not show significant values (cluster analysis, $p = 0.8$ and $p = 0.7$, respectively), suggesting that the spatial attention deployment pattern does not change significantly over time but only modulates its amplitude.

Discussion

Spatiotemporal dynamics

Our paradigm allowed us to estimate, for the first time, a detailed spatiotemporal map for exogenous and endogenous attentional effects, showing both enhancing and inhibitory effects.

The exogenous attention map reveals a significant enhancing effect zone from 150 to 430 ms, extending up to 6 deg from the cue. The enhancing effect is already visible (although not yet significant) at earlier latencies, rising progressively from 50 up to 150 ms. This slow and gradual rise could be due, in part, to forward masking by the cue over the target (Enns & Di Lollo, 2000; Foley & Boynton, 1993), inducing inhibitory effects that could cover up any earlier facilitatory attentional modulation. The enhancing effect in the exogenous attention map goes above 7% of modulation (yellow blobs, Figure 7a) and plateaus from 200 to 350 ms, in a spatial region extending up to 3° from the cue. This sustained effect could indicate a stabilization of the exogenous cuing, known to be triggered by predictive or interesting direct cues (Ward, 2008). The peak of the enhancement effect reaches values of about 10% contrast modulation. This means that, in this spatiotemporal facilitation zone, the target visibility is 10% higher than in the rest of the screen. A weaker inhibitory effect surrounds this zone, with a peak value of about −5% between 100 and 200 ms and reaching about −8% of modulation after 450 ms. However, analysis of individual subjects' data revealed that this later inhibitory zone in the grand-average map was only due to two subjects who adopted a strategy of reporting the absence of the target whenever it appeared after 450 ms. None of the late inhibitory effects is suggestive of inhibition of return (IOR)—i.e., inhibition at previous attended locations. The absence of IOR can be explained by the fact that our exogenous attention map is limited in time to 466.6 ms, whereas IOR is known to appear with different onsets, ranging from 300 to 600 ms (Klein, 2000); thus, it is possible that we did not sample enough delays to reveal IOR in our paradigm. Previous reports have shown earlier modulations of transient attention using different paradigms. In a rapid serial visual presentation (RSVP) paradigm, Weichselgartner and Sperling (1987) measured the recall probability of the stream items occurring with and after the cue. They showed a cuing effect at latencies as early as 20 ms, with a decline at about 200 ms. In a discrimination task with a peripheral cue lasting 33 ms, Nakayama and Mackeben (1989) showed an enhancing peak in accuracy at about 100 ms, with a fast onset (from 0 to ~100 ms) and a slower decline (from ~100 to 500 ms). In a similar setting, Müller and Rabbitt (1989) revealed a peak of performance at 175 ms after the cue onset.

Theeuwes at al. (2000) showed an early facilitation of reaction times at 50 ms, followed by a drop of performance at 100 ms (due to the simultaneous presentation of a distractor), and then a stabilization of reaction times, with the fastest reaction times obtained from 150 to 300 ms. Attentional manipulations in the studies described above probably avoided forward masking by the cue at short SOAs and were thus more likely to obtain early attentional modulations.

Endogenous attention maps showed a peak at the cued side at ~400 ms and between 8 and 10° from the cue. The enhancing effect begins in the periphery (from 5 to 10°) and then spreads toward the cue location, reaching its maximum value of 12% at 10° from the cue at 420 ms. The existence of a second attention locus near the cue location (0°) is also visible as three different peaks (~200, ~350, and ~550 ms). This "second focus" could reveal that some subjects had trouble disengaging the exogenous component of their attention in some trials—thus enhancing target detection whenever it was presented near the cue. The endogenous attentional modulation time course showed in the present work is similar to previous reports using different paradigms. Weichselgartner and Sperling (1987) showed in an RSVP task that a symbolic cue instructing observers to switch the attended stream gated the deployment of attention at latencies of ~300 ms. Müller and Rabbitt (1989) showed that the time necessary to allocate spatial attention to the periphery after a valid central cue was of ~400 ms. In our mean attention map of both exogenous and endogenous attention, we obtained a peak of attentional modulation of around 10%, even though individual subjects often reached higher values (~20%, Figure 6). The modulation peaks across subjects do not necessarily coincide, which could explain the reduction in amplitude of the grand-average effect. The 20% peak of attention modulation from individual subjects falls into the range of amplitudes of attention modulation described in different physiological and psychophysical studies. Although behavioral and physiological data are not directly comparable (Eckstein et al., 2009; Pestilli et al., 2009), our effect seems to be smaller than the effect found in many single-unit reports in macaque monkey (30 to 40% gain in spontaneous activity in V2 and V4 in Luck et al., 1997; ~20% gain in neuronal responsiveness in V4 in Spitzer et al., 1988; 39 and 44% gain in firing rate in V4 and IT, respectively, in Chelazzi et al., 1998) or even in fRMI studies in humans (30% gain in BOLD signal in Reddy et al., 2009). Event-related potentials (ERPs) in humans (Kelly, Gomez-Ramirez, & Foxe, 2008) also reveal an enhancement of about 20% due to spatial attention in area V1. Overall, it could be that physiological response modulations (i.e., spiking rate, BOLD activity, and ERPs) are stronger than their behavioral counterpart. However, our main attention result is also in agreement with the gain found in the contrast response function in humans (Pestilli et al., 2009), where the difference in the threshold of the contrast response function (C50) between the cued and uncued conditions was less than 10%.

Method limitations

Several assumptions and approximations were necessary for our paradigm. For example, we defined the eccentricity function as a series of annular segments centered at fixation, thus assuming that visual acuity decreases homogeneously in both horizontal and vertical directions—an assumption we know to be overly simplistic (Smythies, 1996). Similarly, we sampled attentional effects in only one spatial dimension (i.e., the Euclidean cue–target distance), hence, assuming that attention is distributed radially from the cue location in a homogeneous manner. This assumption is not necessarily true since it has been shown that attention can be deployed preferably either over the vertical or the horizontal axis, depending on the visual context (Botta, Santangelo, Raffone, Lupiáñez, & Belardinelli, 2010). We also assumed that attention maintains its deployment and time course characteristics regardless of whether the cue and target end up in the same or in different hemifields; yet interhemispheric deployment asymmetries and competition between hemifields have often been reported (Fecteau, Enns, & Kingstone, 2000; Mathôt, Hickey, & Theeuwes, 2010; Righi & Ribeiro-do-Valle, 2011). To counter the limitations of our paradigm, a mapping of attention in two spatial dimensions (i.e., in Cartesian x, y coordinates) instead of one (i.e., only Euclidean cue–target distance) would be necessary. However, the introduction of another spatial dimension would multiply the number of trials required and make the study impractical. All in all, our results can be taken as a good approximation to a spatiotemporal map of exogenous and endogenous attention, since many of the abovementioned undesirable manifestations of the spatial heterogeneity of attention will average out due to our counterbalancing the target presentation over all possible locations (i.e., the same cue–target distance but oriented in all directions, presenting cue and target in the same or in different hemifields, etc.).

Another issue is the degree of target location uncertainty in the exogenous versus endogenous condition. In fact, the possible target positions in the exogenous mapping includes all the possible positions on the screen (26 by 19.5°), and in the endogenous condition, the possible target locations includes all the possible positions within the horizontal meridian of 26° of length (13° at each side of the central cue), in both cases encouraging observers to select an extensive attended zone (i.e., a large attended field). Recent models (Reynolds & Heeger, 2009) and psychophysical data (Herrmann, Montaser-Kouhsari, Carrasco, & Heeger, 2010) have suggested that the amount of target uncertainty balances the attention effect

between contrast gain (a left shift in the psychometric curve with an attentional modulation in the intermediate contrast range) and response gain (an upward shift in the psychometric curve with an attentional modulation in the maximum contrast range). Contrast gain effect becomes predominant when the target size is significantly smaller than the zone of target uncertainty. Conversely, response gain becomes predominant when the target size is comparable or larger than the zone of uncertainty. In intermediate cases, the attention modulation becomes a combination of the two effects (contrast and response gain). In our paradigm, the zone of uncertainty is significantly larger than the target size in both exogenous (ratio between uncertainty area and target area equals 507) and endogenous mapping conditions (ratio equals 26). Critically, modeling predicts a predominant contrast gain effect for attention field/target size ratios equal or greater than 10 (Reynolds & Heeger, 2009). On the whole, previous evidence thus suggests that in our paradigm attention predominantly modulates contrast, validating our use of contrast as the dependent variable.

Our maps of exogenous attention, even in the "high-resolution" condition (data not shown) failed to confirm the existence of fine spatial features of attention; for example, we did not find a zone within the near surround of attention (2–3°) where attention declines to rise again at farther eccentricities, as suggested by Hopf et al. (2005) and Tsotsos (1990). This could mean that the signal-to-noise ratio in our paradigm was too low to detect the possible existence of subtle attention motifs.

Space–time independence

Our results suggest that the spatial pattern of both exogenous and endogenous attention does not change significantly across time; only its magnitude is modulated. In other words, the spotlight does not systematically shrink or expand as a function of time nor does it revert its polarity in any specific spatial subregion (e.g., from facilitation to inhibition). This result constrains the neural mechanisms that could support the deployment of visual attention. For example, it is compatible with a simple model composed of two independent neural populations. The first neural population, retinotopically organized, would encode the selected region of the visual field (the shape and the coordinates of the spatial attention pattern) in the form of a "saliency map," as postulated by Itti and Koch (2000). The second neural source would represent the magnitude of attentional modulation as a function of time. In this model, the neural population that represents the spatial attention pattern (i.e., the saliency map) would receive global modulatory input from the second neural source, and there would thus be no dependence between the spatial pattern of attention and its magnitude modulation over time. Several putative anatomical localizations have been suggested for each of these two populations. The equivalent of a "saliency map" for attention has been proposed to involve subcortical areas such as the pulvinar (Laberge & Buchsbaum, 1990; Robinson & Petersen, 1992), the lateral geniculate nucleus (Koch & Ullman, 1985), and the superior colliculus (Kustov & Robinson, 1996), as well as cortical locations such as V1 (Li, 2002), V4 (Mazer & Gallant, 2003), the frontal eye field (Thompson & Schall, 2000), and the posterior parietal cortex (Gottlieb, 2007). Neural populations that would gate the temporal modulations of attention have been identified by neuroimaging techniques in different regions such as the intraparietal sulcus, the lateral inferior premotor cortex, the cerebellum (Coull & Nobre, 1998), frontoparietal areas, and the thalamus (Fan, McCandliss, Fossella, Flombaum, & Posner, 2005; Posner, Sheese, Odludaş, & Tang, 2006). Note finally that the region providing the "temporal signal" for attention may not need to activate the saliency map with the precise time course that we have recorded here. Rather, one could also imagine that a simple "trigger" signal is sent to the saliency map. In this case, the intrinsic temporal properties of neuronal circuits within the saliency map would have to match the temporal modulation patterns observed in our experiments.

Acknowledgments

R.K. was funded by Conicyt and ANR, R.V. was funded by ANR (project 06JCJC-0154) and EURYI.

Commercial relationships: none.
Corresponding author: Roger Koenig-Robert.
Email: roger.koenig@cerco.ups-tlse.fr.
Address: 133 Rte de Narbonne, Toulouse 31062, France.

References

Botta, F., Santangelo, V., Raffone, A., Lupiáñez, J., & Belardinelli, M. O. (2010). Exogenous and endogenous spatial attention effects on visuospatial working memory. *Quarterly Journal of Experimental Psychology, 63,* 1590–1602. [PubMed]

Brainard, D. H. (1997). The Psychophysics Toolbox. *Spatial Vision, 10,* 433–436. [PubMed]

Busse, L., Katzner, S., & Treue, S. (2008). Temporal dynamics of neuronal modulation during exogenous and endogenous shifts of visual attention in macaque area MT. *Proceedings of the National Academy of Sciences of the United States of America, 105,* 16380–16385. [PubMed]

Cameron, E. L., Tai, J. C., & Carrasco, M. (2002). Covert attention affects the psychometric function of contrast sensitivity. *Vision Research, 42,* 949–967. [PubMed]

Carrasco, M., Penpeci-Talgar, C., & Eckstein, M. (2000). Spatial covert attention increases contrast sensitivity across the CSF: Support for signal enhancement. *Vision Research, 40,* 1203–1215. [PubMed]

Carrasco, M., Williams, P. E., & Yeshurun, Y. (2002). Covert attention increases spatial resolution with or without masks: Support for signal enhancement. *Journal of Vision, 2*(6):4, 467–479, http://www.journalofvision.org/content/2/6/4, doi:10.1167/2.6.4. [PubMed] [Article]

Cheal, M., & Lyon, D. R. (1991). Central and peripheral precuing of forced-choice discrimination. *Journal of Experimental Psychology: Applied, 43,* 859–880. [PubMed]

Chelazzi, L., Duncan, J., Miller, E. K., & Desimone, R. (1998). Responses of neurons in inferior temporal cortex during memory-guided visual search. *Journal of Neurophysiology, 80,* 2918–2940. [PubMed]

Chica, A. B., & Lupiañez, J. (2009). Effects of endogenous and exogenous attention on visual processing: An inhibition of return study. *Brain Research, 1278,* 75–85. [PubMed]

Clark, V. P., & Hillyard, S. A. (1996). Spatial selective attention affects early extrastriate but not striate components of the visual evoked potential. *Journal of Cognitive Neuroscience, 8,* 387–402.

Corbetta, M., & Shulman, G. L. (2002). Control of goal-directed and stimulus-driven attention in the brain. *Nature Reviews in Neuroscience, 3,* 201–215. [PubMed]

Coull, J. T., & Nobre, A. C. (1998). Where and when to pay attention: The neural systems for directing attention to spatial locations and to time intervals as revealed by both PET and fMRI. *Journal of Neuroscience, 18,* 7426–7435. [PubMed]

Desimone, R., & Duncan, J. (2000). Neural mechanisms of selective visual attention. *Annual Reviews in Neuroscience, 18,* 193–222. [PubMed]

Dosher, B. A., & Lu, Z. L. (2000). Noise exclusion in spatial attention. *Psychological Science, 11,* 139–146. [PubMed]

Eckstein, M. P., Peterson, M. F., Pham, B. T., & Droll, J. A. (2009). Statistical decision theory to relate neurons to behavior in the study of covert visual attention. *Vision Research, 49,* 1097–1128. [PubMed]

Egeth, H. E., & Yantis, S. (1997). Visual attention: Control, representation, and time course. *Annual Reviews in Psychology, 48,* 269–297. [PubMed]

Enns, J. T., & Di Lollo, V. (2000). What's new in visual masking? *Trends in Cognitive Sciences, 4,* 345–352. [PubMed]

Eriksen, C. W., & St. James, J. D. (1986). Visual attention within and around the field of focal attention: A zoom lens model. *Perception & Psychophysics, 4,* 225–240. [PubMed]

Fan, J., McCandliss, B. D., Fossella, J., Flombaum, J. I., & Posner, M. I. (2005). The activation of attentional networks. *Neuroimage, 26,* 471–479. [PubMed]

Fecteau, J. H., Enns, J. T., & Kingstone, A. (2000). Competition-induced visual field differences in search. *Psychological Science, 11,* 386–393. [PubMed]

Foley, J. M., & Boynton, G. M. (1993). Forward pattern masking and adaptation: Effects of duration, interstimulus interval, contrast, and spatial and temporal frequency. *Vision Research, 33,* 959–980. [PubMed]

Fuller, S., Rodriguez, R. Z., & Carrasco, M. (2008). Apparent contrast differs across the vertical meridian: Visual and attentional factors. *Journal of Vision, 8*(11):16, 11–16, http://www.journalofvision.org/content/8/1/16, doi:10.1167/8.1.16. [PubMed] [Article]

Giordano, A. M., McElree, B., & Carrasco, M. (2009). On the automaticity and flexibility of covert attention: A speed–accuracy trade-off analysis. *Journal of Vision, 9*(3):30, 1–10, http://www.journalofvision.org/content/9/3/30, doi:10.1167/9.3.30. [PubMed] [Article]

Gottlieb, J. (2007). From thought to action: The parietal cortex as a bridge between perception, action, and cognition. *Neuron, 53,* 9–16. [PubMed]

Harter, M. R., Miller, S. L., Price, N. J., LaLonde, M. E., & Keyes, A. L. (1989). Neural processes involved in directing attention. *Journal of Cognitive Neuroscience, 1,* 223–237.

Hein, E., Rolke, B., & Ulrich, R. (2006). Visual attention and temporal discrimination: Differential effects of automatic and voluntary cueing. *Visual Cognition, 13,* 29–50.

Herrmann, K., Montaser-Kouhsari, L., Carrasco, M., & Heeger, D. J. (2010). When size matters: Attention affects performance by contrast or response gain. *Nature Neuroscience, 13,* 1554–1559. [PubMed]

Hillyard, S. A., Teder-Sälejärvi, W. A., & Münte, T. F. (1998). Temporal dynamics of early perceptual processing. *Current Opinion in Neurobiology, 8,* 202–210. [PubMed]

Hopf, J. M., Boehler, C. N., Luck, S. J., Tsotsos, J. K., Heinze, H. J., & Schoenfeld, M. A. (2005). Direct neurophysiological evidence for spatial suppression surrounding the focus of attention in vision. *Proceedings of the National Academy of Sciences of the United States of America, 103,* 1053–1058. [PubMed]

Hopfinger, J. B., Buonocore, M. H., & Mangun, G. R. (2000). The neural mechanisms of top-down attentional control. *Nature Neurosciences, 3,* 284–291. [PubMed]

Huang, L, & Dobkins, K. R. (2005). Attentional effects on contrast discrimination in humans: Evidence for both

contrast gain and response gain. *Vision Research, 45,* 1201–1212. [PubMed]

Itti, L., & Koch, C. (2000). A saliency-based search mechanism for overt and covert shifts of visual attention. *Vision Research, 40,* 1489–1506. [PubMed]

Johnson, C. A., Chauhan, B. C., & Shapiro, L. R. (1992). Properties of staircase procedures for estimating thresholds in automated perimetry. *Investigative Ophthalmology & Visual Science, 33,* 2966–2974. [PubMed]

Kanwisher, N., & Wojciulik, E. (2000). Visual attention: Insights from brain imaging. *Nature Reviews in Neuroscience, 1,* 91–100. [PubMed]

Kelly, S., Gomez-Ramirez, M., & Foxe, J. (2008). Spatial attention modulates initial afferent activity in human primary visual cortex. *Cerebral Cortex, 18,* 2629–2636. [PubMed]

Klein, R. M. (2000). Inhibition of return. *Trends in Cognitive Sciences, 4,* 138–147.

Koch, C., & Ullman, S. (1985). Shifts in selective visual attention: Towards the underlying neural circuitry. *Human Neurobiology, 4,* 219–227. [PubMed]

Kristjánsson, A., & Nakayama, K. (2002). The attentional blink in space and time. *Vision Research, 42,* 2039–2050. [PubMed]

Kustov, A. A., & Robinson, D. L. (1996). Shared neural control of attentional shifts and eye movements. *Nature, 384,* 74–77. [PubMed]

LaBerge, D., & Brown, V. (1989). Theory of attentional operations in shape identification. *Psychological Review, 96,* 101–124.

LaBerge, D., & Buchsbaum, M. S. (1990). Positron emission tomographic measurements of pulvinar activity during an attention task. *Journal of Neuroscience, 10,* 613–619. [PubMed]

Li, Z. (2002). A saliency map in primary visual cortex. *Trends in Cognitive Sciences, 6,* 9–16. [PubMed]

Ling, S., & Carrasco, M. (2006a). Sustained and transient covert attention enhance the signal via different contrast response functions. *Vision Research, 46,* 1210–1220. [PubMed]

Ling, S., & Carrasco, M. (2006b). When sustained attention impairs perception. *Nature Neuroscience, 9,* 1243–1245. [PubMed]

Liu, C. C., Wolfgang, B. J., & Smith, P. L. (2009). Attentional mechanisms in simple visual detection: A speed–accuracy trade-off analysis. *Journal of Experimental Psychology: Human Perception & Performance, 35,* 1329–1345. [PubMed]

Liu, T., Stevens, S. T., & Carrasco, M. (2007). Comparing the time course and efficacy of spatial and feature-based attention. *Vision Research, 47,* 108–113. [PubMed]

Lu, Z. L., & Dosher, B. A. (2000). Spatial attention: Different mechanisms for central and peripheral temporal precues? *Journal of Experimental Psychology: Human Perception and Performance, 26,* 1534–1548. [PubMed]

Lu, Z. L., Lesmes, L. A., & Dosher, B. A. (2002). Spatial attention excludes external noise at the target location. *Journal of Vision, 2*(4):4, 312–323, http://www.journalofvision.org/content/2/4/4, doi:10.1167/2.4.4. [PubMed] [Article]

Luck, S. J., Chelazzi, L., Hillyard, S. A., & Desimone, R. (1997). Neural mechanisms of spatial selective attention in areas V1, V2, and V4 of Macaque visual cortex. *Journal of Neurophysiology, 77,* 24–42. [PubMed]

Lyon, D. R. (1990). Large and rapid improvement in form discrimination accuracy following a location precue. *Acta Psychologica, 73,* 69–82. [PubMed]

Mackeben, M., & Nakayama, K. (1993). Express attentional shifts. *Vision Research, 33,* 85–90. [PubMed]

Mangun, G. R. (1995). Neural mechanisms of visual selective attention. *Psychophysiology, 32,* 4–18. [PubMed]

Mathôt, S., Hickey, C., & Theeuwes, J. (2010) From reorienting of attention to biased competition: Evidence from hemifield effects. *Attention, Perception & Psychophysics, 72,* 651–657. [PubMed]

Mazer, J. A., & Gallant, J. L. (2003). Goal-related activity in area V4 during free viewing visual search: Evidence for a ventral stream salience map. *Neuron, 40,* 1241–1250. [PubMed]

Mitchell, J. F., Sundberg, K. A., & Reynolds, J. H. (2003). Spatial attention decorrelates intrinsic activity fluctuations in macaque area V4. *Neuron, 63,* 879–888. [PubMed]

Müller, H. J., & Rabbitt, P. M. A. (1989). Reflexive and voluntary orienting of visual attention: Time course of activation and resistance to interruption. *Journal of Experimental Psychology: Human Perception & Performance, 15,* 315–330. [PubMed]

Nakayama, K., & Mackeben, M. (1989). Sustained and transient components of focal visual attention. *Vision Research, 29,* 1631–1647. [PubMed]

Nobre, A. C., Sebestyen, G. N., & Miniussi, C. (2000). The dynamics of shifting visuospatial attention revealed by event-related potentials. *Neuropsychologia, 38,* 964–974. [PubMed]

Olivers, C. N., & Meeter, M. (2008). A boost and bounce theory of temporal attention. *Psychological Review, 115,* 836–863. [PubMed]

Pastukhov, A., Fischer, L., & Braun, J. (2009). Visual attention is a single, integrated resource. *Vision Research, 49,* 1166–1173. [PubMed]

Pelli, D. G. (1997). The VideoToolbox software for visual psychophysics: Transforming numbers into movies. *Spatial Vision, 10,* 437–442. [PubMed]

Pestilli, F., & Carrasco, M. (2005). Attention enhances contrast sensitivity at cued and impairs it at uncued locations. *Vision Research, 45,* 1867–1875. [PubMed]

Pestilli, F., Ling, S., & Carrasco, M. (2009). A population-coding model of attention's influence on contrast response: Estimating neural effects from psychophysical data. *Vision Research, 49,* 1144–1153. [PubMed]

Posner, M. I. (1980). Orienting of attention. *The Quarterly Journal of Experimental Psychology, 32,* 3–25. [PubMed]

Posner, M. I., Sheese, B. E., Odludaş, Y., & Tang, Y. (2006) Analyzing and shaping human attentional networks. *Neural Networks, 19,* 1422–1429. [PubMed]

Reddy, L., Kanwisher, N. G., & VanRullen, R. (2009) Attention and biased competition in multi-voxel object representations. *Proceedings of the National Academy of Sciences of the United States of America, 15,* 21447–21452. [PubMed]

Reynolds, J. H., & Heeger, D. J. (2009). The normalization model of attention. *Neuron, 61,* 168–185. [PubMed]

Righi, L. L., & Ribeiro-do-Valle, L. E. (2011). Automatic attention lateral asymmetry in visual discrimination tasks. *Psychological Research, 75,* 24–34. [PubMed]

Robinson, D. L., & Petersen, S. E. (1992). The pulvinar and visual salience. *Trends Neuroscience, 15,* 127–132. [PubMed]

Sagi, D., & Julesz, B. (1986). Enhanced detection in the aperture of focal attention during simple discrimination tasks. *Nature, 321,* 693–695. [PubMed]

Shimozaki, S. S. (2010). Uncued and cued dynamics measured by response classification. *Journal of Vision, 10*(8):10, 1–27, http://www.journalofvision.org/content/10/8/10, doi:10.1167/10.8.10. [PubMed] [Article]

Shulman, G. L., Remington, R., & McLean, J. (1979). Moving attention through visual space. *Journal of Experimental Psychology, 92,* 428–431. [PubMed]

Shulman, G. L., & Wilson, J. (1987). Spatial frequency and selective attention to local and global information. *Perception, 16,* 89–101. [PubMed]

Smythies, J. (1996). A note on the concept of the visual field in neurology, psychology, and visual neuroscience. *Perception, 25,* 369–371. [PubMed]

Spitzer, H., Desimone, R., & Moran, J. (1988). Increased attention enhances both behavioral and neuronal performance. *Science, 15,* 338–340. [PubMed]

Talgar, C. P., Pelli, D. G., & Carrasco, M. (2004). Covert attention enhances letter identification without affecting channel tuning. *Journal of Vision, 4*(1):3, 22–31, http://www.journalofvision.org/content/4/1/3, doi:10.1167/4.1.3. [PubMed] [Article]

Theeuwes, J., Atchley, P., & Kramer, A. F. (2000). On the time course of top-down and bottom-up control of visual attention. In S. Monsell & J. Driver (Eds.), *Attention and performance XVIII* (pp. 105–124). MIT Press.

Thompson, K. G., & Schall, J. D. (2000). Antecedents and correlates of visual detection and awareness in macaque prefrontal cortex. *Vision Research, 40,* 1523–1538. [PubMed]

Tse, P. U. (2004). Mapping visual attention with change blindness: New directions for a new method. *Cognitive Science, 28,* 241–258. [PubMed]

Tsotsos, J. K. (1990). A complexity level analysis of vision. *Behavioral and Brain Sciences, 13,* 423–445.

Ward, L. M. (2008). Attention. *Scholarpedia, 3,* 1538. Available at http://www.scholarpedia.org/article/Attention.

Weichselgartner, E., & Sperling, G. (1987). Dynamics of automatic and controlled visual attention. *Science, 238,* 778–780. [PubMed]

Yantis, S., & Jonides, J. (1990). Abrupt visual onsets and selective attention: Voluntary versus automatic allocation. *Journal of Experimental Psychology: Human Perception and Performance, 16,* 121–134. [PubMed]

Yeshurun, Y., Montagna, B., & Carrasco, M. (2008). On the flexibility of sustained attention and its effects on a texture segmentation task. *Vision Research, 48,* 80–95. [PubMed]

D. Searching for the neural correlates of object recognition

In the previous study we have seen the spatiotemporal deployment of visual attention has a significant effect in the detection of very simple stimuli. Several studies performed over the last decades have suggested that visual attention is the door to the conscious visual perception from detection to discrimination and recognition (for a review on visual attention and its properties on visual perception see Carrasco, 2011). Behind these doors represented by attention we can thus found higher order cognitive processes such as conscious object recognition.

As we have seen, explicit object recognition is supported by preliminary stages which are devoted to encode physical stimulus features in the form of neural activities across different brain areas (Pollen, 1999; Pollen, 2003; DiCarlo, Zoccolan, & Rust, 2012). These stages involve myriads of neural computations in specialized modules which serve to encode stimulus features as activities within specialized neural groups, with neural groups coding for the local contrast in the image and its frequency content (both in the primary visual cortex), figure/ground segregation and border ownership (mostly in V2), form encoding (along the ventral pathway, mostly in V4) etc. These processes are performed automatically and are thought to be largely unconscious (however see Zeki, 2008). An additional step (namely recurrent activity according to Lamme's theory, dynamic core inclusion in Edelman & Tononi's theory or the activation of the global workspace in Dehaene's theory) would render the output of these processes accessible for explicit recognition. However in order to investigate the neural representations beyond these primary or low-level visual processing, one has to somehow dissociate the activities occurring downstream these low-level processes.

A simple assumption is to consider all short-latency processes as low-level processes and those with later latencies as high-level visual processing representing explicit object recognition. However to decide which are early and late visual processes is somehow arbitrary; moreover, we know that high-level areas such as the prefrontal cortex can show very early responses (with earliest responses around 70 ms, Introduction, section G) and it is unclear if these early activities can be considered as low-level processes.

Another commonly approach used to extract the neural activity correlated with explicit recognition is to use subtractive methods, where activity from non-recognized trials is subtracted from activity obtained in recognized trials by simple linear subtraction (see for example Bar et al., 2001; Koivisto et al., 2008). Subtractive methods rely on the assumption that the several stages from low-level visual processing to object recognition are independent and thus it is possible to dissociate by developing a control task containing all the visual process that are *exactly identical*, except for the absence of the recognition processes, and thus, by subtracting the activity in the control condition to recognition condition, it would be possible to dissociate different processes. However, the validity of linear subtractive methods, relying in the implicit premise of a lack of interactions among the neural processes of a task, have been criticized by many authors (Friston et al., 1996; Sidtis, Strother, Anderson, & Rottenberg, 1999; Sartori & Umiltà, 2000; Overgaard, 2004; Banerjee, Tognoli, Assisi, Kelso, & Jirsa, 2008; Logothetis, 2008).

Thus, dissociating between the processes supporting the encoding of physical visual features from object recognition proper has not been an easy task. Can we isolate the neural correlates of object recognition? We shall briefly review two inspiring works that have shed light on the proper ways to approach the study of object recognition.

I. Dissociating visual information extraction from visual recognition. The paper of Carlson et al. 2006

One way to dissociate between recognition and feature extraction processes was brilliantly introduced by (Carlson, Grol, & Verstraten, 2006) which used fMRI in order to identify the brain areas underlying the encoding of visual features and those involved in the actual object recognition. The idea of this work was to dissociate these two processes (feature extraction and recognition) by distinguishing their distinctive dynamics which was assessed by manipulating the temporal dynamics of the information presentation within the stimulation protocol.

The principle was the following: discrete parts of visual information (represented by pictures of famous faces and written words) were unveiled step-by-step in this way distributing across time the amount of image information that was delivered to the visual system (Figure 21A and B). The linear accumulation of information on the screen would lead thus to a linear increase in the activity of areas involved in the feature extraction processes, which can be modeled as a linear increase in the hemodynamic response function (Figure 21C).

The accumulation of visual information eventually triggers the recognition of the object or the word which is represented as a discrete event. The recognition event would entrain a sudden increase in the activity of the areas involved in this process. This activity increase can be thus modeled as a discrete increase in the hemodynamic response locked to the moment of recognition, which is reported by the subject (Figure 21C).

A third response model profile accounted for the task related activity, which is invariant to the amount of visual information presented but continually active over the time needed to complete the task. Thus, a sustained response model was represented by a box car function corresponding to the time subjects were performing the recognition task (Figure 21C).

This approach effectively dissociated between cortical areas involved in visual feature extraction and recognition according to their response characteristics (i.e., information driven, sustained, and recognition-dependent) for the two tested tasks (faces and words).

For the face task, different brain areas were correlated with each one of the models proposed. For the information response model, significant activations were found in the cingulate, frontal and occipital cortex (Figure 22, upper panel, first row). For the sustained response model, significant effects were found in a distributed network involving cingulate cortex, bilateral central sulcus, bilateral intraparietal sulcus, the left insula, the caudate nucleus, the thalamus, bilateral fusiform and lateral occipital regions (Figure 22, upper panel, second row). For the recognition response model, correlated activity was found in thalamus, bilateral fusiform, supplementary motor areas, the anterior cingulate, right superior frontal sulcus, and the left precentral sulcus (Figure 22, upper panel, third row).

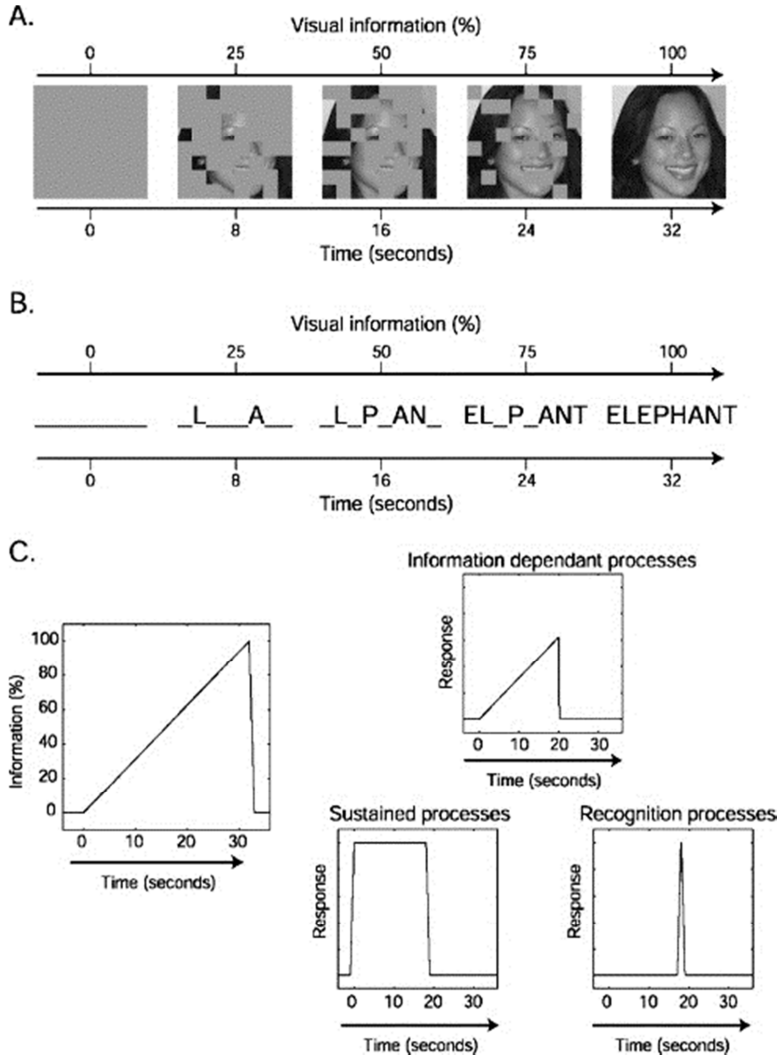

Figure 21. Experimental paradigm used in the study of Carlson et al. A. *Face recognition paradigm. Visual information in the form of small patches of the image was depicted over a period of 32 s.* ***B.*** *Schematic illustration of the word recognition paradigm. Visual information in the form of written words was depicted over the same period.* ***C.*** *Visual information plotted as function of time shown with the three hypothetical response models. Information-dependent response was modeled as linear increase in activity in response to increasing visual information. Sustained response model as box car function corresponding to the time subjects are performing the recognition task. Recognition response was modeled as a discrete event occurring at the moment of recognition. (From Carlson et al., 2006).*

For the word task, the information response model revealed significant patterns of activity in bilateral intraparietal sulcus, bilateral occipital gyri, and the left fusiform (Figure 22, lower panel, first row). For the sustained response model, correlated activity was found in cingulate sulcus, and precuneus (Figure 22, middle panel, second row). For the recognition response model, the areas significantly correlated with the recognition model included supplementary motor areas and the anterior cingulate, the right superior frontal sulcus, bilateral lateral parietal cortex, and bilateral inferior frontal gyrus (Figure 20, middle panel, third row).

A conjunction analysis revealed common activations between the face and the world task (Figure 22, lower panel). While no significant overlapping activations were observed for the information or the sustained response model (Figure 20, lower panel, 2 first rows), a common network of frontal activation was observed for the recognition response model (Figure 22, lower panel, bottom row). These overlaps were observed in supplementary motor areas, the anterior cingulate, bilateral parietal cortex, the right superior frontal sulcus, bilateral inferior frontal gyrus, and the thalamus.

Thus, these results showed that early visual areas are correlated with the information response model, which is consistent with the role of early visual areas in coding local features of the image. On the other hand, activations correlated the sustained response model were found in both LO and FFA and were interpreted as a reflection of a process of maintaining object-based representations which is invariantly to the amount of information received, perhaps representing a pre-activation of object-based representations related to the task expectations. Finally, activations correlated with the recognition response model were identified as activations in high-level areas such as the fusiform, lateral parietal and frontal regions.

This work showed that by manipulating the available image information across time, it is possible to discriminate between brain mechanisms involved in extracting visual features and brain processes involved in visual recognition based in their respective activation time courses.

In the experiment discussed above, the recognition process emerged as result of the accumulation of the image information. In other words the semantic information of the

image was accessible when a sufficient amount of the physical information, represented for the unveiled area of the image, was available. Now, let's consider the following possibility: is it possible to manipulate the semantic information of the image independently of its physical information?

Image processing techniques allow manipulating the particular spatial arrangement of visual features which are associated with objects forms and carry on the semantic properties. These manipulations allow conserving some of their physical properties, such as spatial frequency or contrast. Let's see how the can the tools of image processing be used to manipulate object recognition.

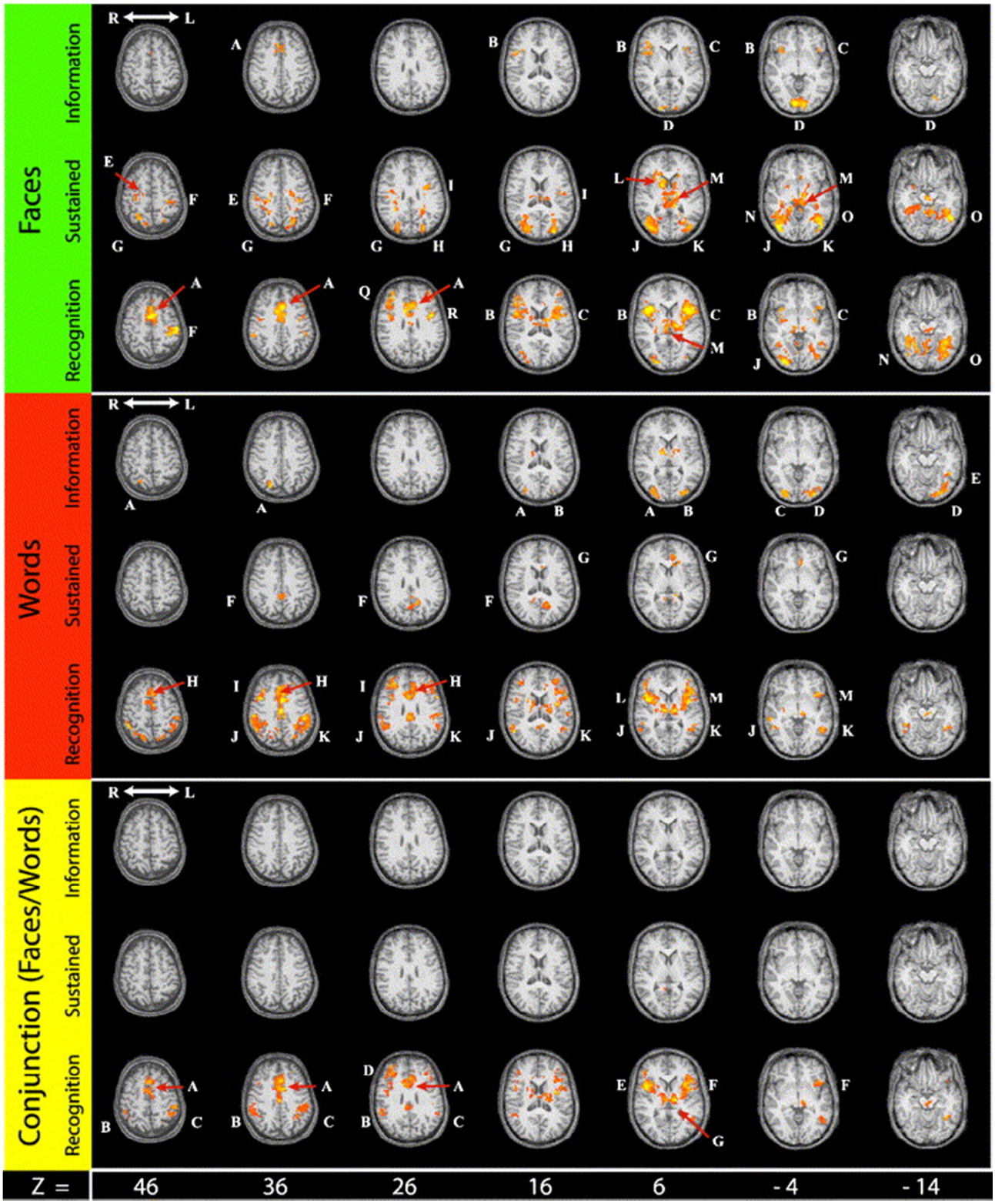
Faces
Information
Sustained
Recognition
Words
Information
Sustained
Recognition
Conjunction (Faces/Words)
Information
Sustained
Recognition
R
L
Z =
46
36
26
16
6
- 4
- 14

Figure 22. Statistical maps showing the activity correlated with the three response models.

Panel 1, face recognition. *The information model (upper row) activations associated with this model were found in supplementary motor areas and anterior cingulate (A), inferior frontal gyrus (B and C), and early visual areas (D). The sustained response model (middle row) was correlated with activations in the central sulcus (E and F), intraparietal sulcus (G and H), the insula (I), occipital gyri (J and K), the caudate (L), the thalamus (M), and fusiform (N and O). The recognition model (lower row) showed activations in supplementary motor areas and anterior cingulate (A), inferior frontal gyrus (B and C), the thalamus (M), fusiform (N and O), superior frontal sulcus (Q), and pre-central sulcus (R).*

Panel 2, word recognition. *The information model (upper row) activations associated with this model were found in intraparietal sulcus (A and B), occipital gyri (C and D), and fusiform (E). The sustained response model (middle row) was correlated with activations in the precuneus (F), and anterior cingulate (G). The recognition model (lower row) was associated with activations in supplementary motor areas and the anterior cingulate (H), superior frontal sulcus (I), lateral parietal cortex (J and K), and inferior frontal gyrus (L and M).*

Panel 3, Conjunction between face and word recognition. *The information model (upper row) No overlap was found between the face and word recognition tasks for this model. The sustained response model (middle row) No overlapping was found. The recognition model (lower row) was associated with activations in supplementary motor areas and the anterior cingulate (A), lateral parietal cortex (B and C), superior frontal sulcus (D), bilateral inferior frontal gyrus (E and F), and the thalamus (G). (From Carlson et al., 2006)*

II. Manipulating the object information in the Fourier domain. The paper of Sadr and Sinha 2004.

The manipulation of the semantic information while preserving some of the physical properties of the image is exploited by the technique called RISE, for Random Image Structure Evolution (Sadr & Sinha, 2004). The RISE technique manipulates visual stimuli which are systematically transformed from recognizable objects to unrecognizable random patterns. This transformation is performed by progressively scrambling the phase of the 2D Fourier coefficients of the image without altering the amplitude of each frequency, thus conserving the spatial frequency content of the image while altering the spatial relationship of their constitutive spatial frequencies, thus precluding the recognition of the object as the scrambling becomes stronger (Figure 23).

By using this approach, it is possible to confine the recognition to a set of frames within the entire RISE sequence as illustrated by the following experiment performed by (Sadr & Sinha, 2004). Five RISE sequences were generated from images of single objects (Figure 24) using the phase-manipulation technique described above (Figure 24). Each of the sequences depicted the evolution of one object.

Each onset and offset subsequence consisted of 75 images ranging in fixed steps from 50 to 85% interpolation of the source and random phase spectra, where 100% interpolation corresponds to the unaltered source image. This results in the images becoming increasing indistinguishable the more they are degraded. Each image in these sequences was presented for 750 ms. Between the presentation of consecutive frames, subjects pressed one of two keys, indicating whether they had or had not recognized the object in the frame just presented.

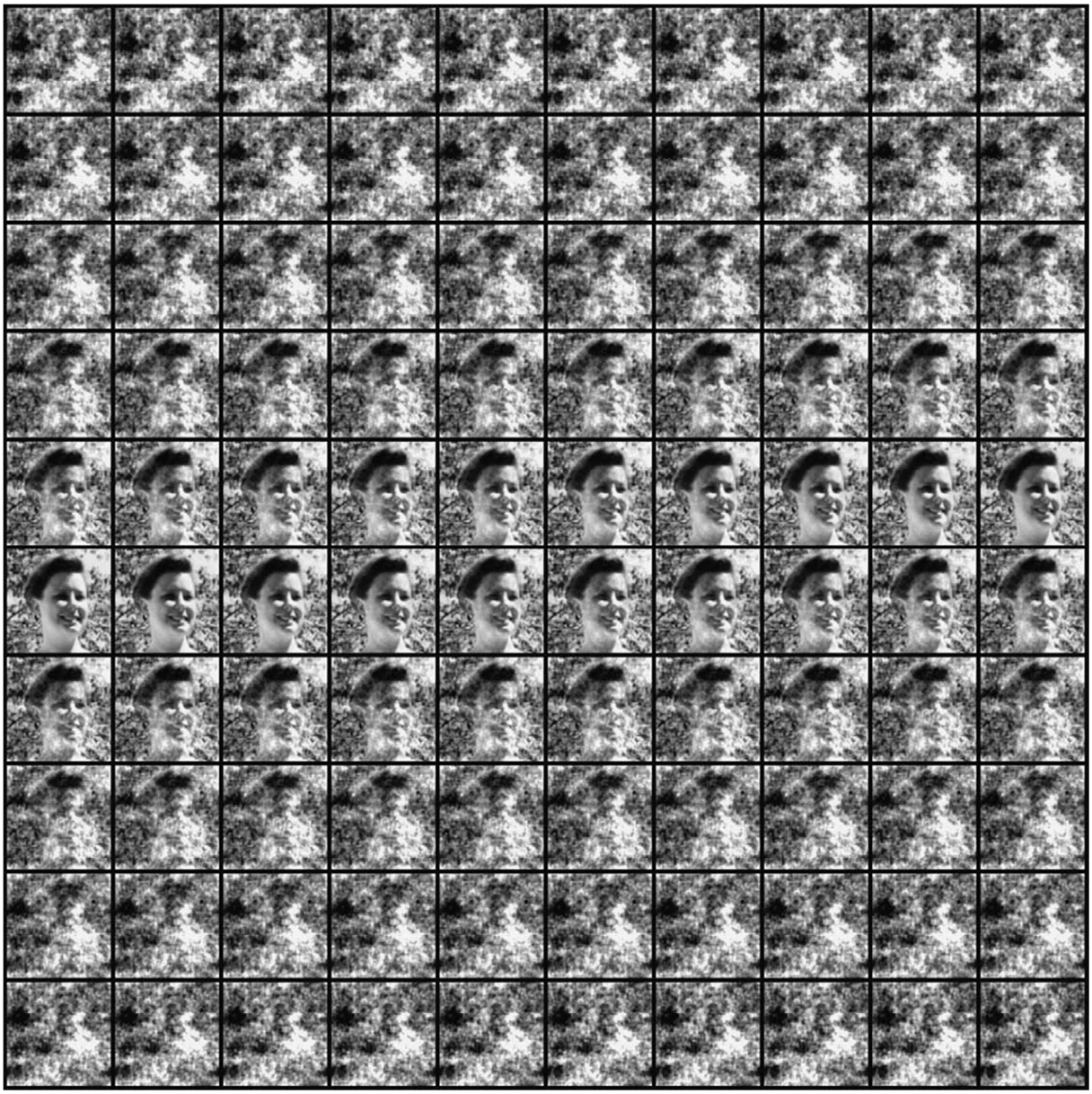

Figure 23. RISE sequence example. *Different frames of a RISE sequence generated by progressive degradation of the phase 2D Fourier coefficients of the source image. This technique progressively disrupts the spatial structure of the image while low-level image properties of the original image, such as the spatial frequency spectrum and overall luminance, are perfectly preserved. (From Sadr & Sinha, 2004).*

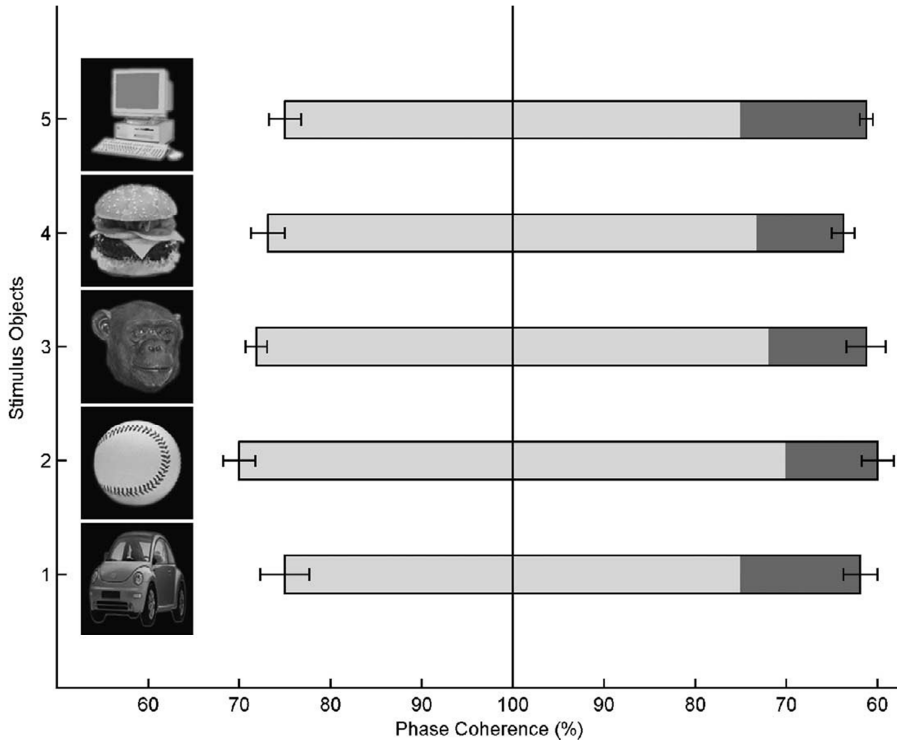

Figure 24. Recognition as a function of phase-coherence. *The recognition of objects was manipulated by the amount of phase-coherence of single frames within a RISE sequence. The onset and the offset parts of the sequence are represented by the left and right side of each bar. Perceptual hysteresis (i.e., recognition at higher levels of phase-scrambling after the recognition of the image) was evident during the offset of the sequence which is represented by the dark gray part of the bar. (From Sadr & Sinha, 2004).*

Figure 24 shows the onset and offset of recognition as a function of phase coherence. The onset of object recognition was situated between 70 and 80% of phase coherence; while the offset was located between 60 and 70% due to hysteresis effects (i.e. the subject already knew the identity of the object).

This work showed that the recognition of an image can be controlled by disturbing its semantic content, while preserving some of their physical attributes. Such an approach is suitable in order to dissociate between the neural correlates of object recognition and the neural correlates of the encoding of its physical features, at least for those involving the encoding of the spatial frequency content and overall luminance. Now, a last element is missing in order to create a stimulation method in which: (1) the semantic content is modulated, (2) the physical features are conserved (3) the responses driven by low-level

stimulation transients are avoided, and (4) the neural activity driven by the object could be tracked using neuroimaging techniques. Let's see how the stimulus representations can be tracked in a dynamic stimulation paradigm which allows directly tagging stimulus representations by frequency.

III. Tracking visual stimuli in brain signals: the frequency-tagging technique

The frequency-tagging technique principle is quite simple: a flickering stimulus entrains a response in the brain at the same frequency of the flickering stimulus (and often its harmonics) thus 'tagging' the stimulus driven activity in the brain at the flickering temporal frequency.

The frequency tagging approach is an application of the steady-state visual evoked potentials (SSVEP) phenomenon. In SSVEP, the constituent discrete frequency component in the evoked potentials remains closely constant in amplitude and phase over long periods of time (Regan 1966, Regan 1982). This regularity is manifest in the frequency domain, allowing tracking the evoked activity by means of a Fourier analysis.

Figure 25 illustrates the differences between a traditional transient visual evoked potential (VEP) and SSVEP. While the transient VEP does not evoke any stationary response, the SSVEP stimulation drives a stationary response which can be measured in the frequency domain by using the Fourier analysis.

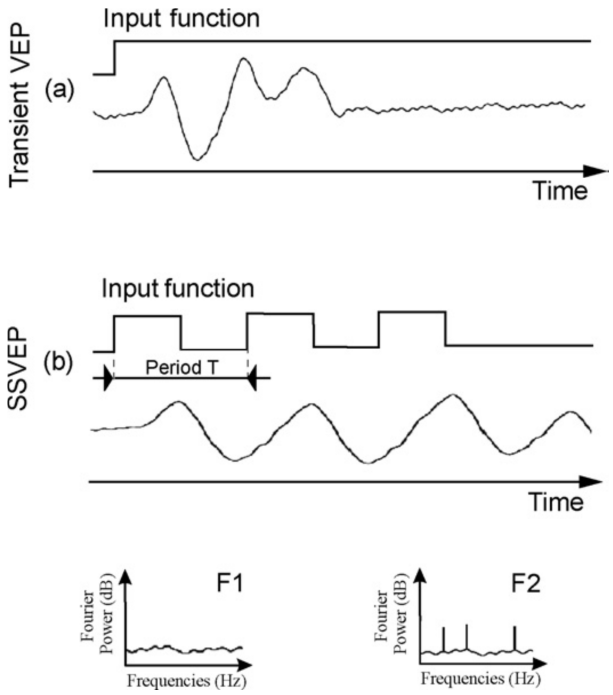

Figure 25. Transient VEP vs. SSVEP—synthetic model. A. *Diagram representing the input function, with a square stimulation (transient); the bottom trace represents a transient VEP.* ***B.*** *The upper diagram represents the input function, a periodic square wave (period T); the bottom trace represents a SSVEP response. A transient VEP response may not show any stationary distinct spectrum (i.e. a distinctive peak at a given temporal frequency) in the corresponding Fourier representation (schematically in F1). SSVEP responses instead generates distinct peaks at the stimulus frequency and its harmonics (as in F2; a square wave elicits responses at the even harmonics). Note that distinct peaks can only be observed if the Fourier spectrum is calculated over a sufficiently large window (i.e., the time window must be at least as large as the period T is). If the window is too short, the SSVEP cannot be observed. For example, for a 1 Hz SSVEP, the recording duration must be at least 1 s. (From Vialatte, Maurice, Dauwels, & Cichocki, 2010).*

SSVEP responses can be obtained using a large range of temporal frequencies, up to at least 90 Hz in humans, revealed using EEG recordings (Herrmann, 2001) and up to 50 Hz in cat early visual cortex, revealed using unitary recordings (Rager & Singer, 1998). SSVEP responses to drifting gratings have also been recorded using cortical EEG on monkeys (Nakayama & Mackeben, 1982). SSVEP responses have been also showed at the delta range (from 0.5 to 5 Hz) in human EEG signals (Vialatte, Maurice, Dauwels, & Cichocki, 2008). SSVEP responses as a function of the temporal frequency of the flickering stimulus (usually a

contrast-reversing check board) have showed three frequency bands centered at ~10Hz, ~20Hz and ~40Hz at which the SSVEP responses amplitude are enhanced (Spekreijse, Estevez, & Reitz, 1977; Regan, 1982; Regan, 1989). These frequency bands are associated with preferred resonance frequencies within the visual system related with its temporal processing dynamics (Vialatte et al., 2010).

IV. Summing-up

By taking elements from each of these paradigms we developed a novel stimulation technique aimed to investigate the neural correlates of high-level representations. From the paradigm of Carlson et al. we take the idea of depicting the semantic image content at discrete amounts in order to dissociate neural activity associated to the encoding of image features and the recognition proper. From the paradigm of Sadr and Sinha we borrowed the concept of manipulation of the image recognizability while conserving some of the image's low-level properties. Finally, we combined those ideas with SSVEP in order to produce a steady flow of low-level features stimulation avoiding thus neural responses evoked by low-level transients and, at the same time, allowing studying the temporal dynamics of high-level representations in the visual system. Let's see how this works.

V. PAPER 3: Koenig-Robert & VanRullen, submitted to Journal of Neuroscience.

Isolating and tracking the neural correlates of object recognition.

Roger Koenig-Robert[1,2] & Rufin VanRullen[1,2]

1 Centre de recherche cerveau et cognition (CerCo), UMR5549, CNRS.

2 Université Paul Sabatier, CHU Purpan, Toulouse, France.

Corresponding author: Roger Koenig-Robert.

Address:

Centre de Recherche Cerveau et Cognition (CerCo) – CNRS

Pavillon Baudot CHU Purpan

BP 25202

31052 Toulouse Cedex – France

email: rogkoenig@gmail.com

Isolating the neural correlates of object recognition and studying their fine temporal dynamics has been a great challenge in neuroscience. A major obstacle has been the difficulty to dissociate low-level feature extraction from the actual object recognition activity. Here we present a new technique called semantic wavelet-induced frequency-tagging (SWIFT), where cyclic wavelet-scrambling allowed us to isolate neural correlates of object recognition from low-level feature extraction. We show that SWIFT is insensitive to unrecognized objects, which were presented up to 30 s, but is highly selective to the recognition of the same objects after their identity has been revealed. The enhancement of object representations by top-down attention was particularly strong with SWIFT due to its selectivity for high-level representations. Finally, SWIFT allowed us to measure the temporal dynamics of conscious object representation: we found it to reach its limit between 4 and 7 conscious representations per second.

Running title: Tracking the neural correlates of object awareness.

How visual objects are represented as meaningful items in our brains and become part of our conscious experience is one of the most fascinating questions in neuroscience. Current models, largely inspired by invasive studies in monkeys, propose a view of the visual system where object representations emerge progressively from a hierarchical cascade of processing stages (Felleman and Van Essen, 1991; Riesenhuber and Poggio, 1999). Early stages are devoted to extracting simple visual features such as luminance (Amthor et al., 2005), contrast (Sclar et al., 1990), contours (Hubel and Wiesel, 1968) and intersecting lines (Hegdé and Van Essen, 2000). Downstream in the ventral pathway, the integration of these simple features implies that neurons become selective to more and more complex forms, e.g. in area V4 (Gallant et al., 1993). At the highest purely visual area in the ventral stream, the inferotemporal cortex (IT), neurons can be selective to single object categories (Tanaka, 1996; Kobatake and Tanaka, 1994). While neuronal selectivities in the ventral stream of the monkey visual system are well understood, their associated semantic value is difficult to access. Where and when do meaningful object representations emerge? Non-invasive techniques have been developed to track visual stimulus representations in the human brain –for which perceptual meaning can be more readily assessed. Functional magnetic resonance imaging (fMRI) has played a major role in understanding the human brain areas engaged in object representations. For example, fMRI has revealed that some regions of the temporal lobe are selective to faces in the FFA (Kanwisher et al., 1997), scenes in the PPA (Epstein et al., 1999) or body parts in sub-regions of the LOC (Downing et al., 2001), and there is good evidence that these regions respond more strongly when the corresponding stimuli are consciously perceived by the subjects (Tong et al., 1998; Grill-Spector et al., 2000; Bar et al., 2001; Hesselmann and Malach, 2011). However, the temporal dynamics of object representations on the scale of a few tenths of a second are unattainable to the slower temporal resolution of fMRI. Electroencephalography (EEG) has been extensively used to explore these temporal dynamics in humans. More particularly, steady-state visual evoked potentials (SSVEP) can track the activity elicited by a given visual stimulus in near-real time. This method, also known as frequency tagging, involves the modulation of a stimulus's intensity over time at a fixed temporal frequency *f0*; a neural response is evoked at the same frequency *f0* (and usually its harmonics), thus providing a frequency label (or tag) for the stimulus representation in the brain(Regan, 1977; Srinivasan et al., 2006; Appelbaum and Norcia, 2009). The frequency-tagged response has been found to depend on attention (Morgan et al., 1996; Müller et al., 1998; Ding et al., 2006; Kim et al., 2007) and on the subject's perceptual state (Tononi et al., 1998; Kaspar et al., 2010; Srinivasan and Petrovic, 2006; Sutoyo and Srinivasan, 2009). One limitation of SSVEP is that they normally rely on the modulation of stimulus contrast or luminance; as a result, both semantic object-representations and low-level feature extraction mechanisms are simultaneously tagged at the modulation frequency. In order to try to disentangle these two processes, we developed a novel

technique called SWIFT (semantic wavelet-induced frequency tagging) in which we equalized low-level physical attributes (luminance, contrast and spatial frequency spectrum) across all frames of a sequence, while modulating, at a fixed frequency *f0,* the mid- and higher-level image properties carried by the spatial configuration of local contours. This novel approach allowed us to isolate the neural correlates of object recognition: we show that SWIFT is insensitive to unrecognized objects presented up to 30 s, but is highly selective to the recognition of the same objects once their identity has been explicitly revealed. As a further confirmation of their high-level nature, we demonstrate that SWIFT signals are strongly modulated by top-down attention –considerably more so than classic SSVEP signals. Finally, SWIFT allowed us to measure the temporal capacity of conscious object representations: we found a limit between 4 and 7 items per second.

Results

SWIFT sequences properties:

By scrambling information in the wavelet domain (see Experimental procedures and Fig 1), we created image sequences in which the contours of the image were disrupted cyclically at a fixed frequency *f0*, while low-level properties (in particular global luminance, local luminance modulation, contrast and spatial frequency spectrum) were preserved at all time-points. As a result, visual processing mechanisms that are sensitive to these low-level features should be equally engaged by all frames in the sequence, and their response profile should thus be independent of *f0*. On the other hand, higher-level mechanisms responsible for extracting semantic information would only come into play once during each cycle: around the onset of the original, unscrambled image. By analyzing the neural activity evoked at *f0* we should thus be able to isolate form-sensitive and higher-level mechanisms.

Our first step was to verify that our SWIFT procedure indeed preserved low-level image features at both the local and global levels. In our procedure (see Methods section), each wavelet was temporally modulated at a different harmonic (i.e. multiple) frequency of *f0*, such that individual contour elements returned to their original orientation several times per cycle –but the entire image was restored only once per cycle. As a result, the luminance of individual pixels was modulated equally over a wide range of frequencies, and the average temporal frequency spectrum of pixel luminance was thus found to be constant around the frequency of interest *f0* (fig 1b, upper panel, red curve); in contrast, classic SSVEP methods using luminance or contrast modulation produce a sharp peak at *f0* in this temporal frequency spectrum (fig 1b, upper panel, black curve). Similarly,

global image contrast was also preserved over time in SWIFT sequences (fig 1b, lower panel, red curve), but not in classic SSVEP sequences (fig 1b, lower panel, black curve). Finally, our wavelet scrambling procedure also conserves the local distribution of spatial frequencies, since (by design) it only affects the orientation, but not the energy or spatial frequency of each wavelet.

Phenomenologically, SWIFT sequences are perceived as a periodic flow of discernible information (i.e. the embedded image) recurringly fading-out into an indistinguishable pattern –like an image reflected in a water surface suddenly vanishing into chaotic ripples (see Movie S1 at http://cerco.ups-tlse.fr/~koenig/SWIFT_manuscript/Movie_S1.avi). The recurrence of the embedded image is pulsatile, rather than sinusoidal. This is a consequence of the introduction of multiple harmonic frequencies in the wavelet scrambling: the original image is only visible when the phases of the different harmonic modulations come into alignment. With the five harmonics used here (see Methods section) the embedded image was recognizable in only ~10% of the individual frames (see Figure S1). This visibility can be manipulated by varying the temporal frequency *f0* and the number of harmonic frequencies used in the wavelet scrambling. We exploited this property to create sequences where the embedded object was difficult to identify. Crucially, after priming the content of the sequence by revealing the original image, the same unrecognized objects became easy to recognize in a second presentation, enabling us to compare EEG activity when subjects were aware and unaware of the embedded object, as illustrated in the next section.

Isolating object recognition awareness:

To determine our method's sensitivity to semantic processing, we compared the activity elicited by SWIFT sequences in three different conditions: (1) when the semantic content was present and perceived, (2) when it was present and not perceived and (3) when there was no semantic content. To create these conditions, SWIFT sequences were produced containing natural images that could be either recognized (i.e. semantic information is available and perceived) or not recognized (i.e. semantic information is available but not perceived); we also produced sequences containing abstract textures (i.e. no semantic information), which were used as a baseline. We showed each sequence twice, the second time after having explicitly revealed the embedded semantic content (when available), such that we could compare the activity elicited by exactly the same sequence before and after the subject had access to the semantic information.

More precisely, we presented SWIFT sequences (n=100) containing either grayscale natural images with one principal visual object (80%) or low-level matched textures (20%). The image contours were

modulated cyclically over time at *f0*=1.5 Hz, meaning that the original image reappeared regularly with a period of ~0.67 s. Importantly, each sequence contained only one embedded image (either a natural image or an abstract texture), and was used only once in the experiment. Each trial consisted of two distinct periods (figure 2a): the first "naïve" period (30 s), followed by a steady presentation of the original image contained in the sequence (2 s), and finally the "cognizant" period (10 s). In the naïve period, subjects saw the SWIFT sequence for the first time; their task consisted in reporting the identification of a visual object (i.e. a non-abstract item) by a button press as fast as possible. Two different response keys were provided corresponding to distinct confidence levels: “I perceive an object-like item, but I am not sure of which object it is” (key 1), and “I see an object and I have identified it confidently” (key 2). It was possible to press the second key directly, or the first key subsequently followed by the second one. When subjects did not perceive any object no key press was required. After the naïve period, the image embedded in the sequence was revealed and presented steadily for 2 s. Subjects were instructed to explore it freely and to seek the features (if any) that had not been recognized during the naïve period. Finally, in the cognizant period the SWIFT sequence was showed again (10 s), and subjects were asked to try and identify the object and/or the details they had missed during the naïve period. The natural images used to construct the sequences contained non-canonical views of bodies, faces, animals and manmade objects, which means that several images were not recognized during the naïve period, but only during the cognizant period, i.e. after their identity had been revealed. This allowed us to compare the activity elicited by SWIFT when the same object was recognized and when it was not.

Trials were classified as 'quickly recognized' when a natural image was presented and the subject recognized an object with high confidence within the first 10 s of the naïve period (22.2% of trials). Trials were classified as 'tardily recognized' when a natural image was presented but the subject did not recognize an object during the 30 sec of the naïve period (22.4% of trials). Trials were classified as 'no-object' when abstract textures where presented (20%, regardless of the subject's response: the false alarm rate at low confidence was 2.86%, and at high confidence only 0.14%). Sequences presenting natural images where the objects were not confidently detected (i.e. only with low confidence, or with high confidence but only after the first 10s of presentation) were not analyzed (35.4% of trials).

We analyzed EEG data (64 channels) of 17 participants. Each wavelet-scrambling cycle (669 ms), starting at the moment when the original image was fully recognizable, was taken as an epoch to compute the event-related potential (ERP). Based on the ERP topography (Fig 2b), we selected 4 central electrodes where the ERP was highest, and we present the corresponding ERP in figure 2b. The ERP for no-object trials can be used as a baseline (green line, fig 2b), since there was no semantic

information present in these trials. The quickly recognized trials (where the semantic information was present and perceived, black line, fig 2b) showed a positive peak around 300 ms, both during the naïve period (with a significant difference to the 'no-object' baseline from 261 to 387ms, two-tailed, paired t-test, $p<0.05$) and during the cognizant period (significant difference from 269 to 411ms). Tardily recognized trials in the naïve period (where the semantic information was present but not yet perceived, red line, Figure 2b, left panel), on the other hand, were not significantly different from no-object trials (two-tailed, paired t-test, $p>0.05$), but only showed a significant difference during the cognizant period (where the semantic information was present and this time perceived, red line, Figure 2b, right panel) from 269 to 388 ms (two-tailed, paired t-test, $p<0.05$). ERP topographies, computed over time points when quickly-recognized ERPs differed from baseline for the naïve period (261 - 387 ms), and over time points when both quickly-recognized ERPs and tardily-recognized ERPs differed from baseline for the cognizant period (269 -388 ms), show a positive central potential which is selective to object recognition: it is present whenever an object is recognized (whether spontaneously, during the naïve period, or after explicit priming, during the cognizant period), but it is absent otherwise.

Finally, the similarity of SWIFT responses across subjects was assessed by computing the phase-locking value of ERPs, band-pass filtered at *f0,* across the subjects' population (see Experimental procedures for details). Whenever an object was recognized (quickly recognized trials in both naïve and cognizant periods, and tardily recognized trials in cognizant period) a significant phase-locking emerged, indicative of a globally similar ERP waveform across subjects (Figure 2c). Importantly, no significant phase locking was observed for unrecognized objects or no-object sequences. Thus, SWIFT responses appear to constitute a reliable index of conscious recognition.

Measuring attention deployment:

Top-down attentional modulations are known to be stronger in higher-level visual areas than in lower-level ones (Lauritzen et al., 2009; Müller and Kleinschmidt, 2003; Beck and Kastner, 2005; McMains and Kastner, 2011). As a result, the conscious representation of an object must be enhanced more strongly by attention than the physical attributes of the same object. Hence, SWIFT responses should be more strongly modulated by attention than the responses from more classic frequency-tagging methods. To test this we quantified attention deployment to a face image using either (on randomly interleaved trials) a simple contrast modulation (classic SSVEP) or our wavelet-scrambling method (SWIFT). In each trial, two faces were presented on either side of fixation, each one oscillating at a different frequency (1.5 Hz or 2.03 Hz, positions counterbalanced across trials). A

central cue, pointing either to the left or right, indicated which face had to be attended (Figure 3a). In order to engage the subjects' attention, the task was to report whether a "deviant" cycle (20% probability) had occurred in the attended sequence (i.e. a cycle in which the circular wavelet scrambling or the SSVEP contrast modulation did not return to the original image, see Experimental procedures for details). The effect of attention was measured as the relative increase of phase-locking values across trials at *f0* over all channels, for the target sequence compared to the distractor sequence (Figure 3b; see Experimental procedures for details). The amplitude of the attentional effect revealed by the classic SSVEP technique was 30.1% (±6%, s.e.m. across 8 subjects), consistent with existing findings (Kim et al., 2007; Müller et al., 1998; Morgan et al., 1996). In SWIFT trials, the attentional effect reached 208.5% (±23%, s.e.m.). This impressive difference ($p<10^{-4}$, two-tailed, paired t-test) confirms that SWIFT selectively tags high-level object representations, which are more strongly modulated by top-down attention than the lower-level feature extraction processes associated with more classic SSVEP sequences.

Probing the temporal dynamics of object representations:

Finally, we used SWIFT to measure the rate at which the visual system can produce semantic object representations. To this aim, we presented SWIFT sequences at different modulation frequencies *f0*: the maximum frequency at which SWIFT can successfully tag object representations should indicate the fastest rate at which the visual system can extract and integrate visual information to lead to a conscious perception. SWIFT sequences containing grayscale natural images (n=20) were shown at 8 frequencies in different trials (1.5, 2.03, 2.62, 3.4, 4.32, 6.96, 8.42 and 12.31 Hz). As in the previous experiment, the subjects' task was to detect any deviant cycle (present in 20% of trials). We measured the tagging as the mean phase-locking factor across trials at *f0* (Figure 4; see Experimental procedures). This tagging was significant from 1.5 to 4.32 Hz (two-tailed, one sample t-test, fdr-corrected, $p = 3.3\cdot10^{-5}$, $2.6\cdot10^{-5}$, $8.5\cdot10^{-4}$, $3.3\cdot10^{-5}$, $2.9\cdot10^{-5}$). Thus, the high-level object representations that are selectively tagged by the SWIFT method appear to reach their limit between 4 and 7 object representations per second.

Discussion

We have developed a new technique to explore the neural correlates of object perception awareness. As a consequence of the conservation of low-level features on each frame, SWIFT isolates

high-level activities –i.e. the brain's time-locked responses to the pulsatile flow of semantic information carried by the frames where the embedded images are visible. As a result, the correlates of object perception awareness can be measured directly as a "tagging" response at the fundamental frequency *f0*, without requiring a comparison or subtraction between perceived and unperceived objects, as many other methods do (Del Cul et al., 2007; Tononi et al., 1998; Sergent et al., 2005; Koivisto et al., 2008; Sutoyo and Srinivasan, 2009). Importantly, in our case there was simply no tagging response for unperceived objects at the selected channels (Figure 2b), thus neural activities that selectively reflect awareness are immediately evident. In addition, SWIFT shares the advantages of more classic SSVEP techniques, i.e. an improved signal-to-noise ratio since a large part of the noise can be discarded by focusing the analysis at the tagging frequency *f0*. The positive perception-related potential revealed by SWIFT was consistent across subjects, both in terms of amplitude and overall shape (fig. 2b and 2c), even though its absolute magnitude was relatively small (~0.2 μV, fig. 2b). This could be due to the fact that the neural populations supporting object recognition awareness are smaller and/or sparser than those encoding the physical features of the stimulus –which eventually determine the major part of the larger evoked responses seen in typical ERPs.

The neural correlates of object recognition revealed with our technique have an onset around 250 ms, peaking at about 350 ms, in accordance with previous reports (Del Cul et al., 2007; Sergent et al., 2005 ; Quiroga et al., 2008; Lamy et al., 2009; Babiloni et al., 2006). This may seem rather tardy when compared with other object recognition-related potentials that have been reported as early as 150-200ms after stimulus onset (Thorpe et al., 1996; Jeffreys, 1996; Bentin et al., 1996; VanRullen and Thorpe, 2001; Fisch et al., 2009 ; Pins and Ffytche, 2003). Of course, neural activities that merely correlate with stimulus perception can be observed at several moments of the visual processing sequence, and even sometimes before the stimulus onset (Busch et al., 2009): in this case, this would only indicate a “readiness state” of the brain that later promotes stimulus detection and recognition. Thus, it is important to distinguish causes and effects when describing neural activities correlated with conscious perception. Based on our results, we propose that activities in the time window from 150 to 200 ms would not directly represent conscious access but rather non-conscious processing (Dehaene et al., 2006), possibly semantic in some cases (Gaillard et al., 2009; Van Opstal et al., 2011), which may ultimately produce consciousness at later stages (Del Cul et al., 2007; Dehaene and Changeux, 2011). On the other hand, the signals elicited by SWIFT (fig 2b) seem to directly index conscious access. The latency and central-parietal topography of the SWIFT response suggests a potential relation to the P300 ERP component and more specifically to the P3b component (Fjell and Walhovd, 2003). The P3b component is the most consistent correlate of visibility found in ERP recordings (Dehaene and Changeux, 2011). It has been reproducibly found to vary with stimulus

perception when comparing trials with or without conscious perception (Babiloni et al., 2006; Del Cul et al., 2007; Fernandez-Duque et al., 2003; Koivisto et al., 2008 ; Lamy et al., 2009; Niedeggen et al., 2001 ; Pins and Ffytche, 2003 ; Sergent et al., 2005). The areas that generate the P3b may include hippocampus and temporal, parietal, and frontal association cortices (Halgren et al., 1998; Mantini et al., 2009), supporting the notion that at this stage of processing the sensory information is broadcasted over a large network or "global workspace", which would serve to promote conscious access (Baars, 1988; Dehaene et al., 2006 ; Dehaene and Changeux, 2011; Tononi, 2004).

Results from experiment 3 (fig 4b) suggest that the visual system can only form a maximum of between 4 and 7 different object representations per second. This may seem at odds with classic reports of semantic recognition in rapid sequences of 10 or more images per second (Potter and Levy, 1969; Potter, 1976; Keysers et al., 2001), but it is in accordance with many experimental findings (Holcombe, 2009), for example from the attentional blink (AB) paradigm, where the second of two targets cannot be detected or identified when it appears around 250ms after the first (Chun and Potter, 1995; Nieuwenstein et al., 2009). The AB phenomenon has been interpreted as a competition between the neural processes underlying the P3b wave evoked by the first target and those reflecting earlier processing of the second target (Sergent et al., 2005). Similarly in our paradigm, an interaction between the P3b elicited about 300ms after semantic information is presented in a given SWIFT cycle and lower-level processing of visual information within the next cycle could explain why the tagging weakens at rates higher than about 4 cycles per second. A similar temporal limit of about 4 conscious events per second has recently been proposed on theoretical grounds (Madl et al., 2011), but direct experimental evidence had been lacking until now.

Finally, SWIFT revealed signal modulations by top-down attention that were much larger than those measured with classic SSVEP techniques. This confirms that SWIFT selectively indexes higher-level object representations, which are more strongly modulated by attention than the lower-level representations tagged using classic SSVEP (Lauritzen et al., 2009; Müller and Kleinschmidt, 2003; Beck and Kastner, 2005; McMains and Kastner, 2011). This property, together with the fact that SWIFT can track object representations for extended time periods, lets us envision the possibility of using SWIFT for brain computer interface (BCI) applications, with subjects controlling peripheral devices by focusing their attention on specific SWIFT-tagged items on a screen.

Future research should characterize the brain areas mediating SWIFT responses. Here, two outcomes are conceivable. First, a strictly hierarchical view of visual processing where conscious perception depends on the engagement of high-level areas (Crick and Koch, 1995; Crick and Koch, 1998; Crick and Koch, 2003; Libedinsky and Livingstone, 2011) should predict SWIFT-related activities to be

restricted to higher levels of the hierarchy (e.g. temporal lobe or frontal regions). A second possibility stems from the notion that conscious perception reflects recurrent activity at multiple stages of the visual system (Baars, 1988; Tononi, 2004; Lamme and Roelfsema, 2000; Dehaene and Changeux, 2011; Dehaene et al., 2006). In this case, SWIFT-related signals should also be found upstream in the visual pathway, indicating recurrent engagement of earlier visual areas.

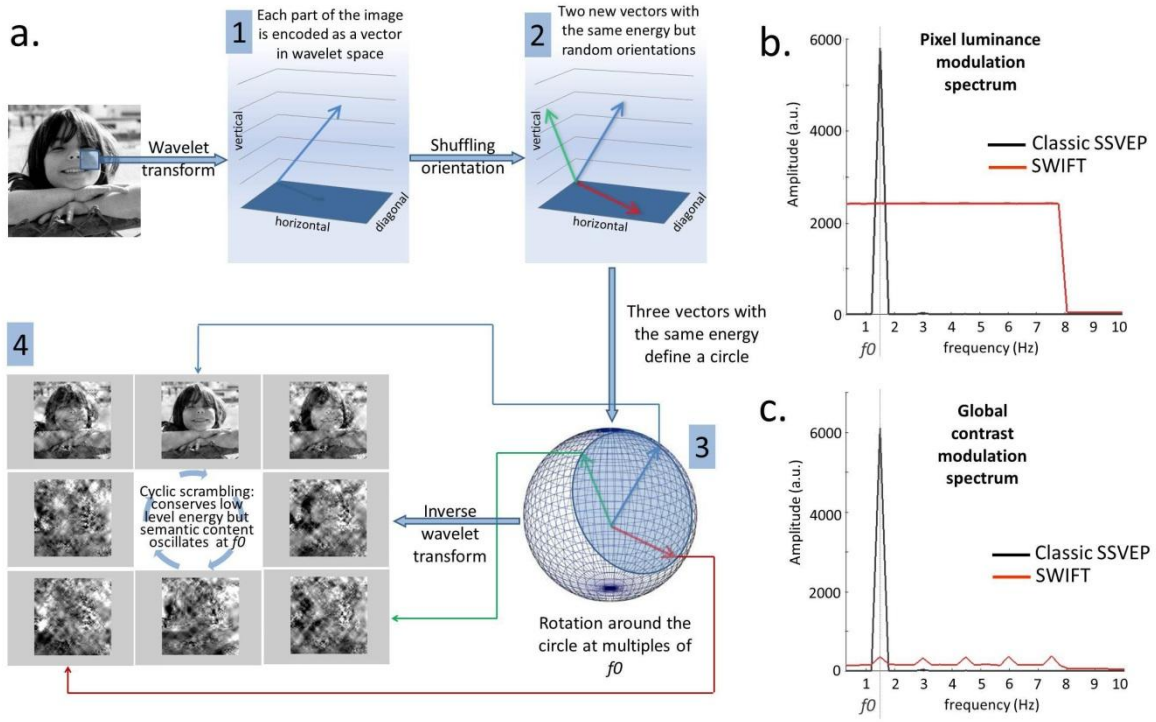

Figure 1. **Construction and properties of SWIFT sequences. A.** (1) The image is transformed into wavelet coefficients, representing local contours' energy and orientation. (2) For each wavelet element represented by a 3D vector, two new vectors with the same length but random orientations are created: low level attributes (spatial frequency, contrast) are conserved but the local contour is disrupted. (3) The 3 vectors define a circular isoenergetic path. The original vector goes around this path at a multiple frequency of *f0* (from 1 to 5). (4) Using the inverse wavelet transform, a cyclic sequence is generated showing the original image once per cycle at *f0*, and conserving low-level attributes at each frame. **B.** Pixel luminance modulation spectrum over time showing the spreading of the local luminance modulation over the harmonic frequencies of the cyclic phase-scrambling (red line). This ensures a continuous modulation of visual stimulation in which the energy is not concentrated in any particular frequency, avoiding low-level evoked responses at *f0*. Note the peak (black line) at *f0* obtained with classic SSVEP using sinusoidal contrast modulation. **C.** Global image contrast modulation spectrum over time. The contrast modulation at *f0* used in classic SSVEP (black line) evokes a strong neural response at the same frequency. In contrast, there is no peak of contrast modulation at *f0* for the SWIFT technique (red line).

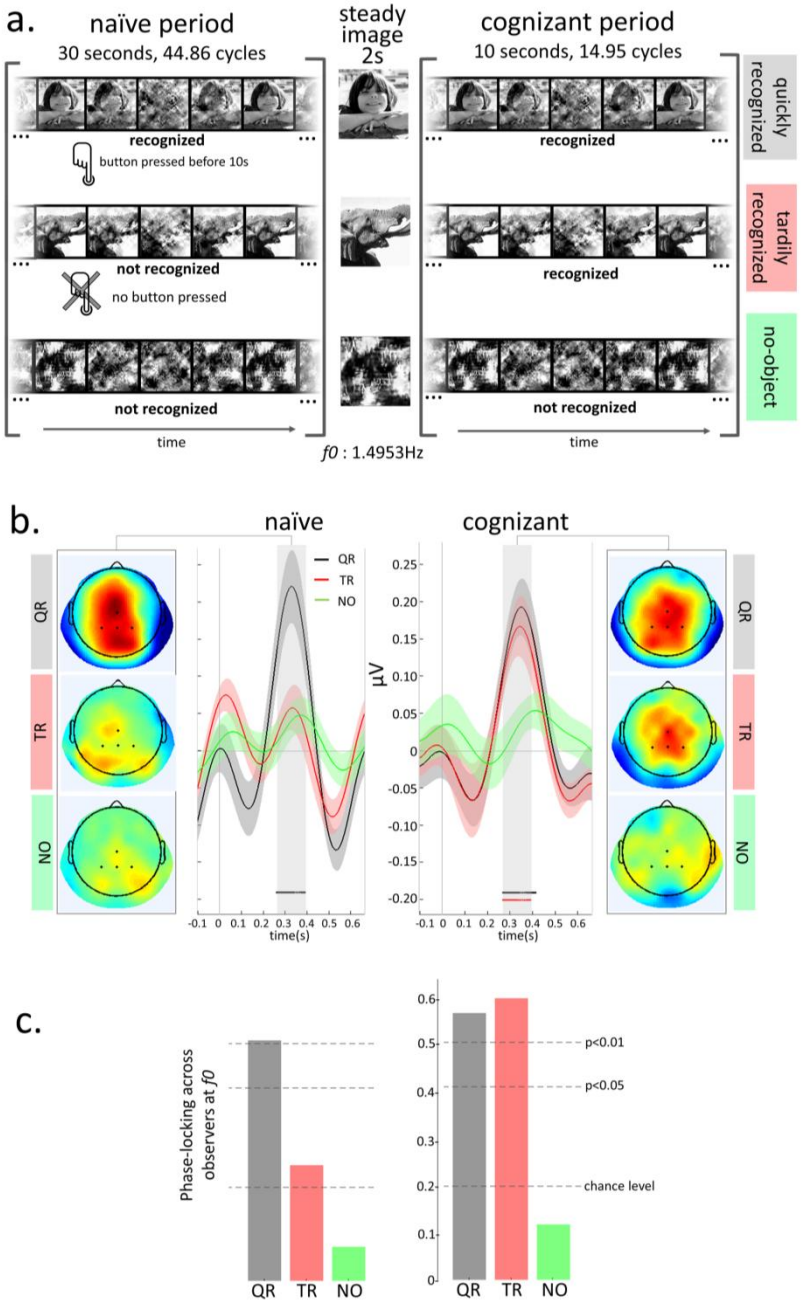

Figure 2. **Isolating object perception awareness. A.** Paradigm to compare activity elicited by SWIFT under recognition and non-recognition of objects (see results section). Two SWIFT epochs composed each trial: the naïve period (30 s, where the sequence was presented for the first time) and the cognizant period (10 s, where the sequence was presented again). In between, the original image was presented steadily for 2 s, ensuring that the object (if any) would be later perceived in the cognizant period. Trials in which the object was detected in the first 10s of the naïve period were labeled as quickly recognized trials (QR). Trials in which objects were recognized only in the cognizant period (no button press during the naïve period) were labeled as tardily recognized trials (TR). In no-object trials (NO), abstract textures were shown and no object was ever recognized. **B.** ERP analysis over 4 central electrodes (marked by a dot in the topographies) taking each wavelet-scrambling cycle (667 ms) as an epoch. Zero time indicates the frame where the original (unscrambled) image was presented. Shaded areas represent S.E.M. During the naïve period, only the activity elicited in QR, but not in TR trials differed ($p < 0.05$, gray box) from the baseline measured in the NO trials. In the cognizant period, however, both the QR and the TR conditions differed from the NO condition ($p < 0.05$, gray box), and the waveforms elicited by QR and TR trials were very similar in this period. To summarize, a significant response only occurred when subjects consciously recognized the objects in the sequences. Topographies were calculated over the time points falling within the gray box (marking statistical significance). Object recognition activity peaked over central electrodes, and was only observed when an object was recognized. **C.** Phase-locking analysis representing the similarity of ERP waveforms across subjects. EEG phase-locking across subjects at *f0* was significant ($p<0.05$) when an object was recognized, but did not differ from chance level when no object was recognized.

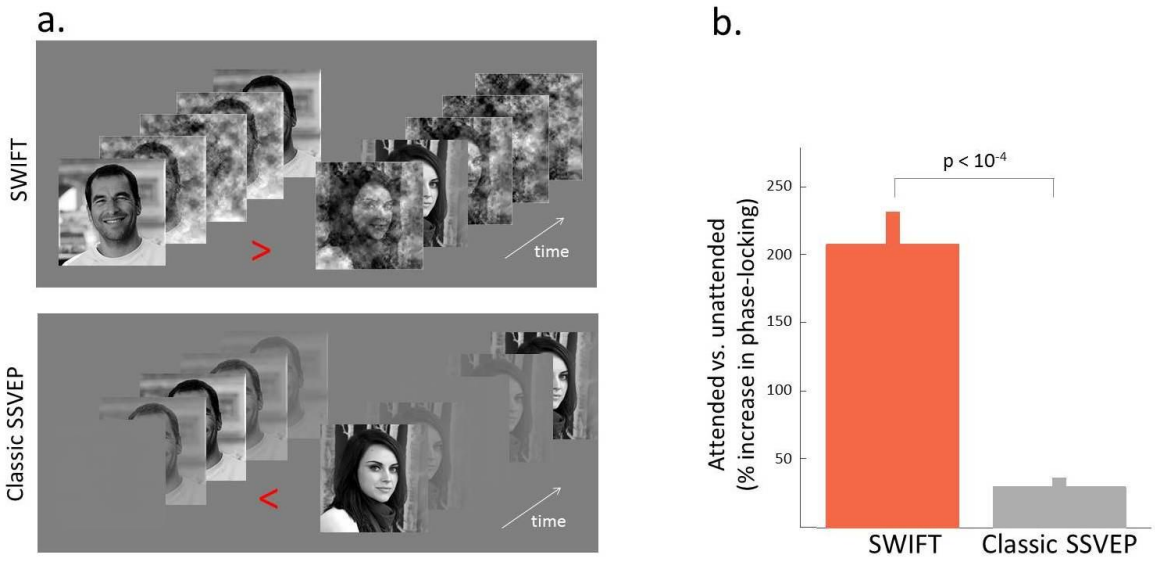

Figure 3. **Measuring attention deployment. A.** The effect of attention on frequency-tagging was calculated using SWIFT (wavelet-scrambling modulation) or classic SSVEP (contrast modulation) in different trials. Two faces were presented on either side of the screen at different modulation frequencies (1.4953 Hz and 2.0253, randomly counterbalanced). Top-down attention was manipulated by a central cue pointing to the face to be attended, and a difficult detection task in the corresponding sequence. **B.** Attention modulation of the frequency-tagging response was measured as the increase in phase-locking at *f0* for the target compared to the distractor stimulus.

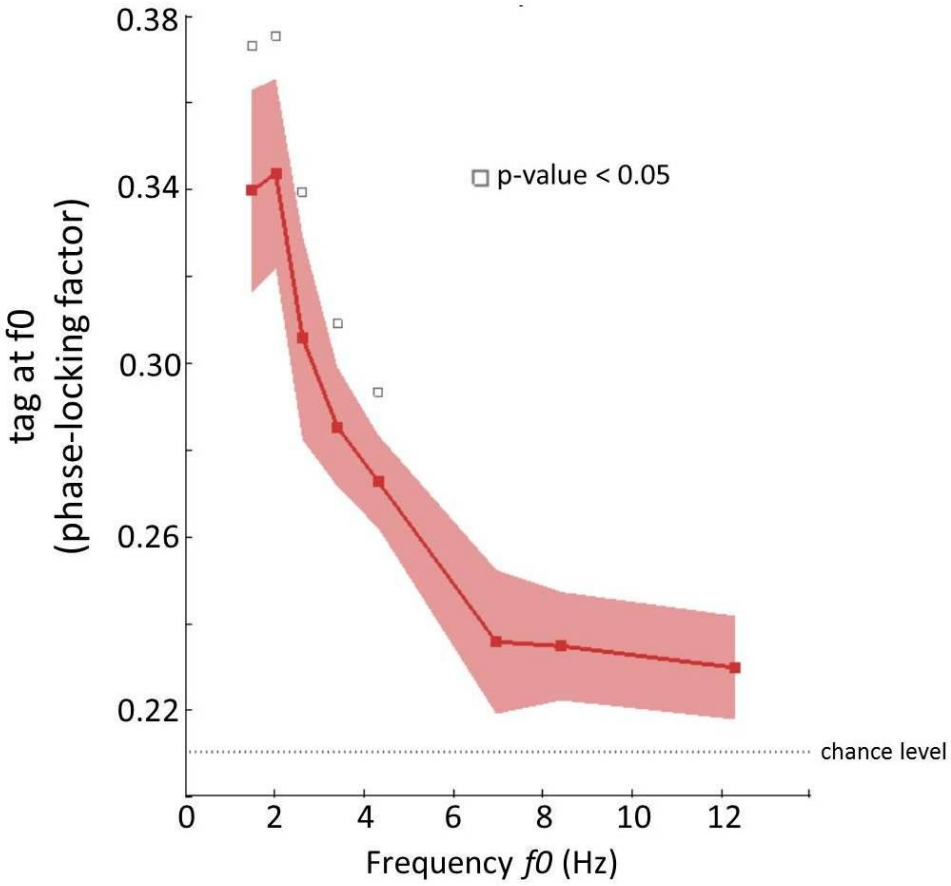

Figure 4. **Temporal dynamics of object recognition.** SWIFT was applied to natural images at 8 different frequencies (from 1.4953 to 12.3077 Hz). The tagging response was calculated as the phase-locking factor across trials at *f0* (after trials were aligned relative to the first appearance of the original unscrambled image in the sequence). A significant tagging ($p < 0.05$) was obtained at frequencies from 1.4953 to 4.3243, but not at frequencies of 6.97Hz and above. This suggests that the visual system can form a maximum of 4 to 7 different high-level representations per second.

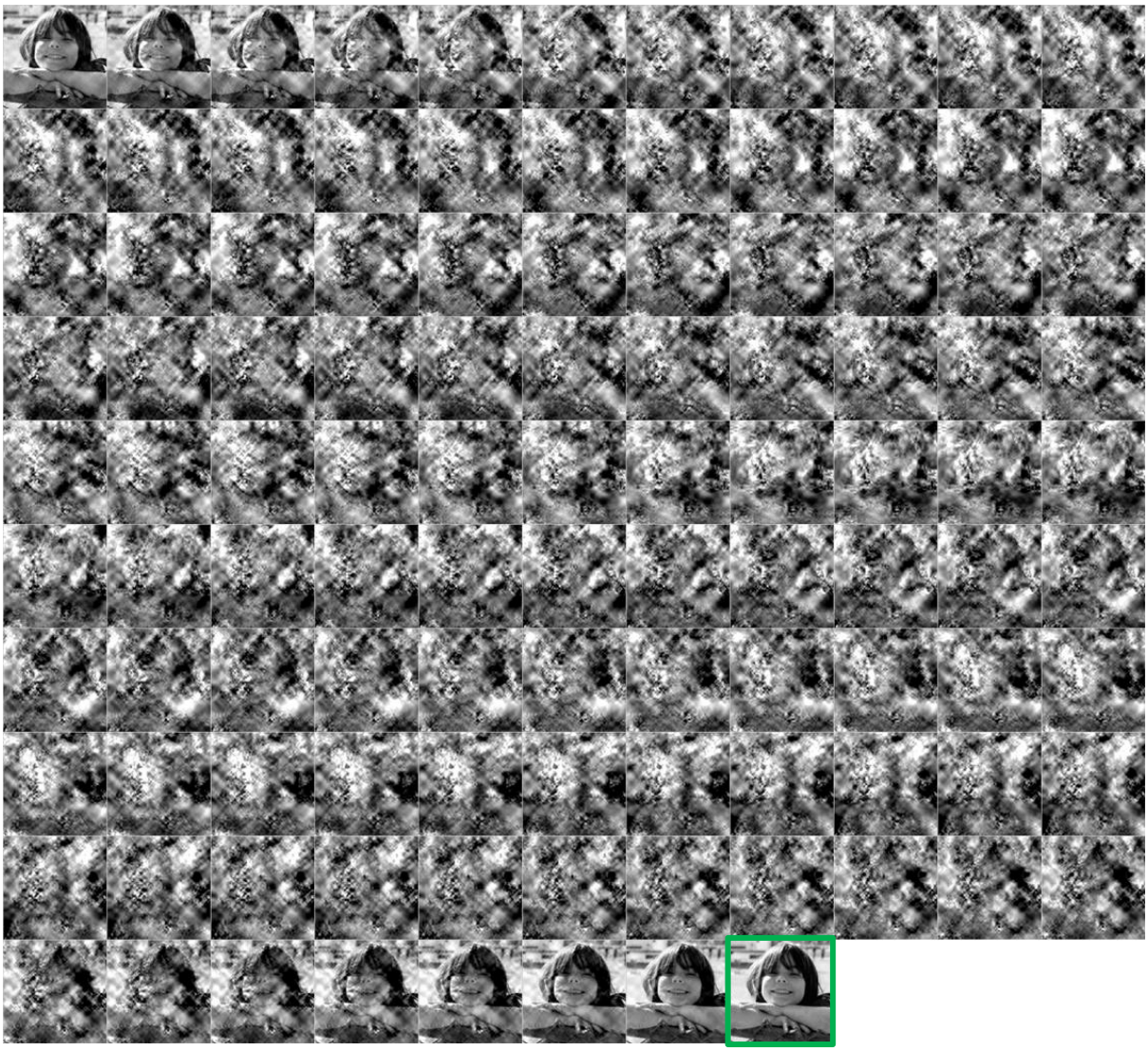

Figure S1. **The 107 frames of a SWIFT sequence modulated at *f0* = 1.4953Hz.** Each frame was presented during 6.25 ms. The green outline (not shown in the experiment), indicates the frame where the semantic information was fully available (unscrambled image), corresponding to zero-time in the ERP analysis and to the reference time for the phase-locking calculation at *f0*.

Methods

SWIFT sequences creation. SWIFT sequences were created by cyclic wavelet scrambling in the wavelets 3D space. We chose wavelet image decomposition rather than other types of image transformation (such as the Fourier transform) because wavelet functions (contrary to Fourier functions) are localized in space: this allowed us to scramble contours while conserving local low-level attributes. The first step was to apply a wavelet transform based on the discrete Meyer (dmey) wavelet and 6 decomposition levels, using the Wavelet toolbox under Matlab (MathWorks); in other words, the image was converted to a multi-scale pyramid of spatially organized maps. At each location and scale, the local contour is represented by a 3D vector $\overrightarrow{v1}$, with the 3 dimensions representing the strengths of horizontal, vertical and diagonal orientations. The vector length $|\overrightarrow{v1}|$ is a measure of local contour energy. In a second step, for each location and scale, two random vectors ($\overrightarrow{v2}$ and $\overrightarrow{v3}$) were defined that shared the length of the original vector ($|\overrightarrow{v1}| = |\overrightarrow{v2}| = |\overrightarrow{v3}|$), thus conserving local energy. By definition, the 3 vectors describe a unique circular path over an isoenergetic sphere where all surface points share the same energy (i.e., the same Euclidian distance from the origin) but represent differently oriented versions of the local image contour. The cyclic wavelet-scrambling was then performed by rotating each original vector (representing the actual image contour), along the circular path defined above. Some wavelet elements (defined by a specific spatial location and decomposition scale) underwent this rotation once per cycle (i.e., at the fundamental frequency *f0*) while others rotated multiple (integer) times per cycle (i.e., at harmonic frequencies of *f0,* from the 2nd up to the 5th harmonic). The introduction of harmonics was crucial to spread the temporal luminance modulation over a broader frequency band, avoiding low-level evoked activity at the tagging frequency *f0*. The 5 harmonic frequencies were distributed equally and randomly among all the wavelet elements. Finally, the inverse wavelet transform was used to obtain the image sequences in the pixel domain. By construction, the original unscrambled image appeared once in each cycle, with a number of intervening wavelet-scrambled frames that depended on the monitor refresh rate and the tagging frequency *f0*. For each original image, several distinct wavelet-scrambling cycles were computed (5 cycles in experiment 1, 2 cycles in experiment 2 and 4 cycles in experiment 3), with different randomly chosen values for the wavelet-scrambling trajectories and the harmonic rotation frequency at each wavelet element. These different cycles were presented in random alternation during the experimental sequences. Two final normalization steps were necessary in order to ensure that the temporal luminance modulation for every pixel was constant (i.e. without any peaks at the individual harmonics frequencies) within the range of harmonic modulation frequencies, and also to ensure the conservation of the mean luminance across frames.

First, we calculated the Fourier transform across frames for every pixel and normalized their luminance modulation spectra. Second, mean frame luminance was equalized over time. (NB: A Matlab script following this procedure to create a wavelet-scrambling sequence based on any given original image is available as supplementary material).

Subjects. All subjects gave informed consent to take part in these studies that were approved by the local ethics committee. A total of 49 observers (26 women, aged 22 to 53) participated in the 3 experiments (19 in Experiment 1, 8 in Experiment 2 and 24 in Experiment 3).

Stimuli and procedure. For all 3 experiments, subjects were placed at 57 cm of a CRT screen with a refresh rate of 170 Hz in a dark room.

In Experiment 1, 100 SWIFT sequences containing either grayscale natural images (bodies with faces 29%, bodies with no visible faces 16%, animals 21% and manmade objects 14%, downloaded from the Internet) or low-level matched textures synthesized using the texture synthesis algorithm developed by Portilla & Simoncelli(Portilla and Simoncelli, 2000) were shown. The image contours were modulated cyclically over time at *f0*=1.4953 Hz. The experiment was divided in 4 blocks of 25 trials each. Each trial lasted 42 sec (30 sec of naïve period + 2 sec of steady image presentation + 10 sec of cognizant period). Sequences (10.5° x 10.5° visual angle) were presented at the center of the screen over a grey background. Subjects were asked to keep their fixation over a red cross at the center of the display during the trial. They gave their responses (presence of a non-abstract item) at any time during the first naïve period by pressing the left arrow of the computer keyboard for the low confidence threshold (key 1: "I perceive an object-like item, but I am not sure of which object it is") and the right arrow for the high confidence threshold (key 2: "I see an object and I have identified it confidently"). Trials were classified as 'quickly recognized' when a natural image was presented and the subject recognized an object with high confidence within the first 10 s of the naïve period. Trials were classified as 'tardily recognized' when a natural image was presented but the subject did not recognize an object during the 30 sec of the naïve period. Trials were classified as 'no-object' when abstract textures were presented. Two of 19 subjects were not considered in the analysis because they had less than 7 tardily recognized trials. For the 17 remaining subjects, the mean number of quickly recognized trials was 22.2, tardily recognized was 22.4 and 20 no-object trials were presented systematically (the remaining trials, corresponding to incomplete or erroneous recognition, were not included in the analysis). Response time for key 2 ("I see an object and I have identified it confidently") in fast recognized trials was 4.4 s (mean) and 3.5 s (median).

In experiment 2, 360 pairs of sequences containing human faces (n = 120, downloaded from the Internet) were presented. The 2 sequences (8.5° x 8.5° visual angle) were presented over a grey

background, on either side of the screen, separated by 5.8° visual angle. In half of the trials both face pictures were modulated in the contrast domain (by manipulating the contrast from 0 to 100% through a sinusoidal envelope: "classic SSVEP") and the other half in the wavelet domain (SWIFT). In each trial, the two sequences were modulated at two different, non-harmonically related frequencies = 1.4953 Hz or 2.0253 Hz (counter balanced per presentation side across trials). The experiment was divided in 4 blocks of 90 trials each. Subjects were instructed to attend the sequence indicated by the central cue (a red arrow of 0.8° visual angle) and ignore the other, while keeping fixation on the central arrow. The task consisted in detecting a deviant cycle (present in 20% of trials) which was only presented in the target sequence. Deviant cycles under SWIFT modulation were produced by inserting a cycle in which the embedded image was itself a wavelet scrambled version of the face showed in the sequence, with the result that the face did not re-appear in this deviant cycle. For the classic SSVEP modulation, the original face was replaced by a wavelet scrambled version in the deviant cycle. Deviant cycles were placed randomly during the trial, excluding the first and last cycle. Each trial lasted 10 seconds and the response (presence/absence of a deviant cycle) was given at the end of the trial by pressing either the left (presence) or right (absence) arrow on a computer keyboard.

In experiment 3, SWIFT sequences (10.5 x 10.5° visual angle) containing natural images (41% animals, 16% faces, 14% bodies with visible faces and 29% manmade, downloaded from the Internet), were presented at the center of the screen over a grey background. Participants were asked to keep fixation over a red cross at the center of the sequence during the trial. SWIFT modulation was performed on different trials at 8 different, non-harmonically related frequencies (*f0* = 1.4953, 2.0253, 2.6230, 3.4043, 4.3243, 6.9665, 8.4211 or 12.3077 Hz). The experimental session contained 160 trials, each lasting 10 sec. The task consisted in detecting the deviant cycles (present 20% of trials) as explained above. The answer was given at the end of the trial by pressing the left arrow key (present) or right arrow key (absent).

EEG acquisition and data processing. Continuous EEG was acquired with a 64-channel ActiveTwo system (Biosemi). Two additional electrodes [CMS (common mode sense) and DRL (driven right leg)] were used as reference and ground. Electrodes were placed according to the international 10/10 system. The vertical and horizontal electrooculogram were recorded by attaching additional electrodes below the left eye and at the outer canthi of both eyes. An active electrode (CMS) and a passive electrode (DRL) were used to compose a feedback loop for amplifier reference. Details of this circuitry can be found on the Biosemi website (www.biosemi.com/faq/cms&drl.htm). All signals were digitized at 1024 Hz, 24-bit A/D conversion. All data were analyzed off-line under Matlab (MathWorks) using the EEGLAB toolbox (Delorme and Makeig, 2004). Average reference was

computed, the data was downsampled at 128 Hz and band-pass filtered between 0.5 and 30 Hz. DC offset was removed from continuous EEG data. The linear trend was removed from each trial, using Andreas Widman's function for EEGLAB. Independent component analysis (ICA plugin from EEGLAB) was performed to remove eye blinks and muscular artifacts. Artifactual components were removed manually (from 2 to 5 out of 64 components per subject) according to their activity time course and topography (frontal for eye blinks and temporal for muscular artifacts).

Event related potentials (ERP) analysis. Data was first low-pass filtered at 3.5 Hz in order to concentrate the analysis on the responses evoked at the tagging frequency (1.4952 Hz). ERP epochs were selected for the naïve and cognizant periods between -0.1 and 0.6688 sec, locked to the onset of the embedded image in each SWIFT cycle (44.86 cycles in the naïve period and 14.95 in the cognizant period; only full cycles were considered). A bootstrap procedure (resampling without replacement, n = 1000) was used to equalize the number of trials entered in the computation of the ERP for all conditions, periods (naïve vs. cognizant) and subjects, resampling 80 epochs at each iteration. 4 central-parietal channels (Cz, CP1, CPz and CP2) were selected as a region of interest using the amplitude of differential activities between perceived/non-perceived conditions as the selection criterion. Onset latencies were evaluated using the statistical criteria proposed by Rugg et al (Rugg et al., 1995): at least 15 consecutive time points with p-values (two-tailed, paired t test) equal or below 0.05.

Phase-locking analysis. Time-locked responses generated at the tagging frequency *f0* were assessed by measuring the response phase delay conservation, relative to the onsets of the semantic information (i.e. the onsets of the embedded image during the trial), at *f0*. Phase-locking analysis was selected over other spectral measures (i.e. spectral power) because of its relative robustness to the noise. By definition, noise is not time locked with the stimulus and can be readily discarded by phase conservation analysis, whereas power analysis is insensitive to the delay of the response and thus more prone to be influenced by noise. The phase of the EEG signals was calculated by means of the fast Fourier transform (FFT) algorithm under Matlab (MathWorks). In experiments 2 and 3, the FFT algorithm was applied over the entire epoch (10 s, 1280 time-points, frequency resolution = 0.1 Hz) and the phase was extracted at the tagging frequency (*f0* = 1.4953 Hz for experiment 1, *f0* = 1.4953, 2.0253 Hz for experiment 2 and *f0* = 1.4953, 2.0253, 2.6230, 3.4043, 4.3243, 6.9665, 8.4211 or 12.3077 Hz for experiment 3). The FFT transform at *f0* of the time-domain signal S for trial k is a complex number in which A represents the amplitude of the signal and φ its phase:

$$F(S_{k,f0}) = A_{k,f0}e^{i\varphi_{k,f0}}$$

Phase-locking factor (PLF, also called inter-trial coherence or phase-locking value) was calculated as follows:

$$PLF_{f0} = \left| \frac{1}{n}\sum_{n=1}^{k} e^{i(\varphi_{k,f0}2\pi)} \right|$$

The PLF measure takes values between 0 and 1. A value of 0 represents absence of synchronization across trials between EEG data and the time- locking events, and a value of 1 indicates perfect synchronization. PLF is computed by normalizing the lengths of the complex vectors (representing amplitude and phase) to 1 for all trials and then computing their complex average. Thus, only the information about the phase of the spectral estimate of each trial is taken into account.

In experiment 2, the attentional effect A was calculated as follows:

$$A_{f0} = 100\left(\frac{PLF_T}{PLF_D} - 1\right)$$

Were PLF_T and PLF_D are the phase-locking factors at the tagging frequency of the target and the distractor, respectively. The ratio was calculated frequency-wise in order to compare activities elicited at the same frequencies. This was done by dividing the PLF of the target and distractor at the same tagging frequency (either both at *f0* = 1.4953 or both at 2.0253 and thus representing activities elicited in different trials). Overall attentional effect A was obtained by averaging the ratios at the 2 tagging frequencies.

In experiment 3, the SWIFT response T as a function of the different tagging frequencies (*f0* = 1.4953, 2.0253, 2.6230, 3.4043, 4.3243, 6.9665, 8.4211 or 12.3077 Hz) was obtained directly as the PLF at the given frequency:

$$T_{f0} = PLF_{f0}$$

PLF values for each *f0* were averaged across subjects and the standard error of the mean (s.e.m.) among them was calculated (shaded area fig 4b). Significance was assessed by comparing the PLF values at each tagging frequency against the null hypothesis that all phases were distributed randomly (the random PLF value over 16 trials = 0.2102, Monte Carlo simulation, 10^6 iterations) by two-tailed, one-sample t-test. To correct for multiple comparisons, we analyzed the resulting distributions of p values with the false discovery rate (FDR) procedure to compute a p threshold that set the expected rate of falsely rejected null hypotheses to 5%.

Inter-subject phase-locking factor in experiment 1 was obtained by applying the FFT transform to the ERP waveform of each subject (0.6641s, 85 time-points, frequency resolution 1.5058 Hz). The same 4 central-parietal channels of the ERP calculation were selected (Cz, CP1, CPz and CP2) and PLF at *f0* = 1.4952 across subjects was calculated as follows:

$$PLF_{f0} = \left| \frac{1}{n} \sum_{n=1}^{s} e^{i(\varphi_{s,f0} 2\pi)} \right|$$

Where s is the number of subjects (n = 17). Significance thresholds were estimated by Monte Carlo simulation. After 10^6 iterations the random PLF value over 17 subjects is 0.2037 (i.e. chance level). Based on the PLF values distribution of the Monte Carlo simulation, 5% confidence interval is represented by a PLF value of 0.4172 and 1% confidence interval by a PLF value = 0.5112.

REFERENCES

Amthor, F.R., Tootle, J.S., and Gawne, T.J. (2005). Retinal ganglion cell coding in simulated active vision. Visual neuroscience *22*, 789–806.

Appelbaum, L.G., and Norcia, A.M. (2009). Attentive and pre-attentive aspects of figural processing. Journal of vision *9*, 18.1–12.

Baars, B.J. (1988). A Cognitive Theory of Consciousness (Cambridge: Cambridge University Press).

Babiloni, C., Vecchio, F., Miriello, M., Romani, G.L., and Rossini, P.M. (2006). Visuo-spatial consciousness and parieto-occipital areas: a high-resolution EEG study. Cerebral cortex (New York, N.Y. : 1991) *16*, 37–46.

Bar, M., Tootell, R.B., Schacter, D.L., Greve, D.N., Fischl, B., Mendola, J.D., Rosen, B.R., and Dale, a M. (2001). Cortical mechanisms specific to explicit visual object recognition. Neuron *29*, 529–535.

Beck, D.M., and Kastner, S. (2005). Stimulus context modulates competition in human extrastriate cortex. Nature neuroscience *8*, 1110–1116.

Bentin, S., Allison, T., Puce, A., Perez, E., and McCarthy, G. (1996). Electrophysiological studies of face perception in humans. Journal of cognitive neuroscience *8*, 551–565.

Busch, N. a, Dubois, J., and VanRullen, R. (2009). The phase of ongoing EEG oscillations predicts visual perception. The Journal of neuroscience : the official journal of the Society for Neuroscience *29*, 7869–7876.

Chun, M.M., and Potter, M.C. (1995). A two-stage model for multiple target detection in rapid serial visual presentation. Journal of experimental psychology. Human perception and performance *21*, 109–127.

Crick, F., and Koch, C. (1995). Are we aware of neural activity in primary visual cortex? Nature *375*, 121–123.

Crick, F., and Koch, C. (1998). Constraints on cortical and thalamic projections: the no-strong-loops hypothesis. Nature *391*, 245–250.

Crick, F., and Koch, C. (2003). A framework for consciousness. Nature neuroscience *6*, 119–126.

Del Cul, A., Baillet, S., and Dehaene, S. (2007). Brain dynamics underlying the nonlinear threshold for access to consciousness. PLoS biology *5*, e260.

Dehaene, S., and Changeux, J.-P. (2011). Experimental and theoretical approaches to conscious processing. Neuron *70*, 200–227.

Dehaene, S., Changeux, J.-P., Naccache, L., Sackur, J., and Sergent, C. (2006). Conscious, preconscious, and subliminal processing: a testable taxonomy. Trends in cognitive sciences *10*, 204–211.

Delorme, A., and Makeig, S. (2004). EEGLAB: an open source toolbox for analysis of single-trial EEG dynamics including independent component analysis. Journal of Neuroscience Methods *134*, 9–21.

Ding, J., Sperling, G., and Srinivasan, R. (2006). Attentional modulation of SSVEP power depends on the network tagged by the flicker frequency. Cerebral cortex (New York, N.Y. : 1991) *16*, 1016–1029.

Downing, P.E., Jiang, Y., Shuman, M., and Kanwisher, N. (2001). A cortical area selective for visual processing of the human body. Science (New York, N.Y.) *293*, 2470–2473.

Epstein, R., Harris, a, Stanley, D., and Kanwisher, N. (1999). The parahippocampal place area: recognition, navigation, or encoding? Neuron *23*, 115–125.

Felleman, D.J., and Van Essen, D.C. (1991). Distributed hierarchical processing in the primate cerebral cortex. Cerebral cortex (New York, N.Y. : 1991) *1*, 1–47.

Fernandez-Duque, D., Grossi, G., Thornton, I.M., and Neville, H.J. (2003). Representation of change: separate electrophysiological markers of attention, awareness, and implicit processing. Journal of cognitive neuroscience *15*, 491–507.

Fisch, L., Privman, E., Ramot, M., Harel, M., Nir, Y., Kipervasser, S., Andelman, F., Neufeld, M.Y., Kramer, U., Fried, I., et al. (2009). Neural "ignition": enhanced activation linked to perceptual awareness in human ventral stream visual cortex. Neuron *64*, 562–574.

Fjell, A.M., and Walhovd, K.B. (2003). On the topography of P3a and P3b across the adult lifespan–a factor-analytic study using orthogonal procrustes rotation. Brain topography *15*, 153–164.

Gaillard, R., Dehaene, S., Adam, C., and Clémenceau, S. (2009). Converging intracranial markers of conscious access. PLoS biology *7*,.

Gallant, J.L., Braun, J., and Van Essen, D.C. (1993). Selectivity for polar, hyperbolic, and Cartesian gratings in macaque visual cortex. Science (New York, N.Y.) *259*, 100–103.

Grill-Spector, K., Kushnir, T., Hendler, T., and Malach, R. (2000). The dynamics of object-selective activation correlate with recognition performance in humans. Nature neuroscience *3*, 837–843.

Halgren, E., Marinkovic, K., and Chauvel, P. (1998). Generators of the late cognitive potentials in auditory and visual oddball tasks. Electroencephalography and clinical neurophysiology *106*, 156–164.

Hegdé, J., and Van Essen, D.C. (2000). Selectivity for complex shapes in primate visual area V2. The Journal of neuroscience : the official journal of the Society for Neuroscience *20*, RC61.

Hesselmann, G., and Malach, R. (2011). The Link between fMRI-BOLD Activation and Perceptual Awareness Is "Stream-Invariant" in the Human Visual System. Cerebral cortex (New York, N.Y. : 1991) *21*, 2829–2837.

Holcombe, A.O. (2009). Seeing slow and seeing fast: two limits on perception. Trends in cognitive sciences *13*, 216–221.

Hubel, D.H., and Wiesel, T.N. (1968). Receptive fields and functional architecture of monkey striate cortex. The Journal of physiology *195*, 215–243.

Jeffreys, D.A. (1996). Evoked Potential Studies of Face and Object Processing. Visual Cognition *3*, 1–38.

Kanwisher, N., McDermott, J., and Chun, M.M. (1997). The fusiform face area: a module in human extrastriate cortex specialized for face perception. The Journal of neuroscience : the official journal of the Society for Neuroscience *17*, 4302–4311.

Kaspar, K., Hassler, U., Martens, U., Trujillo-Barreto, N., and Gruber, T. (2010). Steady-state visually evoked potential correlates of object recognition. Brain research *1343*, 112–121.

Keysers, C., Xiao, D.K., Földiák, P., and Perrett, D.I. (2001). The speed of sight. J Cogn Neurosci *13*, 90–101.

Kim, Y.J., Grabowecky, M., Paller, K. a, Muthu, K., and Suzuki, S. (2007). Attention induces synchronization-based response gain in steady-state visual evoked potentials. Nature neuroscience *10*, 117–125.

Kobatake, E., and Tanaka, K. (1994). Neuronal selectivities to complex object features in the ventral visual pathway of the macaque cerebral cortex. Journal of neurophysiology *71*, 856–867.

Koivisto, M., Lähteenmäki, M., SU00F8 rensen, T.A., Vangkilde, S., Overgaard, M., and Revonsuo, A. (2008). The earliest electrophysiological correlate of visual awareness? Brain and cognition *66*, 91–103.

Lamme, V. a, and Roelfsema, P.R. (2000). The distinct modes of vision offered by feedforward and recurrent processing. Trends in neurosciences *23*, 571–579.

Lamy, D., Salti, M., and Bar-Haim, Y. (2009). Neural correlates of subjective awareness and unconscious processing: an ERP study. Journal of cognitive neuroscience *21*, 1435–1446.

Lauritzen, T.Z., D'Esposito, M., Heeger, D.J., and Silver, M.A. (2009). Top-down flow of visual spatial attention signals from parietal to occipital cortex. J Vis *9*, 18.1–14.

Libedinsky, C., and Livingstone, M. (2011). Role of prefrontal cortex in conscious visual perception. The Journal of neuroscience : the official journal of the Society for Neuroscience *31*, 64–69.

Madl, T., Baars, B.J., and Franklin, S. (2011). The timing of the cognitive cycle. PloS one *6*, e14803.

Mantini, D., Corbetta, M., Perrucci, M.G., Romani, G.L., and Del Gratta, C. (2009). Large-scale brain networks account for sustained and transient activity during target detection. NeuroImage *44*, 265–274.

McMains, S., and Kastner, S. (2011). Interactions of top-down and bottom-up mechanisms in human visual cortex. The Journal of neuroscience : the official journal of the Society for Neuroscience *31*, 587–597.

Morgan, S.T., Hansen, J.C., and Hillyard, S. a (1996). Selective attention to stimulus location modulates the steady-state visual evoked potential. Proceedings of the National Academy of Sciences of the United States of America *93*, 4770–4774.

Müller, M.M., Picton, T.W., Valdes-Sosa, P., Riera, J., Teder-Sälejärvi, W. a, and Hillyard, S. a (1998). Effects of spatial selective attention on the steady-state visual evoked potential in the 20-28 Hz range. Cognitive brain research *6*, 249–261.

Müller, N.G., and Kleinschmidt, A. (2003). Dynamic interaction of object- and space-based attention in retinotopic visual areas. The Journal of neuroscience : the official journal of the Society for Neuroscience *23*, 9812–9816.

Niedeggen, M., Wichmann, P., and Stoerig, P. (2001). Change blindness and time to consciousness. The European journal of neuroscience *14*, 1719–1726.

Nieuwenstein, M., Burg, E.V.D., and Potter, M. (2009). Temporal constraints on conscious vision : On the ubiquitous nature of the attentional blink. Journal of Vision *9*, 1–14.

Van Opstal, F., de Lange, F.P., and Dehaene, S. (2011). Rapid parallel semantic processing of numbers without awareness. Cognition *120*, 136–147.

Pins, D., and Ffytche, D. (2003). The neural correlates of conscious vision. Cerebral cortex (New York, N.Y. : 1991) *13*, 461–474.

Portilla, J., and Simoncelli, E.P. (2000). A Parametric Texture Model Based on Joint Statistics of Complex Wavelet Coefficients. International Journal of Computer Vision *40*, 49–71.

Potter, M.C. (1976). Short-term conceptual memory for pictures. Journal of experimental psychology. Human learning and memory *2*, 509–522.

Potter, M.C., and Levy, E.I. (1969). Recognition memory for a rapid sequence of pictures. Journal of experimental psychology *81*, 10–15.

Quiroga, R.Q., Mukamel, R., Isham, E. a, Malach, R., and Fried, I. (2008). Human single-neuron responses at the threshold of conscious recognition. Proceedings of the National Academy of Sciences of the United States of America *105*, 3599–3604.

Regan, D. (1977). Steady-state evoked potentials. Journal of the Optical Society of America *67*, 1475–1489.

Riesenhuber, M., and Poggio, T. (1999). Hierarchical models of object recognition in cortex. Nature neuroscience *2*, 1019–1025.

Rugg, M.D., Doyle, M.C., and Wells, T. (1995). Word and Nonword Repetition Within- and Across-Modality: An Event-Related Potential Study. Journal of Cognitive Neuroscience *7*, 209–227.

Sclar, G., Maunsell, J.H., and Lennie, P. (1990). Coding of image contrast in central visual pathways of the macaque monkey. Vision research *30*, 1–10.

Sergent, C., Baillet, S., and Dehaene, S. (2005). Timing of the brain events underlying access to consciousness during the attentional blink. Nature neuroscience *8*, 1391–1400.

Srinivasan, R., Bibi, F.A., and Nunez, P.L. (2006). Steady-state visual evoked potentials: distributed local sources and wave-like dynamics are sensitive to flicker frequency. Brain topography *18*, 167–187.

Srinivasan, R., and Petrovic, S. (2006). MEG phase follows conscious perception during binocular rivalry induced by visual stream segregation. Cerebral cortex (New York, N.Y. : 1991) *16*, 597–608.

Sutoyo, D., and Srinivasan, R. (2009). Nonlinear SSVEP responses are sensitive to the perceptual binding of visual hemifields during conventional “eye” rivalry and interocular “percept” rivalry. Brain research *1251*, 245–255.

Tanaka, K. (1996). Inferotemporal cortex and object vision. Annual review of neuroscience *19*, 109–139.

Thorpe, S., Fize, D., and Marlot, C. (1996). Speed of processing in the human visual system. nature *381*, 520–522.

Tong, F., Nakayama, K., Vaughan, J.T., and Kanwisher, N. (1998). Binocular rivalry and visual awareness in human extrastriate cortex. Neuron *21*, 753–759.

Tononi, G. (2004). An information integration theory of consciousness. BMC neuroscience *5*, 42.

Tononi, G., Srinivasan, R., Russell, D.P., and Edelman, G.M. (1998). Investigating neural correlates of conscious perception by frequency-tagged neuromagnetic responses. Proceedings of the National Academy of Sciences of the United States of America *95*, 3198–3203.

VanRullen, R., and Thorpe, S.J. (2001). The time course of visual processing: from early perception to decision-making. Journal of cognitive neuroscience *13*, 454–461.

E. Isolating the neural correlates of conscious vision

In the previous experiment we have seen that our low-level feature equalization frequency-tagging method (SWIFT) allowed us to isolate the neural correlates of conscious object recognition. This result was obtained by presenting a SWIFT movie in which the semantic content could be either consciously perceived or not. However, in both cases the movie itself was always visible and it thus underwent a certain degree of conscious processing (without any conscious association to a semantic value whatsoever when the image was not recognized or when the movie contained an abstract image). Thus, in the previous paradigm, two conscious processes were involved: the conscious visibility of the stimulation and the conscious recognition of the image. While the latter (conscious recognition) was manipulated in the previous paradigm, the former (conscious visibility) was not. Considering the aforementioned, a consequent question arises: by using a paradigm where the conscious visibility is manipulated, which kind of modulations between activities elicited by visible and non-visible stimuli can we obtain using SWIFT?

A suitable paradigm to test this is binocular rivalry. During binocular rivalry, conflicting monocular images compete for access to consciousness alternating every few seconds between one image and the other. Binocular rivalry is produced by the lateral inhibitory interactions between monocular columns in V1. This process is then amplified through successive steps in the visual hierarchy (Figure 26). Nonetheless, information about the suppressed stimulus travels along the visual pathway and can reach higher brain areas (Tong, Meng, & Blake, 2006). Thus neural activity related to the invisible stimulus is still processed by the visual system even though we cannot notice it at all and can be detected in several brain structures such as the amygdala (Pasley, Mayes, & Schultz, 2004), dorsal regions such as the intra-parietal sulcus (IPS) (Fang & He, 2005), the FFA and STS (Jiang & He, 2006). Thus, this paradigm is a great manner to dissociate visual representations which are consciously accessible and those which are not, while both kinds of representations are processed in some amount by the visual system.

Are current frequency-tagging approaches capable of selectively extracting the neural correlates of conscious vision during binocular rivalry? Let's see a previous attempt ussing frequency tagging.

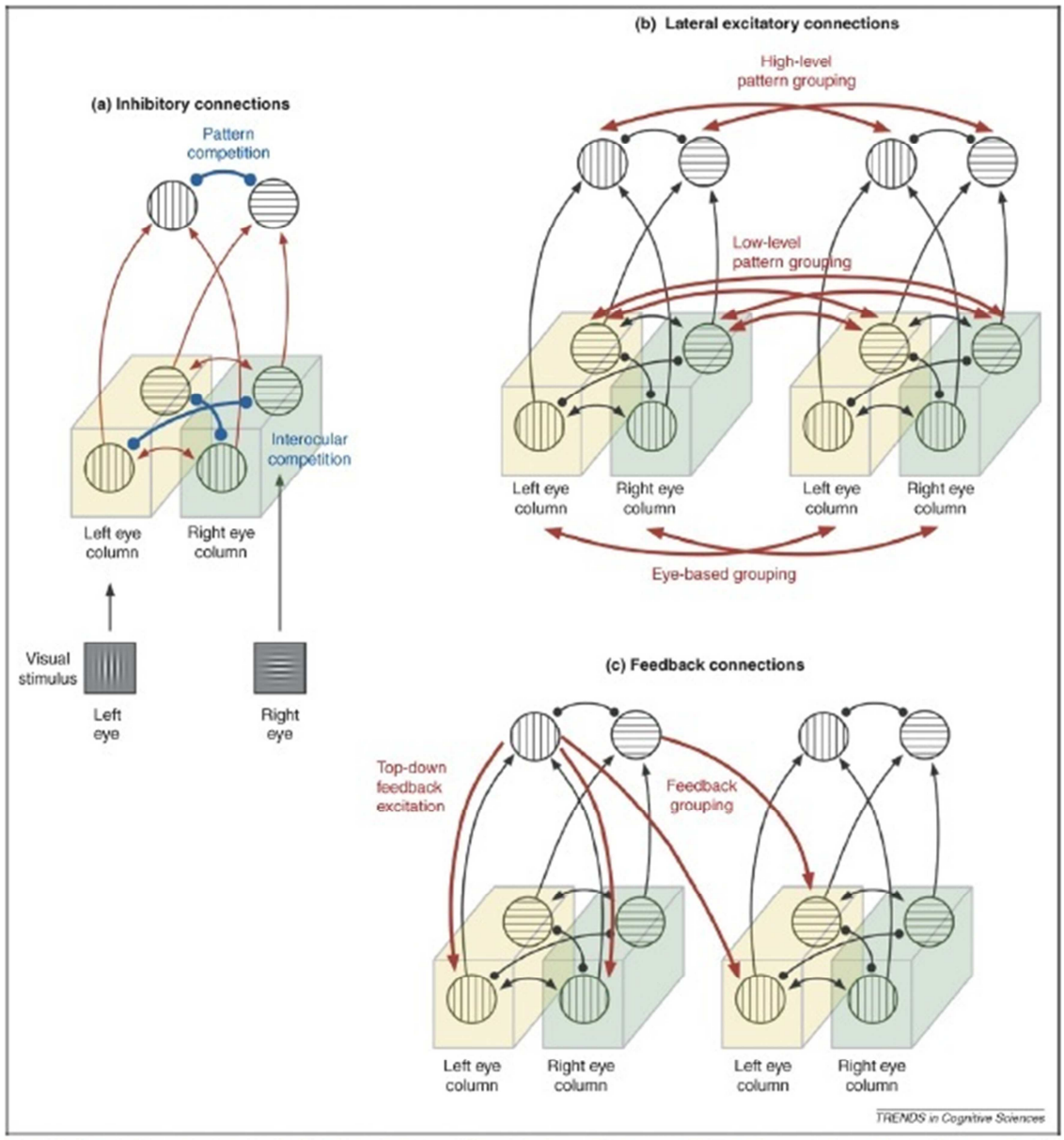

Figure 26. Inhibitory and excitatory connections from the hybrid rivalry model of binocular rivalry. *Inhibitory and excitatory connections are represented by lines with filled circles and lines with arrows, respectively.* ***A. Reciprocal inhibitory connections between monocular neurons and binocular neurons.*** *Inhibitory connections are represented by blue lines with circles. Inhibitory connections between monocular and binocular neurons might account for eye-based and pattern-based visual suppression, respectively.* ***B. Reciprocal excitatory connections.*** *Excitatory connections are represented by red lines with arrows. Excitatory interactions between monocular neurons might account for eye-based grouping, low-level grouping with similar pattern*

preferences including interocular grouping, while reciprocal excitatory connections between binocular neurons would account for high-level pattern-based grouping. ***C. Excitatory feedback projections****. Feedback modulatory connections are represented by red lines with arrows. These projections might account for top-down influences of visual attention and also feedback effects of perceptual grouping. (From Tong et al., 2006).*

I. The paper of Tononi et al, 1998.

A binocular rivalry approach combined with frequency-tagging was used by Tononi et al. (Tononi, Srinivasan, Russell, & Edelman, 1998) in order to capture the consciousness-related activity in the brain. In their protocol, a red vertical grating flickering at one temporal frequency was presented to one eye through a red filter and a blue horizontal grating flickering at a different frequency was presented to the other eye through a blue filter. Steady-state responses at the two tagging frequencies were analyzed by means of the Fourier transform. It was found that a large number of channels showed peaks at both frequencies, arranged in a horseshoe pattern from posterior to anterior regions, whether or not the subject was consciously perceiving the corresponding stimulus (Figure 27). In fact, modulations in the frequency-tagged responses as a function of conscious perception were mild when compared with stimulus alternation, where monocular stimuli were presented alternatively to each eye (Figure 21). This result shows that by using conventional frequency-tagging a significant amount of activity which is not correlated with conscious perception is recorded. Thus, this technique fails to directly (i.e., without using subtractive approaches) dissociate the neural correlates of conscious perception.

The use of binocular rivalry and other forms of dichoptic stimulation such as the continuous flash suppression (CFS) coupled with other recording techniques such as single-unit recordings (Leopold & Logothetis, 1996; Logothetis, 1998) and fMRI (Jiang & He, 2006; Sterzer et al., 2008) have revealed systematic responses to invisible stimuli. In summary, current paradigms fail in directly isolate the neural correlates of consciousness from non-conscious processing.

Is it possible to directly isolate the neural correlates of conscious vision using SWIFT? This is the question that we will address in the next paper.

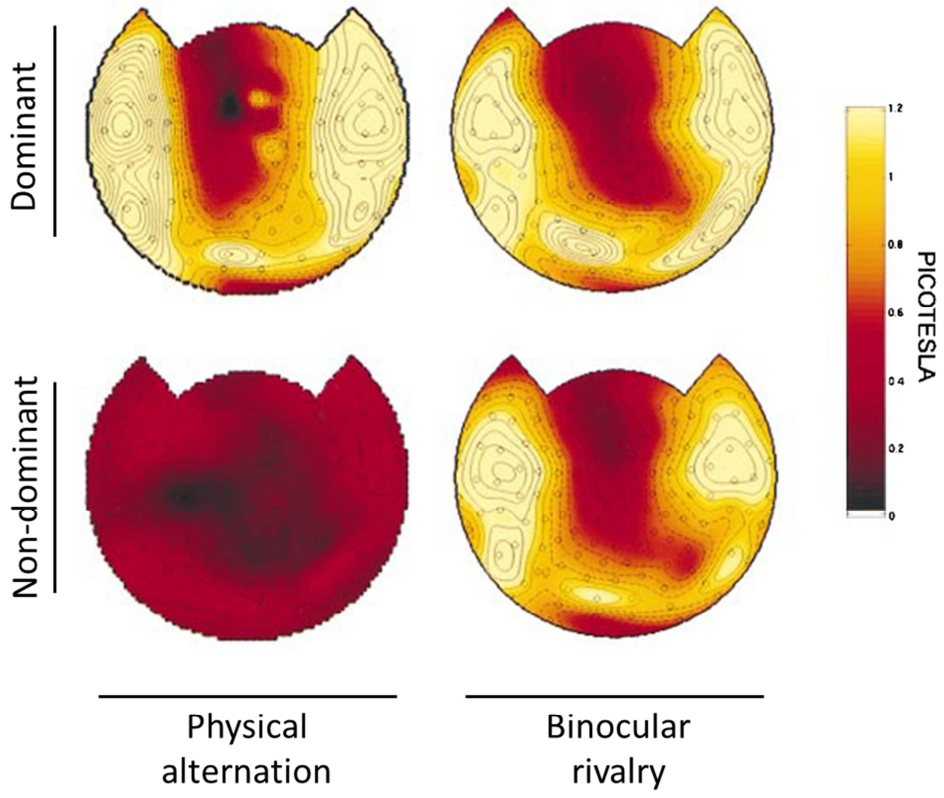

Figure 27. Frequency-tagged responses to flickering monocular gratings during binocular rivalry. *The frequency-tagged responses (measured as the power at 7.41 Hz which was used as the tagging-frequency) corresponding to perceptual dominance (top row) and to perceptual non-dominance (bottom row).* ***Physical alternation.*** *The left column represents stimulus alternation trials, where the stimuli were showed alternatively to each eye. During non-dominance, no frequency-tagged response is seen at frequency of the absent stimulus as expected.* ***Binocular rivalry****. Right column represents binocular rivalry trials. Activities elicited by both dominant and non-dominant stimuli were distributed similarly over the topographies. Modulations in the binocular rivalry condition were less strong than those seen in the physical alternation condition, indicating that the activity associated to the invisible stimulus is present in the frequency-tagged responses obtained with the traditional SSVEP method. (Modified from (Tononi et al., 1998).*

II. PAPER 4 (in preparation). Koenig-Robert & VanRullen.

Temporal consistency of neural activity as the direct correlate of visual consciousness

Roger Koenig-Robert[1,2] & Rufin VanRullen[1,2]

1 Centre de recherche cerveau et cognition (CerCo), UMR5549, CNRS.

2 Université Paul Sabatier, CHU Purpan, Toulouse, France.

Defining the neural correlates of awareness has been difficult due to the lack of selective means to measure consciousness-dependent activity. A widely used paradigm to explore visual awareness is binocular rivalry: conflicting monocular images alternate every few seconds, with the dominant stimulus transiently gaining access to consciousness, while the non-dominant becomes invisible. From single-unit recordings in primates to whole brain EEG or fMRI recordings in humans, current techniques have only found moderate modulations of neural activity when stimuli are dominant versus when they are not; all techniques systematically reveal a significant response to invisible stimuli at different levels of the visual hierarchy. SWIFT (semantic wavelet-induced frequency-tagging) is a recently developed EEG technique which selectively tracks high-level representations with high temporal resolution (Koenig-Robert and VanRullen, submitted). SWIFT uses cyclic wavelet-scrambling to modulate the semantic content of an image at a temporal frequency called the tagging frequency, while conserving low-level features. We used SWIFT to measure perceptual alternations during binocular rivalry. Two face pictures were modulated under SWIFT at different tagging frequencies (1.4894 and 2 Hz) and presented monocularly. Two kinds of alternations were used: binocular rivalry, where the two stimuli were presented simultaneously (and only one was perceived at a time), and physical alternation, where the stimuli were presented alternately in each eye. Fronto-central and occipito-temporal EEG activities were elicited by dominant stimuli, and were comparable in their topography and amplitude in physical alternation and binocular rivalry conditions.

Crucially, invisible stimuli in binocular rivalry elicited no more activity than the response to a blank screen in physical alternation. Considering that visual awareness could cause both increase in the amplitude response and activity synchronization, we found that the feature characterizing consciousness-specific activities is the temporal consistency of brain potentials across onsets of the semantic information in different brain areas, which is consistent with current models of consciousness which highlight massive long-distance interactions.

One of the fundamental aims of neuroscience is to explain conscious experience in terms of brain activity. In the visual modality, several processing steps are completed before light stimulation can be consciously perceived. Since visual stimuli that are not consciously perceived (e.g., suppressed, masked or subliminal images) can activate similar brain areas as consciously perceived stimuli (Moutoussis and Zeki 2002; Tong, Meng, and Blake 2006), it is crucial to characterize the signatures of neural activity which differentiate conscious from unconscious processing. A classic paradigm to study neural activities correlated to conscious representations is to present a single visual stimuli that allows more than one percept. Thus, by recording neural activity as a function of subjective report, it is possible to study neural changes correlated with subjective perception, while the physical stimulation remains constant. Binocular rivalry is an example of such a stimulus. In binocular rivalry, different images are presented to each eye, and, instead of being fused into a single percept, are alternatively perceived, with the dominant image transiently gaining access to consciousness for a few seconds, while the non-dominant becomes invisible. Differential neural activations have been recorded as a function of subjective report (Lansing 1964; Logothetis and Schall 1989; Tononi et al. 1998; Polonsky et al. 2000) and it has been possible to accurately predict perceptual alternations from brain activity (Haynes and Rees 2005). However, current techniques fall short in directly isolating the activities supporting conscious perception. By definition, neural activities supporting conscious perception must exactly mirror subjective states. In the case of binocular rivalry, this implies in practice that neural representations supporting the conscious perception of a given stimulus should systematically emerge when the stimulus is visible and completely vanish when the stimulus becomes invisible. However, neural activity recorded so far systematically includes neural activity belonging to non-

conscious processing, making the distinction between the non-conscious visual processing and the neural correlates of visual awareness a tricky business. From low-level to higher order visual areas, electrophysiological recordings—such as unitary recordings (Logothetis 1998), EEG (Ramesh Srinivasan 2004) and MEG (Tononi et al. 1998)—and functional neuroimaging— such as fMRI (Jiang and He 2006)—show a significant global response to invisible stimuli. Here we report the selective extraction of the neural correlates of conscious perceptual states during binocular rivalry. We used an innovative technique called SWIFT in order to tag high-level visual representations using EEG (Koenig-Robert & VanRullen, SUBMITTED). This technique uses cyclic wavelet-scrambling to modulate the semantic content of an image at a temporal frequency called *tagging frequency*, while conserving low-level features—thus avoiding low-level evoked activity at the tagging frequency—and has been useful in isolating the neural correlates of object recognition (Koenig-Robert & VanRullen, submitted). In the present study, we used dichoptic stimulation by presenting two face pictures modulated under SWIFT at different tagging frequencies (1.4894 and 2 Hz) in each eye. Two kinds of alternations were used: binocular rivalry, where the two stimuli were presented simultaneously (and only one was perceived at a time), and physical alternation, where the stimulus was presented to one eye while the other saw a blank screen, with eye alternations mirroring the dynamics of binocular rivalry spontaneous alternations. Fronto-central and occipito-temporal EEG activities were elicited by dominant stimuli, and were comparable in their topography and amplitude in binocular rivalry and physical alternation conditions. Crucially, invisible stimuli in binocular rivalry elicited no more activity than the response to a blank screen in physical alternation. For the first time, global neural activity recordings representing visual stimuli were found to be modulated in an all-or-none fashion by perceptual alternations in binocular rivalry, exactly mirroring the phenomenal counterpart. Considering that visual awareness could cause both increase in the amplitude response and activity synchronization, we found that consciousness-dependent activities rely on the later which was reflected in temporal consistency of neural potentials, rather than on an increase of the neural activity amplitude. This is consistent with current models of consciousness which highlight massive long-distance interactions mediated by temporal synchrony.

Results

Isolating the neural correlates of visual awareness. We used SWIFT in order to track the high-level representations of faces (Koenig-Robert & VanRullen, submitted). As a consequence of the cyclic modulation performed by SWIFT (see Materials and Methods section for details), stimulus low-level attributes are equalized over time (specifically luminance, contrast and spatial frequency content), while higher-level attributes are modulated at the tagging frequency. Thus, along a cyclic movie, the stimulus is transformed from 'face' to 'noise', at each modulation cycle, without altering the principal statistics of the image. As a result, visual processing mechanisms that are sensitive to the low-level properties should be equally engaged by all frames of the movie, exhibiting a flat response during the presentation. On the other hand, the higher-level mechanisms responsible for extracting semantic information would come into play periodically around the onset of the original image (Figure 1a). By analyzing changes of the neural activity at the tagging frequency it is thus possible to isolate activities supporting high-level visual representations.

By using different tagging frequencies (Frequencies 1 = 1.4894 and Frequency 2 = 2Hz) for each monocular stimulation, it was possible to track the brain responses generated by each one of the SWIFT movies that competed for access to consciousness. We used two kinds of alternations: binocular rivalry, where the two stimuli were presented simultaneously (and only one was perceived at a time), and physical alternation, where the stimuli were presented to an eye while the other saw a blank screen, with eye alternations emulating the dynamics of binocular rivalry (see Figure 1b Material and Methods section for details). The physical alternation condition was used as a control in order to estimate the brain activity elicited at one tagging frequency (e.g., the tagging frequency 1) that we would expect by monocularly presenting only one movie tagged at that frequency—that is, the maximum evoked activity that we would expect—and, on the other hand, to estimate the brain activity at the other tagging frequency (e.g., at the tagging frequency 2) in "response" to an empty screen presented to the other eye—that is, the minimum evoked activity or baseline.

We used an event-related potential (ERP) analysis to measure the scalp potentials locked to the onset of the semantic information—the time when the non-scrambled face was on the

screen for each frequency—which was taken as the zero-time. Each SWIFT cycle was thus taken as an epoch and the data was sorted as a function of the visibility reported by the subject (see Material and Methods section for details). Figure 2a shows the ERP topographies at ~200 ms after semantic onset for both tagging frequencies and different conditions. Consciously perceived movies (dominant) in the binocular rivalry condition generated ERP responses comparable to those elicited by the presentation of a single movie in the physical alternation condition (figure 2a, top panel). Crucially, physically present but non-consciously perceived (non-dominant) movies in the binocular rivalry condition elicited ERP responses comparable to those generated by an empty screen in the physical alternation condition (figure 2a, bottom panel). ERP time course for 10 centro-frontal electrodes is shown in figure 2b. While invisible movies in the binocular rivalry elicited flat activity comparable to an empty screen in physical alternation (Figure 2b, solid and dashed green lines respectively), consciously perceived movies in the binocular rivalry condition elicited significant activation comparable to a movie presented alone in the physical alternation condition. Significant differences ($p<0.01$, two tailed t-test) between dominant and non-dominant stimuli were found between 160 and 215 ms after semantic onset for the frequency 1, and between 176 and 215 ms for frequency 2 (Figure 2b, black line) and between 136 and 207 (Frequency 1) and between 144 and 223 (Frequency 2) for the physical alternation condition (Figure 2b, gray line). These differences are not likely to represent ocular artifacts, as seen in Figure S1 showing that activity recorded on EOG electrodes is not significant.

Temporal consistency as awareness-dependent activity. In order to quantify the brain activity elicited at the tagging frequency by each movie, we calculated spectral amplitude at the tagging-frequency as a function of the movie visibility (see Materials and Methods section for details). Despite the strong differences between visible and invisible movies showed in ERP analysis, traditional amplitude analysis (or power spectrum) at the tagging frequency (see Material and Methods section for details) did not show any significant difference among conditions (data not shown). However, phase-locking analysis at the tagging frequency across cycles—which accounts for the temporal consistency of scalp potentials across stimulus repetitions independently of their relative amplitude—(see Material and Methods for details) revealed the same effects found in the ERP analysis.

Figure 3a shows the topographies of phase-locking effects averaged between the two tagging frequencies. Strong phase-locking at the tagging frequency is present in fronto-central and occipito-temporal regions for dominant stimuli in both binocular rivalry and physical alternation conditions, while for invisible movies the activity is comparable to activity elicited by an empty screen. Figure 3b shows the average phase-locking for all channels. Differences between dominant and non-dominant stimuli were highly significant for both physical alternation and binocular rivalry conditions ($p=5.2\cdot10^{-3}$ and $p=7.3\cdot10^{-4}$ respectively, one-way ANOVA). However, no significant differences were found between physical alternation and binocular rivalry for the activity elicited by dominant ($p=0.98$, one-way ANOVA) and non-dominant stimuli ($p=0.544$, one-way ANOVA).

There is a close relationship between the spectral amplitude and phase-locking for oscillatory signals. While an increase in the signal amplitude can produce an increase in phase-locking, an increase in phase-locking is conceivable without any increment of amplitude. However, contrary to amplitude analysis, phase-locking factor is non-linear, thus it is possible that a significant phase-locking could be produced by a weak (and thus not significant) increase in power. To determine which part of the phase-locking effect can be explained by an increase in signal amplitude we performed a time-frequency analysis to reveal the amplitude and phase-locking values of the signal at each time step and frequencies. This type of analysis allowed us to explore the activities elicited at the tagging frequency as well as activities elicited at higher frequencies—i.e., the neural activities evoked by the onset of the face in different frequency bands. Figure 4a shows the amplitude time-frequency map for the visible stimuli (dominant) in the binocular rivalry condition averaged across subjects and electrodes. As previously, time zero represent the moment at which the semantic information was fully available. The baseline activity (from -200 to 0 ms after the semantic onset) was extracted (see Materials and Methods for details), and thus the map represents amplitude modulations below (Figure 4a, bluish colors) and above (Figure 4a, reddish colors) the baseline. Figure 4b shows the phase-locking time-frequency map for visible stimuli (dominant) averaged across subjects and electrodes. Significant differences between visible and non-visible conditions were found in the phase-locking analysis (Figure 4b, white line, $p<0.05$, FDR-corrected), while no significant differences were found in the amplitude analysis, suggesting thus that phase-locking could appear in absence

of power increment. To test that, we discarded the phase-locking values at the time-frequencies coordinates where amplitude modulations were equal or above zero (i.e., where the amplitude was equal or stronger than baseline), in every subject and electrode map. The remaining phase-locking values represent the phase-locking values at the time-frequency locations where the amplitude modulations were negative (i.e., where the amplitude was weaker than baseline). The mean of these values across subjects and electrodes is represented in Figure 4c, showing that significant phase-locking is still visible (Figure 4c, white line, $p<0.05$, FDR-corrected), thus demonstrating that the phase-locking (i.e., temporal consistency) effect is independent from an increase in amplitude.

Discussion

We have isolated the neural correlates of conscious visibility, which are modulated in an all-or-none fashion by perceptual alternation in binocular rivalry. Previous attempts to measure neural activity changes during binocular rivalry using frequency tagging have shown only mild modulations between consciously perceived and invisible stimuli (Tononi et al. 1998; Srinivasan et al. 1999; Ramesh Srinivasan 2004; Srinivasan and Petrovic 2006; Sutoyo and Srinivasan 2009). Single-unit recordings studies have also been used to measure neural activity changes during binocular rivalry, this time without tagging each stimulus by frequency but rather by studying neurons that respond selectively to the stimulus, showing that neural activity increases its selectivity to consciously perceived stimuli as one ascends on the visual hierarchy. While ~20% of cells are selective to consciously perceived activity in areas V1 and V2 of monkeys, this proportion increases to near 40% in V4 and MT, and up to ~90% in visual temporal areas (Logothetis 1998). It is thus tempting to conclude that the neural correlates of consciousness can be isolated just by picking the activities of higher visual areas, as some functional neuroimaging studies in humans suggest, in which conscious perception modulates neural activity profusely in areas such as FFA (Tong et al. 1998). However, significant activations to invisible stimuli can also be found in these high-level areas (Jiang and He 2006) and, moreover, it is possible to classify well above chance the category-specific information elicited by invisible stimuli in the same areas (Sterzer, Haynes,

and Rees 2008). Thus, our work represents the first result in which neural correlates of awareness are isolated from global brain activity.

Once the neural correlates of conscious vision were isolated, we concentrated our analysis on the nature of these neural activities. Since our paradigm includes a constant influx of visual information, we could either expect an increase of the amplitude response at the onset of the semantic information or a constant amplitude response with a rearranging of the temporal response around the onset of the semantic information. We found that awareness-dependent activities correspond to an increase in temporal consistency across different presentations of the semantic information (i.e., the face), and this effect is independent of the increase in the amplitude response. An increase in the temporal consistency can reflect a key feature of the nervous system such as phase resetting (Shah et al. 2004) that allows the interaction among different brain areas which would support the emergence of consciousness, as proposed by several authors (Rodriguez et al. 1999; Varela et al. 2001; Dehaene, Sergent, and Changeux 2003; Melloni et al. 2007).

Methods

Stimuli generation. We used an innovative technique called SWIFT: semantic wavelet-induced frequency-tagging, which uses manipulations in the wavelet domain to create a movie from a single natural image (Koenig-Robert & VanRullen, submitted). Each frame of the movie equalizes low-level properties of the natural image while modulating its high- and mid-level information content cyclically at a fixed temporal frequency, called tagging frequency. As a result, visual processing mechanisms that are sensitive to the low-level properties should be equally engaged by all frames of the movie, exhibiting a flat response during the presentation. On the other hand, the higher-level mechanisms responsible for extracting semantic information would come into play periodically around the onset of the original image. By analyzing changes of the neural activity at the tagging frequency it is thus possible to isolate activities supporting high-level visual representations. Details of the stimulus construction are published elsewhere (Koenig-Robert & VanRullen, submitted). Briefly, SWIFT movies were created by cyclic wavelet scrambling in the wavelets multi-scale domain. At each location and scale, local image contours were represented by a 3D vector in the wavelets space, with the 3 dimensions representing the strengths of horizontal, vertical

and diagonal orientations. For each location and scale, two new vectors with random orientations but the same length were defined. The unique isoenergetic circular path described by the 3 vectors was used to modulate local contour orientation cyclically, thus obtaining different wavelet-scrambled versions of the image, while conserving low-level properties (local luminance, contrast and spatial frequency) across frames.

Subjects. All subjects gave informed consent to take part in these studies that were approved by the local ethics committee. All nine subjects (4 women, aged 22 to 30) have normal or corrected-to-normal vision. One of them was one of the authors, 6 had intensive experience as observers in psychophysics experiments and 2 were naïve observers.

Experimental setup and procedure. Subjects were placed at 57 cm of a CRT screen with a refresh rate of 100 Hz in a dark room. Six faces (3 women, 3 men), were modulated under SWIFT at 2 different non-harmonic frequencies (1.4894 and 2 Hz). The movies were 10x10° and were separated by 4.3 cm over the computer screen and superimposed on the same region of the visual field of each eye thanks to a stereoscope. Each eye was stimulated by a single face using the 'version 2' stereoscope described by Randolph Blake: http://www.psy.vanderbilt.edu/faculty/blake/Stereoscope/stereoscope.html. Mirrors located close to the eyes allowed each eye to view only half of the computer screen. Mirrors were adjusted for each participant to ensure that both faces overlap exactly in the same portion of the visual field. Each face was colored (red or green) and the subject reported the color of the perceived face by pressing and maintaining a key (left arrow for green and right arrow for red) on a computer keyboard during the whole period of dominance. Subjects were instructed to press no button if dominance was incomplete (i.e., piecemeal). Two types of stimuli alternation were used: binocular rivalry and physical alternation. In binocular rivalry, both stimuli were presented simultaneously. In physical alternation, stimuli were presented alternatively, using smooth transitions that lasted from 0.5 to 1 sec. Dominance durations on physical alternations were defined semi-randomly, following the gamma distribution of binocular rivalry dominance durations of one of the subjects. The 15 possible pairs of different faces were counter-balanced for frequency, color, eye and type of alternation, yielding 240 trials. Each trial lasted 25 seconds and the experiment was divided in 4 blocks lasting about 3 hours. All subjects showed long periods of dominance at both modulation frequencies: mean dominance duration 2.95 (±0.11) sec for 1.4894 Hz and 2.86

(±0.14) sec for 2 Hz. Such stable dominance states are likely to be induced by the dynamic nature of stimuli. For both binocular rivalry and physical alternation conditions mean dominance durations were comparable: 2.94 (±0.23) sec and 3.19 (±0.06) respectively.

EEG acquisition and data processing. Continuous EEG was acquired with a 64-channel ActiveTwo system (Biosemi). Two additional electrodes [CMS (common mode sense) and DRL (driven right leg)] were used as reference and ground. Electrodes were placed according to the international 10/10 system. The vertical and horizontal electrooculogram were recorded by attaching additional electrodes below the left eye and at the outer canthi of both eyes. An active electrode (CMS) and a passive electrode (DRL) were used to compose a feedback loop for amplifier reference. Details of this circuitry can be found on the Biosemi website (www.biosemi.com/faq/cms&drl.htm). All signals were digitized at 1024 Hz, 24-bit A/D conversion. All data were analyzed off-line under Matlab (MathWorks) using the EEGLAB toolbox (Delorme and Makeig 2004). Average reference was computed, the data was downsampled at 512 Hz and no filter was applied. DC offset was removed from continuous EEG data. The linear trend was removed from each trial, using Andreas Widman's function for EEGLAB. Independent component analysis (ICA plugin from EEGLAB) was performed to remove eye blinks and muscular artifacts. Artifactual components were removed manually (from 1 to 5 out of 64 components per subject, mean 2.33) according to their activity time course and topography (frontal for eye blinks and temporal for muscular artifacts).

Event related potentials (ERP) analysis. Data was downsampled to 128 Hz and filtered between 0.5 and 30 Hz. Each SWIFT cycle period (from -100 to 671 ms for 1.4894 Hz and from -100 to 500 ms for 2 Hz) was taken as an epoch, in which zero-time represents the onset of the frame that contains all the semantic information. ERP epochs were sorted as a function of the reported visibility, while a stimulus was reported as dominant the other was labeled as non-dominant. Only complete epochs were considered and epochs occurring at the moment of alternation were discarded. A bootstrap procedure (resampling without replacement, n = 1000) was used to equalize the number of trials entered in the computation of the ERP for conditions (binocular rivalry vs. physical alternation), frequencies

and subjects. Baseline activity from -100 to 0 ms after the semantic onset was extracted. 10 central-frontal channels (AFz, F1, Fz, F2, FC1, FCz, FC2, C1, Cz and C2) were selected as a region of interest using the amplitude of differential activities between dominant and non-dominant conditions as the selection criterion. Onset latencies were evaluated using the statistical criteria proposed by Rugg et al (Rugg, Doyle, and Wells 1995): at least 15 consecutive time points with p-values (two-tailed, paired t test) equal or below 0.05.

Phase-locking analysis. Time-locked responses generated at the tagging frequency (f0) were assessed by measuring the response phase delay conservation, relative to the onsets of the semantic information (i.e. the onsets of the embedded image during the trial), at f0. The phase of the EEG signals was calculated by means of the fast Fourier transform (FFT) algorithm under Matlab (MathWorks). The FFT algorithm was applied over the nearest number of time-points at the sample rate (128 Hz) representing an entire cycle (86 time-points, corresponding to 0.6719 s for 1.4894 Hz, frequency resolution = 1.4884 Hz, and 64 time-points, corresponding to 0.5 seconds for 2 Hz, frequency resolution = 2 Hz) and the phase was extracted by selecting the coefficient representing the first harmonic from the Fourier transform output. The FFT transform at f0 of the time-domain signal S for the cycle k is a complex number in which A represents the amplitude of the signal and φ its phase:

$$F(S_{k,f0}) = A_{k,f0}\, e^{i\varphi_{k,f0}}$$

Phase-locking factor (PLF, also called phase-locking value) was calculated as follows:

$$PLF_{f0} = \left| \frac{1}{n} \sum_{k=1}^{n} e^{i(\varphi_{k,f0})} \right|$$

The PLF measure takes values between 0 and 1. A value of 0 represents absence of synchronization across cycles between EEG data and the time-locking events, and a value of 1 indicates perfect synchronization. PLF is computed by normalizing the lengths of the complex vectors (representing amplitude and phase) to 1 for all cycles and then computing their complex average. Thus, only the information about the phase of the spectral estimate of each cycle is taken into account.

Time-frequency analysis. EEG data (512 Hz, not filtered) was epoched between -600 and 1100 ms around the semantic onset. A bootstrap procedure (resampling without replacement, n = 500) was used to equalize the number of trials entered in the computation for conditions (binocular rivalry vs. physical alternation), frequencies and subjects. A wavelet-based time-frequency decomposition was performed using the EEG lab function 'timefreq'. Each time-frequency map included 348 time-points (from -412 to 913 ms) and 52 frequencies spaced in regular steps (from 3.5 to 50 Hz). Three cycles were used at the lowest frequency and at each frequency step this value was increased by 0.5. The amplitude was computed as the absolute value of the complex time-frequency map. Baseline activity from -100 to 0 ms after semantic onset was subtracted from the amplitude map which thus reflects amplitude modulations above and below the baseline. Phase-locking across cycles was obtained as described above.

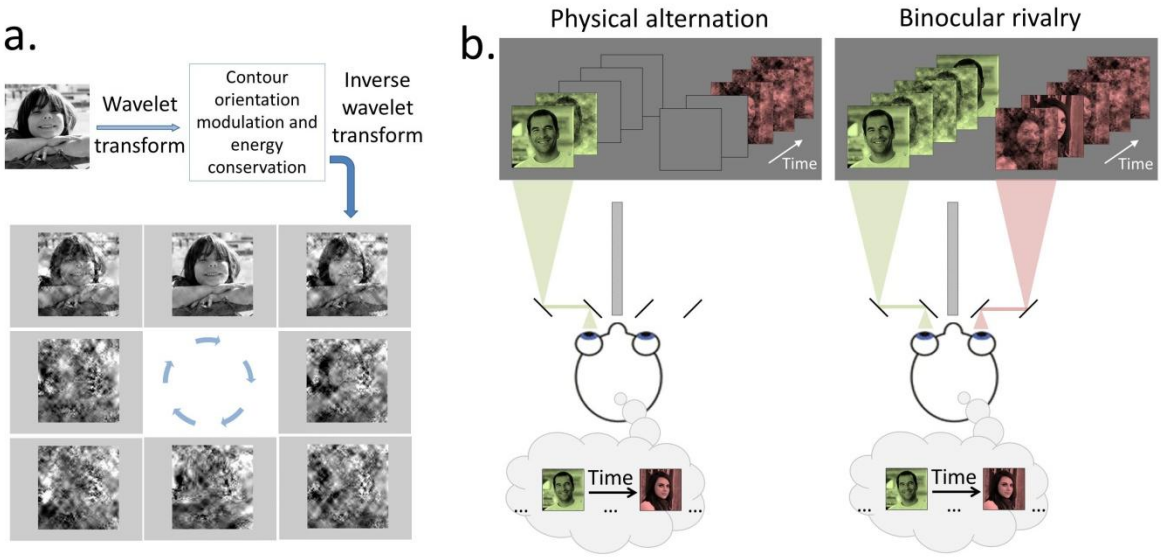

Figure 1. **Paradigm. A. SWIFT method.** Cyclic wavelet-scrambling modulates semantic information at the temporal tagging frequency, while conserving low-level features, thereby allowing tagging high-level representations by frequency. **B. Experimental design.** Two faces modulated at different tagging frequencies (1.4894 and 2 Hz) were shown to each eye. In physical alternation, stimuli were presented alternatively in each eye, mirroring the dynamics of spontaneous alternations recorded in binocular rivalry, where both stimuli were presented simultaneously. Subjects (n=9) had to report the color of the dominant (perceived) face, while EEG (64 channels) was recorded.

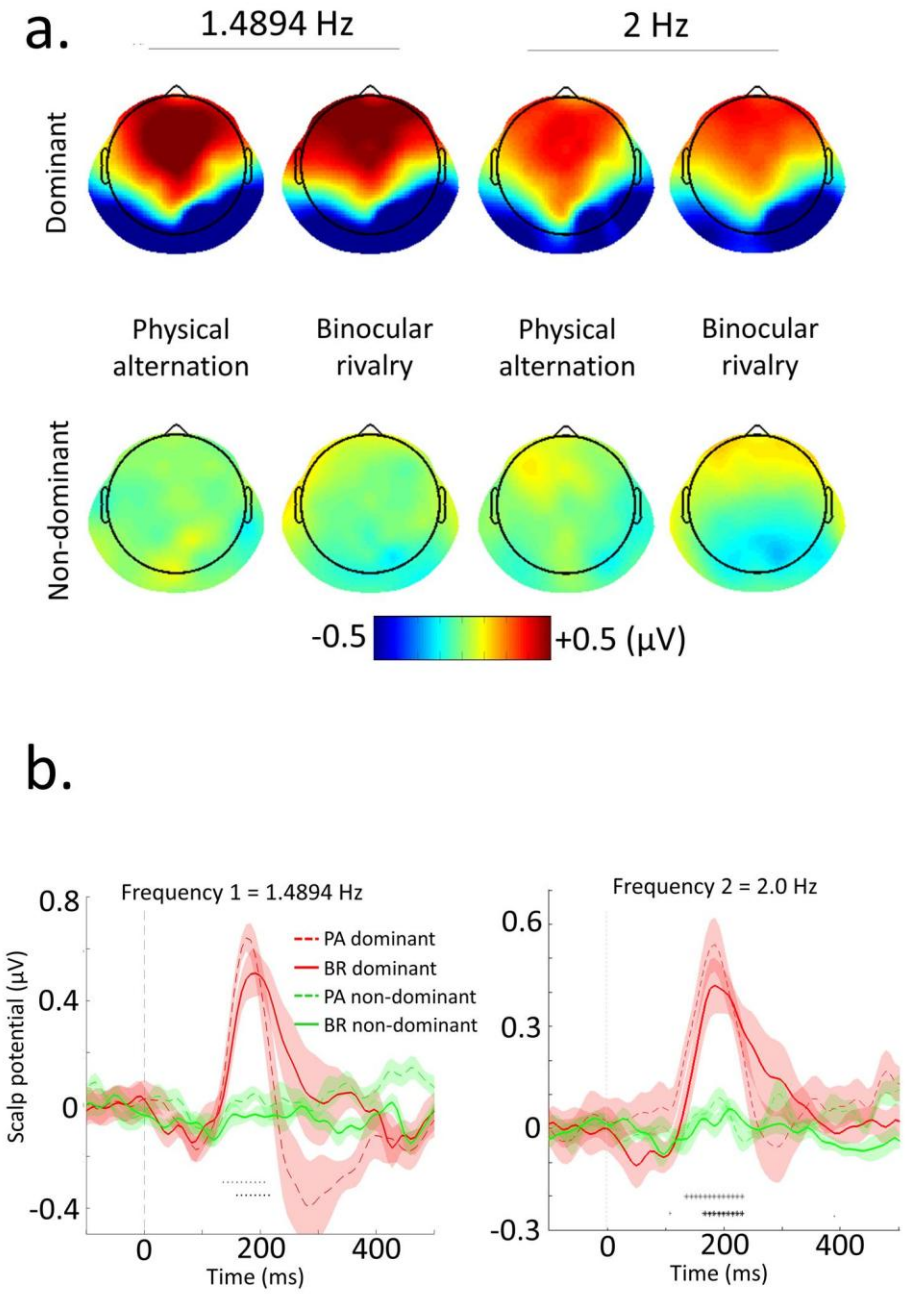

Figure 2. **ERP analysis.** Each cycle of wavelet-scrambling was selected as an epoch (n=1572), with time 0 representing the onset of the face. **A. ERP topography at ~200ms after semantic onset.** Activity elicited by dominant stimuli was comparable between PA and BR conditions. Importantly, the activity elicited by the non-dominant face in BR was comparable to the response to a blank screen in PA. **B**. **Activity time-course of 10 central-frontal electrodes.** The difference between dominant and non-dominant activities was significant ($p<0.05$) around 200 ms after semantic onset, for both physical alternation (grey points) and binocular rivalry (black points) conditions.

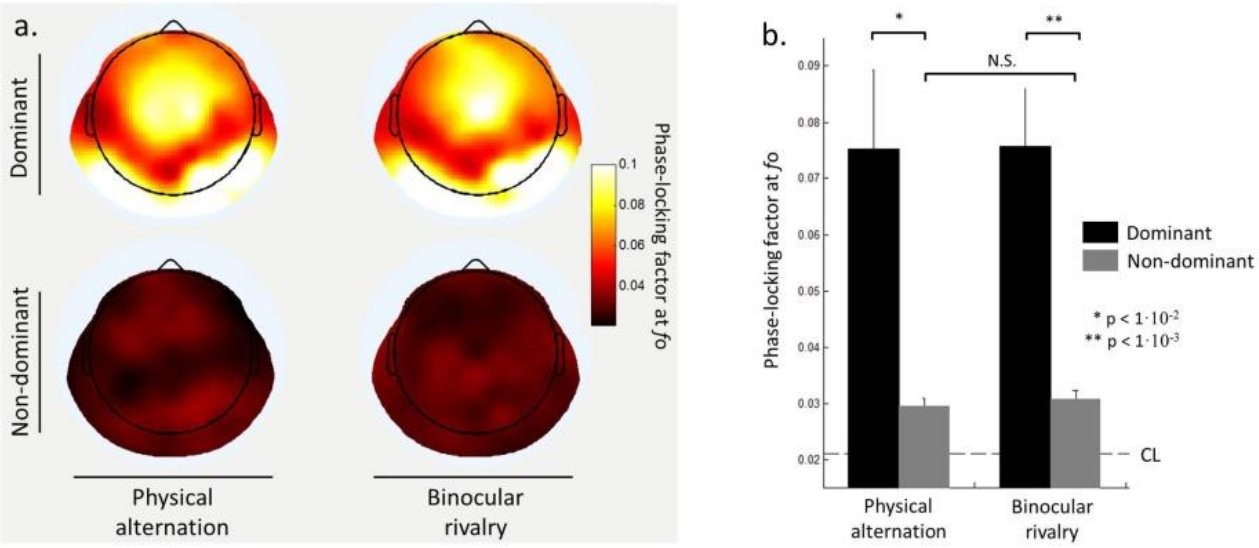

Figure 3. **Phase-locking analysis. A. Topography.** Phase-locking across cycles (n=1572, chance level=0.02) showing the averaged response between the 2 tagging frequencies (1.4894 and 2 Hz). Strong phase-locking at the tagging frequency is present in fronto-central and occipito-temporal regions for dominant stimuli in both physical alternation and binocular rivalry conditions. **b. Average phase-locking for all channels.** Differences between dominant and non-dominant stimuli were highly significant for both physical alternation and binocular rivalry conditions. Importantly, phase-locking elicited by non-dominant faces in binocular rivalry was not different from the activity elicited by the presentation of an empty screen in physical alternation.

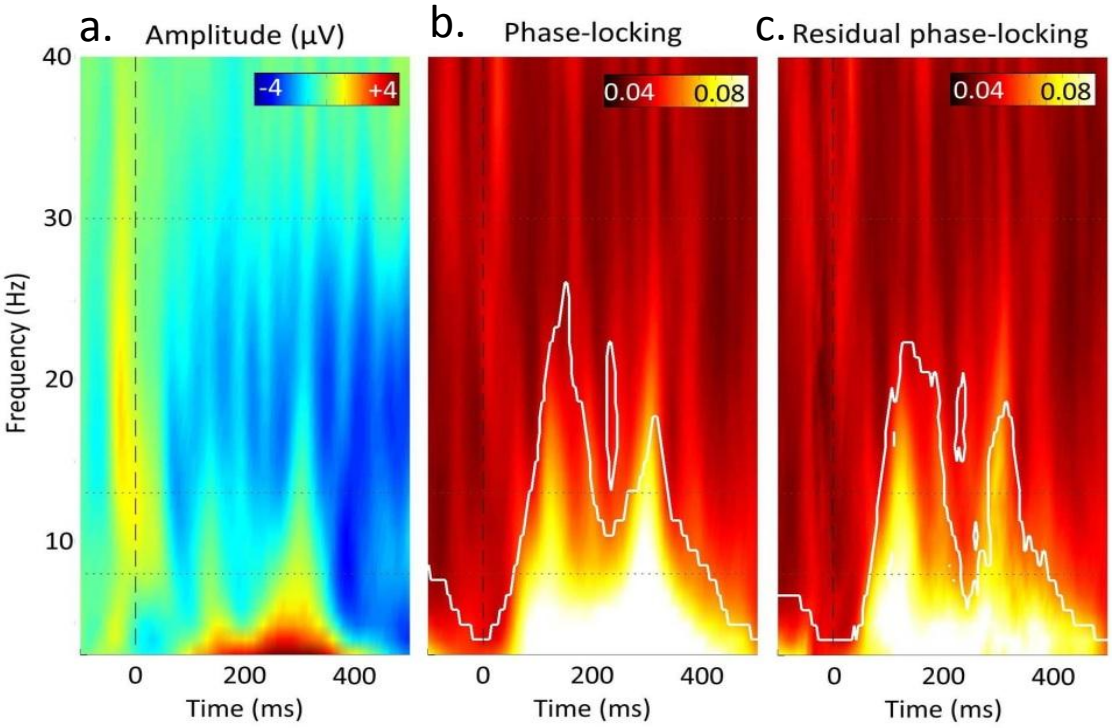

Figure 4. **Time-frequency maps. A. Amplitude map.** Time-frequency map representing amplitude modulations below (bluish colors) and above (reddish colors) the baseline for visible stimuli in the binocular rivalry condition. **B**. **Phase-locking map.** Phase-locking time-frequency map for visible stimuli in the binocular rivalry condition. Significant differences between visible and non-visible conditions ($p<0.05$, FDR-corrected) are delimited by a white line. Note that no significant differences were found between visible and non-visible conditions in the amplitude analysis (panel a). **C. Residual phase-locking map.** Phase-locking at the time-frequencies coordinates where amplitude modulations were below zero. Significant differences between visible and invisible conditions are outlined by a white curve ($p<0.05$, FDR-corrected). This shows that the phase-locking (i.e., temporal consistency) effect is independent from an increase in amplitude

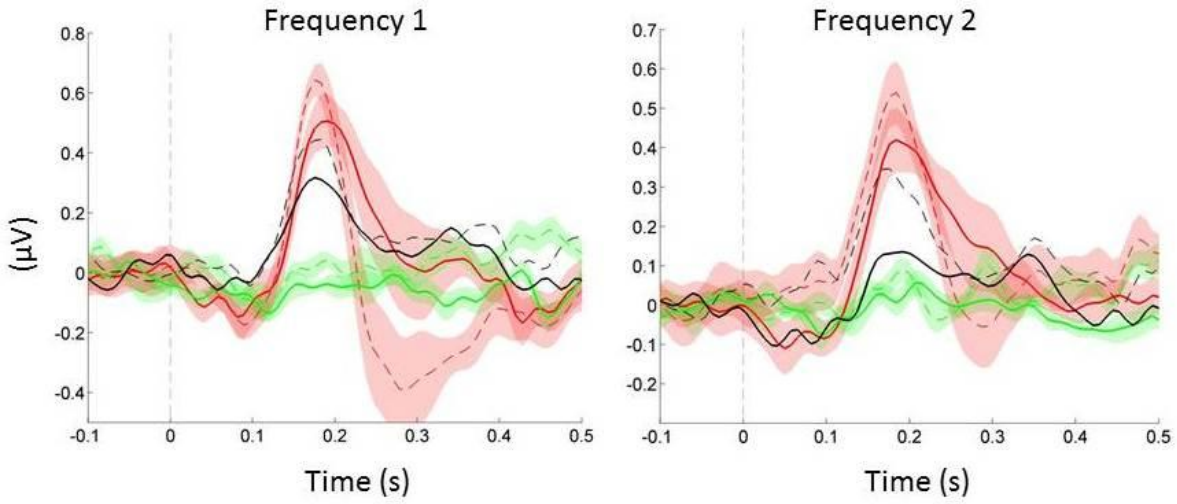

Figure S1. **Electro-oculogram ERP.** Solid and dashed black lines correspond to EOG activity for dominant stimuli in binocular rivalry and physical alternation conditions respectively. These activities were weaker than activities recorded on the scalp and were not significant showing that the effect recorded is not likely to correspond to ocular artifacts.

References

Dehaene, Stanislas, Claire Sergent, and Jean-Pierre Changeux. 2003. “A Neuronal Network Model Linking Subjective Reports and Objective Physiological Data During Conscious Perception.” *Proceedings of the National Academy of Sciences of the United States of America* 100 (14) (July 8): 8520–8525. doi:10.1073/pnas.1332574100.

Delorme, Arnaud, and Scott Makeig. 2004. “EEGLAB: An Open Source Toolbox for Analysis of Single-trial EEG Dynamics Including Independent Component Analysis.” *Journal of Neuroscience Methods* 134 (1) (March 15): 9–21. doi:10.1016/j.jneumeth.2003.10.009.

Haynes, John-Dylan, and Geraint Rees. 2005. “Predicting the Stream of Consciousness from Activity in Human Visual Cortex.” *Current Biology: CB* 15 (14) (July 26): 1301–1307. doi:10.1016/j.cub.2005.06.026.

Jiang, Yi, and Sheng He. 2006. “Cortical Responses to Invisible Faces: Dissociating Subsystems for Facial-information Processing.” *Current Biology: CB* 16 (20) (October 24): 2023–2029. doi:10.1016/j.cub.2006.08.084.

Koenig-Robert, R, and R VanRullen. “Isolating and Tracking the Neural Correlates of Object Recognition.”

Lansing, R W. 1964. “Electroencephalographic Correlates of Binocular Rivalry in Man.” *Science (New York, N.Y.)* 146 (3649) (December 4): 1325–1327.

Logothetis, N K. 1998. “Single Units and Conscious Vision.” *Philosophical Transactions of the Royal Society of London. Series B, Biological Sciences* 353 (1377) (November 29): 1801–1818. doi:10.1098/rstb.1998.0333.

Logothetis, N K, and J D Schall. 1989. “Neuronal Correlates of Subjective Visual Perception.” *Science (New York, N.Y.)* 245 (4919) (August 18): 761–763.

Melloni, Lucia, Carlos Molina, Marcela Pena, David Torres, Wolf Singer, and Eugenio Rodriguez. 2007. “Synchronization of Neural Activity Across Cortical Areas Correlates with Conscious Perception.” *The Journal of Neuroscience: The Official Journal of the Society for Neuroscience* 27 (11) (March 14): 2858–2865. doi:10.1523/JNEUROSCI.4623-06.2007.

Moutoussis, K., and S. Zeki. 2002. “The Relationship Between Cortical Activation and Perception Investigated with Invisible Stimuli.” *Proceedings of the National Academy of Sciences* 99 (14) (June 27): 9527–9532. doi:10.1073/pnas.142305699.

Polonsky, A, R Blake, J Braun, and D J Heeger. 2000. “Neuronal Activity in Human Primary Visual Cortex Correlates with Perception During Binocular Rivalry.” *Nature Neuroscience* 3 (11) (November): 1153–1159. doi:10.1038/80676.

Rodriguez, E, N George, J P Lachaux, J Martinerie, B Renault, and F J Varela. 1999. “Perception’s Shadow: Long-distance Synchronization of Human Brain Activity.” *Nature* 397 (6718) (February 4): 430–433. doi:10.1038/17120.

Rugg, Michael D., Michael C. Doyle, and Tony Wells. 1995. “Word and Nonword Repetition Within- and Across-Modality: An Event-Related Potential Study.” *Journal of Cognitive Neuroscience* 7 (2) (April): 209–227. doi:10.1162/jocn.1995.7.2.209.

Shah, Ankoor S, Steven L Bressler, Kevin H Knuth, Mingzhou Ding, Ashesh D Mehta, Istvan Ulbert, and Charles E Schroeder. 2004. “Neural Dynamics and the Fundamental Mechanisms of Event-related Brain Potentials.” *Cerebral Cortex (New York, N.Y.: 1991)* 14 (5) (May): 476–483. doi:10.1093/cercor/bhh009.

Srinivasan, R, D P Russell, G M Edelman, and G Tononi. 1999. “Increased Synchronization of Neuromagnetic Responses During Conscious Perception.” *The Journal of Neuroscience: The Official Journal of the Society for Neuroscience* 19 (13) (July 1): 5435–5448.

Srinivasan, Ramesh. 2004. “Internal and External Neural Synchronization During Conscious Perception.” *International Journal of Bifurcation and Chaos in Applied Sciences and Engineering* 14 (2) (February): 825–842. doi:10.1142/S0218127404009399.

Srinivasan, Ramesh, and Sanja Petrovic. 2006. “MEG Phase Follows Conscious Perception During Binocular Rivalry Induced by Visual Stream Segregation.” *Cerebral Cortex (New York, N.Y.: 1991)* 16 (5) (May): 597–608. doi:10.1093/cercor/bhj016.

Sterzer, P., J. D. Haynes, and G. Rees. 2008. “Fine-scale Activity Patterns in High-level Visual Areas Encode the Category of Invisible Objects.” *Journal of Vision* 8 (15) (November 1): 10–10. doi:10.1167/8.15.10.

Sutoyo, David, and Ramesh Srinivasan. 2009. “Nonlinear SSVEP Responses Are Sensitive to the Perceptual Binding of Visual Hemifields During Conventional ‘Eye’ Rivalry and Interocular ‘Percept’ Rivalry.” *Brain Research* 1251 (January 28): 245–255. doi:10.1016/j.brainres.2008.09.086.

Tong, F, K Nakayama, J T Vaughan, and N Kanwisher. 1998. “Binocular Rivalry and Visual Awareness in Human Extrastriate Cortex.” *Neuron* 21 (4) (October): 753–759.

Tong, Frank, Ming Meng, and Randolph Blake. 2006. “Neural Bases of Binocular Rivalry.” *Trends in Cognitive Sciences* 10 (11) (November): 502–511. doi:10.1016/j.tics.2006.09.003.

Tononi, G, R Srinivasan, D P Russell, and G M Edelman. 1998. “Investigating Neural Correlates of Conscious Perception by Frequency-tagged Neuromagnetic Responses.” *Proceedings of the National Academy of Sciences of the United States of America* 95 (6) (March 17): 3198–3203.

Varela, F, J P Lachaux, E Rodriguez, and J Martinerie. 2001. “The Brainweb: Phase Synchronization and Large-scale Integration.” *Nature Reviews. Neuroscience* 2 (4) (April): 229–239. doi:10.1038/35067550.

F. Intracranial recordings using SWIFT: ongoing collaborative work

Where and when in the brain does neural activity generate visual consciousness? In order to try to answer this question I wanted to combine SWIFT with intracranial recordings which maximize the advantages of the high-temporal resolving properties of SWIFT adding improved spatial resolution compared with EEG recordings. This method provides both millisecond-level temporal resolution and millimeter-level spatial resolution of brain activity, which cannot be achieved with EEG recordings that lack spatial resolution. The application of this method would provide high spatio-temporal resolution measures of neural activity related to visual consciousness across the brain and, at the same time help us to understand the functional interactions among different areas and how they pinpoint conscious perception.

We had the unique opportunity to use this technique thanks to two fruitful collaborations. A first collaboration with Dr. Emmanuel Barbeau, researcher in our laboratory and Dr. Luc Valton, from the department of epileptology of Rangueil Hospital, allowed us to have access to epileptic patients implanted with deep electrodes (SEEG) for clinical reasons. A second collaboration with Dr. Denis Fize and his Masters student, Anne-Claire Collet, allowed us to have access to one implanted macaque monkey implanted with intracranial electrodes (ECoG).

Using these models we want to address questions such as the causal relationships in the emergence of consciousness in different areas, the propagation of the consciousness related activity across brain areas, the nature of conscious activity and the participation of distinctive activity frequency bands in its generation, among others.

These collaborations are still ongoing and the data collection stage is not yet completed. However, even at this stage, we have obtained very promising results which will be presented in the form of two separate preliminary reports.

I. REPORT 1. Koenig-Robert, Barbeau, Valton & VanRullen.

The time course and spatial distribution of consciousness-dependent activity in the human brain.

Roger Koenig-Robert, Emmanuel Barbeau, Luc Valton & Rufin VanRullen

Exploring neural correlates of awareness with both high spatial and temporal resolution has been a difficult challenge. Current neuroimaging techniques can attain outstanding temporal resolution (EEG and MEG) or great spatial resolution (fMRI) but rarely both. Epileptic patients implanted with deep electrodes for clinical reasons provide a unique opportunity to explore the neural correlates of awareness with both high temporal and spatial resolutions. We used stereotaxic-electroencephalogram (SEEG) to record activity from both superficial and deep structures, mainly from temporal and parietal lobes. We used an innovative technique called SWIFT (semantic wavelet-induced frequency-tagging), in which periodic scrambling in the wavelets domain modulates an image semantic content (object form) over time, without disturbing its low-level attributes. This technique already proved highly effective in isolating conscious object representations by EEG frequency-tagging (Koenig-Robert & VanRullen, submitted). In the present study, we presented to epileptic patients SWIFT sequences containing natural images containing an object, and subjects reported conscious recognition of the object. If it was not recognized after a few scrambling cycles, the original image was shown steadily for 3 seconds to reveal object identity and then the sequence was presented again. Comparing frequency-tagging responses before vs. after conscious object recognition, we found consciousness-dependent activity involving theta, alpha, beta and gamma bands in different brain regions.

Materials and Methods

Subjects. Three patients suffering from drug-resistant epilepsy and candidates for surgery participated in the study. Because the location of the epileptic focus could not be identified using non-invasive methods, the patients underwent intracerebral EEG recordings using stereotactically implanted depth electrodes (SEEG). The selection of electrode implantation sites was solely based on clinical considerations directly related to the presurgical evaluation and without any reference to the present experimental investigations. All patients provided informed consent prior to their participation in the experiment and experimental procedures were approved by the French ethics committee.

Intracerebral recordings. A multi-channel video-SEEG acquisition and monitoring system (Micromed, Treviso, Italy) was used to simultaneously record the intracerebral activity from up to 128 depth-EEG electrodes (512 Hz sampling rate and a 0.1 to 200 Hz bandpass filter). Twelve to fourteen semi-rigid multi-lead electrodes were implanted in each patient. Each electrode had a diameter of 0.8 mm and, depending on the target structure, comprised between 5 and 18 contact leads 2 mm long and 1.5 mm apart (Alcys, Besançon, France). In addition, computer-assisted matching between a post-implantation CT-scan and a pre-implantation 3-D MRI data set allowed for direct visualization of the electrode contacts on the patient's brain anatomy. Bipolar reference was calculated offline.

Experimental procedure. SWIFT sequences containing either grayscale natural images (bodies with faces, bodies with no visible faces, animals and manmade objects, downloaded from the Internet) or no-object pictures (low-level matched textures obtained by using the algorithm developed by Portilla & Simoncelli (Portilla & Simoncelli, 2000)) were shown. The image contours were modulated cyclically over time at two tagging frequencies, f0 = 1.4894 or 1Hz. In each trial a SWIFT movie containing a single natural image was presented in two different periods. In the first period or naïve period, the movie was presented by the first time to the patient. Within this period, the patient could give her response by pressing a computer key (the key was pressed when an object was recognized by the patient). In between the periods, the image contained in the movie was showed steadily as a prime whether the object was recognized or not in the first period. In the second or cognizant

period, the same movie presented in the naïve period was presented again. This assures that all movies containing meaningful natural images (i.e. the movies not containing abstract textures) were recognized in the cognizant period. The experiment was divided in blocks of 25 trials each. Each trial lasted 23 sec (10 sec of naïve period + 3 sec of steady image priming + 10 sec of cognizant period). Subjects completed from 4 to 10 blocks, within a period of several days. Sequences were presented at the center of the screen over a black background. Subjects were asked to keep their fixation over a red cross at the center of the display during the trial. They gave their responses (presence of a non-abstract item) at any time during the first naïve period by pressing the right arrow on a computer keyboard. Our analysis was focused only on the trials that were not recognized during the first period of presentation (i.e., naïve period) and the no-objects trials that were used as a baseline. This yielded three conditions: non-recognized (i.e., unrecognized objects showed in the naïve period, prior to priming), recognized (i.e., the same objects that were recognized in the cognizant period, once the prime was presented) and no-object (trials where an abstract texture was shown).

Responsive recording sites selection. Several electrode contacts were not functional either because they laid on the white matter (~50%) or they were placed on areas that were functionally impaired (i.e., epileptogenic zones), which was the most usual case. Among the functional contacts, we were interested in the brain areas that responded selectively to the semantic visual information. Thus we had to set a criterion in order to select the contacts to focus our analysis. Electrode contact responsiveness was assessed by measuring the phase-locking factor at the tagging frequency, and also at its 2nd harmonic, across trials (see below for details). Phase-locking was defined as significant by comparing it with the null hypothesis of random phase distribution based on the number of trials performed (Monte Carlo simulation, 10^6 iterations). Only electrode contacts showing phase-locking factor at the tagging frequency for the recognition condition above a threshold value (represented by $p=10^{-5}$) and below this threshold for the no-object and non-recognized condition were selected. The selected contacts represented 5.4% of contacts (7 over 128 contacts) for subject 1, 3.4% (4 over 119 contacts) for subject 2, and 5.8% (7 over 120 contacts) for subject 3.

Event-related potential (ERP) analysis. SEEG data (512 Hz sampling rate) was low-pass filtered at 15 Hz and epoched between -100 and 671 ms or between -100 and 1000 ms (depending on the tagging frequency used in a particular subject), taking as 0 time the moment at which the semantic information was fully available within a SWIFT scrambling cycle. Linear detrending correction was performed in order to ensure that potential at time-points 0 and [1/tagging frequency] remained at 0µV for every epoch.

Phase-locking analysis across trials. Time-locked responses generated at the tagging frequency (f0) were assessed by measuring the response phase delay conservation, relative to the onsets of the semantic information (i.e. the onsets of the embedded image during the trial), across trials. A bootstrap procedure (resampling without replacement, n = 500) was used to equalize the number of trials entered in the computation for conditions. The phase of the EEG signals was calculated by means of the fast Fourier transform (FFT) algorithm under Matlab (MathWorks). The FFT algorithm was applied over a whole period of 10 sec (5120 time-points, frequency resolution = 0.1 Hz) and the phase was extracted by selecting the coefficient representing the closest frequency to the tagging frequency from the Fourier transform output. The FFT transform at f0 of the time-domain signal S for the trial k is a complex number in which A represents the amplitude of the signal and φ its phase:

$$F(S_{k,f0}) = A_{k,f0}\, e^{i\varphi_{k,f0}}$$

Phase-locking factor across trials (*tPLF*, also called phase-locking value or inter trial coherence) was calculated as follows:

$$tPLF = \left| \frac{1}{n} \sum_{n=1}^{k} e^{i(\varphi_k)} \right|$$

The PLF measure takes values between 0 and 1. A value of 0 represents absence of synchronization across cycles between EEG data and the time-locking events, and a value of 1 indicates perfect synchronization. *tPLF* is computed by normalizing the lengths of the complex vectors (representing amplitude and phase) to 1 for all cycles and then computing their complex average. Thus, only the information about the phase of the spectral estimate of each trial is taken into account.

Time-frequency analysis. EEG data (512 Hz sample rate, not filtered) was epoched between -500 and 1500 ms around the semantic onset. Wavelet-based time-frequency decomposition was performed using the EEG lab function 'timefreq'. Each time-frequency map included 410 time-points (from -312 to 13162 ms) and 52 frequencies spaced in regular steps (from 1.5 to 100 Hz). Half a cycle were used at the lowest frequency and at each frequency step this value was increased in 0.5.

Phase-locking across cycles (external synchrony) analysis. Oscillatory responses generated at different frequencies phase-locked to the onset of the semantic information across cycles were assessed by phase-locking analysis as follows:

$$cPLF_{t,f} = \left| \frac{1}{n} \sum_{n=1}^{c} e^{i(\varphi_{c,t,f})} \right|$$

Were *cPLF* represents the phase-locking across cycles, φ the phase at the time t and the frequency f.

Inter-electrode phase-locking (internal-synchrony) analysis. The conservation of the phase relationship among electrodes across trials was assessed using phase-locking analysis. We calculated the phase-locking (*ePLF*) between each pair of electrode sites (E1 and E2) as follows:

$$ePLF_{t,f} = \left| \frac{1}{n} \sum_{n=1}^{c} e^{i(\varphi E1_{c,t,f} - \varphi E2_{c,t,f})} \right|$$

Where $\varphi E1_{c,t,f} - \varphi E2_{c,t,f}$ represents the phase difference between each electrode site at the scrambling cycle c, for the frequency f and time t. A value of *ePLF* of 1 denotes perfect conservation of the electrode phase-difference across trials. Significant values of PLF_e were assessed by comparison with the null hypothesis of random inter-electrode phase-locking. In order to do that we shuffled the trials and obtained $\varphi E1_{c1,t,f} - \varphi E2_{c2,t,f}$, were c1 and c2 represent different trials. We repeated this operation 10^3 times and obtained a distribution of the *ePLF* accounting for the null hypothesis of random inter-electrode phase conservation.

Phase-locking as a function of recognition at different frequency bands. Phase-locking time-frequency maps from non-recognized and recognized conditions were averaged across the temporal dimension and different frequency bands were selected (delta 1.5-4Hz, theta 4-8Hz, alpha 8-13Hz, beta 13-30Hz, low-gamma 30-70Hz and high-gamma 70-100Hz). Phase-locking from different electrode sites was normalized in order to compare absolute differences between non-recognized and recognized conditions over recording sites with disparate response strengths, recorded from different subjects and obtained with different number of trials. Normalized phase-locking for recognized (NPL_r) and non-recognized (NPL_n) periods were calculated as follows:

$$NPL_r = \frac{PLr}{PLr + PLn}; \quad NPL_n = \frac{PLn}{PLr + PLn}$$

Were PLr is the phase-locking factor obtained in the recognized period and PLn is the phase-locking obtained in the non-recognized period. The modulations of NPL_r and NPL_n are thus centered at 0.5. In order to plot the results, these values were normalized in order to visually represent the relative amount of phase-locking at difference at the different frequency bands. Note, however, that this last step of normalization has no incidence in the effects presented whatsoever and it is only made for visualization purposes.

Results

Semantic-selective recording sites. Semantic selective electrode contacts were selected based on their response at the tagging frequency harmonics (see Materials and Methods section for details). Only electrode contacts showing a highly significant phase-locking factor ($p<10^{-5}$, Monte Carlo simulation) at one of the first two first harmonics of the tagging frequency for the recognized condition, but showing phase locking below this threshold for the non-recognized or no-object condition were selected (see figure 1 for an example). This

selection was made because several electrode contacts were not functional either because they laid on the white matter (more than 50%) or they were placed on areas that were functionally impaired (i.e., epileptogenic zones). Among the functional contacts, we were interested in the brain areas that responded selectively to the semantic visual information. A mean of 4.9% of the electrode contacts (representing 18 contacts over 3 subjects) fulfilled our selection criterion.

Event related potential analysis. We used an event-related potential (ERP) analysis to measure the scalp potentials locked to the onset of the semantic information—the time when the non-scrambled picture was on the screen—which was taken as the zero-time. Each SWIFT modulation cycle was thus taken as an epoch. Examples of ERPs for different recording sites for the 3 subjects are shown in figure 2. No significant differences between no-objects (Figure 2, green line) and non-recognized objects (Figure 2, black line) were seen in the majority of selected electrodes. Once the same previously non-recognized objects were primed and thus recognized and showed again, ERP responses (Figure 2, red line) became significantly different (Figure 2, black underscore, $p<0.01$, one-way ANOVA) from no-objects (green line). However the significance of these effects is trivial since they are expected from our selection criterion. What is not trivial is the timing of these differences which can be informative regarding the causal relationship among areas in the emergence of activities associated to conscious recognition. Thus, earliest significant differences were found on parietal and temporal electrodes around 100 ms, while most of significant differences were seen between 200 and 300 ms after the semantic onset, with a great amount of jitter among areas (data not shown).

External synchrony analysis. A time-frequency phase-locking analysis allowed us to investigate the neural activities evoked by the semantic information at every SWIFT modulation cycle for the recognized and non-recognized conditions. Significant phase-locking values denote oscillatory activities systematically elicited with the same phase relationship across trials relative to the semantic onset of the stimulation. The time-frequency analysis allows assessing the degree of synchrony of the recorded area relative to the stimulation (from now on called external synchrony) across several frequency bands. Figure 3 shows phase-locking time-frequency maps for the recognized and non-recognized conditions for the 3 subjects (same recording sites as showed in figure 2). A slight increase in

the phase-locking value can be observed in some cases for recognized objects at frequencies below 20 Hz. Note that a high value of phase-locking around the tagging frequency for recognized objects is trivial since it was used as the selection criterion for the electrode contacts. However, significant phase-locking factor at higher frequencies are not *a priori* expected and may denote a phase-resetting evoked by the semantic information. In order to quantify the differences in phase-locking at different frequency bands, we compared the phase-locking across cycles for non-recognized and recognized conditions for all 18 recording sites (Figure 4). Differences in phase-locking between non-recognized and recognized conditions were highly significant in the delta range (1.5-4Hz, $p=2.3\cdot10^{-6}$, one-way ANOVA, although trivial since it was used as the selection criterion), theta range (4-8Hz, $p=8\cdot10^{-5}$, one-way ANOVA), alpha range (8-13Hz, $p=4.5\cdot10^{-3}$, one-way ANOVA) and beta range (13-30Hz, $p=2.4\cdot10^{-3}$, one-way ANOVA). Interestingly, while an increase in phase-locking in the recognized condition was observed at low frequencies (from delta to alpha), the contrary was observed in the beta band, where a decrease in phase-locking was shown (Figure 4).

Inter-electrode (internal) synchrony analysis. Functional connectivity between brain areas was assessed by means of a phase-locking analysis between electrode pairs. Our hypothesis is that if two areas are functionally coupled, their phase relationship would be conserved across trials. Since we were interested by the electrode interactions modulated by the onset of the semantic information, we extracted the baseline activity (from -100 to 0 ms after semantic onset, which reflects intrinsic phase-locking across areas) in order to showcase modulations due to the processing of semantic information during non-recognized and recognized periods (Figure 5). Significant modulations above and below the baseline were shown at different frequencies (Figure 5, outlined regions). Interestingly, inversions in the inter-electrode phase-locking modulation (from positive to negative modulations or inversely) were seen between non-recognized and recognized conditions (i.e., Figure 5, Subject 1, from positive to negative around 40Hz and Subject 2, from negative to positive below 20Hz), denoting inter-area synchronization and de-synchronization as a function of recognition. In order to quantify the global behavior of inter-electrode phase-locking as a function of recognition, we calculated the difference of inter-electrode phase-locking at different frequency bands for all recording sites pairs (Figure 6). While global differences in inter-electrode phase locking were not significant at lower frequencies (Figure 6, delta,

p=0.18; theta, p=0.72, one-way ANOVA), the difference was barely significant in the alpha band (p=0.047) and more significant at higher frequencies (beta, p=0.016; gamma1, p=0.0016, one-way ANOVA) reaching a high significance at the gamma2 range ($p=3.72\cdot10^{-6}$, one-way ANOVA). Interestingly, global modulations in inter-electrode phase-locking suggest both recognition-dependent synchronization and de-synchronization. Inter-area de-synchronization as a function of recognition (i.e., less inter-electrode phase-locking in the non-recognized condition than in the recognized condition) is visible at alpha (though barely significant), beta and gamma1 frequencies, while a highly significant synchronization as a function of recognition is shown at high gamma (Figure 6).

Discussion

These preliminary results are very promising and allow drawing important interim conclusions. First, we found ERP responses that were modulated significantly between non-recognized and recognized conditions, which is trivial considering our selection criterion based on selective phase-locking among conditions. However, the timing or these responses is not trivial and can give us clues about the causal relationship among brain areas in the emergence of activities associated to conscious recognition. In fact a fair degree of temporal variability was shown in these responses, suggesting that there are brain areas which respond earlier than others to the semantic information. A systematic analysis of the latency across areas coupled with measures of causal probability (such as Granger probability) would allow us to understand better the interactions of the brain areas supporting conscious recognition.

Responses selective to the semantic information were found at several electrode contacts in both visual (occipito-temporal, infero-temporal and parietal areas) and non-visual areas (frontal and para-hippocampal areas). We certainly did not exactly replicate the ERP waveforms obtained in previous EEG studies, possibly because by using EEG we have access to neural activities that represent an average of the local sources and with SEEG we are able to directly record from these local sources. Interestingly, only a little part of the recording sites showed semantic selectivity (about 5%). Even though one could expect responsiveness in less than half of contacts (because about a half is located in the white matter, and because the majority is located in epileptogenic, functionally impaired zones), such low ratio of

semantic selectivity suggests a great deal of sparseness in the spatial distribution of the semantic related zones.

Secondly, we assessed the level of synchronization in different brain areas as a function of conscious recognition by means of two different measures: external synchrony and internal synchrony.

The external synchrony measure allowed us to assess the phase consistency (related to the semantic onset of the stimulation) of oscillatory responses of a given recording site across cycles. This measure shows systematic time-locked activity in a given brain area evoked by the semantic information; said otherwise: the synchronization of brain areas with external stimulation which is likely to be originated by phase-resetting involving different frequencies. Globally, time-locked activity respect to the semantic information—external synchrony—was significantly higher when the object was consciously recognized than when it was not in both the theta and alpha bands, showing that brain areas become more synchronized with the semantic onset when the object is consciously recognized. Interestingly, at the beta band, a significant decrease of synchrony with the semantic information is showed when the object is recognized. This can be explained by the relative amount of focused attention involved in the non-recognized and recognized conditions. In the first presentation of the SWIFT movie, the patient efforts to recognize the object imbedded in the SWIFT movie. As we deliberately chosen pictures containing non-canonical views of animals, people, objects, etc. the recognition of these objects needs a high involvement of focused attention during the non-recognized period. On the other hand, in the recognized condition, once the object is primed and recognized, the need of attention decreases as no object must be discovered. Evoked phase-locking responses (i.e. external synchrony) have been documented as attention-related in the high-beta/low-gamma band, using MEG recordings (Vidal, Chaumon, O'Regan, & Tallon-Baudry, 2006). Interestingly, this activity was found in the global activity (grand average across subjects and sensors) and was not related to an increase in power. An early phase-locked response was also found in the beta/low-gamma band in a task with ambiguous stimuli were presented (Tallon-Baudry, Bertrand, Delpuech, & Permier, 1997). The phase-locked response was not modulated by the recognition of the ambiguous object and it may correspond to the involvement of attention needed to perceive the ambiguous object. The increase in the external-synchrony in the

beta-band for the non-recognized condition seems to be consistent with these results; however, we did not detect any significant difference in the gamma band.

The internal synchrony measure or inter-electrode phase-locking assesses a recording-site pair's phase-consistency of oscillatory responses across cycles. This measure represents a way to reveal functional connectivity between areas: two areas that conserve their phase relationship across cycles are more likely to interact than areas without phase consistency. Significant modulations of the synchrony between brain areas evoked by the semantic information were shown; and interestingly, these modulations suffered reversals (from increment to decrease and vice-versa) when the object was consciously recognized compared with the non-recognized period, on pairs of recording sites in all subjects. Global increments and decreases in inter-electrode synchrony were significant for frequencies above 8Hz. Interestingly, a significant global decrease in inter-electrode synchrony was related to conscious recognition at the alpha, beta and low-gamma bands; while a highly significant increase was shown at high-gamma (from 70 to 100 Hz).

The decrease in the internal-synchrony at the beta and low-gamma frequencies when the object was recognized can be explained as an effect produced by the amount of focused attention involved in the two periods. As previously, we hypothesize the patient pays more attention in the non-recognized period, since an active search of the object is made. Single unit recordings have shown attentional effects mostly in the low-gamma but also in the beta band as an increase in the multiunit and LFP coherence (Bichot, 2005); (Womelsdorf et al., 2007); (Chalk et al., 2010) and power (P. Fries, 2001) recorded on different electrodes within a same visual area, and also as an increase in the multiunit and LFP coherence across different brain areas (Gregoriou, Gotts, Zhou, & Desimone, 2009). These effects are explained by the framework of selective attention by selective synchrony, in which a rhythmic inhibition at the high-beta and low-gamma band would select fedforward inputs synchronized with the inhibitory pulse (Womelsdorf & Fries, 2007); (Pascal Fries, Nikolić, & Singer, 2007).

On the other hand, the increase in the internal-synchrony at the high-gamma band related to the conscious recognition can be interpreted as the setting of a resonant network which is the result of the emergence of a conscious meaningful percept. This network would not be

phase-locked to the stimulus onset as it would reflect dynamic and metastable inter-area synchrony.

For the increase in the internal synchrony in the non-recognized we have no compelling explanation until now. It can either be the product of noise or would have a functional role in the formation of transient neuronal assemblies (Palva & Palva, 2007).

The different synchronic response profiles of brain oscillations in different frequency bands may provide new insights into the neural correlates of conscious recognition and also can help us to understand how attention and consciousness are dissociated at the neuronal level. We look forward to reproducing these results in next patients in order to draw more definitive conclusions at that time.

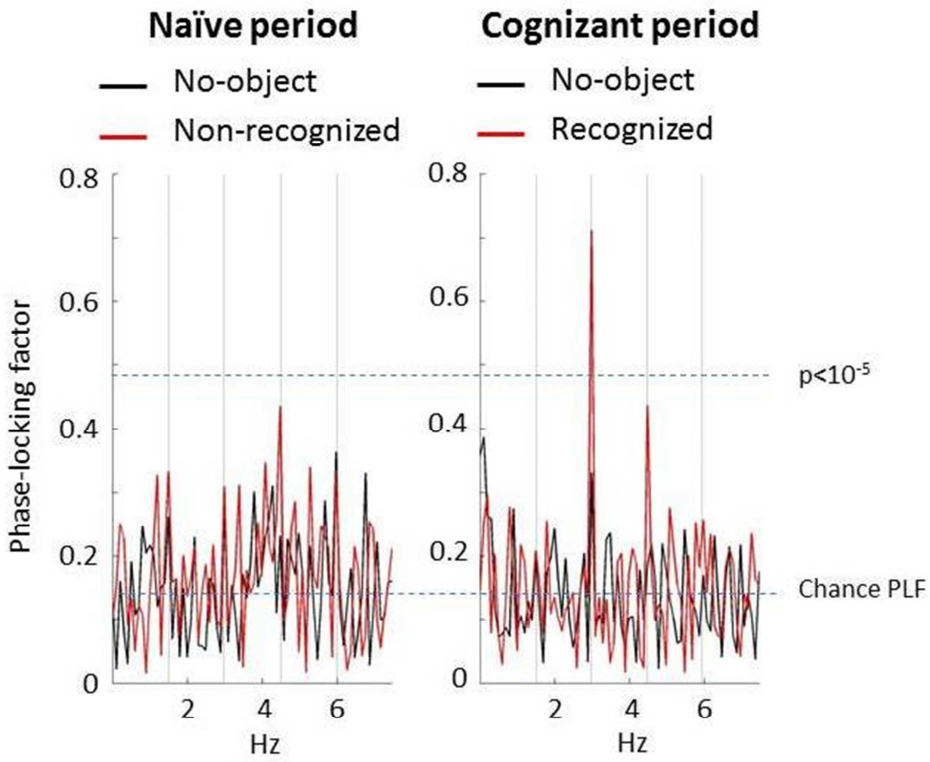

Figure 1. **Semantic-selective recording site selection.** A criterion based on the phase-locking activity evoked by semantic information was used to select responsive contacts. Here an example of a semantic-selective contact. During the naïve period (before priming), neither unrecognized nor abstract textures (no-object) elicited phase-locking values above the threshold for selectivity. In the cognizant period, recognized objects evoked a phase-locking value above the selectivity threshold, but no-object did not pass the threshold. Vertical bars denote the harmonics of the tagging frequency.

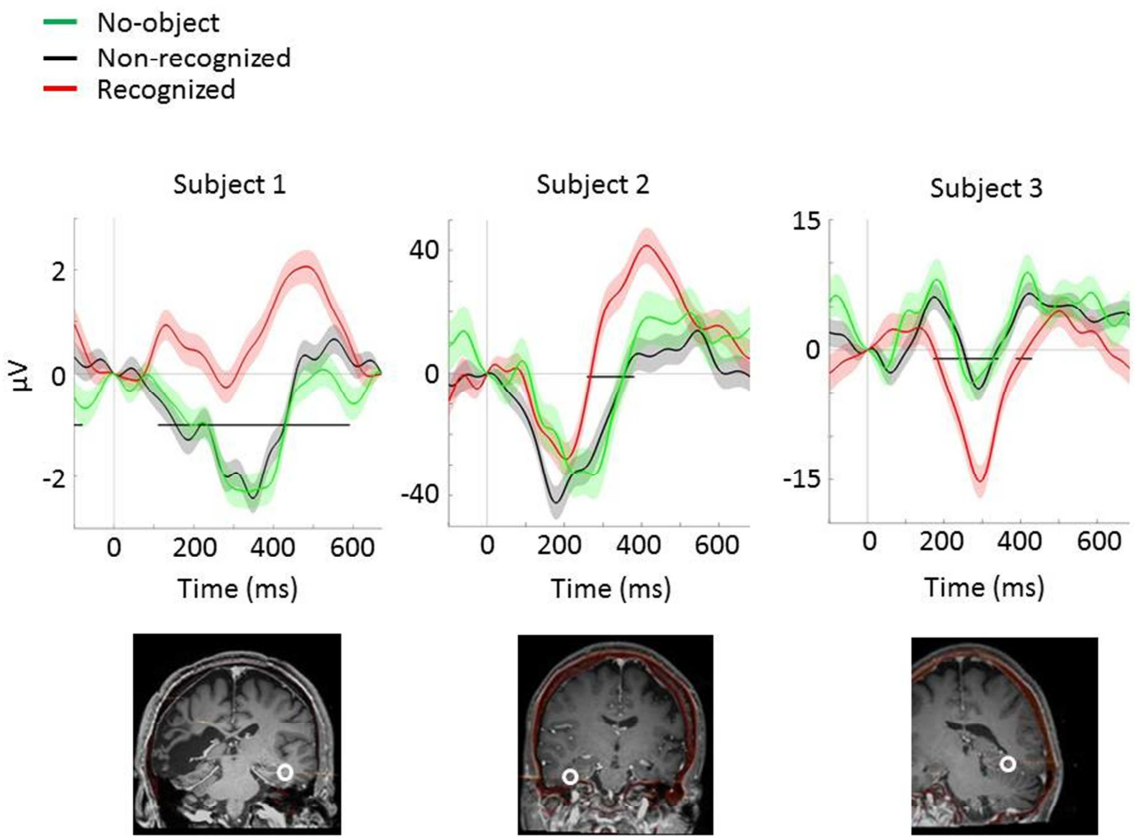

Figure 2. **ERP analysis.** ERP responses from two temporal (two first) and one occipito-temporal (last) recording sites are showed. ERP responses on semantic-selective recording sites showed significant differences ($p<0.01$, ANOVA one-way, black underscore line) between recognized object (red-line) and no-object trials (green-line). No significant differences were found between non-recognized (black-line) and no-object trials (green-line). Note that the fact of finding significant responses in the ERP responses alone is trivial since it is expected from our selection criterion. However the latency of these responses is not trivial and can be informative regarding the temporal sequence of activation in the areas supporting conscious recognition.

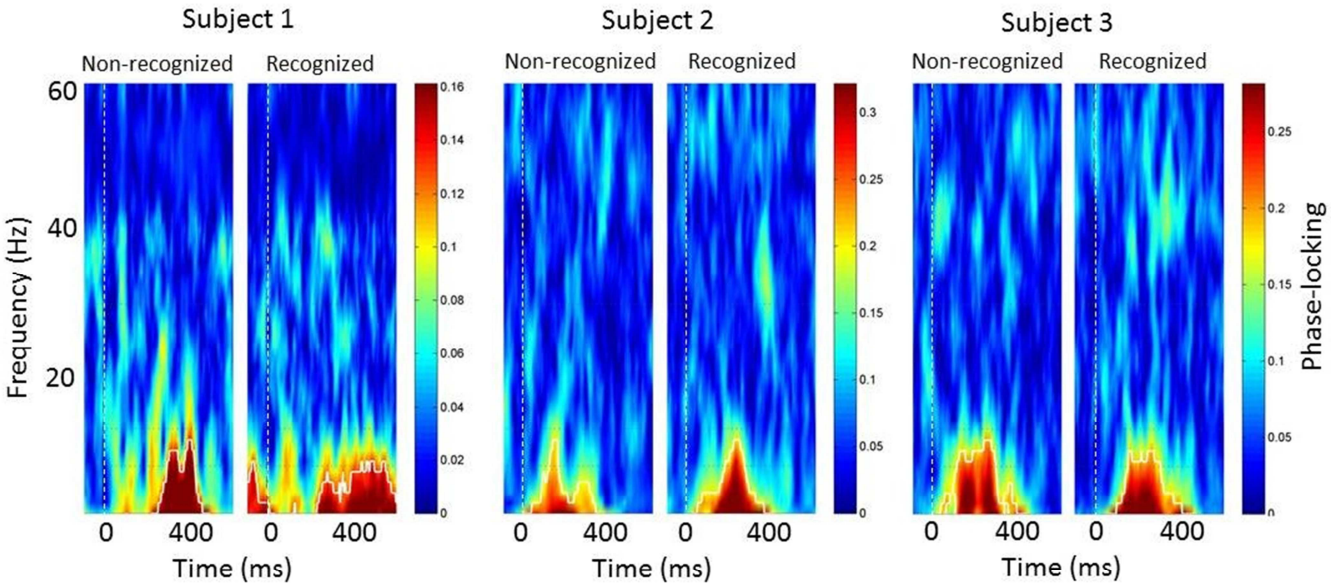

Figure 3. **Phase-locking across cycles (external synchrony) analysis.** Time-frequency maps showing phase-locking values before and after recognition for the same recording sites showed in figure 2. Significant phase-locking values (Monte Carlo simulation 10^6 iterations, taking into account the number of cycles recorded) are outlined by a white line. Note that while significant phase-locking values at the tagging frequency and its second harmonic (up to 3 Hz) are trivial because it corresponded to the selection criterion of recording sites, significant phase-locking at higher frequencies (beyond 3Hz) denote internal synchronization induced by the semantic onset. One can see that phase-locking was moderately greater in the recognized condition than in the non-recognized condition.

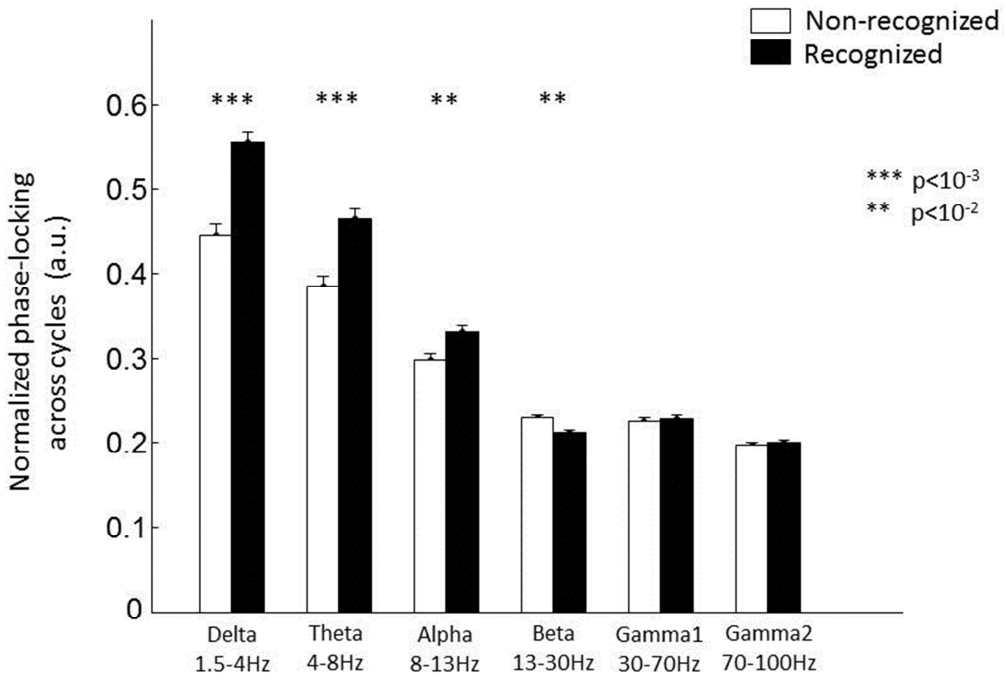

Figure 4. **Phase-locking across trials (external synchrony) as a function of recognition at different frequency bands.** Phase-locking time-frequency maps were averaged across the time dimension and different frequency bands were selected (delta 1.5-4Hz, theta 4-8Hz, alpha 8-13Hz, beta 13-30Hz, low-gamma 30-70Hz and high-gamma 70-100Hz). Phase-locking from different electrode sites (n=18) was normalized across subjects in order to compare phase-locking values obtained with different numbers of trials. Highly significant differences between recognized and non-recognized conditions were found in theta, alpha and beta bands (Note that significant phase locking in the delta range is trivial because it was used as the selection criterion). While phase-locking was stronger after conscious recognition in the theta and alpha range, this pattern is reversed in the beta range.

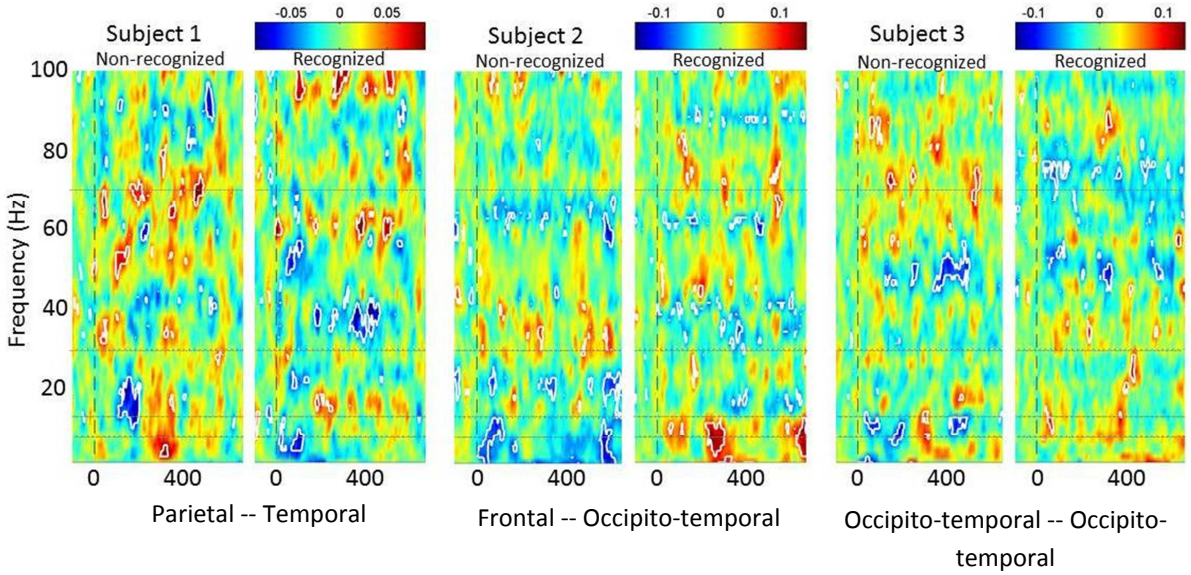

Figure 5. **Inter-electrode (internal) synchrony.** Time-frequency analysis showing the modulations in phase-locking relative to the baseline (from -100 to 0 after semantic onset) between representative electrode pairs for each subject before and after recognition. For subject 1, phase-locking modulations between a left parietal and a right temporal electrode are shown. For subject 2, phase-locking modulations between a frontal and an occipito-temporal contact, both from the left hemisphere, are shown. For subject 3, phase-locking between two contacts from a left occipito-temporal electrode are shown. Outlined areas show significant modulations of phase-locking ($p<0.01$, Monte Carlo simulation, see Materials and Methods for details).

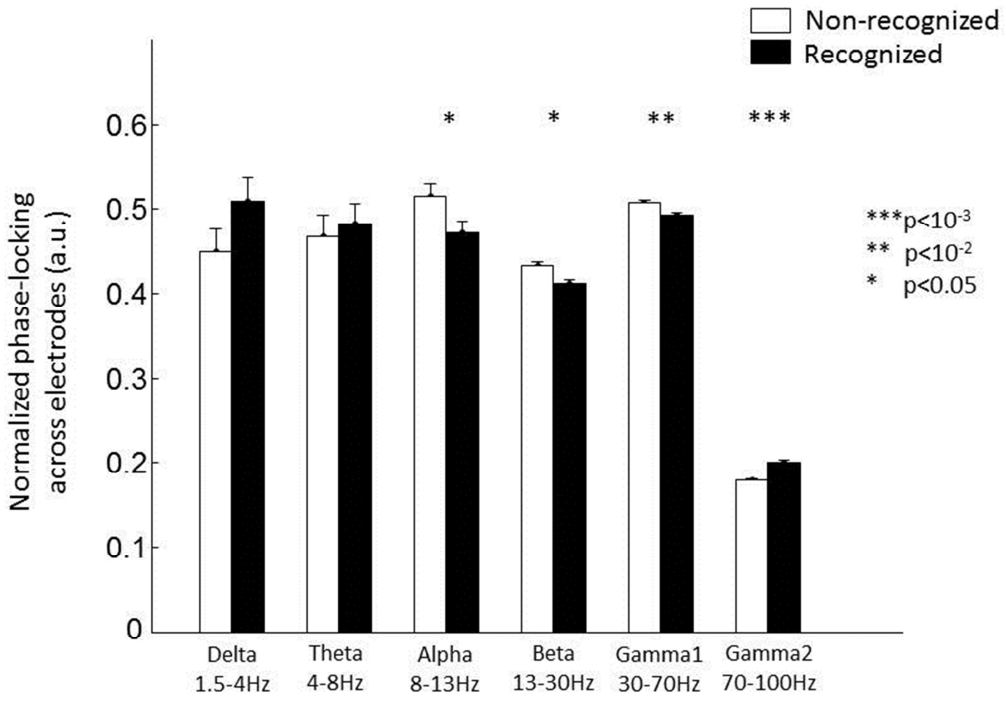

Figure 6. **Phase-locking across electrodes (internal synchrony) as a function of recognition at different frequency bands.** Phase-locking time-frequency maps were averaged across the time dimension and different frequency bands were selected (delta 1.5-4Hz, theta 4-8Hz, alpha 8-13Hz, beta 13-30Hz, low-gamma 30-70Hz and high-gamma 70-100Hz). Phase-locking from different electrode pairs was normalized across subjects in order to compare phase-locking values obtained with different numbers of trials. Significant differences between recognized and non-recognized conditions were found in alpha, beta, gamma1 and gamma2 bands, while no significant effects were found at lower frequencies. Phase-locking between electrodes was smaller after recognition in alpha, beta and gamma1 ranges, denoting inter area de-synchronization after recognition, while in the gamma2 range, recognition elicited synchronization among areas.

II. REPORT 2. Koenig-Robert, Collet, Fize & VanRullen.

All-or-none feedback activity as a correlate of conscious object recognition revealed by SWIFT in monkey ventral visual areas.

Roger Koenig-Robert, Anne-Claire Collet, Denis Fize and Rufin VanRullen

Recurring activity in visual areas has been argued to have an essential role in conscious object recognition. However, this has been hard to prove, mainly due to the difficulty in dissociating low-level feature extraction from the actual object recognition activity. We used an innovative technique called semantic wavelet-induced frequency-tagging (SWIFT), where cyclic wavelet-scrambling allowed us to isolate neural correlates of the semantic extraction from low-level feature processing of the image. Electrocorticogram (ECoG) electrodes placed intracranially over ventral visual areas from V2 to TEO allowed us to record neural activity with both high temporal and spatial resolution. One macaque monkey was trained to perform an animal/non-animal categorization task. In each trial a SWIFT sequence containing either a target (an animal) or a distractor (a landscape, object or meaningless texture) was presented. The monkey reported the presence or absence of a target by a go or no-go manual response respectively. In each session, one third of the trials corresponded to new images, making the task quite challenging (64% correct responses on targets). Event-related potential (ERP) analysis of local sources revealed that correctly recognized targets elicited two ERP components in ventral visual areas. A first positive (P1) component, representing the feedforward sweep, peaked between 100 and 200 ms; while a second positive (P2) component, representing recurring reactivation, appeared from 200 ms after the semantic onset. The P1 component was present whether the target was recognized or not and its amplitude was modulated by stimulus category (low amplitude for meaningless texture distractors, medium amplitude for object distractors and high amplitude for animal targets). On the other hand, the P2 component was only present when the target was recognized, but totally absent otherwise (either

when the target was not recognized, or when a distractor was presented); we controlled that this component was not related to motor response. Thus, P2 was modulated in an all-or-none fashion by conscious target recognition. Importantly, the same P2 modulation was observed when comparing responses to the same image before and after the monkey learned to recognize it as a target, demonstrating that the P2 component is a specific feature related to conscious target recognition. By using SWIFT we were thus able to demonstrate that recurring reactivation of visual areas is necessary for conscious object recognition, a key prediction of the Global Neuronal Workspace model.

Methods

Stimuli generation. We used an innovative technique called SWIFT: semantic wavelet-induced frequency-tagging, which uses manipulations in the wavelet domain to create a movie from a single natural image (Koenig-Robert & VanRullen, submitted). Each frame of the movie equalizes low-level properties of the natural image while modulating its high- and mid-level information content cyclically at a fixed temporal frequency, called the tagging frequency. As a result, visual processing mechanisms that are sensitive to the low-level properties should be equally engaged by all frames of the movie, exhibiting a flat response during the presentation. On the other hand, the higher-level mechanisms responsible for extracting semantic information would come into play periodically around the onset of the original image. By analyzing changes of the neural activity at the tagging frequency it is thus possible to isolate activities supporting high-level visual representations. Details of the stimulus construction are explained elsewhere (Koenig-Robert & VanRullen, submitted). Briefly, SWIFT movies were created by cyclic wavelet scrambling in the wavelets multi-scale domain. At each location and scale, local image contours were represented by a 3D vector in the wavelets space, with the 3 dimensions representing the strengths of horizontal, vertical and diagonal orientations. For each location and scale, two new vectors with random orientations but the same length were defined. The unique isoenergetic circular path

described by the 3 vectors was used to modulate local contour orientation cyclically, thus obtaining different wavelet-scrambled versions of the image, while conserving low-level properties (local luminance, contrast and spatial frequency) across frames.

Behavioral task. One male rhesus monkey (*Maccaca mulata*, aged 19 years, 12 Kg) was used in this study. The animal was an expert in fast animal/non-animal categorization task on natural images. The monkey was trained to perform a go/no-go task to categorize briefly flashed natural scene pictures as containing (or not containing) animals. The animal gave its response by touching the screen as fast as possible (go response) when a target (i.e., an animal picture) was showed, while ignoring the stimuli when they contained a distractor (no-go response). A total of 10 training sessions were necessary in order to adapt the monkey to respond on SWIFT movies and to lengthen trials in order to present up to 3 SWIFT modulations cycles within a trial. On these sessions, familiar stimuli used in previous experiments were presented either as a steady image or modulated under SWIFT. During the training sessions, we lengthened the trials from 100 to 2400 ms while increasing the percentage of SWIFT trials from 0 to 100%. In the experimental sessions (n=21), each trial consisted in the presentation of a SWIFT movie modulated at 1.4894 Hz during 2400 ms. Target trials consisted in SWIFT movies containing an animal natural image (50% of trials) and distractor trials could contain either a landscape or a manmade object image (25% of trials) or an abstract texture (25% of trials). The monkey could give its response anytime during the trial. Correct responses (go-responses to animals or no-go responses to distractors), were rewarded by juice or water drops which were provided at the end of the trial. Incorrect responses (no-go responses to animal or go responses to distractors) were punished by showing the steady image during 1.5 seconds. In each session 60 different SWIFT movies were shown. Twenty of them corresponded to new stimuli, 20 to recent ones (i.e., showed in another session) and 20 to familiar ones (well-known stimuli used in the training sessions). Each one of these images was presented repeatedly during each session, in a semi-random manner. Each session started with 20 trials of familiar stimuli, followed by 600 trials in which new, recent and familiar stimuli were equally represented. In case the monkey performed more than 620 trials, familiar stimuli were shown. In each session, the monkey performed from 300 to 1000 trials (mean ~400 trials), during about 1 hour. All

procedures conformed to French and European standards concerning the use of experimental animals; protocols were approved by the regional ethical committee for experimentation on animals (agreement ref. MP/05/05/01/05).

Electrocorticogram (ECoG) acquisition and data processing. Fourteen intracortical electrodes were implanted over ventral visual areas from V2 to TEO including 2 frontal electrodes, one of them used as the reference, yielding 13 recording sites. Electrode positions were estimated by overlapping the CT-scan of the implanted animal over a standardized monkey atlas. Continuous ECoG was acquired from 13 intracranial electrodes using a NeuroScan device. All signals were digitized at 1000 Hz, 24-bit A/D conversion and high-pass filtered at 0.15 Hz. The data were analyzed off-line under Matlab (MathWorks) using the EEGLAB toolbox (Arnaud Delorme & Makeig, 2004). Data was downsampled at 500 Hz and low-pass filtered at 20 Hz. DC offset was removed from continuous EEG data.

Event related potentials (ERP) analysis. Each SWIFT cycle period (from -100 to 671 ms) was taken as an epoch, in which zero-time represents the onset of the frame that contains all the semantic information (i.e., the frame containing the unscrambled image). ERP epochs were sorted by category (i.e., targets and distractors) and response (i.e., correct and incorrect). Linear detrending correction was performed in order to ensure that potentials at times 0 and [1/tagging frequency] were 0µV.

Results

Behavioral results. Global accuracy on targets was 64%, while on objects and no-object distractors was 89% and 78% respectively. Accuracy for new images was at 48% on targets and 82% and 81% for object and no-object distractors respectively. This shows that the task was quite difficult for new targets.

Early ERP (P1) component. We used an event-related potential (ERP) analysis to measure the cortical local potentials locked to the onset of the semantic information—the time when the non-scrambled picture was on the screen—which was taken as the zero-time. Each

SWIFT modulation cycle was thus taken as an epoch. We only analyzed new images, where the ERP responses were stronger than in familiar and recent ones (data not shown). A positive ERP component (P1) was elicited by all three trial categories: no-object (Figure 2a, green line), recognized targets (Figure 2a, red line) and non-recognized targets (Figure 2a, black line). This P1 component peaked between 100 and 200 ms after the semantic onset. Even though the presence of the P1 component was independent of the category of the stimulus (i.e. target or distractor), its amplitude was modulated both by the object category and the response of the monkey: small amplitude for no-objects (Figure 2a, green line), mid-amplitude for non-recognized targets (Figure 2a, red line) and false alarm object distractors (Figure 2b, blue line), and higher amplitude for recognized targets (Figure 2a, redline). Significant differences ($p<0.01$, one-way ANOVA, red underlying line, Figure 2a) between no-object trials and recognized targets were found in 11 out of 13 contacts (one electrode in V4 and the frontal electrode did not show significant differences). Significant differences were also found between P1 amplitudes elicited by the no-object trials and the non-recognized target trials ($p<0.01$, one-way ANOVA, black underlying line, Figure 2a) in the same electrodes.

Late ERP (P2) component. A second positive component (P2) was evoked specifically by correctly recognized targets (Figure 2a, redline) and otherwise inexistent in other trial categories. The P2 component appeared from 200 ms after the semantic onset and was more sustained than the P1 component, showing an offset around 500 ms. This P2 component was present and significant ($p<0.01$, one-way ANOVA) on 8 out of 13 electrodes (two V4 electrodes, one TEO and one non-visual and the frontal electrode showed no significant P2). The P2 component was present only in correctly recognized trials, where a go-response was made, thus it is conceivable that the motor response could generate this component. Figure 2b shows false alarm object trials (trials containing an object distractor on which the monkey made a go-response, Figure 2b, blue line). No P2 component was present in those false-alarm trials even though a motor response was made. In order to verify that the P2 component represents a specific response to the target recognition and not a response related to a common feature within a subset of target stimuli, we analyzed the same new target stimuli before and after being recognized within the same session

(Figure 2c). No P2 component was present for unrecognized targets (Figure 2c, black line). However, when the same stimulus was later recognized within the session, the P2 component emerged (Figure 2c, red line). This shows that the P2 component is specific to the recognition of target stimuli.

P1 / P2 ratio across brain areas. In order to compare the relative amplitude between the P1 and P2 components across brain areas, we normalized the ERP responses to recognized targets relative to the P2 component, for the new images (Figure 3). We can see that the ratio between P1 and P2 amplitude decreases as the electrode is located in higher-level areas. This shows that the P1 component is more important in lower-level areas, suggesting that this activity is related to sensory driven activity. The P2 activity, on the other hand, tends to be more important in higher level areas indicating recurring activity originating in high-level areas.

Discussion

These preliminary results are very promising and point out the capacity of SWIFT in confirming key predictions of the Global Neuronal Workspace model of consciousness. SWIFT was efficient in dissociating lower-level processes involved in extracting the features necessary for categorization (represented by the P1 component) and the actual neural correlates of conscious object recognition (represented by the P2 component).

A first positive ERP component (P1) was common to all categories, representing the first wave of activation of the visual system. Interestingly, this component was modulated by both object category and the monkey response: low amplitude for meaningless distractors, mid amplitude for missed targets and false alarms in distractors (with a slight stronger response on the latter, see Figure 2b, V2) and the strongest responses for the recognized targets. These results suggest that the P1 component is modulated by relevant visual features for the task at hand, in this case, detecting an animal. In this manner, the relative content of animal features within the stimulus categories would modulate the P1 amplitude, because these features are expected to appear in order to perform the task, and could be amplified by selective attention. Comparisons between the same stimuli before and after its

conscious recognition (Figure 2c) revealed that even for the same set of animal features contained in those stimuli, there was a slight increase in the P1 amplitude after conscious recognition (although not significant) which could be due to a selective tuning for the features contained in the newly recognized targets.

Since the monkey was explicitly trained for many years to recognize animals as targets and to ignore the distractors, it is probable that if he can generate any conscious representation of visual stimuli, these stimuli would likely be animals. This is supported by the fact that a selective neural correlate—the P2 component—was only found when animals were recognized but not for false alarms. What happens with the neural representations of distractors then? We believe that these stimuli are not consciously recognized as such (i.e., the monkey has not been trained to explicitly recognize cars or manmade objects and perhaps he does not assign any semantic value to them: they would be as meaningless as the abstract textures are for us). Then, as the monkey has been trained to perform rapid categorization, it is likely that he mostly uses the first available visual information which is contained in the P1 wave. We believe that the P1 wave represents non-conscious rapid processing and in the case that the stimuli is a recognized animal, a second wave—the P2 component—would emerge, representing a switch in the internal state of the monkey's brain from non-conscious to conscious visual processing. This component is thus likely to represent feedback activity and, interestingly, it has an all-or-none behavior as predicted by the Neuronal Global Workspace theory (Stanislas Dehaene et al., 2003); (Del Cul et al., 2007).

The Neuronal Global Workspace model inherits its general concepts from the Global Workspace theory from (Baars, 1990). It was successfully used in order to describe non-linear access to consciousness observed in attentional blink (Stanislas Dehaene et al., 2003); (Sergent et al., 2005), inattentional blindness (Stanislas Dehaene & Changeux, 2005), and backward masking (Del Cul et al., 2007). This model explains the all-or-none access to consciousness as the result of a phenomenon composed by two steps. First, a burst of activity in early visual areas is needed—which would be represented by the feedforward sweep—which carries sensory information from peripheral to higher areas. Second, a subsequent step of amplification of perceptual processing comes into play. Sustained activity driven by recurrent cortical loops is established. This would lead to interactions across

distant brain regions, creating a functional network (i.e., the global workspace) that would allow broadcasting information among several areas, which would support conscious perception (Stanislas Dehaene et al., 2003); (Stanislas Dehaene & Changeux, 2011).

This model predicts that while the first activation (represented by the feedforward sweep) varies linearly with the amount of relevant visual features in order to perform the task at hand (i.e., this can be modulated by the strength of masking of targets (Del Cul et al., 2007)), the second wave of activation (representing feedback from higher areas) should be modulated non-linearly (i.e., in an all-or-none fashion) by conscious perception. This is exactly what we found in the ECoG results on monkeys: while the P1 component is modulated by object category, the P2 component has an all-or none behavior depending on target recognition. Interestingly, this model also predicts that the ratio P1/P2 would decrease along the visual hierarchy due to the fact that sensory areas generate the P1 component, while high-level areas, including the frontal cortex would trigger the P2 component. This was also verified in our results, as seen in Figure 3, where the ERP were normalized to the P2 peak.

All in all, the present preliminary results extend the Neuronal Global Workspace model to object recognition tasks and suggest that the neural mechanisms that would support conscious perception are present in macaque monkeys.

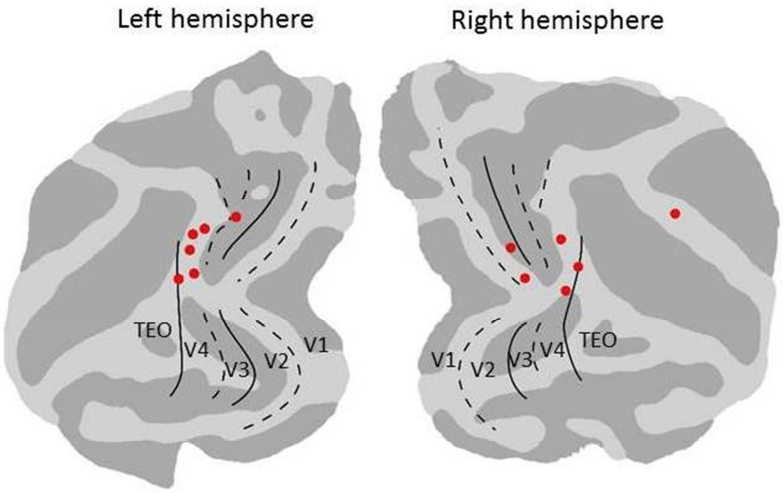

Figure 1. **Electrode implantation.** Electrode positions were estimated based on a CT scan showing the electrode positions over the scalp. These positions were related to putative functional areas using a standardized macaque brain atlas. Fourteen electrodes were placed on occipito-temporal, temporal and frontal areas. Among these electrodes, two electrodes were placed over the right V2 cortex. One electrode was placed on the left V3 cortex. A total of 6 electrodes were placed over the V4 cortex (4 in the left hemisphere and 2 in the right hemisphere). Two electrodes (one over each hemisphere) were placed at the border between V4 and TEO and were classed as TEO electrodes. One electrode was placed anteriorly with respect to the superior temporal sulcus (STS) and thus over cortical areas belonging to non-visual areas. Two more electrodes were implanted in the right frontal cortex and one of them was used as reference.

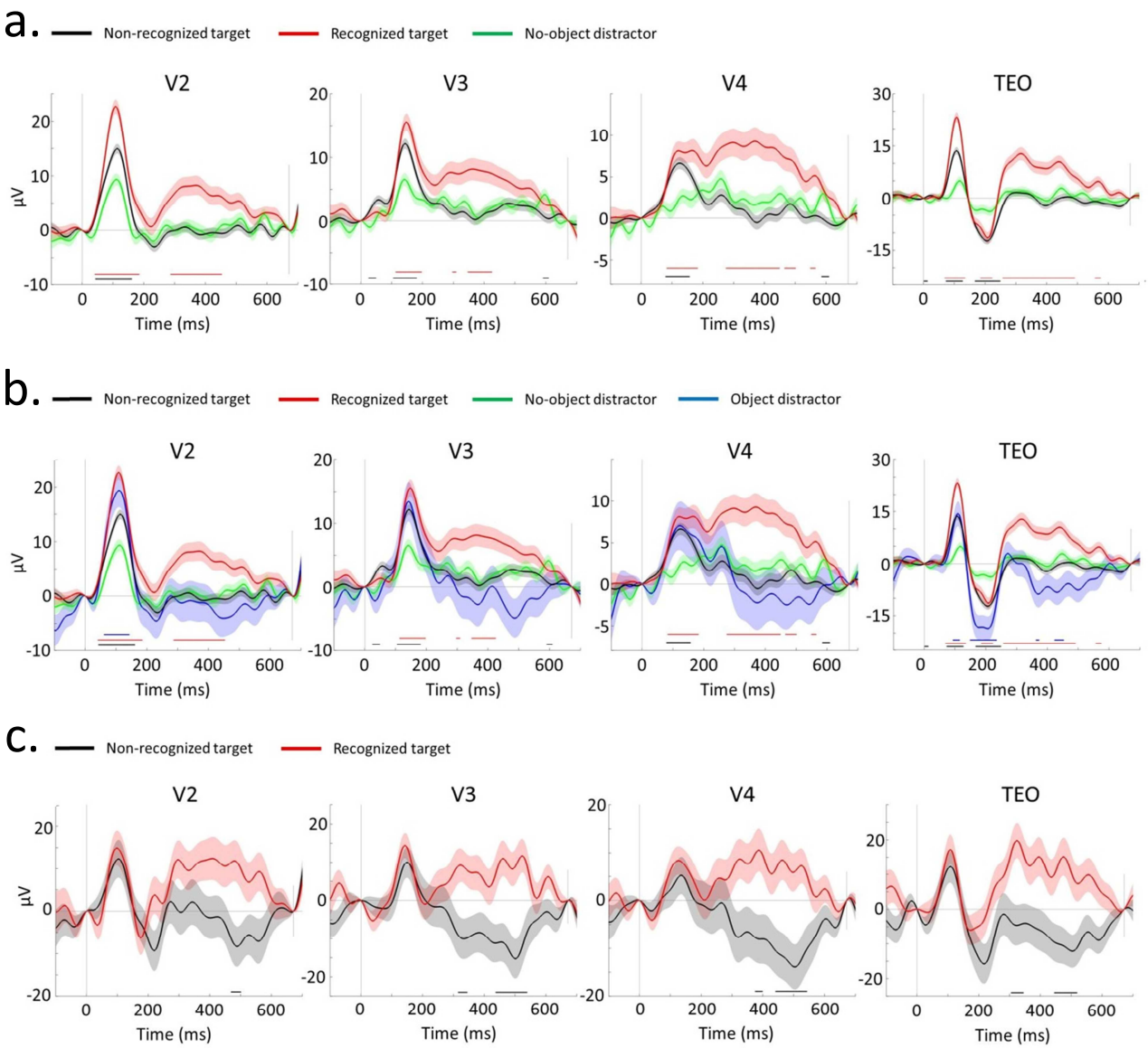

Figure 2. **ERP responses as a function of conscious recognition on ventral visual areas. A. ERP responses for new images.** The green line represents no-object trials, the black line represents non-recognized targets and the red line represents recognized targets. While a first positive potential (P1) is present across all trial categories, a second positive potential (P2) is only present in recognized targets. Significant differences ($p<0.01$, ANOVA one-way) between no-object and non-recognized trials are marked with a black line, while significant differences between no-object and recognized trials are marked with a red line. **B. False alarm responses.** False alarms on object trials (object distractor trials where a go-response was made) are superposed (blue line) on the same ERP traces showed in A. No P2 component is present in these trials, ruling out the possibility that the P2 component were

generated by motor activity. **C. ERP response for the same target stimuli before and after their recognition.** Unrecognized targets did not evoke any P2 component, however the P2 component was present when the same stimuli were recognized later in the session, showing that the P2 component is specific to target recognition.

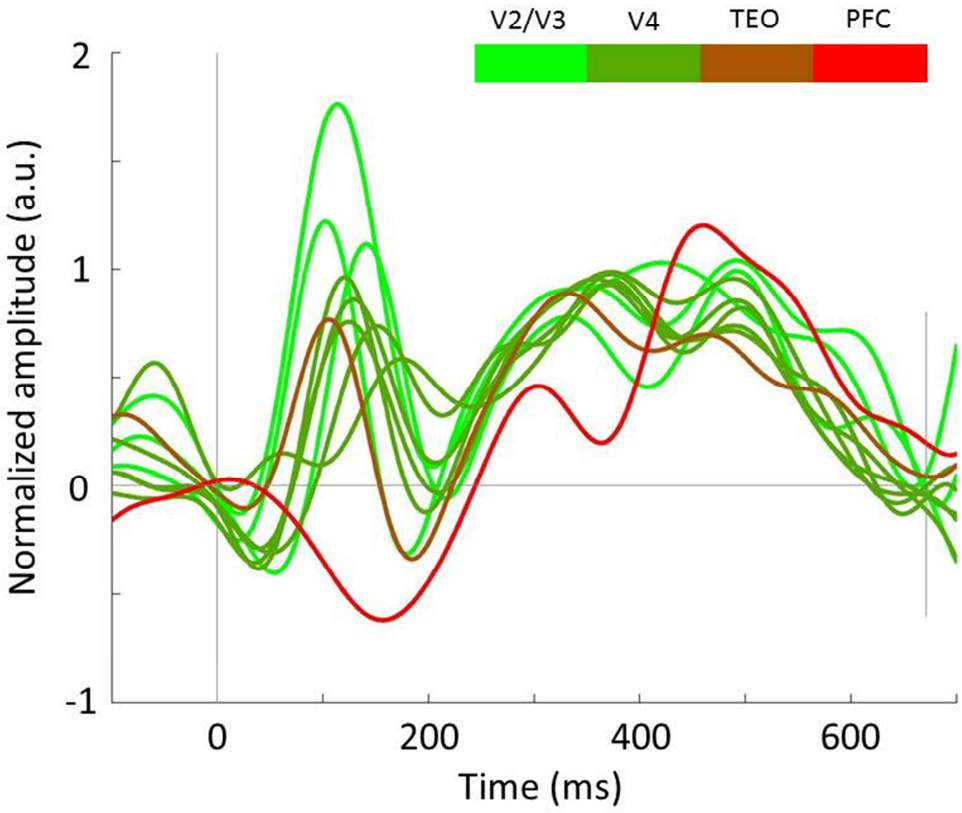

Figure 3. ERP normalized responses for recognized targets on P2 containing electrodes. Electrodes showing a significant P2 component (except for the frontal electrode—red line, where the P2 was not significant) were selected and normalized relatively to their P2 amplitude. Electrodes from earlier visual areas have greater P1/P2 ratios than in higher areas, in accordance with the Neuronal Global Workspace theory.

G. General discussion

I. Recapitulation

We have explored the visual system from categories to awareness. We presented six different works in which diverse questions were addressed at different levels of the visual system, using two different models: monkeys and humans and using both behavior and neural activity recordings (Figure 28). Along this quest, we found answers to the abovementioned questions which represent new contributions to the field (Figure 28). We will recapitulate the most significant conclusions derived from the presented works.

In the first work, we addressed the question of whether ultra-rapid categorization can be performed efficiently for both monkeys and humans when the low-level attributes of the image (namely the Fourier amplitude spectrum) are equalized across categories. We used a saccadic choice task in both monkeys and humans. We found that the fastest reaction times were practically unaltered when compared with other studies were no equalization was used (Girard et al., 2008; Kirchner & Thorpe, 2006). However, taking in to account the global performance, hit rates were significantly degraded for equalized images when compared with studies using intact images. This is explained by the degraded aspect of equalized images and also by the choice of difficult distractor images. Interestingly, in a second experiment we correlated the performance in categorizing a given image with its quality of being recognizable when only its low-frequency spectrum was preserved. This result suggest that the spatial arrangement of low-frequencies in an image is an important feature used by the visual system to perform ultra-rapid categorization, and also points out an involvement of the magnocellular pathway in the processing of visual information.

In the second work we addressed the question of whether the spatial pattern of both exogenous and endogenous spatial attention evolves across time in human subjects. We used a detection task involving a unique cueing paradigm where the background contrast was equalized in order to take into in account the effects of attention, with the aim of creating detailed maps of the spatial deployment of attention as a function of time. We

found that the spatiotemporal map of exogenous attention showed a significant enhancement zone from 150 to 430 ms, extending up to 6° from the cue. For endogenous spatial attention, a peak at the cued side at 400 ms and between 8 and 10° from the cue was found in the spatiotemporal maps. The results from the spatiotemporal maps were well explained by a model of null spatiotemporal interaction, suggesting that the spatial pattern of attention deployment does not change across time and only modulates its amplitude.

In the third work we developed a new stimulation paradigm called SWIFT which equalizes the low-level attributes of an image and modulates its sematic content cyclically. Using this paradigm, we explored its possibilities in tracking high-level visual representations in human subjects. SWIFT was developed using an approach involving image scrambling in the wavelets-domain in combination with frequency-tagging. In a first experiment, using a recognition task, we successfully isolated the neural correlates of conscious object recognition with no need to apply subtractive approaches: non-recognized objects simply did not evoke significant activities over centro-parietal electrodes. In a second experiment we manipulated spatial attention deployed over frequency-tagged face pictures and discovered that attentional effects were tracked more effectively by using SWIFT than with the classic frequency-tagging approach. In a third experiment we tested the temporal limits of SWIFT and we could conclude that a maximum of between 4 and 7 conscious object representations can be produced by the visual system.

In the fourth work we addressed the question of whether, by using SWIFT, we can track visual consciousness when it is modulated between all-or-none states (i.e., between visibility and invisibility). In order to do so, we used the binocular rivalry paradigm in combination with SWIFT in human subjects. We found that frequency-tagged signals evoked by SWIFT were modulated in an all-or-none fashion, just as their phenomenal counterpart. This represents the first time that conscious related activity is isolated from global brain activations. Using these ‘pure conscious’ signals we studied the properties of these signals. Is activity supporting conscious states characterized by an augmentation of the signal amplitude or are they better explained by an increase in synchrony? We found that an increase in synchrony, specifically the temporal consistency of brain signals across presentations, and not an increase in signal amplitude accounted for the conscious states.

In the fifth work we reproduced the conscious recognition experiment using SWIFT on patients implanted with intracranial electrodes which allows obtaining brain activity recordings with both high spatial and high temporal resolution. We addressed the question of how different types of synchrony support conscious object recognition in different frequency bands. We found that brain activity in several regions of the visual cortex and beyond significantly synchronize their activities with the stimulus presentation when an object was recognized at the theta and alpha frequencies but a de-synchronization was revealed at the beta frequency. When we studied the synchrony among brain areas, we found that object recognition elicited a de-synchronization at the alpha, beta and low-gamma frequencies, but an increase of synchrony was shown at high-gamma.

In the sixth work we addressed the question of whether the electrophysiological features of object-recognition could be found in macaques. We adapted the recognition task for a monkey trained in rapid animal/non-animal categorization. We found that feed-back activity registered on electrodes of the ventral visual pathway was present only when targets were correctly recognized. The ERP patterns effectively corresponded to the predictions from the Neuronal Global Workspace model.

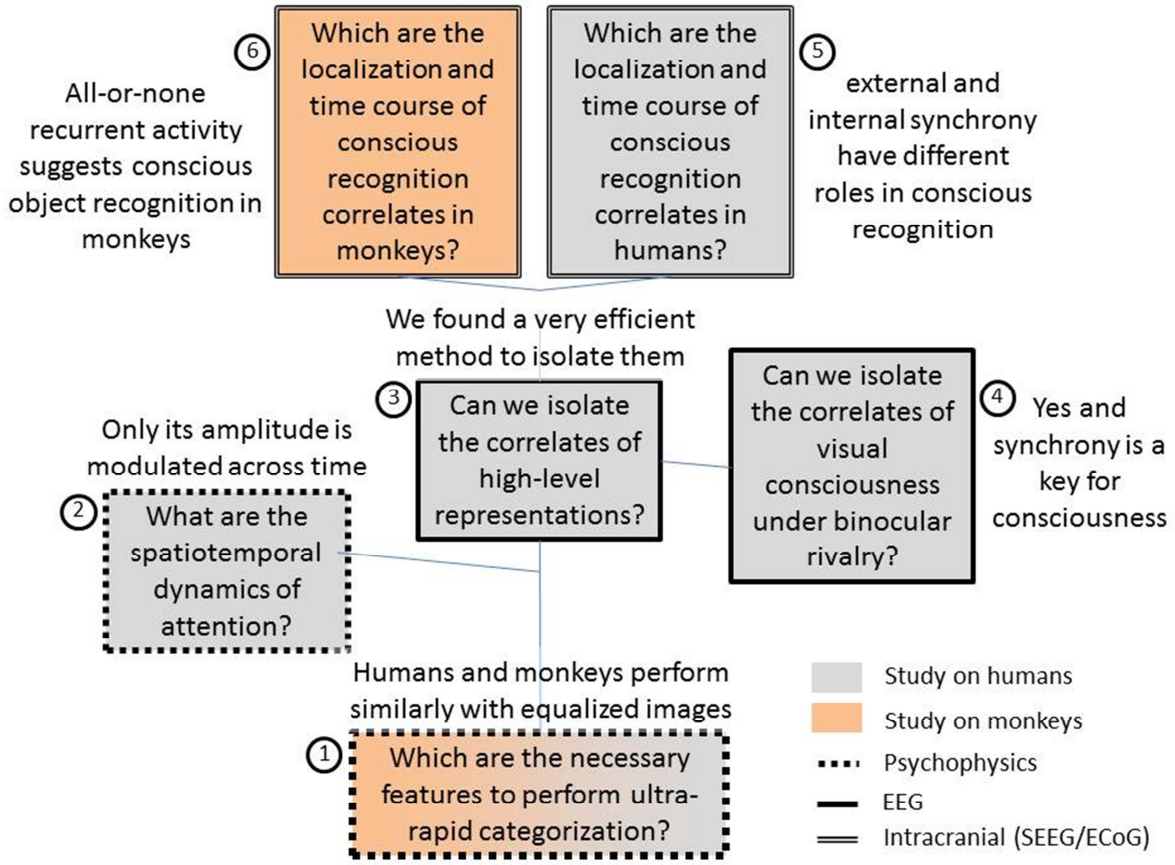

Figure 28. Scheme of the works presented in the thesis summarizing the most relevant results of each study in a concise statement.

II. On the relationship between ultra-rapid categorization and conscious object recognition

Ultra-rapid categorization corresponds to an extremely time-efficient mechanism allowing rapidly exploiting the visual information in order to sort images according to arbitrary semantic categories despite their physical differences. One widely accepted proposal is that categorization can be performed on the basis of diagnostic features, without the need of processing all visual information (Gosselin & Schyns, 2001 ; Ullman et al., 2002; Schyns, Gosselin, & Smith, 2009; Wang et al. 2011). These features can be extracted and represented explicitly in early stages of visual processing. In the specific case of faces, it was argued that diagnostic information could potentially be extracted very early in the visual hierarchy, possibly as early as V1 and V2 (Crouzet & Thorpe, 2011), being thus available within the first stages of the feedforward sweep.

Our behavioral results in ultra-rapid categorization are compatible with a view where incomplete representations of visual objects would suffice to perform rapid categorization. However, our results showed that ultra-rapid categorization does not exclusively rely on the mean Fourier spectrum. Even though performances decreased with amplitude-spectrum equalized images, the minimum reaction time remained comparable with previous results (100 ms for monkeys and 140 ms for humans). Based on a second experiment in which the performance on a given image was correlated with its capacity of being recognized when only its low-frequency content was presented, we conclude that the necessary features to perform ultra-rapid categorization are likely to be included within this coarse version of the images. All in all, these results are compatible with the idea that complete object representations would not be necessary to perform ultra-rapid categorization and a coarse summary of the relevant features contained (represented by the low-frequency information contained in the image) would suffice to perform the task. However, these features would be more complex than the mean frequency spectrum.

In the literature there are numerous reports suggesting that this process can be done with little attention (Li et al., 2002) and non-consciously (Boucart et al., 2010), suggesting that conscious recognition would be a further step in the visual processing. Our work in

implanted macaques has suggested dissociations between visual categorization and conscious object recognition. We have seen that categorization seems to depend on the first positive component (P1) peaking between 50 and 150 ms and corresponding to the feedforward sweep, which amplitude is modulated by the object category, while conscious perception of the target seems to be associated with a second positive wave (P2). This P2 component represents recurrent activation on visual areas, said otherwise, a feedback activation driven relatively later in the visual processing. This latter activation was compatible with the P3 wave recorded in humans with EEG. Another piece of evidence supporting the idea of the implication of the P2 in conscious recognition is represented by the fact that the pattern of activation across ventral areas was compatible with the Neuronal Global Workspace model which predicts non-linear dynamics in the activations supporting conscious perception.

Thus I propose that rapid categorization processes represent a preliminary step in the path leading to conscious object recognition. Rapid categorization would rely on incomplete information of the scene, carried in the feedforward sweep, while conscious object recognition would rely on global feedback reactivation of distributed brain areas that would allow the interaction of different bits of visual information represented by different areas in the visual pathway.

Our study revealed that the features used by humans and monkeys are quite similar, suggesting that rapid visual categorical mechanisms would be conserved in evolution due to their adaptive value. Ecologically, this process is important in order to react rapidly to environmental threats. Rapid categorization is specially needed when the visual system cannot wait to produce a conscious representation (which may be accessed tardily), in situations where important behavioral decisions have to be triggered rapidly. Based on our results it seems that conscious perception need a non-negligible amount of time (at least 200ms), and it thus seems to quite expensive in temporal terms. Perhaps the brain is quite prepared to deal with sensorial information and prepare behavioral responses without any conscious sensation. Due to the slow activation dynamics of consciousness, it may not directly guide our behavior as often as we think and only would be used when is necessary.

III. On the relationship between attention and conscious object recognition

Even though the relationship between attention and consciousness is still highly debated (see for instance Christof Koch & Tsuchiya, 2007; Boxtel et al., 2010), we do believe that attention is necessary for conscious object recognition, although it is not equal to. This idea is supported by our results in the first study using SWIFT, where we manipulated spatial attention while showing frequency-tagged face images. In this experiment we showed two frequency-tagged faces on each side of the screen and a central arrow indicated the face to be attended. In a given trial the faces could be either frequency-tagged using SWIFT or classic frequency-tagging. We thus compared the amount of tagging, represented by the synchrony of brain signals with the onsets of the face—measured as phase-locking—and we compared the amount of tagging elicited by distractors (the non-cued faces) and targets (the cued faces). Besides the main finding—showing that the attentional effect was more noticeable using SWIFT than classic frequency-tagging—we found that the amount of tagging elicited by SWIFT distractors was not different ($p>0.05$) from baseline. If we consider that SWIFT elicited signals correspond to conscious representations, this result means that neural representations devoided of attention would fail to be included in the contents of consciousness.

We propose that the role of attention on conscious recognition would be causal; representing a prior step which is necessary for the activation of metastable resonant state where fragmentary stimulus representations would interact transiently. This interaction driven by attention would compel the possible set of feature conjunctions into a competitive evaluation in a sort of 'arena' represented by initial states of a Neuronal Global Workspace-like assembly. In the case that selective attention would select few features, the number of possible conjunctions would be limited and evaluation of their relevance would be made quickly, thus the winning feature conjunction would emerge rapidly. On the other hand, if attention is distributed among several features (think on the case of subjects trying to make

sense of our ambiguous SWIFT movies) the conjunction among features would be less likely to match a meaningful internal representation.

Based on our preliminary results obtained in the epileptic implanted patients, we propose a compatible model in which the activation of the metastable state by attention would by driven by modulatory feedback inputs that would increase in transient inter-area interactions at the beta and low-gamma frequency bands, which is compatible with the idea of selective attention by selective synchrony (Womelsdorf et al., 2007). This inter-area synchrony would be the neural correlate of the transient evaluation of the possible configurations within the constitutive features. This metastable state would perish soon if no stable assembly emerges, being thus promptly replaced by the next candidate assembly. Stable assemblies would entrain long-distance interactions at high frequencies and superfluous assemblies would perish.

IV. Comparing the study in binocular rivalry with the studies on conscious object recognition

All studies using SWIFT using both EEG and intracranial recordings showed specific activities that were only present in conscious states. Among all the consciousness-specific activities revealed across different experiments, the dissociations found in the binocular rivalry studies were among the clearest. This fact is easy to explain when considering the experimental conditions used in that experiment (Figure 29). I will use an extremely schematic framework to make this point. Let's say that the visual system can produce different levels of visual representations, as illustrated by the color bar in Figure 29. Let's say now that at some point of this hierarchy of different representations one can become conscious, and this point thus defines a threshold of the access to consciousness. In this manner, the visual representations below the threshold will remain devoid of any conscious quality whatsoever (including its visibility); and visual representations above this threshold can be associated with conscious experiences. In the conscious part we will distinguish several levels of conscious representations. Just crossing the threshold of consciousness, the very first level is represented by the capacity of a stimulus to be visible. Beyond this level a

visible stimulus (i.e., a stimulus already possessed at some degree in conscious realm) can be consciously recognized, that is, its semantic quality would now become conscious. The awareness of the semantic values of a stimulus can be also divided in different degrees. For example, we can either define what we see as an animal, a dog or our own dog. That supposes the emergence of more and more specific and refined conscious representations.

As far as the experiments presented here are concerned, in conscious recognition experiments the stimulus was always visible but its semantic value was either consciously accessed or not; whereas in the binocular rivalry experiment, the stimuli were either invisible or consciously recognized. In fact, our selection of faces as stimuli in the binocular rivalry experiment was motivated for the exclusive reason that faces are very easy to recognize and thus the conditions in this experiment are invisible and consciously recognized stimuli (Figure 29).

Thus activities recorded in the binocular rivalry experiment represent invisible representations (which elicited no activity) in the non-dominant condition and consciously recognized ones in the dominant condition; while in the recognition experiments the activities recorded were elicited by visible but non-recognized stimuli (which elicited measurable activity, as seen in the intracranial studies) and recognized ones.

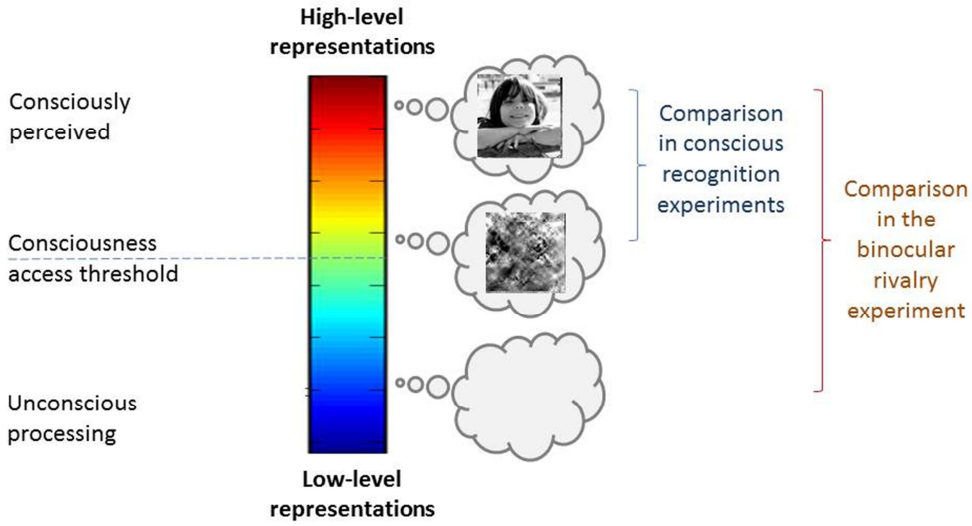

Figure 29. Schematic illustration showing different level of consciousness and their respective representations.

V. Late ERP components, phase-resetting and consciousness

We found very compelling consciousness-related effects in the late components of the ERP waveforms in all experiments performed using SWIFT. We confirmed that these effects were supported by temporal consistency of oscillatory activities across different instances of stimulus presentation, which was measured as an increase in phase locking at the tagging frequency but also at other frequency bands (see the results obtained in the binocular rivalry experiment and the intracranial recordings in epileptic patients). This increase in phase-locking represents the synchronization of the visual system with the external stimulation and was independent of an increase in amplitude of ongoing oscillatory brain signals, as showed in the binocular rivalry experiment. The latter suggests that the first requirement for a stimulus to enter to consciousness it would be a resetting of the phase of ongoing oscillations around 100ms in several brain areas. If this turns to be true, an interesting question arises regarding the role of this external synchronization. What is the role of phase-resetting? Does it set a start signal in order to allow the interaction of different brain areas at certain frequency bands? This would suppose that external synchronization would have a causal role in inter area functional connectivity, which in turn would be important for conscious perception. We found some support for this claim in the preliminary results obtained by intracranial recordings in humans, where inter-area synchrony was increased at high-gamma as a function of conscious recognition.

However, we did not obtained any conclusive result regarding the role of synchrony in the emergence of conscious perception. This is clearly a question to be addressed in future research.

VI. Conscious object recognition in humans and monkeys

Our results support the idea that macaque monkey would have access to conscious object representations. This is supported by the similarities between the results obtained using SWIFT in humans and monkeys in tasks of object recognition. In our first EEG study in humans, we found that a later ERP potential, located in centro-parietal regions and peaking after 300 ms (with an onset between 200 and 300 ms) was present only when objects were recognized. In monkeys a late ERP potential was also found when the target stimuli where correctly identified, along the ventral pathway. This ERP potential was present after 200 ms and is likely to represent recurrent activation in areas of the ventral visual stream. This late potential was preceded by an earlier positive potential, representing the feedforward sweep and which was present for all stimulus categories including meaningless ones. Moreover, the ERP amplitudes of the P1 component relative to the P2 across the visual hierarchy and the fact that the P2 component presents an all-or-none behavior are the hallmarks predicted by the Neuronal Global Workspace model of non-linear access to consciousness (Dehaene et al., 2003; Del Cul et al., 2007).

The commonalities found in the electrophysiological features related to the visual identification of objects in both humans and monkeys suggest the existence of consciousness in macaque monkeys. Further analyses will reveal if other electrophysiological features related with conscious perception such as synchrony at distinctive frequency bands are also present.

VII. Spatial localization and time course of consciousness dependent activity

Intracranial recordings in both human and macaques revealed several brain areas which showed late activities (beyond 200 ms) related with conscious perception. In the macaque, late activations (after 200 ms) along the ventral visual pathway (from V2 to TEO) were associated with conscious recognition. In implanted patients, significant activities correlated

with conscious recognition were found after 200 ms, however significant activations were also found earlier (between 100 and 200 ms). The areas showing selective responses to conscious recognition were found in occipito-temporal, infero-temporal, parietal, and frontal zones.

At this stage we do not have enough data to achieve a clear understanding about the brain areas supporting conscious perception, their profile of temporal activation and the directionality of their communication in order to support consciousness. We hope that the results obtained from more implanted patients would give us the necessary understanding to draw a more complete picture regarding these phenomena.

VIII. How does sense emerge in the visual system?

This last part is devoted to discussing a speculative model aimed to explain how sense emerges in the visual system. This model has no great pretentions and is intended to have some explicative and integrative value concerning the results presented in this thesis as well as to introduce some tentative hypothesis to be tested in future research. Following the classification of theories introduced by Sir Roger Penrose (in which we distinguish among: superb, useful, tentative and misguided), at this point this theory only aspires to a tentative status.

In the model, a first step is represented by extraction of visual features within the feedforward sweep (Figure 30a). At this stage, quite raw and incomplete stimulus representations emerge within visual areas. The sense of the visual information represented at this point consists in the content of coarse visual features in the stimulus, represented in Figure 24 as ‘legs’, ‘face’ or ‘horns’. Nevertheless, these incomplete stimulus informations can be certainly sufficient to diagnose the presence or absence of a category (animal/non-animal) and could guide some forms of simple behaviors such as saccades or go-responses, all this in a feedforward manner and pre-consciously. Such processing would be exploited by rapid categorization experiments.

A second step would depend on the presence of attention (Figure 30b). Attention would select and enhance some of these incomplete stimulus representations and it would introduce them in a process of active feature conjunction formation where different transient versions of joint features would compete for the access to consciousness. Note that this stage is compatible with a Global Workspace architecture where different representations would compete to invade the workspace (Dehaene et al., 1998; Dehaene et al., 2003; Dehaene et al., 2006; Shanahan, 2010). This step represents an attempt to integrate several visual features that emerge in different visual areas at different moments. In this process the role of attention is also necessary to organize and maintain the feature conjunctions which are not explicitly coded by a neural population. At this point, no definitive conjunction of features has been selected, and despite the fact that the current visual representations are quite well integrated, the informativeness of this state is limited since the number of possible conjunctions leaves the perceptual output undetermined and thus the current representation is not differentiated. According to the dynamic core theoretical framework which proposes that the fundamental properties of conscious representations are differentiation and integration (Edelman & Tononi, 2000; Tononi, 2004), this state could not be consciously experienced, since one of the fundamental properties of conscious representations (differentiation) would be missing.

A third step in this model is marked by the selection of a unique conjunction of visual features and its entrance to phenomenal access (Figure 30c). The entrance of the winning feature conjunction to consciousness would be associated with an increase of inter-area synchrony at high-gamma, which would stabilize for a while these metastable representations by inter-area resonance at high-frequencies. At this step, massive recurrent activation of several brain areas is triggered and the phase of ongoing oscillations is reset, which can be seen by an increase in phase-locking. At this stage, the selection of a specific conjunction among several visual features represents integration and informativeness, since many options have been ruled out.

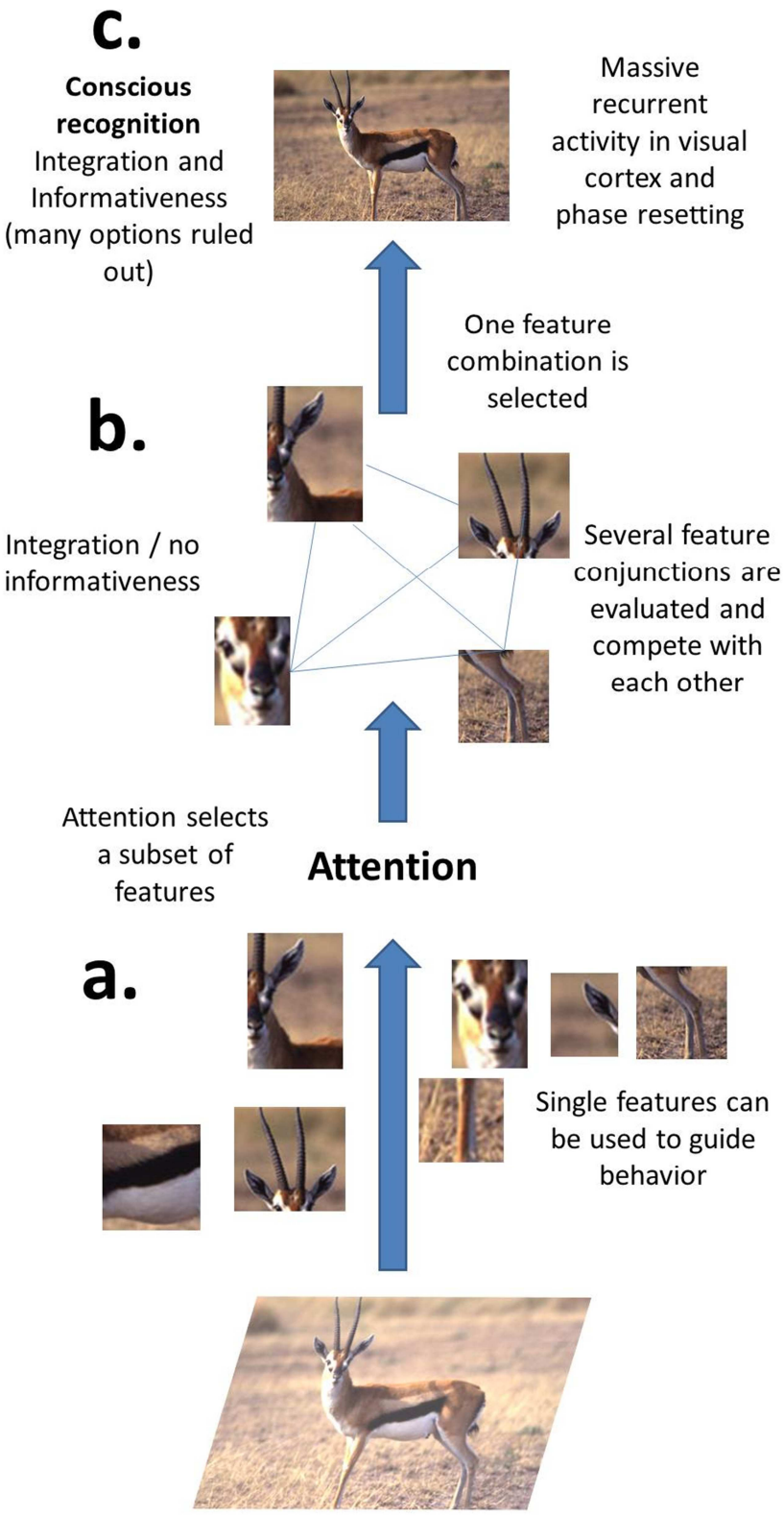
c.
Conscious recognition
Integration and Informativeness (many options ruled out)
Massive recurrent activity in visual cortex and phase resetting
One feature combination is selected
b.
Integration / no informativeness
Several feature conjunctions are evaluated and compete with each other
Attention selects a subset of features
Attention
a.
Single features can be used to guide behavior

Figure 30. Speculative model of visual perception. A. *Visual features are extracted while the information is processed in a bottom-up manner. At this stage a certain sense is extracted from the visual information by diagnosing of the presence or absence of critical features, thus incomplete information can be used at this step to guide simple forms of behavior.* ***B.*** *Attention selects certain visual features, leading them to a state where several feature conjunctions are evaluated and compete with each other. This stage represents a high degree of integration (many possible feature conjunctions are concurrently represented), however the informativeness of this state is limited since the number of possible conjunctions renders the perceptual output undetermined* ***C.*** *If the feature conjunction is resolved (i.e., a neural assembly can code for it in a sufficiently stable manner), a unique combination is selected and enters to consciousness which is accompanied by a massive recurrent activity in several brain regions activating a phase-resetting in different brain zones. This step represents a high degree of both integration and informativeness.*

Based on the results that were collected using SWIFT, it is also possible to speculate about the putative neural signatures of attention and consciousness which would involve synchrony of oscillatory networks in distinctive frequency bands and delays from stimulus presentation. Assuming that SWIFT recordings represent both consciousness- and attention-dependent activities, we could speculate that the earlier effects (<200 ms) seen in the evoked activities would most likely represent the effects of attention and the later (>250 ms) would most likely represent the effects of consciousness. Attention would select and activate (Figure 31a, red and black lines) some visual features in order to lead them into a higher level of activation than the level of activation produced by the bottom-up wave of activation (Figure 31a, green line). The activation of these features would be mediated by a phase resetting at beta and lower frequencies which is compatible with our results in the binocular rivalry experiment and those regarding the external synchrony in the implanted patients. This would promote the interaction of areas coding these features at the beta and low-gamma band, which is compatible with the preliminary results of internal synchrony obtained in patients (Figure 31b) and also with the proposal of selective attention by selective synchrony (Womelsdorf et al., 2007). This activated state would fade out rapidly if no conscious processing is achieved (Figure 31). In a later stage, conscious processing would be reflected by inter-area interaction at high-gamma frequency bands (as suggested by our

results in the implanted patients) associated with a phase-resetting at lower frequencies (<40 Hz).

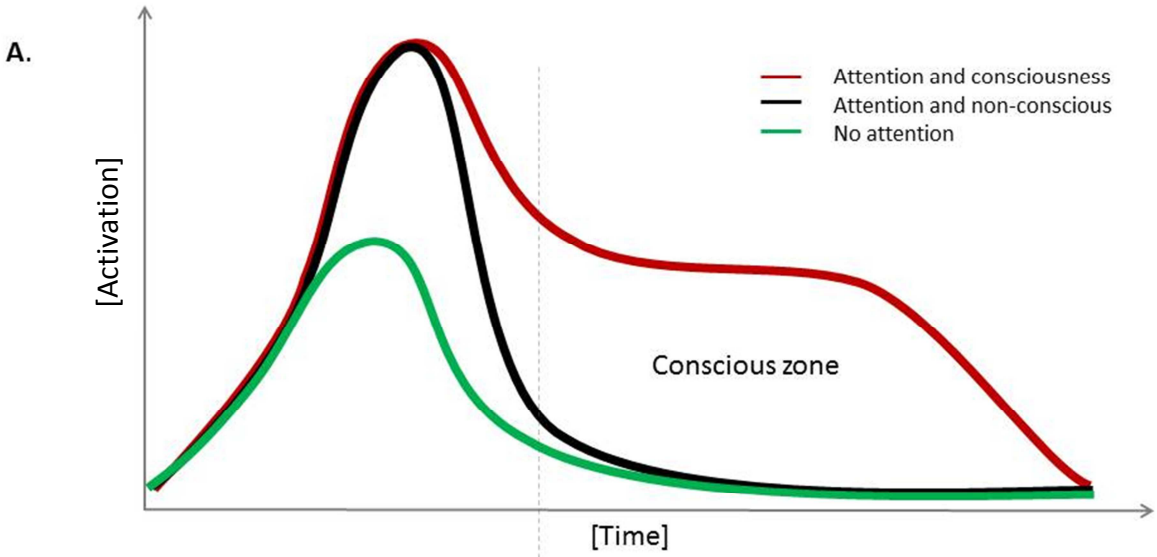

B.

	Attention effects are predominant	
Attention	**Internal synchrony**	**External synchrony**
+	↑ beta, low-gamma	↑ beta and lower
-	↓ all freqs	↓ all freqs

	Consciousness effects are predominant	
Conscious	**Internal synchrony**	**External synchrony**
+	↑ high-gamma	↑ low freqs
-	↓ all freqs	↓ all freqs

***Figure 31. Hypothetical effects of attention and consciousness**. **A.** Effects of attention and consciousness in the activation of brain areas as function of time after the stimulus presentation. Effects of attention would be more manifest in the early part of processing while the effects of consciousness would be more preponderant at later stages. In the earlier part, the bottom-up wave of visual information would activate visual areas and beyond (green line). On top of that, attention would select and activate some visual features leading to a highly activated state (black line). This state is metastable and would fade rapidly if consciousness does not emerge. In the later part of processing, conscious processing would promote a more stable activated state. **B.** Effects of attention and consciousness on synchrony. Attention would activate neural representations by promoting their interactions at the beta and low-gamma frequencies, which would be correlated with a phase-resetting at beta and lower frequencies. Conscious perception would be associated with the stabilization of the neural assemblies coding for these conjunction of features by allowing their interaction at high-gamma frequencies which would be accompanied by a phase-reset at lower frequencies.*

IX. Future directions

The development of the SWIFT technique has opened a door to the exploration of consciousness and I believe that several fundamental questions can be addressed at this point by using this novel paradigm. Future directions on the research using SWIFT involve three fundamental questions to be addressed: where does consciousness emerges in the brain? What is the causal relationship between brain areas in the emergence of consciousness?

Regarding the brain areas supporting consciousness, further research on both implanted patients and monkey will give us more information about the areas showing consciousness-dependent activity. Different electrode implantation schemes across different subjects will allow testing different brain areas and unveiling their role in conscious perception. In another vein, fMRI studies could represent a great alternative to define the brain areas that generate the consciousness-dependent activity under SWIFT stimulation.

The causal relationship among brain areas regarding the emergence of consciousness can be addressed by statistical measures, such as Granger causality, applied to intracranial recordings and fMRI recordings. This will allow us to obtain a clearer idea of the interactions among the components of the conscious brain network.

H. References

Adrian, E. D., & Matthews, R. (1927). The action of light on the eye: Part I. The discharge of impulses in the optic nerve and its relation to the electric changes in the retina. *The Journal of Physiology*, *63*(4), 378–414.

Alamouti, B. (2003). Retinal thickness decreases with age: an OCT study. *British Journal of Ophthalmology*, *87*(7), 899–901. doi:10.1136/bjo.87.7.899

Alonso, J. M., Usrey, W. M., & Reid, R. C. (2001). Rules of connectivity between geniculate cells and simple cells in cat primary visual cortex. *The Journal of Neuroscience: The Official Journal of the Society for Neuroscience*, *21*(11), 4002–4015.

Anderson, J. C., & Martin, K. A. C. (2005). Connection from cortical area V2 to V3 A in macaque monkey. *The Journal of Comparative Neurology*, *488*(3), 320–330. doi:10.1002/cne.20580

Anderson, J. C., & Martin, K. A. C. (2006). Synaptic connection from cortical area V4 to V2 in macaque monkey. *The Journal of Comparative Neurology*, *495*(6), 709–721. doi:10.1002/cne.20914

Anderson, J. C., & Martin, K. A. C. (2009). The synaptic connections between cortical areas V1 and V2 in macaque monkey. *The Journal of Neuroscience: The Official Journal of the Society for Neuroscience*, *29*(36), 11283–11293. doi:10.1523/JNEUROSCI.5757-08.2009

Arrington, C. M., Carr, T. H., Mayer, A. R., & Rao, S. M. (2000). Neural mechanisms of visual attention: object-based selection of a region in space. *Journal of Cognitive Neuroscience*, *12 Suppl 2*, 106–117. doi:10.1162/089892900563975

Attwell, D., & Laughlin, S. B. (2001). An energy budget for signaling in the grey matter of the brain. *Journal of Cerebral Blood Flow and Metabolism: Official Journal of the International Society of Cerebral Blood Flow and Metabolism*, *21*(10), 1133–1145. doi:10.1097/00004647-200110000-00001

Baars, B. J. (1990). *A cognitive theory of consciousness*. Cambridge: Cambridge University Press.

Baars, B. J. (2002). The conscious access hypothesis: origins and recent evidence. *Trends in Cognitive Sciences*, *6*(1), 47–52. doi:10.1016/S1364-6613(00)01819-2

Baars, B. J. (2005). Global workspace theory of consciousness: toward a cognitive neuroscience of human experience. *Progress in Brain Research*, *150*, 45–53. doi:10.1016/S0079-6123(05)50004-9

Baizer, J. S., Ungerleider, L. G., & Desimone, R. (1991). Organization of visual inputs to the inferior temporal and posterior parietal cortex in macaques. *The Journal of Neuroscience: The Official Journal of the Society for Neuroscience*, *11*(1), 168–190.

Banerjee, A., Tognoli, E., Assisi, C. G., Kelso, J. A. S., & Jirsa, V. K. (2008). Mode level cognitive subtraction (MLCS) quantifies spatiotemporal reorganization in large-scale brain topographies. *NeuroImage*, *42*(2), 663–674. doi:10.1016/j.neuroimage.2008.04.260

Bar, M, Kassam, K. S., Ghuman, A. S., Boshyan, J., Schmid, A. M., Schmidt, A. M., Dale, A. M., et al. (2006). Top-down facilitation of visual recognition. *Proceedings of the National Academy of Sciences of the United States of America*, *103*(2), 449–454. doi:10.1073/pnas.0507062103

Bar, M, Tootell, R. B., Schacter, D. L., Greve, D. N., Fischl, B., Mendola, J. D., Rosen, B. R., et al. (2001). Cortical mechanisms specific to explicit visual object recognition. *Neuron*, *29*(2), 529–535.

Bar, Moshe. (2003). A cortical mechanism for triggering top-down facilitation in visual object recognition. *Journal of cognitive neuroscience*, *15*(4), 600–609. doi:10.1162/089892903321662976

Barlow, H. B. (1953). Summation and inhibition in the frog's retina. *The Journal of Physiology*, *119*(1), 69–88.

Baylor, D. A., Lamb, T. D., & Yau, K. W. (1979). Responses of retinal rods to single photons. *The Journal of Physiology*, *288*, 613–634.

Behrmann, M., Zemel, R. S., & Mozer, M. C. (1998). Object-based attention and occlusion: evidence from normal participants and a computational model. *Journal of Experimental Psychology. Human Perception and Performance*, *24*(4), 1011–1036.

Bichot, N. P. (2005). Parallel and Serial Neural Mechanisms for Visual Search in Macaque Area V4. *Science*, *308*(5721), 529–534. doi:10.1126/science.1109676

Binzegger, T., Douglas, R. J., & Martin, K. A. C. (2004). A quantitative map of the circuit of cat primary visual cortex. *The Journal of Neuroscience: The Official Journal of the Society for Neuroscience*, *24*(39), 8441–8453. doi:10.1523/JNEUROSCI.1400-04.2004

Blackmore, S. (2005). *Consciousness: A Very Short Introduction*. Oxford University Press.

Blackmore, S. J., Brelstaff, G., Nelson, K., & Trościanko, T. (1995). Is the richness of our visual world an illusion? Transsaccadic memory for complex scenes. *Perception*, *24*(9), 1075–1081.

Blasdel, G. G., & Lund, J. S. (1983). Termination of afferent axons in macaque striate cortex. *The Journal of Neuroscience: The Official Journal of the Society for Neuroscience*, *3*(7), 1389–1413.

Block, N. (1995). On a confusion about a function of consciousness. *Behavioral and Brain Sciences*, *18*(02), 227. doi:10.1017/S0140525X00038188

Block, N. (2008). Consciousness, accessibility, and the mesh between psychology and neuroscience. *Behavioral and Brain Sciences*, *30*(5-6). doi:10.1017/S0140525X07002786

Blumberg, J., & Kreiman, G. (2010). How cortical neurons help us see: visual recognition in the human brain. *Journal of Clinical Investigation*, *120*(9), 3054–3063. doi:10.1172/JCI42161

Booth, M. C., & Rolls, E. T. (1998). View-invariant representations of familiar objects by neurons in the inferior temporal visual cortex. *Cerebral Cortex (New York, N.Y.: 1991)*, *8*(6), 510–523.

Bor, D., & Seth, A. K. (2012). Consciousness and the prefrontal parietal network: insights from attention, working memory, and chunking. *Frontiers in psychology*, *3*, 63. doi:10.3389/fpsyg.2012.00063

Borowsky, R., Esopenko, C., Cummine, J., & Sarty, G. E. (2007). Neural representations of visual words and objects: a functional MRI study on the modularity of reading and object processing. *Brain Topography*, *20*(2), 89–96. doi:10.1007/s10548-007-0034-1

Boucart, M., Moroni, C., Despretz, P., Pasquier, F., & Fabre-Thorpe, M. (2010). Rapid categorization of faces and objects in a patient with impaired object recognition. *Neurocase*, *16*(2), 157–168. doi:10.1080/13554790903339637

Boxtel, J. J. A. van, Tsuchiya, N., & Koch, C. (2010). Consciousness and attention: on sufficiency and necessity. *Frontiers in Consciousness Research*, *1*, 217. doi:10.3389/fpsyg.2010.00217

Bransford, J. D. (1979). *Human Cognition: Learning, Understanding and Remembering*. Wadsworth Publishing Co Inc.

Breitmeyer, B. G., & Öğmen, H. (2006). *Visual masking: Time slices through conscious and unconscious vision (2nd ed.)*. Oxford psychology series. New York, NY, US: Oxford University Press.

Broadbent, D. E. (1987). *Perception and communication*. Oxford [Oxfordshire]; New York: Oxford University Press.

Brodmann, K. (1909). *Brodmann's: Localisation in the Cerebral Cortex* (1st ed. Softcover of orig. ed. 2006.). Springer-Verlag New York Inc.

Bullier, J. (2001). Integrated model of visual processing. *Brain Research. Brain Research Reviews*, *36*(2-3), 96–107.

Bullier, J., & Kennedy, H. (1983). Projection of the lateral geniculate nucleus onto cortical area V2 in the macaque monkey. *Experimental Brain Research. Experimentelle Hirnforschung. Expérimentation Cérébrale*, *53*(1), 168–172.

Butler, A. B. (2008). Evolution of brains, cognition, and consciousness. *Brain Research Bulletin*, *75*(2-4), 442–449. doi:10.1016/j.brainresbull.2007.10.017

Butler, A. B. (2012). Hallmarks of Consciousness. In C. López-Larrea (Ed.), *Sensing in Nature*, Advances in Experimental Medicine and Biology (Vol. 739, pp. 291–309). Springer US. Retrieved from http://www.springerlink.com.gate1.inist.fr/content/g6j2723463207730/abstract/

Cameron, E. L., Tai, J. C., & Carrasco, M. (2002). Covert attention affects the psychometric function of contrast sensitivity. *Vision Research*, *42*(8), 949–967.

Carlson, J. M., Beacher, F., Reinke, K. S., Habib, R., Harmon-Jones, E., Mujica-Parodi, L. R., & Hajcak, G. (2012). Nonconscious attention bias to threat is correlated with anterior cingulate cortex gray matter volume: a voxel-based morphometry result and replication. *NeuroImage*, *59*(2), 1713–1718. doi:10.1016/j.neuroimage.2011.09.040

Carlson, J. M., Reinke, K. S., LaMontagne, P. J., & Habib, R. (2011). Backward masked fearful faces enhance contralateral occipital cortical activity for visual targets within the spotlight of attention. *Social Cognitive and Affective Neuroscience*, *6*(5), 639–645. doi:10.1093/scan/nsq076

Carlson, T., Grol, M. J., & Verstraten, F. A. J. (2006). Dynamics of visual recognition revealed by fMRI. *NeuroImage*, *32*(2), 892–905. doi:10.1016/j.neuroimage.2006.03.059

Carrasco, M. (2011). Visual attention: the past 25 years. *Vision Research*, *51*(13), 1484–1525. doi:10.1016/j.visres.2011.04.012

Casagrande, V. A., Yazar, F., Jones, K. D., & Ding, Y. (2007). The morphology of the koniocellular axon pathway in the macaque monkey. *Cerebral Cortex (New York, N.Y.: 1991)*, *17*(10), 2334–2345. doi:10.1093/cercor/bhl142

Chalk, M., Herrero, J. L., Gieselmann, M. A., Delicato, L. S., Gotthardt, S., & Thiele, A. (2010). Attention Reduces Stimulus-Driven Gamma Frequency Oscillations and Spike Field Coherence in V1. *Neuron*, *66*(1), 114–125. doi:10.1016/j.neuron.2010.03.013

Chalmers, D. J. (1996). *The conscious mind : in search of a fundamental theory*. New York: Oxford University Press.

Cheal, M., & Lyon, D. R. (1991). Central and peripheral precuing of forced-choice discrimination. *The Quarterly Journal of Experimental Psychology. A, Human Experimental Psychology*, *43*(4), 859–880.

Cheal, M., Lyon, D. R., & Hubbard, D. C. (1991). Does attention have different effects on line orientation and line arrangement discrimination? *The Quarterly Journal of Experimental Psychology. A, Human Experimental Psychology*, *43*(4), 825–857.

Chelazzi, L., Miller, E. K., Duncan, J., & Desimone, R. (1993). A neural basis for visual search in inferior temporal cortex. *Nature*, *363*(6427), 345–347. doi:10.1038/363345a0

Chica, A. B., & Lupiáñez, J. (2009). Effects of endogenous and exogenous attention on visual processing: an Inhibition of Return study. *Brain Research*, *1278*, 75–85. doi:10.1016/j.brainres.2009.04.011

Collins, C. E., Airey, D. C., Young, N. A., Leitch, D. B., & Kaas, J. H. (2010). Neuron densities vary across and within cortical areas in primates. *Proceedings of the National Academy of Sciences of the United States of America*, *107*(36), 15927–15932. doi:10.1073/pnas.1010356107

Corbetta, M, Kincade, J. M., Ollinger, J. M., McAvoy, M. P., & Shulman, G. L. (2000). Voluntary orienting is dissociated from target detection in human posterior parietal cortex. *Nature Neuroscience*, *3*(3), 292–297. doi:10.1038/73009

Corbetta, Maurizio, & Shulman, G. L. (2002a). Control of goal-directed and stimulus-driven attention in the brain. *Nature Reviews. Neuroscience*, *3*(3), 201–215. doi:10.1038/nrn755

Corbetta, Maurizio, & Shulman, G. L. (2002b). Control of goal-directed and stimulus-driven attention in the brain. *Nature Reviews. Neuroscience*, *3*(3), 201–215. doi:10.1038/nrn755

Corbetta, Maurizio, & Shulman, G. L. (2011). Spatial neglect and attention networks. *Annual Review of Neuroscience*, *34*, 569–599. doi:10.1146/annurev-neuro-061010-113731

Crick, F, & Koch, C. (1995). Are we aware of neural activity in primary visual cortex? *Nature*, *375*(6527), 121–123. doi:10.1038/375121a0

Crick, F, & Koch, C. (1998a). Consciousness and neuroscience. *Cerebral cortex (New York, N.Y.: 1991)*, *8*(2), 97–107.

Crick, F, & Koch, C. (1990). Towards a Neurobiological Theory of Consciousness. *Seminars in the Neurosciences*, *2*, 263–275.

Crick, F, & Koch, C. (1998b). Constraints on cortical and thalamic projections: the no-strong-loops hypothesis. *Nature*, *391*(6664), 245–250. doi:10.1038/34584

Crick, Francis, & Koch, C. (2003). A framework for consciousness. *Nature neuroscience*, *6*(2), 119–126. doi:10.1038/nn0203-119

Crouzet, S. M., Kirchner, H., & Thorpe, S. J. (2010). Fast saccades toward faces: face detection in just 100 ms. *Journal of Vision*, *10*(4), 16.1–17. doi:10.1167/10.4.16

Crouzet, S. M., & Thorpe, S. J. (2011). Low-level cues and ultra-fast face detection. *Frontiers in Psychology*, *2*, 342. doi:10.3389/fpsyg.2011.00342

Crouzet, S., Thorpe, S. J., & Kirchner, H. (2007). Category-dependent variations in visual processing time. *Journal of Vision*, *7*(9), 922–922. doi:10.1167/7.9.922

Cutzu, F., & Tsotsos, J. K. (2003). The selective tuning model of attention: psychophysical evidence for a suppressive annulus around an attended item. *Vision Research*, *43*(2), 205–219.

De Brigard, F., & Prinz, J. (2009). Attention and consciousness. *Wiley Interdisciplinary Reviews: Cognitive Science*, *1*(1), 51–59. doi:10.1002/wcs.27

De Valois, R. L., Yund, E. W., & Hepler, N. (1982). The orientation and direction selectivity of cells in macaque visual cortex. *Vision Research*, *22*(5), 531–544.

Dehaene, S. (1989). Discriminability and dimensionality effects in visual search for featural conjunctions: a functional pop-out. *Perception & Psychophysics*, *46*(1), 72–80.

Dehaene, S, Naccache, L., Le Clec'H, G., Koechlin, E., Mueller, M., Dehaene-Lambertz, G., van de Moortele, P. F., et al. (1998). Imaging unconscious semantic priming. *Nature*, *395*(6702), 597–600. doi:10.1038/26967

Dehaene, Stanislas, Kerszberg, M., & Changeux, J.-P. (1998). A Neuronal Model of a Global Workspace in Effortful Cognitive Tasks. *Proceedings of the National Academy of Sciences*, *95*(24), 14529–14534. doi:10.1073/pnas.95.24.14529

Dehaene, Stanislas, & Changeux, J.-P. (2005). Ongoing spontaneous activity controls access to consciousness: a neuronal model for inattentional blindness. *PLoS Biology*, *3*(5), e141. doi:10.1371/journal.pbio.0030141

Dehaene, Stanislas, & Changeux, J.-P. (2011). Experimental and Theoretical Approaches to Conscious Processing. *Neuron*, *70*(2), 200–227. doi:10.1016/j.neuron.2011.03.018

Dehaene, Stanislas, Changeux, J.-P., Naccache, L., Sackur, J., & Sergent, C. (2006). Conscious, preconscious, and subliminal processing: a testable taxonomy. *Trends in Cognitive Sciences*, *10*(5), 204–211. doi:10.1016/j.tics.2006.03.007

Dehaene, Stanislas, Sergent, C., & Changeux, J.-P. (2003). A neuronal network model linking subjective reports and objective physiological data during conscious perception. *Proceedings of the National Academy of Sciences of the United States of America*, *100*(14), 8520–8525. doi:10.1073/pnas.1332574100

Del Cul, A., Baillet, S., & Dehaene, S. (2007). Brain dynamics underlying the nonlinear threshold for access to consciousness. *PLoS Biology*, *5*(10), e260. doi:10.1371/journal.pbio.0050260

Delorme, A, Richard, G., & Fabre-Thorpe, M. (2000). Ultra-rapid categorisation of natural scenes does not rely on colour cues: a study in monkeys and humans. *Vision Research*, *40*(16), 2187–2200.

Delorme, Arnaud, & Makeig, S. (2004). EEGLAB: an open source toolbox for analysis of single-trial EEG dynamics including independent component analysis. *Journal of Neuroscience Methods*, *134*(1), 9–21. doi:10.1016/j.jneumeth.2003.10.009

Denys, K., Vanduffel, W., Fize, D., Nelissen, K., Peuskens, H., Van Essen, D., & Orban, G. A. (2004). The processing of visual shape in the cerebral cortex of human and nonhuman primates: a functional magnetic resonance imaging study. *The Journal of Neuroscience: The Official Journal of the Society for Neuroscience*, *24*(10), 2551–2565. doi:10.1523/JNEUROSCI.3569-03.2004

Descartes, R., Meyer, M., & Timmermans, B. (1649). *Les Passions de l'âme*. Paris: Librairie générale française.

Desimone, R., Albright, T. D., Gross, C. G., & Bruce, C. (1984). Stimulus-selective properties of inferior temporal neurons in the macaque. *The Journal of Neuroscience: The Official Journal of the Society for Neuroscience*, *4*(8), 2051–2062.

Desimone, R., Fleming, J., & Gross, C. G. (1980). Prestriate afferents to inferior temporal cortex: an HRP study. *Brain Research*, *184*(1), 41–55.

Desimone, R., & Schein, S. J. (1987). Visual properties of neurons in area V4 of the macaque: sensitivity to stimulus form. *Journal of Neurophysiology*, *57*(3), 835–868.

Desimone, R., & Ungerleider, L. (1989). *Handbook of neuropsychology* (Vol. 2). Boller, F Grafman, J.

DiCarlo, J. J., Zoccolan, D., & Rust, N. C. (2012). How Does the Brain Solve Visual Object Recognition? *Neuron*, *73*(3), 415–434. doi:10.1016/j.neuron.2012.01.010

Driver, J., Davis, G., Russell, C., Turatto, M., & Freeman, E. (2001). Segmentation, attention and phenomenal visual objects. *Cognition*, *80*(1-2), 61–95.

Duncan, J. (1993). Similarity between concurrent visual discriminations: dimensions and objects. *Perception & Psychophysics*, *54*(4), 425–430.

Edelman, G. M., & Tononi, G. (2000). *A universe of consciousness : how matter becomes imagination*. New York, NY: Basic Books.

Egeth, H. E., & Yantis, S. (1997). Visual attention: control, representation, and time course. *Annual Review of Psychology*, *48*, 269–297. doi:10.1146/annurev.psych.48.1.269

Enns, J. T. (2004). *The thinking eye, the seeing brain : explorations in visual cognition*. New York: W.W. Norton.

Epstein, R., Harris, A., Stanley, D., & Kanwisher, N. (1999). The parahippocampal place area: recognition, navigation, or encoding? *Neuron*, *23*(1), 115–125.

Eriksen, C. W., & St James, J. D. (1986). Visual attention within and around the field of focal attention: a zoom lens model. *Perception & Psychophysics*, *40*(4), 225–240.

Fabre-Thorpe, M, Delorme, A., Marlot, C., & Thorpe, S. (2001). A limit to the speed of processing in ultra-rapid visual categorization of novel natural scenes. *Journal of Cognitive Neuroscience*, *13*(2), 171–180.

Fabre-Thorpe, M, Richard, G., & Thorpe, S. J. (1998). Rapid categorization of natural images by rhesus monkeys. *Neuroreport*, *9*(2), 303–308.

Fabre-Thorpe, Michèle. (2011). The characteristics and limits of rapid visual categorization. *Frontiers in Psychology*, *2*. doi:10.3389/fpsyg.2011.00243

Fang, F., & He, S. (2005). Cortical responses to invisible objects in the human dorsal and ventral pathways. *Nature Neuroscience*, *8*(10), 1380–1385. doi:10.1038/nn1537

Farivar, R. (2009). Dorsal-ventral integration in object recognition. *Brain Research Reviews*, *61*(2), 144–153. doi:10.1016/j.brainresrev.2009.05.006

Felleman, D. J., & Van Essen, D. C. (1991). Distributed hierarchical processing in the primate cerebral cortex. *Cerebral Cortex (New York, N.Y.: 1991)*, *1*(1), 1–47.

Fenske, M. J., Aminoff, E., Gronau, N., & Bar, M. (2006). Top-down facilitation of visual object recognition: object-based and context-based contributions. *Progress in brain research*, *155*, 3–21. doi:10.1016/S0079-6123(06)55001-0

Ferster, D. (1988). Spatially opponent excitation and inhibition in simple cells of the cat visual cortex. *The Journal of Neuroscience: The Official Journal of the Society for Neuroscience*, *8*(4), 1172–1180.

Fetzer, J. H. (2002). *Consciousness Evolving*. John Benjamins Publishing Company.

Fishman, R. S. (2008). Evolution and the eye: the Darwin bicentennial and the sesquicentennial of the origin of species. *Archives of Ophthalmology*, *126*(11), 1586–1592. doi:10.1001/archopht.126.11.1586

Flanagan. (1994). Consciousness reconsidered. Cambridge. *Journal of the History of the Behavioral Sciences*, *30*(1), 61–65. doi:10.1002/1520-6696(199401)30:1<61::AID-JHBS2300300109>3.0.CO;2-5

Freedman, D J, Riesenhuber, M., Poggio, T., & Miller, E. K. (2001). Categorical representation of visual stimuli in the primate prefrontal cortex. *Science (New York, N.Y.)*, *291*(5502), 312–316. doi:10.1126/science.291.5502.312

Freedman, David J, Riesenhuber, M., Poggio, T., & Miller, E. K. (2002). Visual categorization and the primate prefrontal cortex: neurophysiology and behavior. *Journal of Neurophysiology*, *88*(2), 929–941.

Freedman, David J, Riesenhuber, M., Poggio, T., & Miller, E. K. (2003). A comparison of primate prefrontal and inferior temporal cortices during visual categorization. *The Journal of Neuroscience: The Official Journal of the Society for Neuroscience*, *23*(12), 5235–5246.

Fries, P. (2001). Modulation of Oscillatory Neuronal Synchronization by Selective Visual Attention. *Science*, *291*(5508), 1560–1563. doi:10.1126/science.1055465

Fries, Pascal, Nikolić, D., & Singer, W. (2007). The gamma cycle. *Trends in Neurosciences*, *30*(7), 309–316. doi:10.1016/j.tins.2007.05.005

Fries, W. (1981). The projection from the lateral geniculate nucleus to the prestriate cortex of the macaque monkey. *Proceedings of the Royal Society of London. Series B, Containing Papers of a Biological Character. Royal Society (Great Britain)*, *213*(1190), 73–86.

Friston, K. J., Price, C. J., Fletcher, P., Moore, C., Frackowiak, R. S., & Dolan, R. J. (1996). The trouble with cognitive subtraction. *NeuroImage*, *4*(2), 97–104. doi:10.1006/nimg.1996.0033

Fujita, I., Tanaka, K., Ito, M., & Cheng, K. (1992). Columns for visual features of objects in monkey inferotemporal cortex. *Nature*, *360*(6402), 343–346. doi:10.1038/360343a0

Gallant, J. L., Braun, J., & Van Essen, D. C. (1993). Selectivity for polar, hyperbolic, and Cartesian gratings in macaque visual cortex. *Science (New York, N.Y.)*, *259*(5091), 100–103.

Galliot, B., & Quiquand, M. (2011). A two-step process in the emergence of neurogenesis. *European Journal of Neuroscience*, *34*(6), 847–862. doi:10.1111/j.1460-9568.2011.07829.x

Giordano, A. M., McElree, B., & Carrasco, M. (2009). On the automaticity and flexibility of covert attention: A speed-accuracy trade-off analysis. *Journal of Vision*, *9*(3), 30–30. doi:10.1167/9.3.30

Girard, P, Jouffrais, C., & Kirchner, C. H. (2008). Ultra-rapid categorisation in non-human primates. *Animal Cognition*, *11*(3), 485–493. doi:10.1007/s10071-008-0139-2

Girard, Pascal, Lomber, S. G., & Bullier, J. (2002). Shape discrimination deficits during reversible deactivation of area V4 in the macaque monkey. *Cerebral Cortex (New York, N.Y.: 1991)*, *12*(11), 1146–1156.

Goodale, M A, & Milner, A. D. (1992). Separate visual pathways for perception and action. *Trends in Neurosciences*, *15*(1), 20–25.

Goodale, Melvyn A, & Westwood, D. A. (2004). An evolving view of duplex vision: separate but interacting cortical pathways for perception and action. *Current opinion in neurobiology*, *14*(2), 203–211. doi:10.1016/j.conb.2004.03.002

Gosselin, F., & Schyns, P. G. (2001). Bubbles: a technique to reveal the use of information in recognition tasks. *Vision Research*, *41*(17), 2261–2271. doi:10.1016/S0042-6989(01)00097-9

Gottesmann, C. (2008). Noradrenaline involvement in basic and higher integrated REM sleep processes. *Progress in Neurobiology*, *85*(3), 237–272. doi:10.1016/j.pneurobio.2008.04.002

Gregoriou, G. G., Gotts, S. J., Zhou, H., & Desimone, R. (2009). High-frequency, long-range coupling between prefrontal and visual cortex during attention. *Science (New York, N.Y.)*, *324*(5931), 1207–1210. doi:10.1126/science.1171402

Grill-Spector, K. (2003). The neural basis of object perception. *Current Opinion in Neurobiology*, *13*(2), 159–166. doi:10.1016/S0959-4388(03)00040-0

Gross, C. G., Rocha-Miranda, C. E., & Bender, D. B. (1972). Visual properties of neurons in inferotemporal cortex of the Macaque. *Journal of Neurophysiology*, *35*(1), 96–111.

Guyonneau, R., Vanrullen, R., & Thorpe, S. J. (2004). Temporal codes and sparse representations: a key to understanding rapid processing in the visual system. *Journal of Physiology, Paris*, *98*(4-6), 487–497. doi:10.1016/j.jphysparis.2005.09.004

Guyonneau, R., VanRullen, R., & Thorpe, S. J. (2005). Neurons tune to the earliest spikes through STDP. *Neural Computation*, *17*(4), 859–879. doi:10.1162/0899766053429390

Hameroff, S. (1998). Quantum Computation in Brain Microtubules? The Penrose–Hameroff 'Orch OR' Model of Consciousness. *Philosophical Transactions of the Royal Society of London. Series A: Mathematical, Physical and Engineering Sciences*, *356*(1743), 1869–1896. doi:10.1098/rsta.1998.0254

Hartline, H. K. (1938). The response of single optic nerve fibers of the vertebrate eye to illumination of the retina. *American J Physiol*, *121*, 400–415.

Haxby, J. V., Grady, C. L., Horwitz, B., Ungerleider, L. G., Mishkin, M., Carson, R. E., Herscovitch, P., et al. (1991). Dissociation of object and spatial visual processing pathways in human extrastriate cortex. *Proceedings of the National Academy of Sciences of the United States of America*, *88*(5), 1621–1625.

He, B. J., Snyder, A. Z., Vincent, J. L., Epstein, A., Shulman, G. L., & Corbetta, M. (2007). Breakdown of functional connectivity in frontoparietal networks underlies behavioral deficits in spatial neglect. *Neuron*, *53*(6), 905–918. doi:10.1016/j.neuron.2007.02.013

Hegdé, J, & Van Essen, D. C. (2000). Selectivity for complex shapes in primate visual area V2. *The Journal of Neuroscience: The Official Journal of the Society for Neuroscience*, *20*(5), RC61.

Hegdé, Jay, & Van Essen, D. C. (2003). Strategies of shape representation in macaque visual area V2. *Visual Neuroscience*, *20*(3), 313–328.

Hegdé, Jay, & Van Essen, D. C. (2005). Role of primate visual area V4 in the processing of 3-D shape characteristics defined by disparity. *Journal of Neurophysiology*, *94*(4), 2856–2866. doi:10.1152/jn.00802.2004

Hegdé, Jay, & Van Essen, D. C. (2006). Temporal dynamics of 2D and 3D shape representation in macaque visual area V4. *Visual Neuroscience*, *23*(5), 749–763. doi:10.1017/S0952523806230074

Hegdé, Jay, & Van Essen, D. C. (2007). A comparative study of shape representation in macaque visual areas v2 and v4. *Cerebral Cortex (New York, N.Y.: 1991)*, *17*(5), 1100–1116. doi:10.1093/cercor/bhl020

Hein, E., Rolke, B., & Ulrich, R. (2006). Visual attention and temporal discrimination: Differential effects of automatic and voluntary cueing. *Visual Cognition*, *13*(1), 29–50. doi:10.1080/13506280500143524

Helmholtz, H. von. (1867). *Helmholtz's treatise on physiological optics*. Bristol, England; Sterling, VA: Thoemmes.

Hendry, S. H., & Reid, R. C. (2000). The koniocellular pathway in primate vision. *Annual Review of Neuroscience*, *23*, 127–153. doi:10.1146/annurev.neuro.23.1.127

Hernández-González, A., Cavada, C., & Reinoso-Suárez, F. (1994). The lateral geniculate nucleus projects to the inferior temporal cortex in the macaque monkey. *Neuroreport*, *5*(18), 2693–2696.

Herrmann, C. S. (2001). Human EEG responses to 1-100 Hz flicker: resonance phenomena in visual cortex and their potential correlation to cognitive phenomena. *Experimental Brain Research. Experimentelle Hirnforschung. Expérimentation Cérébrale*, *137*(3-4), 346–353.

Hesselmann, G., Naccache, L., Cohen, L., & Dehaene, S. (2012). Splitting of the P3 component during dual-task processing in a patient with posterior callosal section. *Cortex*, (0). doi:10.1016/j.cortex.2012.03.014

Honey, C., Kirchner, H., & VanRullen, R. (2008). Faces in the cloud: Fourier power spectrum biases ultrarapid face detection. *Journal of Vision*, *8*(12), 9–9. doi:10.1167/8.12.9

Hopfinger, J. B., Buonocore, M. H., & Mangun, G. R. (2000). The neural mechanisms of top-down attentional control. *Nature Neuroscience*, *3*(3), 284–291. doi:10.1038/72999

Howarth, C., Gleeson, P., & Attwell, D. (2012). Updated energy budgets for neural computation in the neocortex and cerebellum. *Journal of Cerebral Blood Flow and Metabolism: Official Journal of the International Society of Cerebral Blood Flow and Metabolism*. doi:10.1038/jcbfm.2012.35

Huang, J. Y., Wang, C., & Dreher, B. (2007). The effects of reversible inactivation of postero-temporal visual cortex on neuronal activities in cat's area 17. *Brain Research*, *1138*, 111–128. doi:10.1016/j.brainres.2006.12.081

Hubel, D. H., & Wiesel, T. N. (1959). Receptive fields of single neurones in the cat's striate cortex. *The Journal of Physiology*, *148*, 574–591.

Hubel, D. H., & Wiesel, T. N. (1962). Receptive fields, binocular interaction and functional architecture in the cat's visual cortex. *The Journal of Physiology*, *160*, 106–154.

Hubel, D. H., & Wiesel, T. N. (1965). RECEPTIVE FIELDS AND FUNCTIONAL ARCHITECTURE IN TWO NONSTRIATE VISUAL AREAS (18 AND 19) OF THE CAT. *Journal of Neurophysiology*, *28*, 229–289.

Hubel, D. H., & Wiesel, T. N. (1968). Receptive fields and functional architecture of monkey striate cortex. *The Journal of Physiology*, *195*(1), 215–243.

Hupé, J. M., James, A. C., Payne, B. R., Lomber, S. G., Girard, P., & Bullier, J. (1998). Cortical feedback improves discrimination between figure and background by V1, V2 and V3 neurons. *Nature*, *394*(6695), 784–787. doi:10.1038/29537

James, W. (1890). *The principles of psychology. Vol. 1*. New York; Toronto; [s. l.]: Dover ; General Publishing Company ; Constable and Company.

Jiang, Y., & He, S. (2006). Cortical responses to invisible faces: dissociating subsystems for facial-information processing. *Current Biology: CB*, *16*(20), 2023–2029. doi:10.1016/j.cub.2006.08.084

Jones, B. E. (2003). Arousal systems. *Frontiers in Bioscience: A Journal and Virtual Library*, *8*, s438–451.

Joubert, O. R., Fize, D., Rousselet, G. A., & Fabre-Thorpe, M. (2008). Early Interference of Context Congruence on Object Processing in Rapid Visual Categorization of Natural Scenes. *Journal of Vision*, *8*(13). doi:10.1167/8.13.11

Judd, C. H. (1910). Evolution and consciousness. *Psychological Review*, *17*(2), 77–97. doi:10.1037/h0071801

Kaas, J. H., Huerta, M. F., Weber, J. T., & Harting, J. K. (1978). Patterns of retinal terminations and laminar organization of the lateral geniculate nucleus of primates. *The Journal of Comparative Neurology*, *182*(3), 517–553. doi:10.1002/cne.901820308

Kanwisher, N, McDermott, J., & Chun, M. M. (1997). The fusiform face area: a module in human extrastriate cortex specialized for face perception. *The Journal of Neuroscience: The Official Journal of the Society for Neuroscience*, *17*(11), 4302–4311.

Kanwisher, N, Woods, R. P., Iacoboni, M., & Mazziotta, J. C. (1997). A Locus in Human Extrastriate Cortex for Visual Shape Analysis. *Journal of Cognitive Neuroscience*, *9*(1), 133–142. doi:10.1162/jocn.1997.9.1.133

Kastner, S., Pinsk, M. A., De Weerd, P., Desimone, R., & Ungerleider, L. G. (1999). Increased activity in human visual cortex during directed attention in the absence of visual stimulation. *Neuron*, *22*(4), 751–761.

Kefalov, V. J. (2012). Rod and cone visual pigments and phototransduction through pharmacological, genetic, and physiological approaches. *The Journal of Biological Chemistry*, *287*(3), 1635–1641. doi:10.1074/jbc.R111.303008

Kennedy, H., & Bullier, J. (1985). A double-labeling investigation of the afferent connectivity to cortical areas V1 and V2 of the macaque monkey. *The Journal of Neuroscience: The Official Journal of the Society for Neuroscience*, *5*(10), 2815–2830.

Kentridge, R. W., Heywood, C. A., & Weiskrantz, L. (1999). Attention without awareness in blindsight. *Proceedings. Biological Sciences / The Royal Society*, *266*(1430), 1805–1811. doi:10.1098/rspb.1999.0850

Kentridge, R. W., Heywood, C. A., & Weiskrantz, L. (2004). Spatial attention speeds discrimination without awareness in blindsight. *Neuropsychologia*, *42*(6), 831–835. doi:10.1016/j.neuropsychologia.2003.11.001

Kentridge, R. W., Nijboer, T. C. W., & Heywood, C. A. (2008). Attended but unseen: visual attention is not sufficient for visual awareness. *Neuropsychologia*, *46*(3), 864–869. doi:10.1016/j.neuropsychologia.2007.11.036

Kincade, J. M., Abrams, R. A., Astafiev, S. V., Shulman, G. L., & Corbetta, M. (2005). An event-related functional magnetic resonance imaging study of voluntary and stimulus-driven orienting of attention. *The Journal of Neuroscience: The Official Journal of the Society for Neuroscience*, *25*(18), 4593–4604. doi:10.1523/JNEUROSCI.0236-05.2005

Kirchner, H., & Thorpe, S. J. (2006). Ultra-rapid object detection with saccadic eye movements: visual processing speed revisited. *Vision Research*, *46*(11), 1762–1776. doi:10.1016/j.visres.2005.10.002

Kirk, R. (1974). Sentience and Behaviour. *Mind*, *LXXXIII*(329), 43–60. doi:10.1093/mind/LXXXIII.329.43

Kobatake, E., & Tanaka, K. (1994). Neuronal selectivities to complex object features in the ventral visual pathway of the macaque cerebral cortex. *Journal of Neurophysiology*, *71*(3), 856–867.

Koch, C, & Ullman, S. (1985). Shifts in selective visual attention: towards the underlying neural circuitry. *Human Neurobiology*, *4*(4), 219–227.

Koch, C. (2004). *The quest for consciousness : a neurobiological approach*. Englewood: CO : Roberts and Company Publishers.

Koch, C, & Tsuchiya, N. (2007). Attention and consciousness: two distinct brain processes. *Trends in Cognitive Sciences*, *11*(1), 16–22. doi:10.1016/j.tics.2006.10.012

Koivisto, M., Kainulainen, P., & Revonsuo, A. (2009). The relationship between awareness and attention: Evidence from ERP responses. *Neuropsychologia*, *47*(13), 2891–2899. doi:10.1016/j.neuropsychologia.2009.06.016

Koivisto, M., Lähteenmäki, M., Sørensen, T. A., Vangkilde, S., Overgaard, M., & Revonsuo, A. (2008). The earliest electrophysiological correlate of visual awareness? *Brain and Cognition*, *66*(1), 91–103. doi:10.1016/j.bandc.2007.05.010

Kreiman, G., Koch, C., & Fried, I. (2000). Category-specific visual responses of single neurons in the human medial temporal lobe. *Nature Neuroscience*, *3*(9), 946–953. doi:10.1038/78868

Kuffler, S. W. (1953). Discharge patterns and functional organization of mammalian retina. *Journal of Neurophysiology*, *16*(1), 37–68.

Kustov, A. A., & Robinson, D. L. (1996). Shared neural control of attentional shifts and eye movements. *Nature*, *384*(6604), 74–77. doi:10.1038/384074a0

Kveraga, K., Boshyan, J., & Bar, M. (2007). Magnocellular projections as the trigger of top-down facilitation in recognition. *The Journal of Neuroscience: The Official Journal of the Society for Neuroscience*, *27*(48), 13232–13240. doi:10.1523/JNEUROSCI.3481-07.2007

LaBerge, D., & Brown, V. (1989). Theory of attentional operations in shape identification. *Psychological Review*, *96*(1), 101–124. doi:10.1037/0033-295X.96.1.101

Lachica, E. A., Beck, P. D., & Casagrande, V. A. (1992). Parallel pathways in macaque monkey striate cortex: anatomically defined columns in layer III. *Proceedings of the National Academy of Sciences of the United States of America*, *89*(8), 3566–3570.

Lamb, T. D., Arendt, D., & Collin, S. P. (2009). The evolution of phototransduction and eyes. *Philosophical Transactions of the Royal Society B: Biological Sciences*, *364*(1531), 2791–2793. doi:10.1098/rstb.2009.0106

Lamme, V A F. (2004). Separate neural definitions of visual consciousness and visual attention; a case for phenomenal awareness. *Neural Networks: The Official Journal of the International Neural Network Society*, *17*(5-6), 861–872. doi:10.1016/j.neunet.2004.02.005

Lamme, V. (2000). Neural Mechanisms of Visual Awareness: A Linking Proposition. *Brain and Mind*, *1*(3), 385–406. doi:10.1023/A:1011569019782

Lamme, Victor A.F. (2003). Why visual attention and awareness are different. *Trends in Cognitive Sciences*, *7*(1), 12–18.

Lamme, V. A., Supèr, H., & Spekreijse, H. (1998). Feedforward, horizontal, and feedback processing in the visual cortex. *Current Opinion in Neurobiology*, *8*(4), 529–535.

Laughlin, S. B. (2001). Energy as a constraint on the coding and processing of sensory information. *Current Opinion in Neurobiology*, *11*(4), 475–480.

Lavenex, P., & Amaral, D. G. (2000). Hippocampal-neocortical interaction: a hierarchy of associativity. *Hippocampus*, *10*(4), 420–430. doi:10.1002/1098-1063(2000)10:4<420::AID-HIPO8>3.0.CO;2-5

Lee, B. B., Martin, P. R., & Grünert, U. (2010). Retinal connectivity and primate vision. *Progress in retinal and eye research*, *29*(6), 622–639. doi:10.1016/j.preteyeres.2010.08.004

Lehky, S. R., & Sereno, A. B. (2007). Comparison of shape encoding in primate dorsal and ventral visual pathways. *Journal of Neurophysiology*, *97*(1), 307–319. doi:10.1152/jn.00168.2006

Lennie, P. (2003). The cost of cortical computation. *Current Biology: CB*, *13*(6), 493–497.

Leopold, D. A., & Logothetis, N. K. (1996). Activity changes in early visual cortex reflect monkeys' percepts during binocular rivalry. *Nature*, *379*(6565), 549–553. doi:10.1038/379549a0

Leventhal, A. G., Thompson, K. G., Liu, D., Zhou, Y., & Ault, S. J. (1995). Concomitant sensitivity to orientation, direction, and color of cells in layers 2, 3, and 4 of monkey striate cortex. *The Journal of Neuroscience: The Official Journal of the Society for Neuroscience*, *15*(3 Pt 1), 1808–1818.

Levitt, J. B., Kiper, D. C., & Movshon, J. A. (1994). Receptive fields and functional architecture of macaque V2. *Journal of Neurophysiology*, *71*(6), 2517–2542.

Li, F. F., VanRullen, R., Koch, C., & Perona, P. (2002). Rapid natural scene categorization in the near absence of attention. *Proceedings of the National Academy of Sciences of the United States of America*, *99*(14), 9596–9601. doi:10.1073/pnas.092277599

Likova, L. T., & Tyler, C. W. (2008). Occipital network for figure/ground organization. *Experimental Brain Research. Experimentelle Hirnforschung. Expérimentation Cérébrale*, *189*(3), 257–267. doi:10.1007/s00221-008-1417-6

Liu, T., Stevens, S. T., & Carrasco, M. (2007). Comparing the time course and efficacy of spatial and feature-based attention. *Vision Research*, *47*(1), 108–113. doi:10.1016/j.visres.2006.09.017

Llinás, R. (2002). *I of the vortex : from neurons to self*. Cambridge, Mass.: MIT.

Llinás, R. R. (1988). The intrinsic electrophysiological properties of mammalian neurons: insights into central nervous system function. *Science (New York, N.Y.)*, *242*(4886), 1654–1664.

Logothetis, N K. (1998). Single units and conscious vision. *Philosophical Transactions of the Royal Society of London. Series B, Biological Sciences*, *353*(1377), 1801–1818. doi:10.1098/rstb.1998.0333

Logothetis, N K, Pauls, J., & Poggio, T. (1995). Shape representation in the inferior temporal cortex of monkeys. *Current Biology: CB*, *5*(5), 552–563.

Logothetis, N K, & Sheinberg, D. L. (1996). Visual object recognition. *Annual Review of Neuroscience*, *19*, 577–621. doi:10.1146/annurev.ne.19.030196.003045

Logothetis, Nikos K. (2008). What we can do and what we cannot do with fMRI. *Nature*, *453*(7197), 869–878. doi:10.1038/nature06976

Lomber, S. G., & Payne, B. R. (1996). Removal of Two Halves Restores the Whole: Reversal of Visual Hemineglect During Bilateral Cortical or Collicular Inactivation in the Cat. *Visual Neuroscience*, *13*(06), 1143–1156. doi:10.1017/S0952523800007781

Lomber, S. G., Payne, B. R., & Horel, J. A. (1999). The cryoloop: an adaptable reversible cooling deactivation method for behavioral or electrophysiological assessment of neural function. *Journal of Neuroscience Methods*, *86*(2), 179–194. doi:10.1016/S0165-0270(98)00165-4

Lőrincz, M. L., Kékesi, K. A., Juhász, G., Crunelli, V., & Hughes, S. W. (2009). Temporal Framing of Thalamic Relay-Mode Firing by Phasic Inhibition during the Alpha Rhythm. *Neuron*, *63*(5), 683–696. doi:10.1016/j.neuron.2009.08.012

Lu, S., Cai, Y., Shen, M., Zhou, Y., & Han, S. (2012). Alerting and orienting of attention without visual awareness. *Consciousness and Cognition*. doi:10.1016/j.concog.2012.03.012

Luck, S. J., Chelazzi, L., Hillyard, S. A., & Desimone, R. (1997). Neural mechanisms of spatial selective attention in areas V1, V2, and V4 of macaque visual cortex. *Journal of Neurophysiology*, *77*(1), 24–42.

Lumer, E. D., Edelman, G. M., & Tononi, G. (1997). Neural dynamics in a model of the thalamocortical system. I. Layers, loops and the emergence of fast synchronous rhythms. *Cerebral Cortex (New York, N.Y.: 1991)*, *7*(3), 207–227.

Lund, J. S. (1973). Organization of neurons in the visual cortex, area 17, of the monkey (Macaca mulatta). *The Journal of Comparative Neurology*, *147*(4), 455–496. doi:10.1002/cne.901470404

Lund, J. S. (1988). Anatomical organization of macaque monkey striate visual cortex. *Annual review of neuroscience*, *11*, 253–288. doi:10.1146/annurev.ne.11.030188.001345

Luppi, P.-H., Gervasoni, D., Verret, L., Goutagny, R., Peyron, C., Salvert, D., Leger, L., et al. (2006). Paradoxical (REM) sleep genesis: the switch from an aminergic-cholinergic to a GABAergic-glutamatergic hypothesis. *Journal of Physiology, Paris*, *100*(5-6), 271–283. doi:10.1016/j.jphysparis.2007.05.006

Mack, A., & Rock, I. (1998). *Inattentional blindness*. Cambridge, Mass.: MIT Press. Retrieved from http://search.ebscohost.com/login.aspx?direct=true&scope=site&db=nlebk&db=nlabk&AN=1439

Malach, R., Reppas, J. B., Benson, R. R., Kwong, K. K., Jiang, H., Kennedy, W. A., Ledden, P. J., et al. (1995). Object-related activity revealed by functional magnetic resonance imaging in human occipital cortex. *Proceedings of the National Academy of Sciences of the United States of America*, *92*(18), 8135–8139.

Marr, D. (1976). Early processing of visual information. *Philosophical transactions of the Royal Society of London. Series B, Biological sciences*, *275*(942), 483–519.

Martínez-García, F., Puelles, L., Donkelaar, H. J. T., & González, A. (2012). Adaptive function and brain evolution. *Frontiers in Neuroanatomy*, 17. doi:10.3389/fnana.2012.00017

Martin-Malivel, J., & Fagot, J. (2001). Cross-modal integration and conceptual categorization in baboons. *Behavioural Brain Research*, *122*(2), 209–213.

Maturana, H., & Varela, F. J. (1992). *The Tree of Knowledge: The Biological Roots of Human Understanding* (3rd Revised ed.). Shambhala Publications Inc.

Maunsell, J. H., Ghose, G. M., Assad, J. A., McAdams, C. J., Boudreau, C. E., & Noerager, B. D. (1999). Visual response latencies of magnocellular and parvocellular LGN neurons in macaque monkeys. *Visual Neuroscience*, *16*(1), 1–14.

Maunsell, J. H., & van Essen, D. C. (1983). The connections of the middle temporal visual area (MT) and their relationship to a cortical hierarchy in the macaque monkey. *The Journal of Neuroscience: The Official Journal of the Society for Neuroscience*, *3*(12), 2563–2586.

Miller, E. K., Gochin, P. M., & Gross, C. G. (1993). Suppression of visual responses of neurons in inferior temporal cortex of the awake macaque by addition of a second stimulus. *Brain Research*, *616*(1-2), 25–29.

Mishkin, M., & Ungerleider, L. G. (1982). Contribution of striate inputs to the visuospatial functions of parieto-preoccipital cortex in monkeys. *Behavioural Brain Research*, *6*(1), 57–77. doi:10.1016/0166-4328(82)90081-X

Mishkin, M., Ungerleider, L. G., & Macko, K. A. (1983). Object vision and spatial vision: two cortical pathways. *Trends in Neurosciences*, *6*, 414–417. doi:10.1016/0166-2236(83)90190-X

Miyashita, Y., & Hayashi, T. (2000). Neural representation of visual objects: encoding and top-down activation. *Current Opinion in Neurobiology*, *10*(2), 187–194.

Mole, C. (2008). Attention and Consciousness. *Journal of Consciousness Studies*, *15*(4), 86–104.

Moran, J., & Desimone, R. (1985). Selective attention gates visual processing in the extrastriate cortex. *Science (New York, N.Y.)*, *229*(4715), 782–784.

Most, S. B., Simons, D. J., Scholl, B. J., Jimenez, R., Clifford, E., & Chabris, C. F. (2001). How not to be seen: the contribution of similarity and selective ignoring to sustained inattentional blindness. *Psychological science*, *12*(1), 9–17.

Moutoussis, K., & Zeki, S. (2002). The relationship between cortical activation and perception investigated with invisible stimuli. *Proceedings of the National Academy of Sciences of the United States of America*, *99*(14), 9527–9532. doi:10.1073/pnas.142305699

Müller, H. J., & Rabbitt, P. M. (1989). Reflexive and voluntary orienting of visual attention: time course of activation and resistance to interruption. *Journal of Experimental Psychology. Human Perception and Performance*, *15*(2), 315–330.

Mumford, D. (1991). On the computational architecture of the neocortex. I. The role of the thalamo-cortical loop. *Biological Cybernetics*, *65*(2), 135–145.

Naccache, L., Blandin, E., & Dehaene, S. (2002). Unconscious masked priming depends on temporal attention. *Psychological Science*, *13*(5), 416–424.

Nakayama, K., & Mackeben, M. (1982). Steady state visual evoked potentials in the alert primate. *Vision Research*, *22*(10), 1261–1271.

Nakayama, K., & Mackeben, M. (1989). Sustained and transient components of focal visual attention. *Vision Research*, *29*(11), 1631–1647.

Nasr, S., Liu, N., Devaney, K. J., Yue, X., Rajimehr, R., Ungerleider, L. G., & Tootell, R. B. H. (2011). Scene-Selective Cortical Regions in Human and Nonhuman Primates. *The Journal of Neuroscience*, *31*(39), 13771–13785. doi:10.1523/JNEUROSCI.2792-11.2011

Neggers, S. F. W., Huijbers, W., Vrijlandt, C. M., Vlaskamp, B. N. S., Schutter, D. J. L. G., & Kenemans, J. L. (2007). TMS pulses on the frontal eye fields break coupling between visuospatial attention and eye movements. *Journal of Neurophysiology*, *98*(5), 2765–2778. doi:10.1152/jn.00357.2007

Neisser, U., & Becklen, R. (1975). Selective looking: Attending to visually specified events. *Cognitive Psychology*, *7*(4), 480–494. doi:10.1016/0010-0285(75)90019-5

Newcombe, F., Ratcliff, G., & Damasio, H. (1987). Dissociable visual and spatial impairments following right posterior cerebral lesions: clinical, neuropsychological and anatomical evidence. *Neuropsychologia*, *25*(1B), 149–161.

O'Kusky, J., & Colonnier, M. (1982). A laminar analysis of the number of neurons, glia, and synapses in the adult cortex (area 17) of adult macaque monkeys. *The Journal of Comparative Neurology*, *210*(3), 278–290. doi:10.1002/cne.902100307

O'Regan, J. K., & Noë, A. (2001). A sensorimotor account of vision and visual consciousness. *The Behavioral and Brain Sciences*, *24*(5), 939–973; discussion 973–1031.

Oliva, A., & Torralba, A. (2006). Chapter 2 Building the gist of a scene: the role of global image features in recognition. *Progress in Brain Research* (Vol. 155, pp. 23–36). Elsevier. Retrieved from http://linkinghub.elsevier.com/retrieve/pii/S0079612306550022

Orban, G. A. (2008). Higher Order Visual Processing in Macaque Extrastriate Cortex. *Physiological Reviews*, *88*(1), 59–89. doi:10.1152/physrev.00008.2007

Orban, Guy A., Van Essen, D., & Vanduffel, W. (2004). Comparative mapping of higher visual areas in monkeys and humans. *Trends in Cognitive Sciences*, *8*(7), 315–324. doi:10.1016/j.tics.2004.05.009

Overgaard, M. (2004). Confounding Factors in Contrastive Analysis. *Synthese*, *141*(2), 217–231. doi:10.1023/B:SYNT.0000043019.64052.e0

Palmer, L. A., & Davis, T. L. (1981). Receptive-field structure in cat striate cortex. *Journal of Neurophysiology*, *46*(2), 260–276.

Palva, S., & Palva, J. M. (2007). New vistas for alpha-frequency band oscillations. *Trends in Neurosciences*, *30*(4), 150–158. doi:10.1016/j.tins.2007.02.001

Pasley, B. N., Mayes, L. C., & Schultz, R. T. (2004). Subcortical discrimination of unperceived objects during binocular rivalry. *Neuron*, *42*(1), 163–172.

Pasupathy, A., & Connor, C. E. (1999). Responses to contour features in macaque area V4. *Journal of Neurophysiology*, *82*(5), 2490–2502.

Penrose, R. (1990). *The Emperor's New Mind: Concerning Computers, Minds and the Laws of Physics* (New ed.). Vintage.

Peterhans, E., & von der Heydt, R. (1993). Functional organization of area V2 in the alert macaque. *The European Journal of Neuroscience*, *5*(5), 509–524.

Pinsk, M. A., Arcaro, M., Weiner, K. S., Kalkus, J. F., Inati, S. J., Gross, C. G., & Kastner, S. (2009). Neural representations of faces and body parts in macaque and human cortex: a comparative FMRI study. *Journal of Neurophysiology*, *101*(5), 2581–2600. doi:10.1152/jn.91198.2008

Pollen, D A. (1999). On the neural correlates of visual perception. *Cerebral Cortex (New York, N.Y.: 1991)*, *9*(1), 4–19.

Pollen, Daniel A. (2003). Explicit neural representations, recursive neural networks and conscious visual perception. *Cerebral Cortex (New York, N.Y.: 1991)*, *13*(8), 807–814.

Portilla, J., & Simoncelli, E. P. (2000). A Parametric Texture Model Based on Joint Statistics of Complex Wavelet Coefficients. *Int. J. Comput. Vision*, *40*(1), 49–70. doi:10.1023/A:1026553619983

Posner, M I. (1980). Orienting of attention. *The Quarterly Journal of Experimental Psychology*, *32*(1), 3–25.

Posner, M I. (1994). Attention: the mechanisms of consciousness. *Proceedings of the National Academy of Sciences of the United States of America*, *91*(16), 7398–7403.

Posner, M I, Snyder, C. R., & Davidson, B. J. (1980). Attention and the detection of signals. *Journal of Experimental Psychology*, *109*(2), 160–174.

Posner, Michael I. (2012). Attentional networks and consciousness. *Frontiers in Psychology*, *3*, 64. doi:10.3389/fpsyg.2012.00064

Postma, A., Sterken, Y., de Vries, L., & de Haan, E. H. (2000). Spatial localization in patients with unilateral posterior left or right hemisphere lesions. *Experimental Brain Research. Experimentelle Hirnforschung. Expérimentation Cérébrale*, *134*(2), 220–227.

Price, C. J., & Devlin, J. T. (2003). The myth of the visual word form area. *NeuroImage*, *19*(3), 473–481.

Prinz. (2010). *Perceiving the World*. Oxford University Press.

Puce, A., Allison, T., Asgari, M., Gore, J. C., & McCarthy, G. (1996). Differential sensitivity of human visual cortex to faces, letterstrings, and textures: a functional magnetic resonance imaging study. *The Journal of Neuroscience: The Official Journal of the Society for Neuroscience*, *16*(16), 5205–5215.

Puce, A., Allison, T., Gore, J. C., & McCarthy, G. (1995). Face-sensitive regions in human extrastriate cortex studied by functional MRI. *Journal of Neurophysiology*, *74*(3), 1192–1199.

Quiroga, R. Q., Kreiman, G., Koch, C., & Fried, I. (2008). Sparse but not “Grandmother-cell” coding in the medial temporal lobe. *Trends in Cognitive Sciences*, *12*(3), 87–91. doi:10.1016/j.tics.2007.12.003

Quiroga, R. Q., Reddy, L., Kreiman, G., Koch, C., & Fried, I. (2005). Invariant visual representation by single neurons in the human brain. *Nature*, *435*(7045), 1102–1107. doi:10.1038/nature03687

Rager, G., & Singer, W. (1998). The response of cat visual cortex to flicker stimuli of variable frequency. *The European Journal of Neuroscience*, *10*(5), 1856–1877.

Reddy, L., Reddy, L., & Koch, C. (2006). Face identification in the near-absence of focal attention. *Vision Research*, *46*(15), 2336–2343. doi:10.1016/j.visres.2006.01.020

Regan, D. (1966). Some characteristics of average steady-state and transient responses evoked by modulated light. *Electroencephalography and Clinical Neurophysiology*, *20*(3), 238–248. doi:10.1016/0013-4694(66)90088-5

Regan, D. (1982). Comparison of transient and steady-state methods. *Annals of the New York Academy of Sciences*, *388*, 45–71.

Regan, David. (1989). *Human Brain Electrophysiology: Evoked Potentials and Evoked Magnetic Fields in Science and Medicine*. Appleton & Lange.

Remington, R. W., Johnston, J. C., & Yantis, S. (1992). Involuntary attentional capture by abrupt onsets. *Perception & Psychophysics*, *51*(3), 279–290.

Rensink, R. (2005). Change Blindness. *McGraw-Hill Yearbook of Science & Technology* (pp. 44–46). McGraw-Hill.

Rensink, R. A. (2000). When good observers go bad: Change blindness, inattentional blindness, and visual experience. *Psyche*.

Rensink, R. A., O'Regan, J. K., & Clark, J. J. (1997). To See or not to See: The Need for Attention to Perceive Changes in Scenes. *Psychological Science*, *8*(5), 368–373. doi:10.1111/j.1467-9280.1997.tb00427.x

Rensink, Ronald A. (2002). Change detection. *Annual review of psychology*, *53*, 245–277. doi:10.1146/annurev.psych.53.100901.135125

Reynolds, J. H., Chelazzi, L., & Desimone, R. (1999). Competitive mechanisms subserve attention in macaque areas V2 and V4. *The Journal of Neuroscience: The Official Journal of the Society for Neuroscience*, *19*(5), 1736–1753.

Reynolds, J. H., & Desimone, R. (1999). The role of neural mechanisms of attention in solving the binding problem. *Neuron*, *24*(1), 19–29, 111–125.

Rizzolatti, G., & Berti, A. (1990). Neglect as a neural representation deficit. *Revue Neurologique*, *146*(10), 626–634.

Rockland, K. S., & Drash, G. W. (1996). Collateralized divergent feedback connections that target multiple cortical areas. *The Journal of Comparative Neurology*, *373*(4), 529–548. doi:10.1002/(SICI)1096-9861(19960930)373:4<529::AID-CNE5>3.0.CO;2-3

Rockland, K. S., & Pandya, D. N. (1979). Laminar origins and terminations of cortical connections of the occipital lobe in the rhesus monkey. *Brain Research*, *179*(1), 3–20.

Rockland, K. S., & Van Hoesen, G. W. (1994). Direct temporal-occipital feedback connections to striate cortex (V1) in the macaque monkey. *Cerebral Cortex (New York, N.Y.: 1991)*, *4*(3), 300–313.

Roelfsema, P. R., Lamme, V. A. F., Spekreijse, H., & Bosch, H. (2002). Figure-ground segregation in a recurrent network architecture. *Journal of Cognitive Neuroscience*, *14*(4), 525–537. doi:10.1162/08989290260045756

Rolls, E T, & Tovee, M. J. (1995). The responses of single neurons in the temporal visual cortical areas of the macaque when more than one stimulus is present in the receptive field. *Experimental Brain Research. Experimentelle Hirnforschung. Expérimentation Cérébrale*, *103*(3), 409–420.

Rolls, Edmund T, Aggelopoulos, N. C., & Zheng, F. (2003). The receptive fields of inferior temporal cortex neurons in natural scenes. *The Journal of Neuroscience: The Official Journal of the Society for Neuroscience*, *23*(1), 339–348.

Rossi, A. F., Pessoa, L., Desimone, R., & Ungerleider, L. G. (2009). The prefrontal cortex and the executive control of attention. *Experimental Brain Research. Experimentelle Hirnforschung. Expérimentation Cérébrale*, *192*(3), 489–497. doi:10.1007/s00221-008-1642-z

Rousselet, G. A., Fabre-Thorpe, M., & Thorpe, S. J. (2002). Parallel processing in high-level categorization of natural images. *Nature Neuroscience*, *5*(7), 629–630. doi:10.1038/nn866

Rousselet, G. A., Macé, M. J.-M., & Fabre-Thorpe, M. (2003). Is it an animal? Is it a human face? Fast processing in upright and inverted natural scenes. *Journal of Vision*, *3*(6), 440–455. doi:10:1167/3.6.5

Rust, N. C., & Dicarlo, J. J. (2010). Selectivity and tolerance ("invariance") both increase as visual information propagates from cortical area V4 to IT. *The Journal of Neuroscience: The Official Journal of the Society for Neuroscience*, *30*(39), 12978–12995. doi:10.1523/JNEUROSCI.0179-10.2010

Sadr, J., & Sinha, P. (2004). Object recognition and random image structure evolution. *Cognitive Science*, *28*, 259–287.

Sagi, D., & Julesz, B. (1986). Enhanced detection in the aperture of focal attention during simple discrimination tasks. *Nature*, *321*(6071), 693–695. doi:10.1038/321693a0

Saleem, K. S., & Tanaka, K. (1996). Divergent projections from the anterior inferotemporal area TE to the perirhinal and entorhinal cortices in the macaque monkey. *The Journal of Neuroscience: The Official Journal of the Society for Neuroscience*, *16*(15), 4757–4775.

Salin, P. A., & Bullier, J. (1995). Corticocortical connections in the visual system: structure and function. *Physiological Reviews*, *75*(1), 107–154.

Salsbury, K., & Horel, J. (1983). A cryogenic implant for producing reversible functional brain lesions. *Behavior Research Methods*, *15*(4), 433–436. doi:10.3758/BF03203678

Sanders, A. F. (1997). A summary of resource theories from a behavioral perspective. *Biological Psychology*, *45*(1-3), 5–18.

Sartori, G., & Umiltà, C. (2000). How to Avoid the Fallacies of Cognitive Subtraction in Brain Imaging. *Brain and Language*, *74*(2), 191–212. doi:10.1006/brln.2000.2334

Sauseng, P., & Klimesch, W. (2008). What does phase information of oscillatory brain activity tell us about cognitive processes? *Neuroscience and Biobehavioral Reviews*, *32*(5), 1001–1013. doi:10.1016/j.neubiorev.2008.03.014

Schenkman, B. N., & Nilsson, M. E. (2010). Human echolocation: Blind and sighted persons' ability to detect sounds recorded in the presence of a reflecting object. *Perception*, *39*(4), 483–501.

Schenkman, B. N., & Nilsson, M. E. (2011). Human echolocation: pitch versus loudness information. *Perception*, *40*(7), 840–852.

Schiller, P. H. (1995). Effect of lesions in visual cortical area V4 on the recognition of transformed objects. *Nature*, *376*(6538), 342–344. doi:10.1038/376342a0

Schiller, P. H., Finlay, B. L., & Volman, S. F. (1976). Quantitative studies of single-cell properties in monkey striate cortex. I. Spatiotemporal organization of receptive fields. *Journal of Neurophysiology*, *39*(6), 1288–1319.

Schiller, P. H., & Lee, K. (1991). The role of the primate extrastriate area V4 in vision. *Science (New York, N.Y.)*, *251*(4998), 1251–1253.

Schmid, A. M. (2008). The processing of feature discontinuities for different cue types in primary visual cortex. *Brain Research*, *1238*, 59–74. doi:10.1016/j.brainres.2008.08.029

Schmolesky, M. T., Wang, Y., Hanes, D. P., Thompson, K. G., Leutgeb, S., Schall, J. D., & Leventhal, A. G. (1998). Signal timing across the macaque visual system. *Journal of Neurophysiology*, *79*(6), 3272–3278.

Schmolesky, M. T., Wang, Y., Pu, M., & Leventhal, A. G. (2000). Degradation of stimulus selectivity of visual cortical cells in senescent rhesus monkeys. *Nature neuroscience*, *3*(4), 384–390. doi:10.1038/73957

Scholl, B. J., & Pylyshyn, Z. W. (1999). Tracking multiple items through occlusion: clues to visual objecthood. *Cognitive Psychology*, *38*(2), 259–290. doi:10.1006/cogp.1998.0698

Scholte, H. S., Jolij, J., Fahrenfort, J. J., & Lamme, V. A. F. (2008). Feedforward and recurrent processing in scene segmentation: electroencephalography and functional magnetic resonance imaging. *Journal of Cognitive Neuroscience*, *20*(11), 2097–2109. doi:10.1162/jocn.2008.20142

Schyns, P. G., Gosselin, F., & Smith, M. L. (2009). Information processing algorithms in the brain. *Trends in Cognitive Sciences*, *13*(1), 20–26. doi:10.1016/j.tics.2008.09.008

Seghier, M. L., & Vuilleumier, P. (2006). Functional neuroimaging findings on the human perception of illusory contours. *Neuroscience and Biobehavioral Reviews*, *30*(5), 595–612. doi:10.1016/j.neubiorev.2005.11.002

Sereno, A. B., & Maunsell, J. H. (1998). Shape selectivity in primate lateral intraparietal cortex. *Nature*, *395*(6701), 500–503. doi:10.1038/26752

Sergent, C., Baillet, S., & Dehaene, S. (2005). Timing of the brain events underlying access to consciousness during the attentional blink. *Nature Neuroscience*, *8*(10), 1391–1400. doi:10.1038/nn1549

Shanahan, M. (2010). *Embodiment and the inner life : cognition and consciousness in the space of possible minds*. Oxford; New York: Oxford University Press.

Sherman, S. M., & Guillery, R. W. (1998). On the actions that one nerve cell can have on another: distinguishing “drivers” from “modulators.” *Proceedings of the National Academy of Sciences of the United States of America*, *95*(12), 7121–7126.

Shulman, G. L., Remington, R. W., & McLean, J. P. (1979). Moving attention through visual space. *Journal of Experimental Psychology. Human Perception and Performance*, *5*(3), 522–526.

Shulman, G. L., & Wilson, J. (1987). Spatial frequency and selective attention to local and global information. *Perception*, *16*(1), 89–101.

Sidtis, J. J., Strother, S. C., Anderson, J. R., & Rottenberg, D. A. (1999). Are Brain Functions Really Additive? *NeuroImage*, *9*(5), 490–496. doi:10.1006/nimg.1999.0423

Sigala, N. (2004). Visual categorization and the inferior temporal cortex. *Behavioural Brain Research*, *149*(1), 1–7. doi:10.1016/S0166-4328(03)00224-9

Sigala, Natasha, & Logothetis, N. K. (2002). Visual categorization shapes feature selectivity in the primate temporal cortex. *Nature*, *415*(6869), 318–320. doi:10.1038/415318a

Simons, D J, & Chabris, C. F. (1999). Gorillas in our midst: sustained inattentional blindness for dynamic events. *Perception*, *28*(9), 1059–1074.

Simons, D J, Franconeri, S. L., & Reimer, R. L. (2000). Change blindness in the absence of a visual disruption. *Perception*, *29*(10), 1143–1154.

Simons, Daniel J., & Rensink, R. A. (2003). Induced Failures of Visual Awareness. *Journal of Vision*, *3*(1). doi:10.1167/3.1.i

Sincich, L. C., Adams, D. L., & Horton, J. C. (2003). Complete flatmounting of the macaque cerebral cortex. *Visual Neuroscience*, *20*(6), 663–686.

Sincich, L. C., Park, K. F., Wohlgemuth, M. J., & Horton, J. C. (2004). Bypassing V1: a direct geniculate input to area MT. *Nature Neuroscience*, *7*(10), 1123–1128. doi:10.1038/nn1318

Solari, S. V. H., & Stoner, R. (2011). Cognitive consilience: primate non-primary neuroanatomical circuits underlying cognition. *Frontiers in neuroanatomy*, *5*, 65. doi:10.3389/fnana.2011.00065

Soltani, A., & Koch, C. (2010). Visual saliency computations: mechanisms, constraints, and the effect of feedback. *The Journal of Neuroscience: The Official Journal of the Society for Neuroscience*, *30*(38), 12831–12843. doi:10.1523/JNEUROSCI.1517-10.2010

Spatz, W. B., Tigges, J., & Tigges, M. (1970). Subcortical projections, cortical associations, and some intrinsic interlaminar connections of the striate cortex in the squirrel monkey (Saimiri). *The Journal of Comparative Neurology*, *140*(2), 155–174. doi:10.1002/cne.901400203

Spekreijse, Estevez, & Reitz. (1977). Visual evoked potential and the physiological analysis of visual process in man. *Visual Evoked Potentials in Man: New Developments* (pp. 16–85). Oxford: Clarendon.

Steriade, M., Oakson, G., & Ropert, N. (1982). Firing rates and patterns of midbrain reticular neurons during steady and transitional states of the sleep-waking cycle. *Experimental Brain Research. Experimentelle Hirnforschung. Expérimentation Cérébrale*, *46*(1), 37–51.

Sterzer, P., Haynes, J. D., & Rees, G. (2008). Fine-scale activity patterns in high-level visual areas encode the category of invisible objects. *Journal of Vision*, *8*(15), 10–10. doi:10.1167/8.15.10

Suzuki, W A. (1999). The long and the short of it: memory signals in the medial temporal lobe. *Neuron*, *24*(2), 295–298.

Suzuki, Wendy A. (1996). The anatomy, physiology and functions of the perirhinal cortex. *Current Opinion in Neurobiology*, *6*(2), 179–186. doi:10.1016/S0959-4388(96)80071-7

Tallon-Baudry, C., Bertrand, O., Delpuech, C., & Permier, J. (1997). Oscillatory gamma-band (30-70 Hz) activity induced by a visual search task in humans. *The Journal of Neuroscience: The Official Journal of the Society for Neuroscience*, *17*(2), 722–734.

Tanaka, K. (1997). Mechanisms of visual object recognition: monkey and human studies. *Current Opinion in Neurobiology*, *7*(4), 523–529.

Tanaka, K. (1983). Cross-correlation analysis of geniculostriate neuronal relationships in cats. *Journal of Neurophysiology*, *49*(6), 1303–1318.

Tanaka, Keiji. (1996). Representation of Visual Features of Objects in the Inferotemporal Cortex. *Neural Networks: The Official Journal of the International Neural Network Society*, *9*(8), 1459–1475.

Tanaka, Keiji. (2003). Columns for complex visual object features in the inferotemporal cortex: clustering of cells with similar but slightly different stimulus selectivities. *Cerebral Cortex (New York, N.Y.: 1991)*, *13*(1), 90–99.

Tanaka, M., Lindsley, E., Lausmann, S., & Creutzfeldt, O. D. (1990). Afferent connections of the prelunate visual association cortex (areas V4 and DP). *Anatomy and Embryology*, *181*(1), 19–30.

Teng, S., Puri, A., & Whitney, D. (2012). Ultrafine spatial acuity of blind expert human echolocators. *Experimental Brain Research. Experimentelle Hirnforschung. Expérimentation Cérébrale*, *216*(4), 483–488. doi:10.1007/s00221-011-2951-1

Thomas, O. M., Cumming, B. G., & Parker, A. J. (2002). A specialization for relative disparity in V2. *Nature Neuroscience*, *5*(5), 472–478. doi:10.1038/nn837

Thorpe, S., Fize, D., & Marlot, C. (1996). Speed of processing in the human visual system. *Nature*, *381*(6582), 520–522. doi:10.1038/381520a0

Thorpe, S. J., & Fabre-Thorpe, M. (2001). Neuroscience. Seeking categories in the brain. *Science (New York, N.Y.)*, *291*(5502), 260–263.

Tombu, M., & Tsotsos, J. K. (2008). Attending to orientation results in an inhibitory surround in orientation space. *Perception & Psychophysics*, *70*(1), 30–35.

Tomycz, N. D., & Friedlander, R. M. (2011). Neuromodulation of the locus coeruleus: a key to controlling wakefulness. *Neurosurgery*, *68*(2), N14–15. doi:10.1227/01.neu.0000393589.31014.61

Tong, F, Nakayama, K., Vaughan, J. T., & Kanwisher, N. (1998). Binocular rivalry and visual awareness in human extrastriate cortex. *Neuron*, *21*(4), 753–759.

Tong, Frank, Meng, M., & Blake, R. (2006). Neural bases of binocular rivalry. *Trends in Cognitive Sciences*, *10*(11), 502–511. doi:10.1016/j.tics.2006.09.003

Tononi, G, Srinivasan, R., Russell, D. P., & Edelman, G. M. (1998). Investigating neural correlates of conscious perception by frequency-tagged neuromagnetic responses. *Proceedings of the National Academy of Sciences of the United States of America*, *95*(6), 3198–3203.

Tononi, Giulio. (2004). An information integration theory of consciousness. *BMC Neuroscience*, *5*, 42. doi:10.1186/1471-2202-5-42

Tootell, R. B., Dale, A. M., Sereno, M. I., & Malach, R. (1996). New images from human visual cortex. *Trends in Neurosciences*, *19*(11), 481–489.

Torralba, A., & Oliva, A. (2003). Statistics of natural image categories. *Network (Bristol, England)*, *14*(3), 391–412.

Treisman, A. (1988). Features and objects: the fourteenth Bartlett memorial lecture. *The Quarterly Journal of Experimental Psychology. A, Human Experimental Psychology*, *40*(2), 201–237.

Treisman, A., & Sato, S. (1990). Conjunction search revisited. *Journal of Experimental Psychology. Human Perception and Performance*, *16*(3), 459–478.

Treue, S., & Maunsell, J. H. (1996). Attentional modulation of visual motion processing in cortical areas MT and MST. *Nature*, *382*(6591), 539–541. doi:10.1038/382539a0

Tse, P. U. (2004). Mapping visual attention with change blindness: new directions for a new method. *Cognitive Science*, *28*(2), 241–258. doi:10.1016/j.cogsci.2003.12.002

Tsotsos, J K. (1997). Limited capacity of any realizable perceptual system is a sufficient reason for attentive behavior. *Consciousness and Cognition*, *6*(2-3), 429–436. doi:10.1006/ccog.1997.0302

Tsotsos, John K., Culhane, S. M., Kei Wai, W. Y., Lai, Y., Davis, N., & Nuflo, F. (1995). Modeling visual attention via selective tuning. *Artificial Intelligence*, *78*(1-2), 507–545. doi:10.1016/0004-3702(95)00025-9

Tsunoda, K., Yamane, Y., Nishizaki, M., & Tanifuji, M. (2001). Complex objects are represented in macaque inferotemporal cortex by the combination of feature columns. *Nature Neuroscience*, *4*(8), 832–838. doi:10.1038/90547

Ullman, S. (1984). Visual routines. *Cognition*, *18*(1-3), 97–159.

Ullman, Shimon, Vidal-Naquet, M., & Sali, E. (2002). Visual features of intermediate complexity and their use in classification. *Nature Neuroscience*. doi:10.1038/nn870

Ungerleider, L G, & Haxby, J. V. (1994). “What” and “where” in the human brain. *Current Opinion in Neurobiology*, *4*(2), 157–165.

Ungerleider, Leslie G., & Mishkin, M. (1982). *Analysis of visual behavior : (articles first presented to the NATO advanced study institute on new advances in the analysis of visual behavior; Waltham - Mass, June 1978)*. (M. NATO Advanced Study Institute on New Advances in the Analysis of Visual Behavior (1978 ; Waltham, Ed.). Cambridge - Mass.& London: MIT Press.

Van Essen, D. C., & Gallant, J. L. (1994). Neural mechanisms of form and motion processing in the primate visual system. *Neuron*, *13*(1), 1–10.

van Gaal, S., de Lange, F. P., & Cohen, M. X. (2012). The role of consciousness in cognitive control and decision making. *Frontiers in Human Neuroscience*, *6*. doi:10.3389/fnhum.2012.00121

Van Horn, S. C., Erişir, A., & Sherman, S. M. (2000). Relative distribution of synapses in the A-laminae of the lateral geniculate nucleus of the cat. *The Journal of Comparative Neurology*, *416*(4), 509–520.

VanRullen, R. (2006). On second glance: still no high-level pop-out effect for faces. *Vision Research*, *46*(18), 3017–3027. doi:10.1016/j.visres.2005.07.009

VanRullen, R., Guyonneau, R., & Thorpe, S. J. (2005). Spike times make sense. *Trends in Neurosciences*, *28*(1), 1–4. doi:10.1016/j.tins.2004.10.010

VanRullen, R., & Koch, C. (2003). Visual selective behavior can be triggered by a feed-forward process. *Journal of Cognitive Neuroscience*, *15*(2), 209–217. doi:10.1162/089892903321208141

VanRullen, R., & Thorpe, S. J. (2002). Surfing a spike wave down the ventral stream. *Vision Research*, *42*(23), 2593–2615.

Vecera, S. P., & Farah, M. J. (1994). Does visual attention select objects or locations? *Journal of Experimental Psychology. General*, *123*(2), 146–160.

Vialatte, François-Benoît, Maurice, M., Dauwels, J., & Cichocki, A. (2010). Steady-state visually evoked potentials: Focus on essential paradigms and future perspectives. *Progress in Neurobiology*, *90*(4), 418–438. doi:10.1016/j.pneurobio.2009.11.005

Vialatte, François-Benoit, Maurice, M., Dauwels, J., & Cichocki, A. (2008). Steady state visual evoked potentials in the delta range (0.5-5 Hz) (pp. 400–407). Presented at the Proceedings of the 15th international conference on Advances in neuro-information processing - Volume Part I, Springer-Verlag. Retrieved from http://dl.acm.org/citation.cfm?id=1813488.1813540

Vidal, J. R., Chaumon, M., O'Regan, J. K., & Tallon-Baudry, C. (2006). Visual Grouping and the Focusing of Attention Induce Gamma-band Oscillations at Different Frequencies in Human Magnetoencephalogram Signals. *J. Cognitive Neuroscience*, *18*(11), 1850–1862. doi:10.1162/jocn.2006.18.11.1850

von der Heydt, R., Peterhans, E., & Baumgartner, G. (1984). Illusory contours and cortical neuron responses. *Science (New York, N.Y.)*, *224*(4654), 1260–1262.

Voogd, J., Schraa-Tam, C. K. L., van der Geest, J. N., & De Zeeuw, C. I. (2010). Visuomotor Cerebellum in Human and Nonhuman Primates. *Cerebellum (London, England)*. doi:10.1007/s12311-010-0204-7

Vossel, S., Thiel, C. M., & Fink, G. R. (2006). Cue validity modulates the neural correlates of covert endogenous orienting of attention in parietal and frontal cortex. *NeuroImage*, *32*(3), 1257–1264. doi:10.1016/j.neuroimage.2006.05.019

Wang, H. F., Friel, N., Gosselin, F., & Schyns, P. G. (2011). Efficient bubbles for visual categorization tasks. *Vision Research*, *51*(12), 1318–1323. doi:10.1016/j.visres.2011.04.007

Wang, X.-J. (2010). Neurophysiological and computational principles of cortical rhythms in cognition. *Physiological Reviews*, *90*(3), 1195–1268. doi:10.1152/physrev.00035.2008

Ward, L. M. (2011). The thalamic dynamic core theory of conscious experience. *Consciousness and Cognition*, *20*(2), 464–486. doi:10.1016/j.concog.2011.01.007

Ward, R., & Jackson, S. R. (2002). Visual attention in blindsight: sensitivity in the blind field increased by targets in the sighted field. *Neuroreport*, *13*(3), 301–304.

Warrington, E. K. (1982). Neuropsychological studies of object recognition. *Philosophical Transactions of the Royal Society of London. Series B, Biological Sciences*, *298*(1089), 15–33.

Watanabe, M., Cheng, K., Murayama, Y., Ueno, K., Asamizuya, T., Tanaka, K., & Logothetis, N. (2011). Attention But Not Awareness Modulates the BOLD Signal in the Human V1 During Binocular Suppression. *Science*, *334*(6057), 829–831. doi:10.1126/science.1203161

Wiesel, T. N., & Hubel, D. H. (1966). Spatial and chromatic interactions in the lateral geniculate body of the rhesus monkey. *Journal of Neurophysiology*, *29*(6), 1115–1156.

Wilson, M. E., & Cragg, B. G. (1967). Projections from the lateral geniculate nucleus in the cat and monkey. *Journal of Anatomy*, *101*(Pt 4), 677–692.

Wolfe, J. M., Cave, K. R., & Franzel, S. L. (1989). Guided search: an alternative to the feature integration model for visual search. *Journal of Experimental Psychology. Human Perception and Performance*, *15*(3), 419–433.

Womelsdorf, T., & Fries, P. (2007). The role of neuronal synchronization in selective attention. *Current Opinion in Neurobiology*, *17*(2), 154–160. doi:10.1016/j.conb.2007.02.002

Womelsdorf, T., Schoffelen, J.-M., Oostenveld, R., Singer, W., Desimone, R., Engel, A. K., & Fries, P. (2007). Modulation of Neuronal Interactions Through Neuronal Synchronization. *Science*, *316*(5831), 1609–1612. doi:10.1126/science.1139597

Wong-Riley, M. (1978). Reciprocal connections between striate and prestriate cortex in squirrel monkey as demonstrated by combined peroxidase histochemistry and autoradiography. *Brain Research*, *147*(1), 159–164.

Wong-Riley, M. T. (1977). Connections between the pulvinar nucleus and the prestriate cortex in the squirrel monkey as revealed by peroxidase histochemistry and autoradiography. *Brain Research*, *134*(2), 249–267.

Wright, R. D., & Ward, L. M. (2008). *Orienting of attention*. Oxford; New York: Oxford University Press.

Xu, X., Ichida, J. M., Allison, J. D., Boyd, J. D., Bonds, A. B., & Casagrande, V. A. (2001). A comparison of koniocellular, magnocellular and parvocellular receptive field properties in the lateral geniculate nucleus of the owl monkey (Aotus trivirgatus). *The Journal of Physiology*, *531*(Pt 1), 203–218.

Yantis, S., & Jonides, J. (1990). Abrupt visual onsets and selective attention: voluntary versus automatic allocation. *Journal of Experimental Psychology. Human Perception and Performance*, *16*(1), 121–134.

Yeshurun, Y., Montagna, B., & Carrasco, M. (2008). On the flexibility of sustained attention and its effects on a texture segmentation task. *Vision Research*, *48*(1), 80–95. doi:10.1016/j.visres.2007.10.015

Yoshida, K., & Benevento, L. A. (1981). The projection from the dorsal lateral geniculate nucleus of the thalamus to extrastriate visual association cortex in the macaque monkey. *Neuroscience Letters*, *22*(2), 103–108.

Young, M. P., & Yamane, S. (1992). Sparse population coding of faces in the inferotemporal cortex. *Science (New York, N.Y.)*, *256*(5061), 1327–1331.

Zeki, S. (1995). The motion vision of the blind. *NeuroImage*, *2*(3), 231–235. doi:10.1006/nimg.1995.1030

Zeki, S. (2003). The disunity of consciousness. *Trends in Cognitive Sciences*, *7*(5), 214–218.

Zeki, S, & Bartels, A. (1999). Toward a theory of visual consciousness. *Consciousness and Cognition*, *8*(2), 225–259. doi:10.1006/ccog.1999.0390

Zeki, Semir. (2008). The disunity of consciousness. *Progress in Brain Research*, *168*, 11–18. doi:10.1016/S0079-6123(07)68002-9

Zhan, C. A., & Baker, C. L., Jr. (2008). Critical spatial frequencies for illusory contour processing in early visual cortex. *Cerebral Cortex (New York, N.Y.: 1991)*, *18*(5), 1029–1041. doi:10.1093/cercor/bhm139

Zhaoping, L. (2005). Border ownership from intracortical interactions in visual area v2. *Neuron*, *47*(1), 143–153. doi:10.1016/j.neuron.2005.04.005

Zhou, H., Friedman, H. S., & von der Heydt, R. (2000). Coding of border ownership in monkey visual cortex. *The Journal of Neuroscience: The Official Journal of the Society for Neuroscience*, *20*(17), 6594–6611.